



UNIVERSITY
OF
JOHANNESBURG

COPYRIGHT AND CITATION CONSIDERATIONS FOR THIS THESIS/ DISSERTATION

 creative
commons



- Attribution — You must give appropriate credit, provide a link to the license, and indicate if changes were made. You may do so in any reasonable manner, but not in any way that suggests the licensor endorses you or your use.
- NonCommercial — You may not use the material for commercial purposes.
- ShareAlike — If you remix, transform, or build upon the material, you must distribute your contributions under the same license as the original.

How to cite this thesis

Surname, Initial(s). (2012) Title of the thesis or dissertation. PhD. (Chemistry)/ M.Sc. (Physics)/ M.A. (Philosophy)/M.Com. (Finance) etc. [Unpublished]: [University of Johannesburg](https://ujcontent.uj.ac.za/vital/access/manager/Index?site_name=Research%20Output). Retrieved from: https://ujcontent.uj.ac.za/vital/access/manager/Index?site_name=Research%20Output (Accessed: Date).



RESEARCH DISSERTATION

**CHARACTERIZATION OF TITANIUM ALLOY AND BORON
CARBIDE METAL MATRIX COMPOSITES (MMCs) FOR SURFACE
ENGINEERING APPLICATIONS**

By

Ogunlana M O

Submitted in partial fulfilment for the requirements of the degree

Masters of Engineering

In

Mechanical Engineering
Department of Mechanical Engineering Science
Faculty of Engineering and the Built Environment

Student Number: 201510083

At the

UNIVERSITY OF JOHANNESBURG

Supervisor: Prof E. T. Akinlabi

January, 2016

DECLARATION

- I, **Ogunlana Musibau Olalekan**, hereby declares that this dissertation is wholly my own work and has not been submitted anywhere else for academic credit either by myself or another person.

- I understand what plagiarism implies and declare that this dissertation is my own ideas, words, phrases, arguments, graphics, figures, results, and organization except where reference is explicitly made to another's work.

- I understand further that any unethical academic behaviour, which includes plagiarism, is seen in a serious light by the University of Johannesburg and is punishable by disciplinary action.

Signed:

Date: January, 2016

ACKNOWLEDGEMENTS

Unto the Lord be the glory, honour and adoration for His infinite mercies and favour upon my life. Thanks and glory be to the Name of God for the privilege to achieve this great height in my career.

I would like to express my most sincere gratitude to my supervisor, Prof Esther Akinlabi for her guidance and immense support during the course of this research work. However, the successful completion of this work would not have been achieved without her great assistance. My gratitude and appreciation goes to Mr Erinosh Mutiu, Dr Kenny Sobiyi, Dr Kazeem Sanusi and Dr Onitiri Modupe for their inestimable and ceaseless assistance during the course of this research work. I would also like to thank my fellow researchers, the presently registered Masters' and Doctoral students for their assistance and moral support. I am also grateful to my colleagues and friends in the University of Johannesburg for their encouragements and support.

My special gratitude goes to my parents, Late Chief Alhaji Sakariyau Olalekan Ogunlana, who was my source of inspiration in academic pursuits. To my mother, Alhaja Bilawu Olalekan Ogunlana and my brothers, sisters, cousins, nephews, nieces and friends for their moral support and prayers. I would also like to express my special gratitude to my brother Mr Monsuru (Raymond) Ogunlana for his invaluable contributions financially and in the provision of shelter for me during the course of this research work. I don't know what I would have done without your assistance and support. Thank you very much my brother, May God reward you with uncommon blessings and may you live to enjoy the fruits of your labour. I can not thank you enough.

I would like to acknowledge the Head of Department of Mechanical Engineering Science, University of Johannesburg who also happened to be my supervisor and sponsored my Masters programme from her personal research fund. I am very grateful to you Prof Esther Akinlabi.

ABSTRACT

Surface engineering applications has brought titanium and its alloys into limelight in the manufacturing industries such as the aerospace, automobile, marine, food processing and chemical processing industry. Despite the growths experienced in the use of this material, Ti and its alloys are plagued with poor wear behaviour especially when in contact with other materials during application. This limitation of Ti-based components has led to a search for techniques and processes to modify, restructure and re-engineer such materials for extended lifespan and for reuse. Among various techniques for restoring and protecting the material is by the use of the laser metal deposition (LMD) technique otherwise called the laser cladding process. The LMD is a technique used to achieve a coating on components which allow the addition of reinforcing particles to improve the surface properties of titanium-based materials. These properties include hardness, wear amongst others.

This research study involves the use of the LMD process to deposit composite coatings on titanium alloy (Ti6Al4V) substrate using Rofin Sinar 3.0 KW Ytterbium fibre laser system. The reinforcement titanium alloy (Ti6Al4V) and boron carbide (B_4C) ceramic powder were employed to deposit Ti6Al4V- B_4C composite coatings on Ti6Al4V substrate. The microstructural evaluation, geometrical analysis, porosity analysis, microhardness profiling and the wear characteristics of laser clad composite coatings were investigated. Samples from the as-deposited laser clad composite coatings were characterized using optical microscopy (OM), scanning electron microscopy (SEM) with energy dispersive spectroscopy (EDS) and x-ray diffraction (XRD). Both geometrical and porosity analyses were carried out to investigate the rate of dilution and defects such as porosity and cracks on the deposited composite coatings. Furthermore, performance characteristics were investigated using microhardness tester and CETRUMT-2 tribometer for the wear test analysis of the laser clad composite coatings of Ti6Al4V- B_4C composite coatings.

This research work is also aimed to establish process parameters that will result in defect-free composite coatings. The microstructure of the Ti6Al4V- B_4C composite coatings revealed a pore and crack free clad when observed at laser power of 2200 W. The SEM analysis revealed that there is uniform distribution of the ceramic particles in the titanium matrix at higher laser power. The geometrical analysis of the samples revealed that the aspect ratio (AR) and the dilution (D) increases with an increase in the laser power. The results obtained further revealed the dilution of approximately between 34% and 46% with aspect ratio between 2.16 and 3.58 were the best in terms of defectology for the combined with acceptable geometrical characteristics. The EDS and the XRD results revealed that there is a relationship between intermetallic phase of $\alpha+\beta$ titanium alloy and boron carbide in which certain amount of peaks between 40.69° and 71.57° were observed in most of the samples. The hardness of the composite coatings ranged between 371 and 471 Hv. Improvement in the hardness property was however achieved in the laser clad composite coatings when compared to the substrate with approximately 360 Hv. The wear results revealed that the sample produced at a laser power of 1800 W has the lowest wear depth of 74.6 μm while the sample produced at a laser power of 2200 W has the highest wear depth of 646.3 μm . Furthermore, both the wear volume and the wear rate were characterized by irregular pattern of increase and decrease behaviour. Sample produced at a laser power of 800 W has the lowest wear volume and rate with $35.2 \times 10^{-3} \text{ mm}^3$ and $6.42 \times 10^{-4} \text{ mm}^3/\text{Nm}$ respectively, while sample at 2000 W experienced the highest


wear volume and rate with $93.3 \times 10^{-3} \text{ mm}^3$ and $2.62 \times 10^{-3} \text{ mm}^3/\text{Nm}$ respectively. Friction coefficient values for the wear test revealed that the Coefficient of Friction (COF) for the samples is between 0.5 and 0.56. The laser cladded composites with the lowest COF is characterized with fair resistance to wear damage.



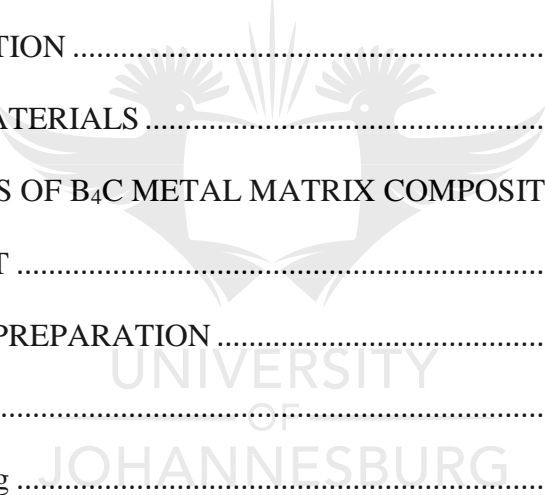
TABLE OF CONTENTS

DECLARATION.....	i
ACKNOWLEDGEMENTS	ii
ABSTRACT	iii
TABLE OF CONTENTS	v
LIST OF FIGURES	x
LIST OF TABLES	xiv
GLOSSARY OF TERMS.....	xv
LIST OF SYMBOLS.....	xx
ABBREVIATIONS	xxi
CHAPTER ONE.....	1
INTRODUCTION	1
1.0 BACKGROUND	1
1.1 BRIEF REVIEW.....	3
1.2 PROBLEM STATEMENT.....	6
1.3 HYPOTHESIS STATEMENT	7
1.4 METHODOLOGY	7
1.5 RESEARCH OBJECTIVES	8
1.6 SIGNIFICANCE OF RESEARCH.....	8
1.7 OVERVIEW OF DISSERTATION	9
1.8 SUMMARY.....	10
CHAPTER TWO.....	11
LITERATURE REVIEW	11
2.0 INTRODUCTION	11


2.1	METAL MATRIX COMPOSITES (MMCs).....	13
2.1.1	Material Selection for Metal Matrix Composites (MMCs).....	18
2.1.2	Reinforcement Selection.....	19
2.1.3	Metal Matrix Selection.....	21
2.2	TITANIUM MATRIX COMPOSITES (TMCs).....	21
2.2.1	Boron Compounds as Reinforcements for TMCs.....	26
2.2.2	Titanium Monoboride (TiB).....	27
2.2.3	Titanium Diboride (TiB ₂).....	29
2.2.4	Titanium Carbide (TiC).....	32
2.2.5	Titanium-Aluminium-Vanadium alloy (Ti-6Al-4V).....	34
2.2.6	Boron Carbide with Titanium (B ₄ C – Ti) Composites.....	37
2.3	PROCESSING OF TITANIUM MATRIX COMPOSITES (TMCs).....	38
2.3.1	Mechanical Alloying (MA).....	39
2.3.2	Powder Metallurgy (PM).....	41
2.3.3	Laser Additive Manufacturing (LAM).....	42
2.3.4	Reactive Hot Pressing (RHP).....	48
2.3.5	Rapid Solidification Processing (RSP).....	49
2.3.6	Self-Propagating High-temperature Synthesis (SHS).....	49
2.3.7	Exothermic Dispersion (XD) Process.....	51
2.3.8	Chemical Vapour Deposition (CVD).....	52
2.4	THERMODYNAMICS OF IN SITU REACTION SYSTEM.....	52
2.4.1	Ti – C System.....	53
2.4.2	Ti – B and Ti – TiB ₂ System.....	53
2.4.3	Ti – B ₄ C System.....	54
2.4.4	Ti –TiC/Ti - B ₄ C system.....	56



2.5	MECHANICAL PROPERTIES OF IN-SITU TMCs	56
2.6	MICROSTRUCTURAL CHARACTERISTICS OF IN-SITU TMCs.....	60
2.6.1	Morphology, size and distribution of in-situ reinforcements in Ti – based Composites	62
2.6.2	Factor affecting particle size and morphology	63
2.7	MICROHARDNESS CHARACTERIZATION OF CLADDED TMCs	64
2.8	WEAR CHARACTERISTICS OF CLADDED TMCs.....	66
2.9	SUMMARY.....	69
CHAPTER THREE		70
EXPERIMENTAL PROCEDURE.....		70
3.1	INTRODUCTION	70
3.2	PARENT MATERIALS	70
3.3	PROPERTIES OF B ₄ C METAL MATRIX COMPOSITES.....	71
3.4	EQUIPMENT	71
3.5	SPECIMEN PREPARATION	73
3.5.1	Cutting	74
3.5.2	Mounting	76
3.5.3	Grinding and Polishing.....	77
3.5.4	Etching.....	79
3.6	MIXING OF Ti6Al4V-B ₄ C POWDER	81
3.7	CHARACTERIZATION OF LASER PRERARED SAMPLES	83
3.7.1	Scanning Electron Microscopy (SEM).....	84
3.7.2	X-Ray Diffraction (XRD).....	85
3.7.3	Optical Microscopy	86
3.8	MICROHARDNESS PROFILING	88



3.9 WEAR ANALYSIS	89
3.10 SUMMARY	90
CHAPTER FOUR	91
RESULTS AND DISCUSSION.....	91
4.1 INTRODUCTION	91
4.2 PHYSICAL APPEARANCES OF DEPOSITIONS.....	91
4.3 GEOMETRICAL ANALYSIS AND CHARACTERIZATION	93
4.4 MICROSTRUCTURAL EVALUATION	99
4.4.1 Microstructural Characterization.....	101
4.4.2 Porosity Analysis and Characterization.....	112
4.4.3 Scanning Electron Microscopy (SEM) Analysis.....	115
4.4.4 X-Ray Diffraction (XRD) Analysis.....	123
4.5 MICROHARDNESS PROFILING	128
4.6 WEAR CHARACTERIZATION	129
4.6.1 SEM characterization of wear track	129
4.6.2 Dry Wear Characteristics of the Deposited Coatings.....	134
4.7 SUMMARY.....	138
CHAPTER FIVE.....	139
CONCLUSIONS AND FUTURE WORK.....	139
5.1 INTRODUCTION	139
5.2 CONCLUSIONS	140
5.3 FUTURE WORK.....	142
REFERENCES	145
APPENDIX A	156
PROERTIES OF BORON CARBIDE (B ₄ C) POWDER AS-RECEIVED.....	156



APPENDIX B.....	161
GEOMETRICAL MEASUREMENT OF LASER CLAD DEPOSITIONS.....	161
APPENDIX C.....	163
POROSITY ANALYSIS OF LASER CLAD DEPOSITIONS	163
APPENDIX D	164
SEM AND EDS ANALYSIS OF LASER CLAD SAMPLES	164
D1. SEM of the deposited clad samples	164
D2. EDS of the deposited clad samples.....	165
APPENDIX E.....	167
XRD ANALYSIS OF LASER CLAD SAMPLES	167
APPENDIX F.....	169
WEAR ANALYSIS OF LASER CLAD SAMPLES.....	169
APPENDIX G	170
WEAR TRACK MEASUREMENT ANALYSIS AND VARIABLE EVALUATION.....	170



LIST OF FIGURES

CHAPTER 2

Figure 2. 1: Ti-B phase diagram [1].....	27
Figure 2. 2: Ti-C phase diagram [1].....	33
Figure 2. 3: Crystal structure of titanium (a) α -titanium phase, HCP; (b) β -titanium phase, BCC [20, 22].....	35
Figure 2. 4: Schematic of laser cladding process [50].....	46
Figure 2. 5: A typical cross section of a single clad bead [22].....	47
Figure 2. 6: The change of Gibbs free energy ΔG as a function of temperature for reaction equation 2.2, 2.3 and 2.4 [1].....	54
Figure 2. 7: Change of Gibbs free energy ΔG as a function of temperature for reactions of equation 2.5 and 2.6 [1].....	55
Figure 2. 8: Variation of compressive yield strength with temperature for 15 vol.% TiB/Ti and 15 vol.% (TiB+TiC)/Ti composites and unreinforced Ti [4].....	58
Figure 2. 9: Variation of steady-state creep rate with applied stress for unreinforced Ti (solid symbol) and 25 vol.% Ti ₂ C/Ti composite (open symbol) [1].....	59

CHAPTER 3

Figure 3. 1: Laser metal deposition machine connected to kuka robot with coaxial nozzle; Courtesy CSIR, Pretoria.....	72
Figure 3. 2: Powder mixer analyser connected with hoppers; Courtesy CSIR, Pretoria.	73
Figure 3. 3: Sandblasting machine; Courtesy National Laser Centre CSIR, Pretoria.	74
Figure 3. 4: Schematic view of cutting machine.....	75
Figure 3. 5: Schematic view of a hot mounting press.....	76

Figure 3. 6: Schematic view of hot mounted samples	77
Figure 3. 7: Schematic view of an automatic polishing machine with two rotating discs.....	78
Figure 3. 8: (a) deposition of melt pool on the surface of titanium alloy substrate, (b) single track deposition and (c) multiple track deposition.....	83
Figure 3. 9: Schematic view of scanning electron microscopy with energy dispersion spectroscopy.....	85
Figure 3. 10: Schematic view of x-ray diffraction machine	86
Figure 3. 11: Optical Microscope, courtesy Olympus BX51M.....	87
Figure 3. 12: Digital Microhardness Tester	89
Figure 3. 13: Schematic view of CETRUMT-2 Tribometer.....	90
 CHAPTER 4	
Figure 4. 1: The photograph of single track laser metal deposited samples S1-S9 on the substrate	92
Figure 4. 2: The photograph of multiple track laser metal deposition of samples S1, S5 and S9	93
Figure 4. 3: Schematic view of cross section morphology of a single laser clad track showing main geometrical quantities [73]	94
Figure 4. 4: Optical micrographs showed geometrical measurement for different composites	95
Figure 4. 5: Dilution ratio of B ₄ C-Ti6Al4V single clad track composite coatings.....	99
Figure 4. 6: (a) Optical microstructure of the substrate, (b), (c) and (d) Macrographs of B ₄ C-Ti6Al4V composites deposited with laser power of 800 W, 1000 W and 1200 W.....	101
Figure 4. 7: Optical micrographs of laser deposited Ti6Al4V-B ₄ C composites deposited at varying laser powers, (a) 2000 W; (b) 2200 W; (c) 2400 W	102



Figure 4. 8: Optical micrographs of B ₄ C-Ti6Al4V composite deposited at 1800 W laser power.....	103
Figure 4. 9: Optical micrographs of B ₄ C-Ti6Al4V composite deposited at 2000 W laser power.....	105
Figure 4. 10: Optical micrographs of B ₄ C-Ti6Al4V composite deposited at 2200 W laser power.....	107
Figure 4. 11: Optical micrographs of B ₄ C-Ti6Al4V composite deposited at 2400 W laser power.....	111
Figure 4. 12: Micrographs of samples (S4 and S6) at (a) 1400 W laser power, (b) 1800 W laser power	113
Figure 4. 13: Micrographs of sample 4 and 6 (S4 and S6) at high magnification with laser power of (a) 1400 W and (b) 1800 W	113
Figure 4. 14: Micrograph of Ti6Al4V-B ₄ C composite of sample S8 at laser power of 2200 W	114
Figure 4. 15: The Figure shown illustrates the variation of average porosity and maximum pore size of composites for different samples.....	115
Figure 4. 16: SEM micrographs of B ₄ C-Ti6Al4V composite at laser power of 800 W at low and high magnification	116
Figure 4. 17: SEM micrographs of B ₄ C-Ti6Al4V composite at laser power of 1000 W at low and high magnification	116
Figure 4. 18: SEM micrographs of B ₄ C-Ti6Al4V composite at laser power of 2000 W at low and high magnification	117
Figure 4. 19: SEM micrographs of B ₄ C-Ti6Al4V composite at laser power of 2200 W at low and high magnification	117
Figure 4. 20: SEM micrograph showing backscattered morphology of B ₄ C-Ti6Al4V composite at laser power of 2200 W at magnification of 677 x	118



Figure 4. 21: SEM micrographs of B ₄ C-Ti6Al4V composite at laser power of 2400 W at low and high magnification	118
Figure 4. 22: The SEM images and EDS spectrum of B ₄ C-Ti6Al4V composite at 800 W laser power.....	119
Figure 4. 23: The SEM image and EDS spectrum of B ₄ C-Ti6Al4V composite at 1000 W laser power.....	120
Figure 4. 24: The SEM image and EDS spectrum of B ₄ C-Ti6Al4V composite at 1400 W laser power.....	120
Figure 4. 25: The SEM image and EDS spectrum of B ₄ C-Ti6Al4V composite at 2000 W laser power.....	121
Figure 4. 26: The SEM images and EDS spectrum of B ₄ C-Ti6Al4V composite at 2200 W laser power	122
Figure 4. 27: The SEM image and EDS spectrum of B ₄ C-Ti6Al4V composite at 2400 W laser power.....	122
Figure 4. 28: x-ray diffraction (XRD) patterns of sample S1, S6, S8 and S9 at laser power 800 W, 1800 W, 2200 W and 2400 W respectively	125
Figure 4. 29: Average Vickers microhardness profiles of the deposited composites.....	128
Figure 4. 30: The SEM images of wear scar on the deposited B ₄ C-Ti6Al4V composite flat that was worn against a tungsten carbide, WC ball; (a) sample S1 at laser power of 800W, (b) sample S2 at laser power of 1000 W, (c) sample S3 at laser power of 1200 W, (d) sample S7 at laser power of 2000 W, (e) sample S8 at laser power of 2200 W and (f) sample S9 at laser power of 2400 W	130
Figure 4. 31: Multiple bar charts of the wear depth, width, stroke length, wear volume and wear rate for the deposited composites samples	133
Figure 4. 32: Friction coefficients (COF) of deposited composites coatings versus time taken at constant normal load of 25N and 5mm/s speed under varying laser power of samples in a dry condition	137

LIST OF TABLES

CHAPTER 2

Table 2. 1 Properties and typical applications of wrought titanium alloys (Source: Types of material, IE 351 lecture 3, page 26) [12], accessed August 2014..... 16

Table 2. 2 Properties of ceramic reinforcements commonly used in metal matrix composites (MMCs) [1].....20

Table 2. 3 Properties of ceramic reinforcements commonly used in TMCs [1].....25

Table 2. 4 Apparent stress exponent and apparent activation energy for creep of composites titanium matrix composites (TMCs) and unreinforced titanium, Ti [1, 4]60

CHAPTER 3

Table 3. 1 commonly used etchants for metals and alloys [61].....80

Table 3. 2 Experimental matrix for the laser metal deposition.....81

Table 3. 3 Powders with respective mixing proportion82

CHAPTER 4

Table 4. 1: Processing parameters and geometrical quantities of single laser tracks96

Table 4. 2: Average percentage porosity and maximum pore size of various samples 114

Table 4. 3: Phase analysis 126



GLOSSARY OF TERMS

A

- **Alloy** – A substance having metallic properties and being composed of two or more chemical elements, of which at least one is a metal.
- **Alloying element** – An element added to and remaining in metal, which changes its structure and properties.

B

- **Body Centred Cube** – The body centred cube unit is a cube with an atom at each corner of the unit cell, and an atom in the centre of the unit cell.
- **Brittleness** – The tendency of a material to fracture without first undergoing significant plastic deformation.
- **Brittle fracture** – Rapid fracture preceded by little or no plastic deformation.

C

- **Coalescence** – The merging of two or more materials (metals) into one.

D

- **Defect** - A discontinuity or discontinuities that accumulate to render a weld or part unable to meet minimum acceptance standards or criteria of the design specifications.
- **Deformation** – This is a change in the form of a body due to stress, thermal, or other causes.
- **Diffraction** - The scattering of electrons by any crystalline material, through discrete angles depending only on the lattice spacing of the material and the velocity of the electrons.
- **Ductility** - The ability of a material to deform plastically before fracture.

- **Dwell time** - The period of time after the rotating tool has been plunged into the work and for which it remains stationary, generating frictional heat and plasticizing the materials, before commencing the traverse along the joint (seconds).

E

- **Etchant** - A chemical solution used to etch a metal to reveal structural details.
- **Etching** – This involves subjecting the surface of a metal to preferential chemical or electrolytic attack to reveal structural details for metallographic examination.

F

- **Face Centred Cube** - This is a crystal system where atoms are arranged at the corners and centre of each cube face of the cell.
- **Fusion** - The melting together of filler metal and base metal, or of base metal only, which results in coalescence.
- **Friction** -The force required to cause one body in contact with another to begin to move.

G

- **Grain** - An individual crystallite in metals.
- **Grain growth** - This is a phenomenon which occurs when the temperature of a metal is raised, the grains begin to grow and their size may eventually exceed the original grain size.
- **Grain size** - A measure of the areas or volumes of grains in a polycrystalline metal or alloy, usually expressed as an average when the individual sizes are fairly uniform. Grain size is reported in terms of number of grains per unit area or volume, average diameter, or as a number derived from area measurements.
- **Grain boundary** – This is an interface separating two grains, where the orientation of the lattice changes from that of one grain to that of the other. When the orientation

change is very small, the boundary is sometimes referred to as a sub-boundary structure.

- **Grinding** – This involves the removing material from the surface of a work piece by using a grinding wheel or abrasive grinding papers.

H

- **Hardness** - A term used for describing the resistance of a material to plastic deformation.
- **Hardness test** – It measures the resistance of a material to penetration by a sharp object.
- **Heat-Affected Zone** - The portion of the base metal which has not been melted, but whose mechanical properties have been altered by the heat of welding or cutting.
- **Homogeneous** - A chemical composition and physical state of any physical small portion, and that is the same as that of any other portion.

I

- **Indentation hardness** - This is the hardness, as evaluated from the measurements of an area of an indentation made by pressing a specified indenter into the surface of a material under specified static loading conditions.
- **Intensity (X-rays)** - The energy per unit time of a beam per unit area perpendicular to the direction of propagation.
- **Intermetallic bonding** – This is a bond in any solid materials or powders, composed of two or more metal atoms in a definite proportion, which have a definite structure which differs from those of its constituent metals.

M

- **Macrograph** - A graphic reproduction of a prepared surface of a specimen at a magnification not exceeding 25x.

- **Macrostructure** - The structure of metals as revealed by macroscopic examination of the etched surface of a polished specimen.
- **Magnification** - The ratio of the length of a line in the image plane to the length of a line on the imaged material.
- **Mechanical properties** - The properties of a material that reveal its elastic or inelastic behaviour when force is applied, indicating the suitable mechanical applications.
- **Mechanical testing** - The determination of mechanical properties.
- **Metallurgy** - The science and technology of metals and their alloys including methods of extraction and use.
- **Microstructure** - The structure of a prepared surface of a metal, as revealed by a microscope at a particular magnification.

O

- **Oxidation** - The addition of oxygen to a compound.

P

- **Parameter** - The minimum and maximum parameters that will describe the operating range of a variable.
- **Parent material** - This is the sheet-metal plate in its as manufactured form, as supplied.
- **Polished surface** - A surface that reflects a large proportion of the incident light in a peculiar manner.
- **Porosity** - A rounded or elongated cavity formed by gas entrapment during cool down or solidification.

R

- **Recrystallization** - A change from one crystal structure to another, such as that occurring upon heating and / or cooling through a critical temperature.
- **Residual stress** – The stress in a body which is at rest, in equilibrium, and at uniform temperature in the absence of any external force.



S

- **Scanning Electron Microscope** - An electron microscope in which the image is formed by a beam operating simultaneously with an electron probe scanning the object.

T

- **Tensile strength** - The maximum tensile stress which a material is capable of sustaining. Tensile strength is calculated from the maximum load during a tension test carried out to rupture, and the original cross-sectional area of the specimen.
- **Tensile test** - Measures the response of a material to a slowly applied axial force. The yield strength, tensile strength, modulus of elasticity and ductility are obtained.

V

- **Vickers hardness number** - A number related to the applied load and the surface area of the permanent impression made by a square-based pyramid diamond indenter.



LIST OF SYMBOLS

D	Dilution (%)
AR	Aspect Ratio (No unit)
H	Clad height (μm)
W	Clad width (μm)
Ac	Clad area (μm)
Am	Molten area (μm)
V_f	wear volume (mm^3)
s	sliding distance (μm)
h_f	wear depth (μm)
R_f	wear track radius (μm)
Ls	stroke length (μm)
F_N	normal load (N)
K	wear rate (mm^3/Nm)



ABBREVIATIONS

AM	- Additive Manufacturing
ASTM	- American Society for Testing and Materials
BCC	- Body Centred Cubic
BE	- Blended Elemental
CAC	- Combustion Assisted Casting
CAD	- Computer Aided Design
CMC	- Ceramic Matrix Composite
COF	- Coefficient of Friction
CP	- Commercially Pure
CTE	- Coefficient of Thermal Expansion
CVD	- Chemical Vapour Deposition
DLF	- Direct Laser Fabrication
DMD	- Direct Metal Deposition
DRTMC	- Discontinuous Reinforced Titanium Matrix Composite
EDM	- Electrical Discharge Machining
EDS	- Energy Dispersion Spectroscopy
FEA	- Finite Element Analysis
FRP	- Fibre Reinforced Polymers
FZ	- Fusion Zone
HAZ	- Heat Affected Zone
HCP	- Hexagonal Closed Packed
HIP	- Hot Isostatic Pressing
IM	- Ingot Metallurgy
LAM	- Laser Additive Manufacturing
LENS	- Laser Engineered Net Shaping
LMD	- Laser Metal Deposition
LPD	- Laser Powder Deposition
LSC	- Laser Surface Cladding
MA	- Mechanical Alloying
MACC	- Minimum Area of Contact Cutting



MMC	- Metal Matrix Composite
OM	- Optical Microscope
PA	- Pre-Alloyed
PAMCA	- Plasma Arc Melting with Centrifugal Atomization
PIRAC	- Powder Immersion Reaction Assisted Coating
PM	- Powder Metallurgy
PMC	- Polymer Matrix Composite
PVD	- Physical Vapour Deposition
RHP	- Reactive Hot Pressing
RSP	- Rapid Solidification Processing
SEM	- Scanning Electron Microscope
SHS	- Self-Propagating High-Temperature Synthesis
TMC	- Titanium Matrix Composite
TPPP	- Transient Plastic Phase Processing
UTS	- Ultimate Tensile Strength
XD	- Exothermic Dispersion
XRD	- X-Ray Diffraction



CHAPTER ONE

INTRODUCTION

1.0 BACKGROUND

The subject of this thesis is to research the possibility of enhancing the microstructural and mechanical properties through the characterization analyses of both laser deposited titanium alloy (grade 5) and boron carbide using the processing parameters. The properties to be characterized are hardness, wear, and corrosion and however manipulating the microstructure of titanium alloy, Ti6Al4V with boron carbide, B₄C materials by the application of laser additive manufacturing (LAM) processing and thereby improving the material's mechanical properties. Titanium and its alloys are used for highly demanding applications such as in the fabrication of some of the most critical and highly-stressed civilian and military aircraft parts, chemical processing, automobile industries, nuclear power plants, food processing plants and oil refinery heat exchangers. This wide range of applications have been attributed to its excellent properties such as low density, high specific strength, heat resistance, corrosion resistance, low temperature resistance and excellent biocompatibility. However, the applications of titanium and titanium alloys to other fields are limited by several other shortcomings that include poor plastic deformation, low modulus, high friction coefficient, low thermal conductivity coefficient and low wear resistance, and in addition is high cost of production.

Suggestions have been made that the physical and mechanical properties of titanium can be improved through the incorporation of reinforcing compounds using the principle of metal matrix composites (MMCs). This is because MMCs combine the properties of ceramics and metals to produce materials with attractive properties like good shear strength, high temperature strength etc. However, titanium matrix composites (TMCs) were identified as the best form of MMCs that can provide the best combination of high specific strength, rigidity, corrosion resistance, and good wear resistance required for drastic enhancement of titanium and titanium alloy's physical and mechanical properties. Titanium matrix composites (TMCs) also face challenges that include the selection of an ideal reinforcement, as well as high performance processing methods.



Among the existing reinforcements, titanium monoboride (TiB) has been judged the best compared to the existing reinforcing compounds like TiC, SiC, TiB₂, B₄C, Al₃O₄, TiN, and Si₃N₄ because of its outstanding physical and mechanical properties with linear coefficient of thermal expansion that is approximately the same as that of titanium alloys. However, boron carbide, B₄C powder is a promising reinforcement ceramic material of Ti and Ti alloys for a variety of applications that require elevated hardness, good wear and corrosion resistance and above all, it is a good source for TiB, TiB₂ and TiC particulate for reinforcing titanium matrix. Therefore, the introduction of B₄C powder would lead to a reasonable cost reduction in comparison to using commercial TiB and TiC powder separately to reinforce titanium matrix [1].

Boron carbide, which has a high melting point, outstanding hardness, good mechanical properties, low specific weight and great resistance to chemical agents, is currently used in high-technology industries fast-breeders, lightweight armours and high-temperature thermoelectric conversion. In the group of the most important non-metallic hard materials (alumina, silicon carbide, silicon nitride, diamond or cubic boron nitride), boron carbide occupies a specific place. A boron carbide compound was discovered in 1858, and then Joly in 1883 and Moissan in 1894. These compounds were prepared and identified as B₃C and B₆C, respectively. The 'stoichiometric formula' B₄C was only assigned in 1934, and then many diverse formulae were proposed by the Russian authors. After 1950, numerous studies were carried out, especially concerning structures and properties of boron carbide [2].

Nevertheless, owing to the poor tribological resistance and being prone to galling, the applications of titanium alloys under severe wear conditions are highly restricted. In addition, titanium alloys present limited high temperature oxidation resistance because of their high affinity towards oxygen at elevated temperature in air. Surface treatments can effectively improve the properties of titanium alloys.

Of all the surface treatment techniques, laser treatments are widely used in surface modification of many kinds of metals. Laser treatments have several advantages over commonly used heat treatment techniques, including precise control over the width and depth

of processing, the ability to selectively process specific areas of a component, and the ability to process complex parts. The researches of laser alloying of titanium alloys to improve their wear and oxidation resistance have been performed previously with fabricated coatings containing TiN, Ti₂AlN and Ti₂N compounds on the surface of pure titanium by laser alloying with aluminium powder in a nitrogen atmosphere [3].

The results of laser alloying pure titanium with powder mixtures of silicon and aluminium showed that the laser treated samples were much more resistant to oxidation than the untreated titanium. The tests carried out after the application of laser nitriding to Ti6Al4V showed that the wear resistance of the treated samples was enhanced. The results of laser alloying of powder mixtures of (Mo) Molybdenum and WC (Tungsten Carbide) on the surface of Ti6Al4V alloy indicated that the sliding wear resistance of the coatings was five times higher than that of the original Ti6Al4V alloy. However, the investigations of laser boronizing of titanium alloys have been seldom reported. As known, titanium borides have very high hardness, excellent wear resistance, and high stability at elevated temperature [3]. The aim of this work is to identify the characteristics of titanium alloy with boron carbide metal matrix composites (MMCs) by a laser alloying technique and to investigate the microstructure, microhardness and wear resistance through additive manufacturing process.

1.1 BRIEF REVIEW

Considering this section which reviews the available research works that has been done in the area of investigating and experimenting the characteristics of titanium and its alloys using the principle of metal matrix composite (MMC). Metal matrix composites (MMCs) refer to a kind of synthesized material in which rigid ceramics reinforcement is embedded in a ductile metal or alloy matrix. The synthesized material combines the excellent properties of ceramics (high strength and modulus) and metals (ductility and toughness), leading to a greater strength in shear and compression and to higher service temperature capabilities [4, 5]. Tjong et al. [4] reported extensively on the attractive physical and mechanical properties such as high specific modulus, strength, and thermal stability and others that can be achieved with MMCs.

The interest in MMCs, for use in aerospace, automotive and other structural applications has increased over the past 25 years and this has been attributed to the availability of relatively

inexpensive reinforcements, and development of various processing routes which result in reproducible microstructures and properties [4]. A good advantage of MMC as it affects the aerospace industry is reduction in structural weight; this can be achieved not only by reducing the alloy density but also by increasing its modulus. For instance, a 50% increase in modulus through substitution of a discontinuous silicon carbide reinforced aluminium alloy for an unreinforced wrought counterpart resulted in a 10% reduction in weight [1, 4].

Titanium matrix composites (TMCs) are advanced materials made of titanium or titanium alloy matrices mixed either with continuous or discontinuous reinforcements. They exhibit several excellent properties such as corrosion resistance, high specific strength, high specific modulus, heat resistance etc. [6]. There are two families of titanium matrix composites, continuously reinforced and discontinuously reinforced TMCs [7]. The early work on titanium matrix composites considered continuous fibre reinforced composites and the industrial use of the composites produced was restricted to highly specialized applications. The reasons attributed were prohibitive cost of continuous fibres, complex fabrication routes, limited formability and high anisotropic properties of composites produced. Discontinuously reinforced (particulate) TMCs have attracted more attention compared to continuous fibre reinforced composites. This is because of their properties of isotropy, easy secondary operation, improved mechanical properties and economic benefits. Typical applications for discontinuous or particulate titanium matrix composites include:

- Creep resistant engine components,
- Wear parts such as gears, bearings and shafts,
- Erosion-corrosion resistant tubing.

Following the significance of titanium matrix composites in engineering applications, several reinforced materials have been examined but boron carbide-titanium (B₄C-Ti) composites proved to be one of the widely used in the manufacturing industries. Boron carbide is an extremely promising material for a variety of applications that require elevated hardness, good wear and corrosion resistance [7]. Application of boron carbide, B₄C in the highlighted areas is due to its excellent properties that include high hardness, high wear resistance, high melting point and high thermal conductivity.

This material is reported as the third hardest (after diamond and cubic boron nitride) of the technically useful materials. Boron carbide, B₄C currently finds application in the nuclear industry and high-temperature thermo-electric conversion but there is restriction to its wide industrial application because of low strength (about 200-400 MPa), low fracture toughness (2-3 MPa/m^{0.5}), as well as poor sinterability that results from its low self-diffusion coefficient. However, several B₄C based composites, such as B₄C-SiC, B₄C-Al, B₄C-CrB₂, B₄C-(W, Ti) C, B₄C-TiB₂ etc., have been developed and used in various applications.

Recent research focuses more attention on the use of Ti and B₄C powder in the manufacturing of in situ TMCs. This is because of the excellent and unique properties exhibited by reinforced particulate TMCs produced when combined reinforcement of particles of TiB and TiC is used, and the possibility of obtaining both reinforcements simultaneously from the reaction of B₄C and Ti powders. However few works have been reported using Ti-B₄C systems.

The aim of this research and experimental study is to add boron carbide, B₄C metal matrix composites to a titanium alloy, (Ti6Al4V) matrices from a starting powder mixture of the two single phase constituents. In addition to enhanced strength arising from the presence of the B₄C matrix, there occurs an increase in fracture toughness and an overall enhancement in cracking resistance of the Ti6Al4V-B₄C composites.

Thus the variable used to assess the strengthening effect of these composite's microstructure is the content of titanium, aluminium, vanadium, in the Ti6Al4V alloy. However, this study will examine the influence of B₄C on microstructural development and microhardness of the laser deposited Ti6Al4V-B₄C composites and thereby making reference to the improved properties.

1.2 PROBLEM STATEMENT

Components used in many engineering applications, especially in the aerospace and automobile industries and defence, are required to meet certain property requirements, such as possession of a certain specific strength, elastic modulus, toughness, etc. Conventional metallic materials rarely meet such requirements. However, recent advancements in the field of metal matrix composites have overcome this difficulty, and many metal matrix composites developed in recent years have the characteristics to meet various combinations of property requirements.

Titanium-based composites constitute an important group of such metal matrix composites. Though, titanium-based composites are mostly used for aerospace applications, but are finding increasing use in other applications such as in the fabrication of automotive components and consumer utilities. Titanium alloy-based composites possess several advantageous properties such as high specific modulus, high specific strength, good corrosion resistance and good wear resistance. Various reinforcements are used in titanium alloy as required composites.

The incorporation of reinforcements such as SiC or Al₂O₃ leads to the formation of undesirable reaction products, which act as major barriers to the development of viable titanium composites. However, titanium alloy, Ti6Al4V with B₄C is well suited for use as reinforcement due to the presence of microstructural and mechanical properties involved. Moreover, B₄C reinforcement has certain desirable characteristics such as high elastic modulus, good thermal stability at high temperature and a density nearly equal to that of titanium.

Many research studies on the processing of TiB₂-B₄C composites using many techniques such as solidification, rapid solidification, combustion synthesis and laser cladding have been reported. In all of these techniques, B₄C reinforcement is developed either by an in situ method or by the addition of ceramic particles of B₄C [1]. Fibre-reinforced composites involve the addition of costly fibres and intricate processing steps. However, in situ composites are created using simpler fabrication steps and hence are more cost effective than fibre reinforced composites. Additionally, in situ titanium alloying with matrix composites

overcome the shortcomings associated with the casting process, such as the pollution of reinforcements and the wettability between ceramic particles and a matrix.

Considerable research study will be carried out to understand the mechanical properties of Ti6Al4V-B₄C composites with respect to hardness, wear and the elastic properties of the composites. Therefore the purpose of this research is to carry out the experimental procedures on the characteristics of titanium alloy with boron carbide metal matrix composites and to analyse the probable behaviours like microstructure, microhardness, wear and how the composites adjust to high temperature applications. Hence, the parent material, Ti6Al4V-B₄C composite will undergo characterization as a case study because titanium alloy composites are of interest in many applications due to their multi-functionality deriving from their unique combinations of properties and their application in automobile and aerospace industries.

1.3 HYPOTHESIS STATEMENT

Titanium and its alloys, due to their intrinsic properties such as high specific strength, good oxidation and corrosion resistance, are extensively used in the aeronautical, marine and chemical industries. Metal matrix composites of titanium alloy and boron carbide will be produced through laser metal deposition process by varying the process parameters such as the laser power. It is expected that the optimum processing parameters will result in composites with good characteristic properties that will impact positively on wear behaviour, the microstructure, microhardness and its profiles.

1.4 METHODOLOGY

Varying these process parameters will influence the properties stated in the hypothesis. Establishing these relationships will enable the control of the process to achieve a desirable outcome or finished products of the titanium alloy and boron carbide composite which is an important material in chemical processing, automobile industries, nuclear power plants, food processing plants and oil refinery heat exchangers. However, in the process parameter used, the laser power was varied between 800 W and 2400 W while other parameters such as the scanning speed, the powder flow rate and the gas flow rate were kept constant throughout the experiment.

1.5 RESEARCH OBJECTIVES

The aim and objective of this research study is given as follows:

- Investigate the characteristics and mechanical behaviour of titanium alloy with reinforcement composites through a comprehensive experimental procedure as starting material for the production of reinforced titanium matrix composites using a powder metallurgy processing method with laser metal deposition (LMD).
- Also, to develop models from laser metal deposition (LMD) process parameters for the manufacture of a range of titanium alloy with boron carbide composites for various applications.

1.6 SIGNIFICANCE OF RESEARCH

Titanium alloy with boron carbide metal matrix composites offers various characteristic properties which helps in improving the modern industrialization of manufacturing industries. Amongst these various characteristics are the microstructure, microhardness, wear behaviour and the high temperature application of titanium matrix composites. Thus, hardness is the property of a material that enables it to resist plastic deformation, penetration, indentation, and scratching. Therefore, hardness is important from an engineering point of view because resistance to wear by either friction or erosion, by steam, oil, and water generally increases with hardness. Hardness of a metal depends on relative density, interstitial content and grain size. The superior specific strength and corrosion resistance of titanium and its alloys over many commonly available ferrous- and non-ferrous-based metals has drawn considerable attention to these materials within areas such as medical device manufacturing, automotive production, aerospace frame construction and armoured material fabrication.

The results of this research work will make information available to the manufacturing industry on the effect of these process parameters on manufactured part so that the life of the part can be extended. Furthermore, the results of this research will provide an experimental database of process parameters and an empirical model, a function of the interaction of the identified process parameters on material properties, from which required process parameters can be selected for required functional properties.

1.7 OVERVIEW OF DISSERTATION

This research study is aim to carry out experimental analysis on Titanium alloy, Ti6Al4V with Boron Carbide, B₄C. The dissertation has been structured into five chapters with all the set objectives covered. Each chapter starts with an introduction stating the contents of the chapter and ends with a summary. Furthermore, a list of references cited in the entire research work will be provided at the end of the thesis. Also, additional information are provided in the appendices section after the list of references. Thus, the dissertation overview is given as follows:

- Chapter 1 provides the introduction to the entire research work.
- Chapter 2 gives the details on review of literature on titanium alloy and different titanium matrix composites (TMCs) processes with focus on laser processing of Ti6Al4V with Boron Carbide, B₄C as reinforced material. However based on the reviews, research opportunities are identified and objectives formulated.
- Chapter 3 will provide information on various experimental procedures observed including deposition, material characterization and testing procedures employed to carry out the research work. Thus, deposition of Ti6Al4V and B₄C powders on a Ti6Al4V substrate through laser metal deposition (LMD) process will be carefully observed in order to identify suitable processing parameter ranges thereby determining the influence of laser processing parameters in which laser power will be the commanding parameter on the characteristics of beads/tracks and as well as efficiency of the deposition.
- Chapter 4 will present the results obtained from the experimental study of the samples to evaluate the microstructural, microhardness, wear and corrosion evolutions of the material for the laser metal deposition process and subsequent experimental analysis such as scanning electron microscopy (SEM), optical microscopy (OM) and energy dispersion spectroscopy (EDS) will then be presented in which the analysis of the experimental study with results follow. Also, the reports of the obtained results of laser deposition of Ti6Al4V reinforced with B₄C particles will be presented. This chapter however contains the discussion on the microstructural characterization of the composite deposits.

- Chapter 5 will provide the conclusions and as well as the recommendations on the entire research work with the results obtained. It also discussed on the areas of future work. However, a list of references follows and thereafter the appendix.

1.8 SUMMARY

Titanium alloy with boron carbide for the production of matrix composites through the process of laser metal additive is considered to be adopted in this research. However, the experimental analysis will focus into the characteristics of this titanium alloy with boron carbide metal matrix composites to be able to test and predict the best performance to the manufacturing industries in terms of wear and hardness.



CHAPTER TWO

LITERATURE REVIEW

2.0 INTRODUCTION

This section reviews the available research works that has been done in the area of improving the properties of titanium and its alloys using the principle of metal matrix composites (MMCs) with the application of laser additive manufacturing (LAM). However, composite materials are composed of at least two phases; a matrix phase and a reinforcement phase [1]. Matrix and reinforcement phase work together to produce combination of material properties that cannot be met by the conventional materials [1, 8]. In most of the composites, reinforcement is added to matrix and the bulk material to increase the strength and stiffness of the matrix. The most common composites can be divided into three main groups:

- **Polymer Matrix Composites (PMCs):** Polymer matrix composites are also known as Fibre Reinforced Polymers (FRP) or Plastics. These materials use a polymer-based resin as the matrix, and a variety of fibres such as glass, carbon and aramid as the reinforcement.
- **Metal Matrix Composites (MMCs):** Metal matrix composites are increasingly found in the aerospace and automotive industries. These materials use a metal such as aluminium as the matrix, and reinforce it with fibres, particulates or whiskers such as silicon carbide.
- **Ceramic Matrix Composites (CMCs):** Ceramic matrix composites are used in very high temperature environments. These materials use a ceramic as the matrix and reinforce it with short fibres, or whiskers such as those made from silicon carbide and boron nitride [8].

The reductions in material density or increases in stiffness, yield strength, ultimate tensile strength can be directly translated to reductions in structural weight. This led the aerospace industry to develop and examine new materials with combinations of low density, improved stiffness and high strength as attractive alternatives to existing high-strength aluminium alloys and titanium alloys. These high-strength metal matrix composites combine the high strength and hardness of reinforcing phase with ductility and toughness of light metals. Moreover, the need for improved design procedures has resulted from an attempt to achieve



significant improvement in structural efficiency, reliability and overall performance through reductions in either absolute weight or increases in strength-to-weight ratio. Recent research results have made it possible to imagine or visualize combining these effects through the development of reinforced lightweight alloys [8]. Metal-matrix composites, in general, consist of at least two components: one is the metal matrix and the second component is the reinforcement. In all cases the matrix is defined as a metal, but a pure metal is rarely used as the matrix, it is generally an alloy. The distinction of metal-matrix composites from other two or more phase alloys come about from the processing of the composite. In the production of the composite, the matrix and the reinforcement are mixed together. This is to distinguish a composite from a two or more, phase alloy, where the second phase forms as a particulate and a phase separation such as a eutectic or a eutectoid reaction occurs [8]. The metal-matrix composites offer a spectrum of advantages that are important for their selection and use as structural materials. A few such advantages include the combination of high strength, high elastic modulus, high toughness and impact resistance, low sensitivity to changes in temperature or thermal shock, high surface durability, low sensitivity to surface flaws, high electrical and thermal conductivity, minimum exposure to the potential problem of moisture absorption resulting in environmental degradation and improved fabricability with conventional metal working equipment [8]. Metal-matrix composite reinforcements can be generally divided into five major categories: (a) Continuous fibres (b) Discontinuous fibres (c) Whiskers (d) Wires (e) Particulates. With the exception of wires, which are metals, reinforcements are generally ceramics. Typically these ceramics are oxides, carbides and nitrides, which are used because of their excellent combinations of specific strength and stiffness at both ambient temperature and at elevated temperatures. Silicon carbide, boron carbide and aluminium oxide are the key particulate reinforcements and can be obtained in varying levels of purity and size distribution. Silicon carbide particulates are also produced as a by-product of the processes used to make whiskers of these materials [8].

The particulate-reinforced metal-matrix composites have emerged as attractive candidates for use in a spectrum of applications to include industrial, military and space-related. The renewed interest in metal-matrix composites has been aided by the development of reinforcement material, which provides either improved properties or reduced cost when compared with existing monolithic materials [8]. Due to the fact that composite materials constitute a significant proportion of the engineered materials market ranging from everyday

products to sophisticated suitable applications, they have already proven their worth as weight-saving materials. Thus increasingly enabled by the introduction of newer polymer resin matrix materials and high performance reinforcement fibres of glass, carbon and aramid, the penetration of these advanced materials has witnessed a steady expansion in uses and volume [9]. Furthermore, the need of composite for lighter construction materials and more seismic resistant structures has placed high emphasis on the use of new and advanced materials that not only decreases dead weight but also absorbs the shock and vibration through tailored microstructures. Composites are now extensively being used for strengthening of pre-existing structures that have to be retrofitted to make them seismic resistant, or to repair damage caused by seismic activity. Unlike conventional materials (e.g., steel), the properties of the composite material can be designed considering the structural aspects. The design of a structural component using composites involves both material and structural design. Composite properties (e.g. stiffness, thermal expansion etc.) can be varied continuously over a broad range of values under the control of the designer. Careful selection of reinforcement type enables finished product characteristics to be tailored to almost any specific engineering requirement. Whilst the use of composites will be a clear choice in many instances, material selection in others will depend on factors such as working lifetime requirements, number of items to be produced (run length), complexity of product shape, possible savings in assembly costs and on the experience and skills used by the designer in tapping the optimum potential of composites. In some instances, best results may be achieved through the use of composites in conjunction with traditional materials [9].

2.1 METAL MATRIX COMPOSITES (MMCs)

Metal Matrix Composites (MMCs) are increasingly found in the automotive industry. They consist of a metal such as aluminium as the matrix, and a reinforcement that could be continuous fibres such as silicon carbide, graphite or alumina, wires such as tungsten, beryllium, titanium and molybdenum, and discontinuous materials [10]. MMCs are said to be materials for the demands of the future, when the demands for high thermal conductivity, reduced weight, heat dissipation, and high strength are factors for design. MMCs represent the Next Generation of solutions for today's electronic requirements. Metal matrix

composites are either in use or prototyping for the Space Shuttle, commercial airliners, electronic substrates, bicycles, automobiles, golf clubs, and a variety of other applications. While the vast majority are aluminium matrix composites, a growing number of applications require the matrix properties of superalloys, titanium, copper, magnesium, or iron. Regardless of the variations, however, aluminium composites offer the advantage of low cost over most other MMCs. In addition [10, 11] they offer excellent thermal conductivity, high shear strength, excellent abrasion resistance, high-temperature operation, nonflammability, minimal attack by fuels and solvents, and the ability to be formed and treated on conventional equipment. Aluminium MMCs are applied in brake rotors, pistons, and other automotive components, as well as golf clubs, bicycles, machinery components, electronic substrates, extruded angles and channels, and a wide variety of other structural and electronic applications [10]. Titanium [12, 13] on the other hand is expensive, has high strength-to-weight ratio and corrosion resistance. Used as components for aircrafts, jet-engines, racing-cars and marine crafts.

Metal Matrix Composites are composed of a metallic matrix Aluminium (Al), Magnesium (Mg), Iron (Fe), Copper (Cu) etc. and a dispersed ceramic (oxide, carbides) or metallic phase Lead (Pb), Molybdenum (Mo), Tungsten (W) etc. Ceramic reinforcement may be silicon carbide, boron, alumina, silicon nitride, boron carbide, boron nitride etc. whereas metallic reinforcement may be tungsten, beryllium etc. [14]. MMCs are used for Space Shuttle, commercial airliners, electronic substrates, bicycles, automobiles, golf clubs and a variety of other applications. From a material point of view, when compared to polymer matrix composites, the advantages of MMCs lie in their retention of strength and stiffness at elevated temperature, good abrasion and creep resistance properties. Most MMCs are still in the development stage or the early stages of production and are not so widely established as polymer matrix composites. The biggest disadvantages of MMCs are their high costs of fabrication, which has placed limitations on their actual applications [14].

There are also advantages in some of the physical attributes of MMCs such as no significant moisture absorption properties, non-inflammability, low electrical and thermal conductivities and resistance to most radiations. MMCs have existed for the past three-to-four decades and a wide range of MMCs have been studied. Numerous combinations of matrices and reinforcements have been tried since work on MMCs began in the late 1950s [14]. However,

MMCs technology is still in the early stages of development, and other important systems undoubtedly will emerge. Numerous metals have been used as matrices in which the most important have been aluminium, titanium, magnesium, and copper alloys and superalloys. Some selected properties and typical applications of wrought titanium alloys are shown in Table 2.1(a) and 2.1(b):

Table 2. 1(a): Properties and typical applications of wrought titanium alloys (Source: Types of material, IE 351 lecture 3, page 26) [12], accessed August 2014.

Normal Composition (%)	UNS	Condition	Temperature (K)	Ultimate tensile strength (MPa)	Yield strength (MPa)	Elongation (%)	Typical applications
99.5 Ti	R50250	Annealed	298	330	240	30	Airframes, chemical, desalination and marine parts, plate- type heat exchangers.
			575	150	95	32	
5Al, 2.5Sn	R54520	Annealed	298	860	810	16	Aircraft- engine compressor blades and ducting, steam- turbine blades.
			573	565	450	18	



Table 2. 1(b): Properties and typical applications of wrought titanium alloys (Source: Types of material, IE 351 lecture 3, page 26) [12], accessed August 2014.

Normal Composition (%)	UNS	Condition	Temperature (K)	Ultimate tensile strength (MPa)	Yield strength (MPa)	Elongation (%)	Typical applications
6Al, 4V	R56400	Annealed	298	1000	925	14	Rocket motor cases, blades and disks for aircraft
			573	725	650	14	
			698	670	570	18	
			823	530	430	35	
		Solution + age	298	1175	1100	10	turbines and compressor, orthopaedic implants, structural forgings, fasteners.
			573	980	900	10	
13V, 11Cr, 3Al	R58010	Solution + age	298	1275	1210	8	High- strength fasteners, aerospace components, honey comb panels.
			698	1100	830	12	

The challenge and demand for developing metal matrix composites for use in high performance structural and functional applications including aerospace industries, automobile sector, defence etc. have significantly increased in the recent times [15]. The need to develop new materials with combinations of low density, improved stiffness and high strength in order to overcome the limitations of existing high-strength aluminium alloys and titanium alloys improved the design procedures and has resulted to achieve improvements in overall efficiency, reliability and performance by reducing either absolute weight or increases in strength-to-weight ratio. For this purpose, materials of high ultimate tensile strength, high

stiffness, yield strength and low density are required. Metal matrix composites consist of at least two components. Among two components one is matrix phase usually a continuous phase like aluminium, magnesium and second component is discontinuous phase like fibers, whiskers or particles called reinforcement. The objective of developing metal matrix composite materials is to combine the desirable properties of metal and particulates. The matrix holds the reinforcement to form the desired shape and reinforcement improves most of the mechanical properties of composite [15]. Aluminium metal matrix composites are preferred over other materials due to its properties like greater strength, improved stiffness, reduced density, improved temperature properties, controlled thermal expansion and improved wear resistance. Considering the fact that metal matrix composites (MMCs) refer to a kind of material in which rigid ceramic reinforcements are embedded in a ductile metal or alloy matrix. MMCs combine metallic properties (ductility and toughness) with ceramic characteristics (high strength and modulus), leading to greater strength in shear and compression and to higher service temperature capabilities. The interest in MMCs for use in the aerospace and automotive industries, and other structural applications, has increased over the past few decades as a result of the availability of relatively inexpensive reinforcements and the development of various processing routes which result in reproducible microstructure and properties [4, 15].

The family of discontinuously reinforced MMCs includes both particulates and whiskers or short fibers in which this class of MMCs has attracted considerable attention as a result of (a) availability of various types of reinforcement at competitive costs, (b) the successful development of manufacturing processes to produce MMCs with reproducible structure and properties and (c) the availability of standard or near-standard metal working methods which can be utilized to fabricate these MMCs. The particulate-reinforced MMCs are of particular interest due to their ease of fabrication, lower costs, and isotropic properties. Traditionally, discontinuously reinforced MMCs have been produced by several processing routes such as powder metallurgy (PM), spray deposition, mechanical alloying (MA) and various casting techniques, i.e. squeeze casting, rheocasting and compocasting [4]. All these techniques are based on the addition of ceramic reinforcements to the matrix materials which may be in molten or powder form. For the conventional MMCs, the reinforcing phases are prepared separately prior to the composite fabrication. It is widely recognized that the properties of

MMCs are controlled by the size and volume fraction of the reinforcements as well as the nature of the matrix-reinforcement interfaces. An optimum set of mechanical properties can be achieved when fine and thermally stable ceramic particulates are dispersed uniformly in the metal matrix. Thus, efforts has to be made to meet such requirements. Due to the great potential that in situ MMCs offer for widespread applications, a variety of processing techniques have been developed for production during the past decades. Using these routes, in situ MMCs with a wide range of matrix materials (including aluminium, titanium, copper, nickel and iron) and second-phase particles (including borides, carbides, nitrides, oxides and their mixtures) have been produced [4]. In this research work, current developments in microstructure and mechanical properties of the composites reinforced with ceramic phases will be addressed. Particular attention will be focused on the mechanisms responsible for the formation of reinforcements, and for creep failure of the titanium-based matrix composites.

2.1.1 Material Selection for Metal Matrix Composites (MMCs)

The demands on the material selection for the composites are many, i.e. they may need the temperature variations, have moisture sensitivity etc. This may offer weight advantages, ease of handling and other merits which may also become applicable depending on the purpose for which the matrices are chosen. Solids that accommodate stress to incorporate other constituents provide strong bonds for the reinforcing phase are potential matrix materials. A few inorganic materials, polymers and metals have found applications as matrix materials in the designing of structural composites, with commendable success. These materials remain elastic till failure occurs and show decreased failure strain, when loaded in tension and compression. Composites cannot be made from constituents with divergent linear expansion characteristics. The interface is the area of contact between the reinforcement and the matrix materials. In some cases, the region is a distinct added phase. Whenever there is interphase, there has to be two interphases between each side of the interphase and its adjoint constituent. Some composites provide interphases when surfaces with dissimilar constituents interact with each other. Choice of fabrication method depends on matrix properties and the effect of matrix on properties of reinforcements. One of the prime considerations in the selection and

fabrication of composites is that the constituents should be chemically inert, i.e. non-reactive [16].

Most metals and alloys make good matrices. However, practically, the choices for low temperature applications are not many. Only light metals are responsive, with their low density proving an advantage. Titanium, aluminium and magnesium are the popular matrix metals currently in vogue, which are particularly useful for aircraft applications. If metallic matrix materials have to offer high strength, they require high modulus reinforcements. The strength-to-weight ratios of resulting composites can be higher than most alloys. The melting point, physical and mechanical properties of the composite at various temperatures determine the service temperature of composites. Most metals, ceramics and compounds can be used with matrices of low melting point alloys. The choice of reinforcements becomes more stunted with increase in the melting temperature of matrix materials. Therefore, in selecting matrix material, the following factors may be taken into consideration [16]:

- The matrix must have a mechanical strength commensurate with that of the reinforcement i.e. both should be compatible. Thus, if a high strength fibre is used as the reinforcement, there is no point using a low strength matrix, which will not transmit stresses efficiently to the reinforcement.
- The matrix must stand up to the service conditions, viz., temperature, humidity, exposure to ultra-violet environment, exposure to chemical atmosphere, abrasion by dust particles, etc.
- The matrix must be easy to use in the selected fabrication process.
- Smoke requirements.
- Life expectancy.
- The resultant composite should be cost effective.

2.1.2 Reinforcement Selection

The role of the reinforcement in a composite material is fundamentally to increase the mechanical properties of composite [15]. There are necessary criteria or conditions that must be satisfied for the selection of a ceramic as reinforcement in the manufacture of good and standard metal matrix composites. Such criteria include density, melting temperature, size

and shape, elastic modulus, tensile strength, thermal stability, compatibility with matrix material, coefficient of thermal expansion, and cost. Ceramic materials have properties that make them ideal candidates for many applications where hardness, wear resistance, stiffness, and elevated temperature stability are required. Due to the refractory character of ceramics, [1, 17] they often are the only choice for a material that can potentially satisfy the most demanding requirements. Some selected properties of commonly used ceramics in MMCs are shown in Table 2.2:

Table 2. 2: Properties of ceramic reinforcements commonly used in metal matrix composites (MMCs) [1]

Metals	Ceramic	Density ($\times 10^3$ kgm^{-3})	Expansivity ($10^{-6} \text{ } ^\circ\text{C}^{-1}$)	Young's Modulus (GPa) (saito,2004)	Knoop Hardness (GPa) (saito,2004)	Elastic Modulus (GPa)
Al, Mg	Al_2O_3	3.98	7.92	350	22.5	379
Ti	AlN	3.26	4.84	-	-	310
Ti, Al, Mg, Cu	B_4C	2.52	6.08	449	27.5	448
Ti, Cu, Al, Mg	Si	2.33	3.06	-	-	112
Al, Mg, Cu, Ti	SiC	3.21	5.40	420	25.0	430
Ti	TiB	4.56	11.32	-	-	427
Ti, Superalloys	TiB_2	4.52	8.28	529	34.0	500
Ti, Cu	TiC	4.93	7.60	460	24.7	440
Al, Ti	VC	5.77	7.16	-	-	434
Superalloys	WC	15.63	5.09	-	-	669
Al, Ti	ZrB_2	6.09	8.28	-	-	503

However, monolithic ceramics and ceramic composites such as cermets are finding increasing applications, and there is a need to design them for resistance against impact loading. Ceramics and ceramic composites are in general very hard and brittle and hence their failures occur at small strains of less than one percent (1%). An understanding of damage initiation and evolution under dynamic loading conditions is important in the analysis of structures made of such brittle materials [18].

2.1.3 Metal Matrix Selection

Selection of metal or its alloy as matrix for production of MMC depends on the type, required properties and the kind of application where such composite is required. For instance, requirements of low density, with reasonably high thermal conductivity, have made aluminium and magnesium alloys the most commonly used matrices. However, among various MMCs developed, titanium matrix composites (TMCs) provide the best combination of high specific strength, rigidity, and good wear resistance required for drastic enhancement of physical and mechanical properties of titanium and titanium alloys, thus, providing the justification for selection of titanium as a matrix in the production of metal based composites [1].

2.2 TITANIUM MATRIX COMPOSITES (TMCs)

Nevertheless, titanium has often been referred to as the ‘wonder metal’ with excellent strength, ductility, and fracture resistant characteristics in combination with superior environmental resistance. However, significant difficulties in obtaining titanium from its ores (mainly rutile and ilmenite), combined with stringent processing requirements (both factors implying high cost), greatly slowed commercialization. However, today there is a vibrant titanium industry potential poised for breakthrough into the high-volume, cost-competitive automobile marketplace. Titanium is a metal element of Group IVB of the periodic table, with a melting point of 1675°C , an atomic weight of 47.9 g/mol , an atomic number of twenty-two (22) and a density of 4.5 g/cm^3 . The element is the fourth most abundant structural metal in Earth’s crust (behind Al, Fe, and Mg), occurring mainly as rutile (TiO_2) and ilmenite

(FeTiO₃) [19, 20]. Metallic titanium use can be divided into two main categories: corrosion resistance (essentially titanium alloyed to a minor extent) and structural use (for which titanium is more highly alloyed to increase the strength level while maintaining usable levels of other mechanical properties such as ductility). While the market for metallic titanium is showing a generally upward trend, the major use of titanium, as TiO₂ a white compound with high refractive index, is as a pigment ‘whitener’ in paints, paper, rubber, plastics, and the like at about twenty (20) times the use level of metallic titanium. Titanium has been recognized as an element for more than two-hundred (200) years since it was first identified in 1790 by a Cornish United Kingdom (UK) clergyman called William Gregor and named ‘‘titan’’ by a German chemist in 1795 [19].

Titanium alloys may be divided into two major categories: corrosion-resistant and structural alloys. The corrosion-resistant alloys are generally based on the single-phase α with dilute additions of solid solution strengthening and α -stabilizing elements like oxygen, palladium, ruthenium, and aluminium. These alloys are used in the chemical, energy, paper, and food processing industries to produce highly corrosion-resistant tubings, heat exchangers, valve housings, and containers. The single-phase α alloys provide excellent corrosion resistance, good weldability, and easy processing and fabrication but at a relatively low strength. The structural alloys can be divided into four categories: the near- α alloys, the $\alpha + \beta$ alloys, the β alloys, and the titanium aluminide intermetallics. Titanium Matrix Composites (TMCs) are however advanced materials made of titanium or titanium alloy matrices mixed either with continuous or discontinuous reinforcements. They exhibit several excellent properties such as corrosion resistance, high specific strength, high specific modulus, heat resistance etc. There are two families of titanium matrix composites, continuously reinforced and discontinuously reinforced TMCs. The early work on titanium matrix composites considered continuous fibre reinforced composites and the industrial use of the composites produced was restricted to highly specialized applications. The reasons attributed were prohibitive cost of continuous fibres, complex fabrication routes, limited formability and high anisotropic properties of composites produced [1, 19]. Discontinuously reinforced (particulate) TMCs have attracted more attention compared to continuous fibre reinforced composites. This is because of their properties of isotropy, easy secondary operation, improved mechanical properties and

economic benefits. Typical applications for discontinuous or particulate titanium matrix composites include:

- Creep resistant engine components,
- Wear parts such as gears, bearings and shafts,
- Erosion-corrosion resistant tubing.

However, particulate titanium matrix composites (TMCs) are also faced with challenges that include selection of ideal reinforcements, as well as high performance processing methods. Despite the highlighted properties and advantages exhibited by the particulate reinforced titanium matrix composites (which enhanced their industrial applications), many complex problems still exist that affect the overall mechanical properties of the final composites. Such problems include the need to obtain a clean matrix/particle interface because in TMCs, many reinforcements are unstable and different types of reaction products form depending on the reinforcing phase. It is therefore necessary to understand the factors that influence the physical and mechanical properties of the composites since they are sensitive to the type of reinforcement, method of manufacture and processing/heat treatment used [1]. However, the statement stated below illustrates the summaries of the tensile properties of various titanium matrix composites (TMCs) at room temperature. Almost all the reported studies on TMCs used commercial titanium powder as the matrix for their investigations. The commercial titanium powder, apart from being expensive also contains some impurities (e.g. oxygen, manganese, chlorine, nitrogen, iron, silicon, magnesium etc.) and thereby raising questions on the total quality (purity) of the final composites.

Furthermore, various researchers have elaborated on the summary of room temperature tensile properties of titanium matrix composites (TMCs) [1]. Many researchers have worked on the tensile properties of titanium matrix composites at room temperature and the summary of their results are illustrated as follows: Johnson et al. (1991), reported that at 0% volume of Ti as reinforced material using melting as the processing method. The modulus, yield stress and ultimate tensile strength (UTS) were 108, 367 and 474 MPa respectively. Thus, the percentage elongation of the reinforced material is 8.3%. But at 37% volume of the reinforced material (TiC/Ti) matrix using melting as the processing method; the modulus, yield stress as well as the UTS were reported with the values of 140, 444 and 573 MPa, respectively with 1.9% elongation. Similarly, Chen et al. (1989), reported the

physical/mechanical properties of Ti/TiC at room temperature with volume of reinforcement between 40 and 50% using induction melting as the processing method. The results obtained were given as: modulus and yield stress provided with no values but UTS has a value of 1113 MPa with percentage elongation between 1 and 2%. Ranganath, (1996), reported the results using TiB-Ti₂/Ti as the reinforced material and the following values were obtained at room temperature. At 15% volume of reinforced materials, the values obtained are as follows: 137 MPa for modulus, 690 and 757 MPa for both yield stress and UTS, respectively.

On the other hand, Loretto et al. (1990), obtained the following results for modulus, yield stress and UTS as 0, 944 and 999 MPa, respectively with percentage elongation of 2% using hot pressing as the processing method for TiC/Ti64 of 10% volume reinforcement. Similarly, the same reinforced materials at 10% volume were processed using cold and hot pressing process. The values obtained were reported as 792 MPa for yield stress, 799 MPa for UTS and 1.1% elongation whereby leaving the modulus at 0 MPa, by Abkowitz et al. (1989). Shang et al. (1990), however obtained different values using the same reinforcement and same process as Loretto and Abkowitz et al., but different volume reinforced materials as 20% volume. The results obtained are as follows: modulus with 139 MPa, yield stress with 943 MPa and UTS with 959 MPa. The percentage elongation was reported as 0.3%. Furthermore, Lederich et al. (1994), reported the values of TiB/Ti6Al4V at 3.1% reinforcement volume using rapid solidification processing (RSP) method. The modulus, yield stress and UTS were 121 MPa, 1000 MPa and 1107 MPa, respectively with 7% elongation. Smith et al. (1984), performed similar experiment using B₄C/Ti6Al4V as reinforced materials at volume between 35% and 40% using vacuum hot pressing method in which only the values obtained were modulus UTS at 205 MPa and 1055 MPa respectively. Therefore, all these researchers' results were put together by Abdulfatai [1].

An ideal reinforcing compound for TMCs manufacture places special demands that must be fulfilled, and such demands include: high hardness, heat resistance and rigidity, thermodynamic stability in the titanium and titanium alloys at the sintering temperature, insolubility in the titanium matrix and the titanium atoms in the reinforcing compound (minimum mutual solubility), and "crystallographic" stable matrix/particle boundaries. It should be noted that structural efficiency of discontinuously reinforced TMCs is a function of the density, elastic modulus, and tensile strength of the reinforcing phases. Chemical stability

and compatibility of the reinforcements with the matrix materials are very important both during fabrication and for the end application [1]. Also, lack of stability of the second phase can lead to the formation of undesirable interfacial products. Both situations can therefore lead to premature failure of the components produced from such materials during service. Besides, the difference between the coefficients of thermal expansion of the reinforcement and matrix must be minimized in order to minimize strain accumulation, especially for composites that will be exposed to thermal cycling. Some selected properties of commonly used ceramics in TMCs are shown in Table 2.3:

Table 2.3: Properties of ceramic reinforcements commonly used in TMCs [1]

Ceramic	Density (g/cm ³)	M.Pt. (K)	Thermal Conductivity (J.cm ⁻² .S ⁻¹ .K ⁻¹)	Thermal Expansion (10 ⁶ °C ⁻¹)	Poisson's Ratio	Elastic Modulus (MPa)	Tensile Strength (MPa)
B ₄ C	2.51	2720	0.273-0.290	4.78 (25-500 °C)	0.207	445	158 (980 °C)
TiB*	4.56	-	-	7.15-11.32 (20-1380 °C)	0.11 & 0.16	427 & 371	-
TiB ₂	4.52	3253	0.244-0.260	4.6-8.1	0.09-0.28	500	129
TiC	4.99	3433	0.172-0.311	6.52-7.15 (25-500 °C)	0.188	440	120 (1000 °C)
SiC	3.19	2970	0.168	4.63 (25-500 °C)	0.183-0.192	430	-
ZrB ₂	6.09	3373	0.231-0.244	5.69 (25-500 °C)	0.144	503	201

Several reinforcing phases have been used in producing TMCs and these include SiC, TiC, TiB₂, Al₂O₃, TiN, Si₃N₄, TiB, Nd₂O₃, Y₂O₃, B₄C etc. [1]. Titanium monoboride (TiB) has been identified as the best reinforcement for TMCs, because of its chemical compatibility with Ti, outstanding physical and mechanical properties (such as high elastic modulus) with

linear coefficient of thermal expansion that is approximately the same as that of titanium and titanium alloys. Similarly, TiC has been reported as having potential as a good reinforcement for TMCs because of its high hardness, high modulus and high flexural strength. Therefore, composites combining TiB and TiC as reinforcements offer an attractive combination of excellent mechanical properties, good wear resistance and corrosion resistance. Abdulfatai [1] also confirmed that the combination of both TiC and TiB as reinforcement in TMCs is considered as the best reinforcement. Review of relevant literature has shown that in addition to commercial TiB and TiC powders, commercial TiB₂ and graphite powder had also been used for the in-situ formation of stable TiB and TiC particles reinforcement. Recent researches however have shown that B₄C powder is also a promising reinforcement ceramic material of Ti alloys for a variety of applications that require elevated hardness, good wear and corrosion resistance. Above all, it is a good source for TiB, TiB₂ and TiC particulate for reinforcing titanium.

2.2.1 Boron Compounds as Reinforcements for TMCs

There are three boron compounds existing in the Ti-B system which is illustrated in Figure 2.1. These include TiB, Ti₃B₄, and TiB₂. Based on the phase diagram shown in Figure 2.1, the equilibrium phases of the titanium-boron system are classified into: (i) High-temperature body-centered cubic (beta) titanium, low temperature hexagonal close-packed (alpha) titanium, and rhombohedral (beta) boron. (ii) Intermetallic compounds-TiB (monoboride) and TiB₂ (diboride), as well as Ti₃B₄ (formed only in a narrow temperature range) [1, 20, 21, 22].

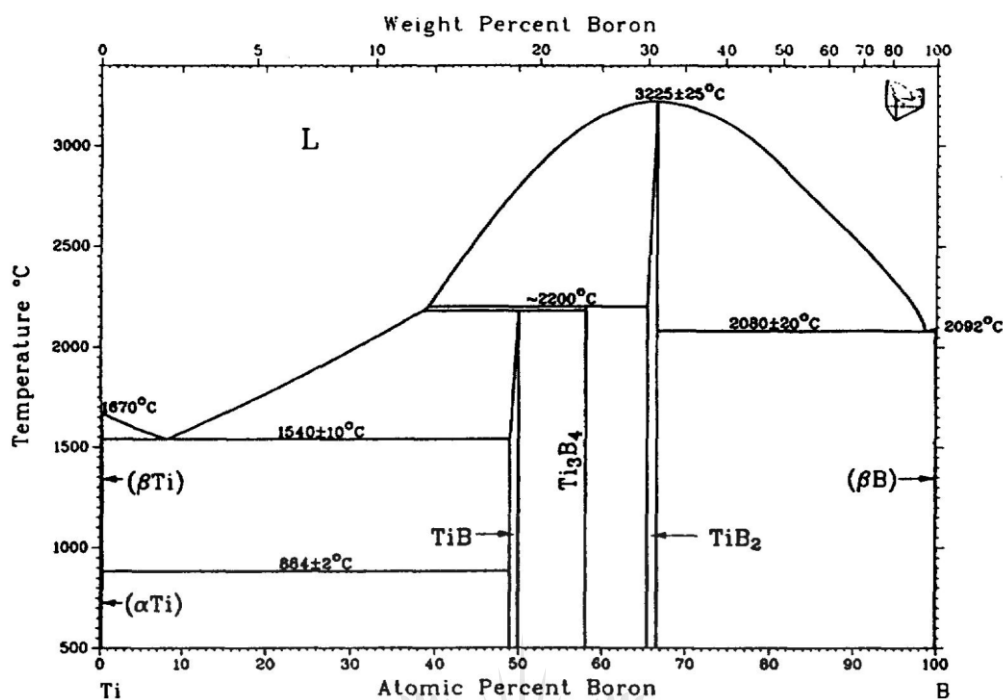


Figure 2. 1: Ti-B phase diagram [1]

As seen in Figure 2.1, the technically important titanium-rich section of the Ti-B binary system has a eutectic reaction (liquid \rightarrow beta titanium + TiB) at 1540°C and 1.64 wt. % boron, B (6.88 at. % B). TiB has a tendency to rapidly segregate to the grain boundaries, and boron itself is slightly soluble with solubility of less than 1 atmosphere percentage (1 at. %) in the high-temperature (beta) and low-temperature (alpha) titanium. Consequently, intermetallic compounds of titanium-base alloys may be increased by the precipitation of TiB intermetallic phase. However, the ductility and fracture toughness are retained only if the amount of boron is less than the eutectic composition (hypo-eutectic Ti-B alloys). It is important to emphasize that the eutectic point can shift significantly when other alloying elements are added.

2.2.2 Titanium Monoboride (TiB)

Components used in many engineering applications, especially in the aerospace and automobile industries and defence, are required to meet certain property requirements, such as possessing a certain specific strength, elastic modulus, toughness, etc. Conventional

metallic materials rarely meet such requirements. However, recent advancements in the field of metal matrix composites have overcome this difficulty, and many metal matrix composites developed in recent years have the characteristics to meet various combinations of property requirements. Titanium-based composites constitute an important group of such metal matrix composites. Though titanium-based composites are mostly used for aerospace applications, they are finding increasing use in other applications such as in the fabrication of automotive components and consumer utilities [23]. Titanium-based composites possess several advantageous properties such as high specific modulus, high specific strength, good corrosion resistance and good wear resistance. Various reinforcements are used in titanium-based composites. The incorporation of reinforcements such as SiC, Al₂O₃ and B₄C leads to the formation of undesirable reaction products, which act as major barriers to the development of viable titanium composites. However, titanium boride (TiB) is well suited for use as reinforcement due to the absence of any intermediate phase between Ti and TiB. Moreover, TiB reinforcement has certain desirable characteristics such as high elastic modulus, good thermal stability at high temperature and a density nearly equal to that of titanium [24].

However, the in situ TiB whisker (TiBw) reinforcement can be simply synthesized by reacting Ti powders with B powders at high temperatures via reactive sintering or pressing [4]. Several researchers have identified TiBw as an effective reinforcement for TMCs. The in situ TiBw promote composite strengthening via a load-transfer mechanism. Moreover, in situ TiBw also enhances the wear resistance of Ti. Hence, with improvements in processing and microstructure control, and proper understanding of structural–property relationship, high performance TMCs with desired mechanical properties for advanced structural applications can be developed. Thus, resistance to fatigue failure is one of the critical design issues for using such materials in automotive and aerospace sectors [25]. During high-cycle fatigue deformation, in situ TiBw/Ti composites show higher fatigue resistance than pure titanium and its alloys due to the reinforcing effect of TiB whiskers. In general, the formation of in situ TiB whiskers in Ti-based alloys also leads to lower creep rates. The creep resistance of TiBw/Ti composite is characterized by high values of apparent stress exponent and apparent activation energy [25]. In general, in situ TiBw-reinforced composites are formed through the exothermic reaction between the reactant powders, or compacts of reactant powders, and densified in a one-step process via hot compaction techniques such as hot pressing and hot

isostatic pressing (HIP). This process is also referred to as Reactive Hot Pressing (RHP). The advantages of RHP are its simplicity, and ease of operation by using conventional hot-press facility. Tjong et al. [4] prepared 12-15 volume % TiB_w/Ti composites by the RHP route using four reactive systems: Ti–TiB₂, Ti–B, Ti–B₄C and Ti–BN [4]. Exothermic reactions between compacted reactant powders of the Ti–B, Ti–B₄C and Ti–BN systems take place during hot pressing. Thus, formation of TiB from elemental Ti and B is a highly exothermic process with the enthalpy of formation of -160 kJ/mol [25].

2.2.3 Titanium Diboride (TiB₂)

Titanium diboride (TiB₂) is an interesting material for its high melting point, high hardness, moderate density, high Young's modulus and low thermal expansion co-efficient. It has been used in applications such as cutting tools, a wear resistance material, for metal melting crucibles and electrodes. TiB₂ powder is prepared by a variety of methods such as the borothermic reduction of titanium, fused-salt electrolysis, and solution phase processing or carbothermal reduction. Among the above mentioned processing techniques, the carbothermal reduction process is commercially used as the cheapest method because of inexpensive raw materials and it is a simple process. Also for each mole of TiB₂ produced, the process generates carbon monoxide (CO) gas, which will release energy when burnt with oxygen. Bahman et al. [26] found a carbothermal reduction process for the synthesis of TiB₂, which has a vapour–liquid–solid growth mechanism [26]. They found that TiB₂ was formed at temperatures greater than or equal to 1300 degrees. Abdulfatai [1] however, revealed that TiB₂ is produced by the reduction of TiC and B₂O₃ when the reaction temperature goes beyond 1367 degrees [1, 26]. Also, Srivatsan et al. [25] found that diboride of titanium (i.e., TiB₂) has shown the potential for use in diverse areas such as spanning cutting tools, armour materials, and even as cathode material for refining aluminium using the Hall–Heroult cell [23, 25]. This is essentially because they possess combinations of high hardness, good elastic

modulus, good electric conductivity and resistance to corrosion in molten metal environments. Due to their high electrical conductivity, they can be easily machined using the technique of electrical discharge machining (EDM). This makes them suitable for use in performance-critical applications [23].

However, application of TiB₂ to its fullest potential has been curbed primarily because of economic considerations. The most important concerns are:

- The cost of densifying the material at high temperatures,
- The uncontrollable variability in mechanical properties such as flexural strength, and
- Relatively moderate to low sinterability.

On account of these drawbacks, there exists an inherent difficulty in producing fully dense products of titanium diboride. Since TiB₂ is both an ionic and covalently bonded compound it can withstand high sintering temperatures. Temperatures above 2200 degrees (°C) are required for pressure-less sintering, and density of the resultant sample can reach a value as high as 95% of theoretical density. In addition, the relatively low crystalline boundary diffusion coefficient of the TiB₂ slows down the densification speed and prolongs the time required for sintering. In order to decrease the sintering temperature, hot pressing is often used. A recent study has shown that hot pressing aids in increasing the density of the TiB₂ sample while concurrently decreasing sintering time and ensuring that the sample has a near uniform microstructure. However, the presence of a thin oxygen-rich layer (rich in TiO₂ and B₂O₃ compounds) on the surface of commercial TiB₂ powder is detrimental to densification [1, 23].

Bahman et al. [26] produced the effect of TiB₂ nanopowder by mechanically induced self-sustaining reaction. For instance ultra-high temperature ceramics are a group of advanced materials that are chemically and physically stable at very high temperatures in extreme reactive environments. Several borides, carbides, and nitrides of groups IV and V elements have similar properties, like high melting point and hardness because of the strong covalent

bonding and consequently are anticipated to be potentially suitable for such applications. Among them, titanium diboride (TiB_2) and its composites have become important ceramics as they possess a number of desirable properties. TiB_2 is representative of refractory compounds with a very high melting point, high hardness, and extraordinary resistance to plastic deformation at high temperatures. Due to these outstanding properties, TiB_2 has many technological applications such as impact-resistant armour, wear components, cutting tools, heating elements and cathodes in Hall–Heroult aluminium smelting [27]. Presently, Self-propagating High-temperature Synthesis (SHS), Mechanical Alloying (MA), combustion synthesis by direct reaction of elemental reagents, arc-plasma method as well as Magnesiothermic, Aluminothermic and Carbothermic reductions of metal oxide-boron oxide mixture [1, 27] were investigated to fabricate TiB_2 -based ceramics. Among them, the MA process is used to produce any quantity of nanopowder with controlled microstructure because the melting and precisely controlled conditions are not essential. In addition, this method has the advantages of simplicity, reproducibility and low processing cost. During the past few decades, numerous attempts have been made to develop TiB_2 -based ceramics by various solid-state processes. Tjong et al. (2007), investigated the mechano-chemical synthesis of TiB_2 using the activation of $\text{TiO}_2\text{--B}_2\text{O}_3\text{--Mg}$ ternary system. They reported that the mechano-chemical reaction occurred after 15 hours of milling [27].

In the same system, TiB_2 nanoparticles were produced after short milling time (lower than 2 hours), synthesized TiB_2 nanopowder was however produced using a mechano-chemical reaction between LiBH_4 , LiH and transition-metal chloride (TiCl_3). Moreover, TiB_2 nanopowder was synthesized by mechanical alloying of Ti-67B elemental powder mixture after 60 hours. TiB_2 powders with submicrometer size were also prepared using the mixture of elemental Ti and B powders after prolonged periods of milling (210 hours). Furthermore, in many instances, TiB_2 -based ceramics were not directly produced by milling, but only after a suitable heat treatment. Whiskers of TiB_2 were produced through carbothermal reduction of

TiO₂ and B₂O₃ in temperature range 940–1200 degrees (°C). The mechano-chemical behaviour of TiO₂–B₂O₃–Si system was studied to produce TiB₂ nanoparticles. It was found that milling up to 50 hours could not lead to the formation of TiB₂. After thermal treatment of the milled powders at 1300 degrees (°C), the phase compositions were TiB₂, Ti₂O₃, Si and SiO₂. It should be realized that the level of contamination increases and some undesirable phases form if the powder is milled for times longer than required [27]. In conclusion, titanium diboride appears to be an attractive candidate for a high-temperature reinforcing fibre for intermetallic-matrix composites. Titanium diboride has high modulus, reasonably low density, a moderate thermal expansion coefficient and is thermodynamically compatible with a number of potential intermetallic matrices. TiB₂ is a high-temperature material with a melting point near 3000°C. The retention of its room temperature strength and elastic modulus to temperatures as high as 1500°C and the absence of any plastic deformation up to 1700°C make it an excellent candidate for consideration as a creep-resistant, high-strength fibre. In addition, the relatively high coefficient of thermal expansion (CTE) of TiB₂ is $8.7 \times 10^{-6} \text{ } ^\circ\text{C}^{-1}$ in the temperature range between 25–750°C which makes it an excellent match with low CTE metallics such as Inconel 903. In addition to physical compatibility, TiB₂ is chemically compatible with many intermetallics such as titanium aluminides, nickel aluminides, and molybdenum disilicide [27 - 28].

2.2.4 Titanium Carbide (TiC)

Titanium carbide, TiC is an extremely hard refractory ceramic material. It has the highest specific strength and specific modulus (among the transition metal carbides), high melting point and relatively high electrical and thermal conductivities. TiC has the boron iodide, BI or sodium chloride, NaCl-type crystal structure type where the titanium atoms are situated in a face-centered cubic closed-packed arrangement with the octahedral interstitial sites being

occupied by the carbon atoms. Due to the excellent physical and mechanical properties exhibited by TiC, it has been widely used as reinforcement in titanium matrix composites (TMCs). At the beginning, TMCs produced with TiC as reinforcement were manufactured using either powder metallurgy or casting techniques with TiC particles directly incorporated into solid or liquid matrices [1].

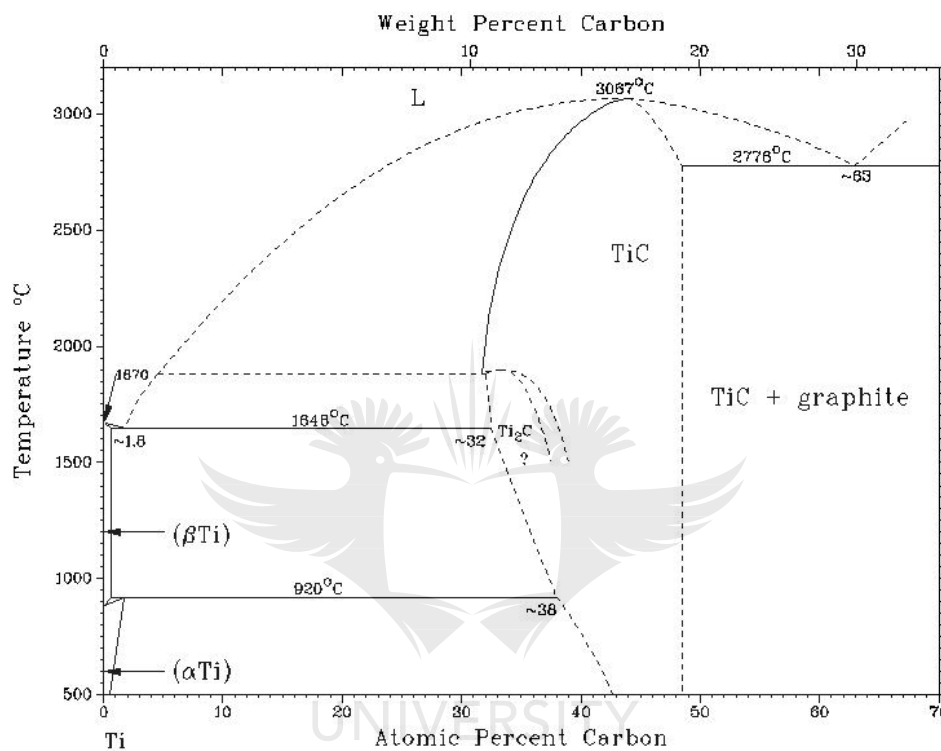


Figure 2. 2: Ti-C phase diagram [1]

On the other hand, TiB₂/TiC composites represent promising materials using for wear resistant parts, such as forming dies and cutting tools. They also exhibit good behaviour as high-temperature structural components in heat exchangers and engines due to their high hardness, good wear resistance and chemical inertness [29]. Furthermore, the superior thermal and electrical conductivities of TiB₂/TiC composites also suggest the potential use in non-structural applications like wall tiles in nuclear fusion reactors, cathodes in Hall–Heroult cells and vaporizing elements in vacuum-metal deposition installations. However, dense TiB₂/TiC composites fabricated starting from TiB₂ and TiC are very difficult by traditional

processing techniques due to their high melting points and low diffusion coefficients. Recently, TiB₂/TiC composites have been prepared by consolidation of mechanically activated or ball-milled powders from Ti–B₄C or Ti–B₄C–C systems. Several techniques, such as powder metallurgy method, transient plastic phase processing (TPPP), self-propagating high temperature synthesis (SHS), reactive hot pressing (RHP) and plasma sintering technique, have been employed for the sintering/densification step. However, there is only limited information about the phase evolution and microstructures of the powder mixtures with the increased milling time, and the role of milling for the subsequent pressureless sintering, which is highly significant especially in terms of possibly commercializing the fabrication process. TiB₂/TiC composites have attracted enormous interests in the recent years due to their superior properties, such as high hardness, good wear resistance, high electrical and thermal conductivities, and high fracture toughness, comparing to their single-phase ceramics [29]. Electron microscope studies of the annealing of Ti-C thin films indicated that, at less than 750 Kelvin (K) only TiC is formed in the film. Saturation of the titanium (Ti) film by carbon (C) occurs as a result of C-atom diffusion into Ti. At less than 750 Kelvin (K), the formation and growth of TiC_xO_{1-x} is observed, as a result of C- and O-atom diffusion into TiC. At less than 1000 Kelvin (K), oxidation of TiC occurs, giving off TiO [30].

2.2.5 Titanium-Aluminium-Vanadium alloy (Ti-6Al-4V)

Ti6Al4V alloy has been widely used in artificial joint and tooth application because of its excellent mechanical properties and biocompatibility, and moreover, its density is nearly to the body bone. However, when the implanted Ti6Al4V alloy was employed in wear conditions, there were large black debris around it which displays the wear resistance property of the alloy should be improved more. Titanium alloy matrix composites reinforced with ceramics particles have significant potential in the field of biomedical materials due to their high hardness, excellent wear properties, good biocompatibility and corrosion resistance, and its close elastic modulus to human tissue [13, 20-21, 31]. Furthermore, titanium and its alloys

are the important materials for aerospace, biomedical and other applications. This is due to an attractive combination of low density, good mechanical properties, high corrosion resistance and biocompatibility. An important engineering alloy of titanium is Ti6Al4V, which exists in three types which include: alpha (α), beta (β), and two phase alpha-beta (α - β) in which however consists of two phases, namely: Alpha, hexagonal close packed (HCP) crystal structure and Beta, body centred cubic (BCC) crystal structure, at room temperature [21]. Figure 2.3 shows the crystal structure of the α – Ti and β – Ti phases:

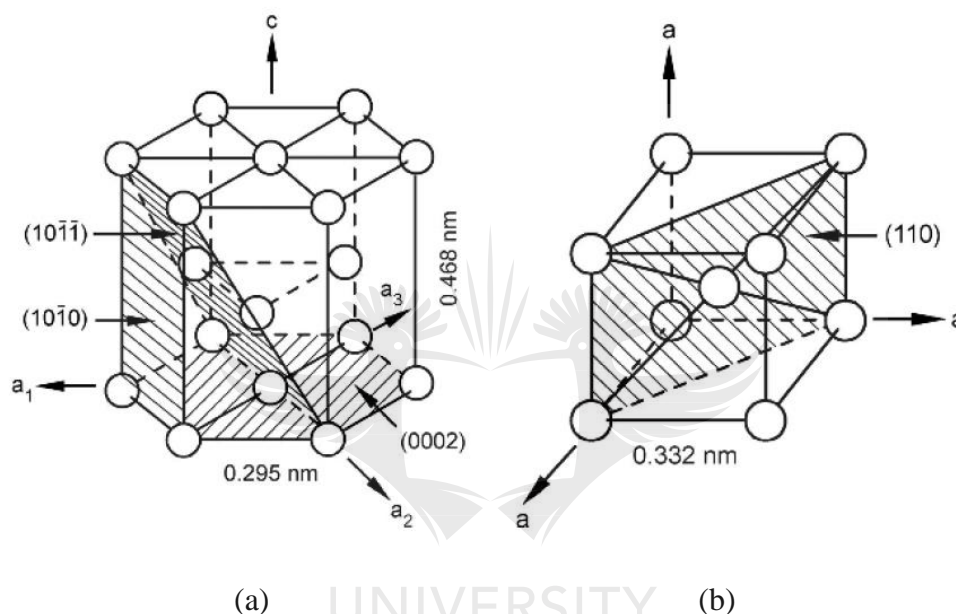


Figure 2. 3: Crystal structure of titanium (a) α -titanium phase, HCP; (b) β -titanium phase, BCC [20, 22]

Recently, researchers have observed significant refinement in the cast structure and improvement of mechanical properties like tensile ductility, strength and hardness for titanium and Ti-0.5Si alloys with a small amount (~ 0.086 to 0.14 mass %) of boron addition. Similar grain refinement has been reported by Tamirisakandala et al. [32] for the alloy Ti6Al4V by about an order of magnitude (from 1700 to 200 micrometre). Grain refined boron modified Ti6Al4V alloy has shown significant improvement in strength, stiffness, fatigue resistance and fracture toughness. However, researchers showed the enhanced formability of boron modified alloy during large deformation without cracking as opposed to the normal alloy. Owing to the fact that microstructural evolution during hot deformation has an important influence on the mechanical properties of the final product, understanding the

processing-microstructure relationship during thermo-mechanical processing of boron modified Ti-6Al-4V is of great importance [33-34].

Titanium alloys can be classified based on the value of the aluminium (Al) and molybdenum (Mo) equivalent parameters. The Al equivalent value indicates the capacity of the alloy to obtain a given hardness, whereas the Mo equivalent value indicates the capacity to obtain an ultimate tensile strength (UTS) and hardness in the aged condition. The first well developed and studied titanium alloy is the alpha-beta Ti6Al4V alloy, which is still one of the most popular and employed and as well represents the ‘work-horse’ of the titanium industry. The aerospace industry accounts for a large percentage of the total consumption and other sectors such as medical, automotive, marine and chemical share the rest of the market. Titanium, as well as its alloys, can be produced by conventional processes, like casting, primary working and machining, and by powder metallurgy where powders are consolidated and sintered to produce near-net-shape products. There are two general approaches when working with powder metallurgy methods which differ by the way in which the alloying elements are added to titanium powder. In the first one, the blended elemental (BE), titanium powder is mixed with alloying elements powders or with master alloy powders; meanwhile, in the second one, the pre-alloyed (PA) approach, each powder particle already had the final composition [35].

Among Ti alloys, Ti6Al4V (hereafter referred to as Ti64) is widely used in aerospace structures and propulsion systems and there is a continuous drive to improve its mechanical properties through alloy design. Conventionally cast Ti64 possesses a coarse grain size, typically of the order of several millimetres, and extensive thermo-mechanical processing is employed to break down this coarse cast structure [32]. Metalworking of titanium and its alloys generally involves series of thermo-mechanical processing steps at temperatures above or below the β -transition. The two phase titanium alloys, e.g. Ti6Al4V in the cast condition or after the intermediate β processing, are typically characterized by lamellar ($\alpha + \beta$) microstructure. Such microstructures are not desirable for manufacturing processes, most notably via superplastic forming in the ($\alpha + \beta$) regime wherein an equiaxed microstructure is required for superior ductility. The processing schedule for two-phase titanium alloys invariably includes secondary thermo-mechanical working steps in the ($\alpha + \beta$) regime which leads to microstructural conversion from lamellar to equiaxed morphology. Thus, the

deformation behaviour in ($\alpha + \beta$)-phase field is of particular interest in successfully designing the processing schedules [36]. At room temperature, the microstructure of pure Ti consists of 100% α . For $\alpha + \beta$ alloys, when α and β stabilizers (such as aluminium and vanadium) are added as alloy constituents, the beta phase begins to appear at grain boundaries. Other alloying elements can be added, and each alters the $\alpha \rightarrow \beta$ transition temperature. When α stabilizers are added (e.g. aluminium), the $\alpha \rightarrow \beta$ transition temperature is increased, and when β stabilizers are added (e.g. vanadium), the $\alpha \rightarrow \beta$ transition temperature is decreased. For instance, for pure Ti, the transition temperature is 885 degree ($^{\circ}\text{C}$) and for the Ti-6Al-4V alloy the transition temperature increases to 995 degree ($^{\circ}\text{C}$).

In the case of the Ti6Al4V alloy, thermo-mechanical processing also has an effect on the amount of β -phase in the final microstructure, where the percent β -phase increases with increasing process temperature in the $\alpha + \beta$ phase, with 100% β formation when processed in the β phase, with or without deformation. The α -phase is observed in Ti6Al4V as equiaxed or acicular, and acicular morphology is present in $\alpha + \beta$ alloys that have been processed above the β -phase. The geometry of the α -platelets will depend on the amount of deformation and cooling rate from the β -phase, and decrease in width with increase in cooling rate. With extensive deformation, the α -platelets break-up into a spheroidized structure. Thus, there exists the possibility of producing Ti6Al4V components with a variety of microstructures and associated properties by varying the mechanical and thermal processing, and possibly the part dimensions, since larger components exhibit slower cooling rates [37].

2.2.6 Boron Carbide with Titanium ($\text{B}_4\text{C} - \text{Ti}$) Composites

Boron carbide, B_4C , is an attractive candidate material for reinforcement in metal matrix composites, whose application is severely hampered by its reactions with most engineering alloys at the high processing or service temperatures. The reactivity of B_4C with some of the metals, however, may be made use of to create protective coatings on its surface [38]. Mogilevsky et al., [38] found that coatings obtained by treating B_4C in Ti powder were found to contain titanium carbide (TiC_{1-x}) and titanium borides (TiB_2 and TiB). A relatively thin

inner layer of the coating was carbide free and contained only borides, while the major part of the coating was a mixture of TiC_{1-x} and TiB. The growth of the coatings was controlled by diffusion, the activation energy for the growth of B₄C/Ti coating being approximately 175 KJ/mol. The phase composition, layer sequence and morphology of the coatings obtained were interpreted on the basis of kinetic and thermodynamic data of the ternary systems involved. However, non-oxide ceramics are important materials having a high potential for advanced structural and electronic applications, as well as reinforcements for metal matrix composites (MMCs). Boron carbide, B₄C, is especially attractive due to its very low density, high hardness and relatively low cost, at least in the particulate form [38].

However, the use of B₄C (as well as other non-oxide ceramics) as a reinforcement for (Iron) Fe-, (Nickel) Ni- and (Cobalt) Co-base alloys is severely hampered by reactions that occur at the ceramic/metal matrix interface at the high processing and service temperatures. The formation of undesirable reaction products, as well as the dissolution of the ceramic in a metal, results in the degradation of the reinforcement and in the deterioration of the mechanical properties of the matrix and of the MMCs as a whole. Since the performance of MMCs is, to a large extent, controlled by the structure and properties of ceramic/metal interfaces, it is important to prevent or, at least, to minimize the reactions at these interfaces. This may be achieved by creating diffusion barriers. One of the possible ways of creating a diffusion barrier is by coating the ceramic prior to inserting it into a metal matrix. It has been recently shown that non-oxide ceramics such as SiC, Si₃N₄ and B₄C, can be coated employing their interaction with powders of metals having high affinity for carbon, silicon and boron, and a new powder immersion reaction assisted coating method (PIRAC) has been proposed [38].

2.3 PROCESSING OF TITANIUM MATRIX COMPOSITES (TMCs)

For particulate-reinforced TMCs to gain industrial viability, their processing methods must be economically feasible, reliable and must be designed in such away as to produce a composite with a microstructure that will optimize their critical properties. Abdulfatai [1] also reported

that high melting point and high reactivity (especially in liquid state) of titanium have been identified as major limitations encountered in the process of manufacturing particulate-reinforced TMCs. However, despite these problems, few techniques like solidification processing, Combustion synthesis or Self-propagating high temperature synthesis (SHS) and as well as cold and hot isostatic pressing were reportedly used to produce particulate-reinforced composites with some success [1]. In a recent view, it was reported that, several methods have been used by in-situ techniques to produce TMCs. Such methods include self-propagating high temperature synthesis (SHS), mechanical alloying (MA), powder metallurgy (PM), rapid solidification powder processing (RSP), reactive hot pressing (RHP), ingot metallurgy techniques (IM) and liquid-liquid or liquid-solid or solid-solid reactions. Among these available techniques for producing TMCs, the solidification processes are more attractive due to their simplicity, flexibility and economy. Simply because of the high chemical reactivity of Ti, fabrication methods based on ingot metallurgy are unsuitable for processing TMCs reinforced with ex situ ceramic particulates [1, 27].

In recent years, several novel processing techniques for synthesizing the in situ ceramic reinforcements have been developed. The techniques for fabrication of discontinuously reinforced TMCs include reactive sintering, mechanical alloying, spark plasma sintering, high temperature self-propagating synthesis, combustion-assisted cast, ingot metallurgy and gas-solid reaction. Two types of in situ ceramic reinforcements, i.e. TiCp and TiBw or a combination of both have been synthesized successfully by many researchers. The in situ TiB whisker is particularly attractive as a reinforcing material owing to its high modulus and hardness, chemical compatibility with Ti. Furthermore, the density of TiB (4.56 g/cm^3) is nearly the same as titanium (4.5 g/cm^3). Thus, the TiB content in TMCs can be increased to a very large extent. Comparing to the ex situ route, in situ processing techniques offer several advantages such as easy fabrication, lower energy consumption and higher purity of ceramic reinforcements produced [27].

2.3.1 Mechanical Alloying (MA)

Mechanical alloying (MA) is a solid state powder processing method which involves repeated cold drawing and fracture of particles resulting from high energy ball-sample collision Tjong

et al. [4]. In this process, the starting constituent phases (powder mixture) are subjected to mechanical milling techniques (e.g. ball milling), after which the milled powder mixture is heat treated at the desired temperature [1, 4]. Materials processing based on mechanical alloying (MA) is used extensively as a mechano-chemical process to prepare metastable phases, amorphous alloys and composites. MA is a solid-state processing technique which involves repeated cold drawing and fracture of particles as a result of the high energy ball-sample collisions. High energy ball milling is normally carried out in the planetary mills or vibratory mills. The process can promote the reactivity of the system, thereby inducing chemical reactions in a variety of powder mixtures. The optimum balance between cold welding and fracturing is essential for mechanical activation of the chemical reactions [27]. However, MA provides a unique means to synthesize TMCs with better homogeneity, particularly a significant size discrepancy exists between the ceramic reinforcement and titanium powders. The disadvantages of MA process include low productivity of high energy ball mills, and powder contaminations from the milling media due to decomposition of the agent. Recently, researchers synthesized 10 vol. % TiB/Ti-4Fe-3.7Mo composite via MA process using either boron (B) or titanium diboride (TiB₂) powder as the boron source [27].

On the other hand, Mechanical alloying (MA) with heavy working of powder particles results in intimate alloying by repeated welding and fracturing. This technique allows dispersoids to be produced, solubility extension, novel phase production, and microstructural refinement [19]. Srivatsan et al. [39] discovered that, in mechanical alloying (MA), pure metal powder and alloying ingredients are mechanically alloyed using high energy ball mills, while concurrently incorporating sub-micron oxide or carbide filler to form discontinuously-reinforced MMCs. During this process heavy working of the powder particles results in an effective alloying by a process of repeated welding, fracturing and re-welding. The mechanically alloyed product (the composite powder) is subsequently consolidated into suitable shapes. The technique is particularly useful in developing materials with large alloying additions for the purpose of improving mechanical properties at elevated temperatures [39]. Tjong et al. [4], found that MA can be used to produce fine-grained alloyed powder particles in metal-metal and metal-ceramic systems. In recent years, the MA technique has been extensively used to fabricate in situ ceramic particle reinforced MMCs [4]. Meyers et al. [40], found that Mechanical alloying produces nanostructured materials by

the structural disintegration of coarse-grained structure as a result of severe plastic deformation. Mechanical alloying consists of repeated deformation (welding, fracturing and rewelding) of powder particles in a dry high-energy ball mill until the desired composition is achieved. In this process, mixtures of elemental or pre-alloyed powders are subjected to grinding under a protective atmosphere in equipment capable of high-energy compressive impact forces such as attrition mills, shaker mills and ball mills [40].

2.3.2 Powder Metallurgy (PM)

Jianbo et al. [41], recently researched that, powder metallurgy (PM) technique is of special interest since high degrees of chemical homogeneities can be obtained and large scale segregations are avoided. Titanium alloys fabricated by PM, starting from the elemental or pre-alloyed powders is a feasible route considering its costs, versatility and also allowing to manufacturing parts with complex geometry and near to the final dimensions. Therefore, the PM technique is of special interest in many titanium alloys recently [41]. The powder-metallurgical process of fabricating composites consists of mixing matrix and reinforcing powders, cold isostatic processing (CIP), vacuum sintering and hot isostatic pressing (HIP) or hot working. The process is difficult for production of composites having relatively high reinforcement content because of difficulties in uniform mixing, cold compaction and also the size control of the reinforcements. However, researchers recently reported the use of powder metallurgy technique to fabricate titanium matrix composites (TMCs). The process has also been described as the most viable and promising route for cost effective fabrication of titanium alloy composites. Powder Metallurgy (PA) also incorporates elemental cold-compactable titanium powder. In this elemental powder blending technique, the correct proportion of master alloy and base elemental powders are blended to obtain a uniform distribution of the required chemical composition. This processing technique has been used to produce 10-20vol.% TiC particulate-reinforced Ti6Al4V composites as well as TiB-Ti composite. Major advantages of this technique are that no additional expensive tools are required and raw material utilization can be maximized. However, the cost of investment is still on the high side when compared to conventional and other emerging techniques.

Powder metallurgy is a commonly used fabrication method in metal matrix composites (MMCs) fabrication. Solid phase processes [1, 8, 27] involve the blending of rapidly solidified powders with particulates, platelets or whiskers, through a series of steps. The sequence of steps include:

- Sieving of the rapidly solidified particles,
- Blending of the particles with reinforcement phases,
- Compressing the reinforcement and particulate mixture to approximately 75% density,
- Degassing and final consolidation by extrusion, forging, rolling or any other hot working method.

In the powder metallurgy (PM) approach, the reinforcement material is blended with rapidly solidified powders. The blend is then consolidated into billets by cold compaction, outgassed and hot isostatic or vacuum hot pressed to form starting products (billets) for subsequent fabrication. The cold compaction density is controlled in order to maintain an open, interconnecting porosity. The process of outgassing involves removal of the adsorbed gases and chemically combined water and any other volatile species, through the synergistic action of heat, vacuum and inert gas flushing. The outgassing reactions, however, are a function of the reinforcement surface chemistry. An advantage of the powder metallurgy technique is an ability to use the improved properties of advanced rapidly solidified powder technology in the composite. In conclusion, this technique has the added advantage of offering near-isotropic properties in the composite body [39].

2.3.3 Laser Additive Manufacturing (LAM)

Laser additive manufacturing (LAM) is a powder based process that allows designer to create parts that are hard or impossible to manufacture with conventional methods. The laser additive manufacturing has gained considerable interest in past few years. The biggest issue on this interest is that the quality of the laser additive manufactured parts is on such high level that the parts can be used in different industrial fields as functional parts. Also the possibility to create geometrically complex parts and working prototypes has raised the interest. Also the possibility to optimize part weight and strength is an advantage of this

technology. Parts are built layer by layer as the laser beam melts the next layer on top of the previous one. However, laser additive manufacturing (LAM) process is layer-wise material addition technique which allows manufacturing of complex three-dimensional (3-D) parts by selective solidification of consecutive layers of powder material on top of each other. Solid structure is achieved by thermal energy supplied by focused and computer guided laser beam. The process produces almost full dense parts and they do not usually need any other post-processing than surface finishing [42]. The advantages of laser additive manufacturing are geometrical freedom, mass customization and material flexibility. The laser additive manufacturing can be used for building visual concept models, customized medical parts and also tooling moulds, tooling inserts and functional parts with long term consistency. This manufacturing process can provide consistency over the products entire lifeline. It is also important that processes accuracy and ability to manufacture complex geometrical structures are on a good level. Also the process reliability, performance and economical aspects like production time and cost will play in a big role in order to use this manufacturing technique in mass production [42].

Similarly to laser additive manufacturing, laser powder deposition (LPD) has been shown to be a flexible manufacturing process enabling the fabrication of fully dense functional parts via a layer-by-layer additive deposition process, which can greatly reduce the production time from the initial design concept to the finished part and can quickly respond to design changes. The process allows a high degree of flexibility in the control of the deposited part's geometry, composition and microstructural properties. LPD has been successfully used to fabricate ribbon-web structures from titanium alloy for the aeronautical industry, and to repair high-value components for advanced industries, such as worn blades and the blisks of engines, etc. A unique characteristic of LPD is its ability to deposit dissimilar materials, however in such applications, residual stress and deformation due to high temperature gradients and mismatch of thermal expansion coefficients between different materials can generate detrimental effects. In order to compensate for these effects a great deal of research has been conducted into the design of compositional gradients between different materials to reduce the residual stress induced during deposition. Recently, work was done on functionally gradient materials of Invar and TiC, Ti to Ti-25 at.% V, Ti to Ti-25 at.% Mo and NiCrBSi and Cr₃C₂ has been investigated in order to obtain unique properties or to develop new materials [43].

On the other hand, Akinlabi et al. [44], researched on laser metal deposition (LMD) as an additive manufacturing (AM) technique which serves as a recommended technique for processing titanium and its alloy because it addresses most of the problems of the traditional manufacturing methods simply because AM technique is a tool-less process. However, AM technology is a promising aerospace manufacturing technique as it has the potential of reducing the buy-to-fly ratio and it is useful for the repair of high valued parts. There are various methods for coating surfaces of materials, some of them includes chemical vapour deposition, physical vapour deposition, spraying, etc. but the Laser Metal Deposition (LMD) process, is an additive manufacturing process and it is believed to have a greater advantage when compared to other deposition processes. Some of the advantages of using the LMD process include the ability to produce parts directly from the 3-Dimensional (3D) computer-aided design (CAD) model of the part with the required surface coating in one single step, as against only coating achievable with other surface coating techniques. Another important advantage of the LMD process is in its ability to be used to repair existing worn out parts that were not repairable in the past. Also, complex parts can be produced with the LMD without requiring later assembly, since the part can be made as one single component, this will greatly reduce the buy-to-fly ratio of aerospace parts [44-48]. However, discontinuous reinforced titanium matrix composites (DRTMCs) have received considerable interests in past decades due to their high specific strength, stiffness, isotropic properties and relative easiness of fabrication compared with fibre reinforced titanium matrix composites.

A number of manufacturing technologies especially the in situ synthesis methods have been developed for the production of DRTMCs. Significant improvements in various mechanical properties over monolithic matrix alloys were obtained [49]. Laser rapid solidification materials processing and manufacturing such as laser engineered net shaping (LENS), originally developed at the US Sandia National Laboratory [27], direct laser fabrication (DLF), laser powder deposition (LPD), laser melting deposition (LMD), etc. have been proved to be useful methods to fabricate fully dense near-net-shape metallic components. These processes are based on layer-by-layer materials melting and deposition process to build a complete workpiece. These methods are very suitable for making complex components of difficult-to-process materials like titanium alloys and their composites. TiC is widely used as reinforcing material in DRTMCs for its excellent mechanical properties. Thus, a variety of

TiC particle reinforced titanium alloy matrix composites and TiC/Ti functionally gradient materials (FGMs) have been successfully manufactured through LENS, DLF and LPD processes, confirming the feasibility of laser assisted forming methods for the production of DRTMCs [49]. Surface treatments can effectively improve the properties of titanium alloys. Of all the surface treatment techniques, laser treatments are widely used in surface modification of many kinds of metals. Laser treatments have several advantages over commonly used heat treatment techniques, including precise control over the width and depth of processing, the ability to selectively process specific areas of a component, and the ability to process complex parts [3]. Tian et al. [3], researched on the fabricated coatings containing TiN, Ti₂AlN and Ti₂N compounds on the surface of pure titanium by laser alloying with aluminium powder in a nitrogen atmosphere.

The results of laser alloying pure titanium with powder mixtures of silicon and aluminium showed that the laser treated samples were much more resistant to oxidation than the untreated titanium. Also found that the significance of applied laser nitriding to Ti6Al4V and the test results showed that the wear resistance of the treated samples was significantly enhanced. The results laser alloying of powder mixtures of Molybdenum (Mo) and Tungsten carbide (WC) on the surface of Ti6Al4V alloy indicated that the sliding wear resistance of the coatings was five (5) times as high as that of the original Ti6Al4V alloy [3]. Laser beams are widely used in surface modification of different metals, owing to their high coherence, directionality and high energy density. Furthermore, laser surface remelting, laser alloying, and laser cladding have been researched by Fei et al. [50], to improve the surface properties of many kinds of metals. It is noteworthy that the coatings prepared by laser cladding show dense microstructure and exhibit strong metallurgical bonding with the substrates. Figure 2.4 shows the schematic of laser cladding process by filling cladding materials in synchronous feeding way.

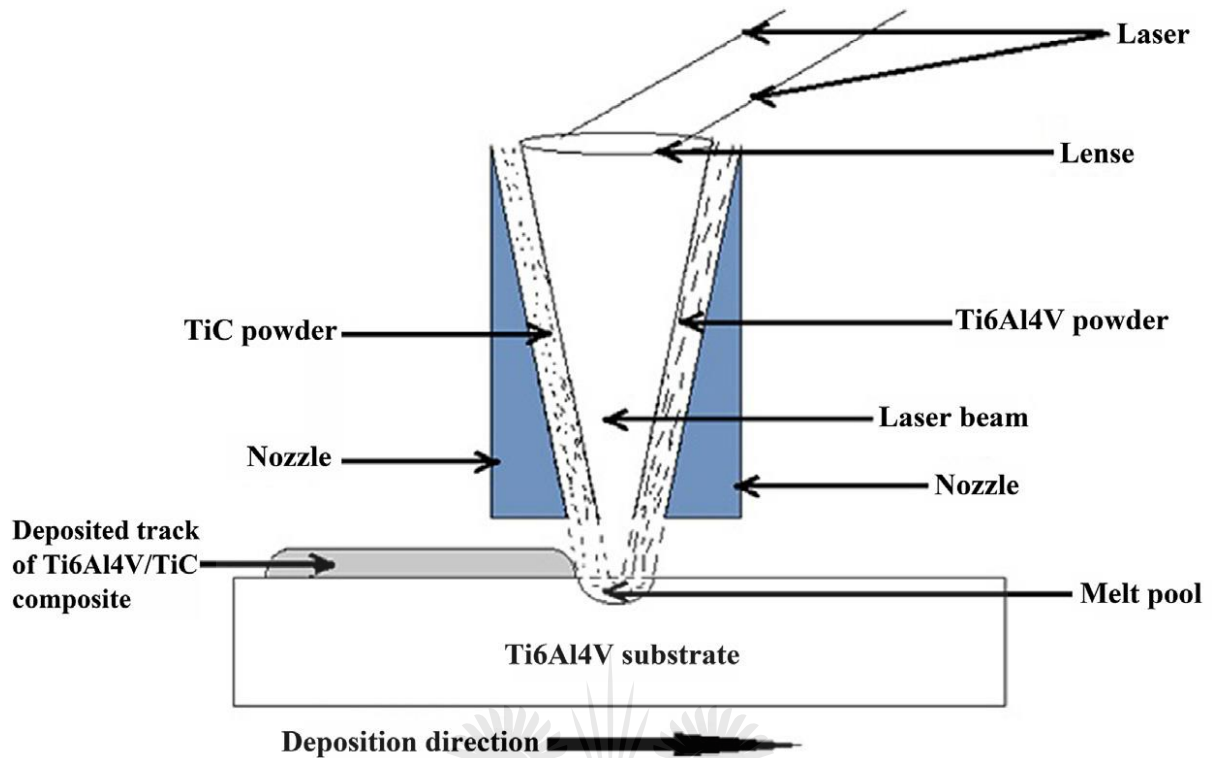


Figure 2. 4: Schematic of laser cladding process [50]

During laser cladding, the most important issue is melting the cladding materials onto the substrate [50]. Anoop et al. [51], however studied the source of energy in laser additive manufacturing (LAM) which is a laser acronym for Light Amplification by Stimulated Emission of Radiation. High density optical energy is incident on the surface of the workpiece and the material is removed by melting, dissociation/decomposition (broken chemical bonds causes the material to dissociate/decompose), evaporation and material expulsion from the area of laser-material interaction [51]. Yilbas et al. [52], also reported that, laser surface processing provides advantages over conventional melting methods such as plasma arc melting. Some of these advantages include high speed processing, non-mechanical contact between the workpiece and the heat source, precision of operation, and local treatment. However, laser control melting involves high temperature heating of the surface within small area, which is limited with the irradiated spot diameter. This, in turn, results in high temperature gradients across the irradiated spot while causing high thermal strain and stress development in the irradiated region. Although microhardness enhances at the surface, fracture toughness reduces because of high hardness and high residual stress

formation in the laser treated layer [52]. Figure 2.5 shows a typical single clad bead cross section with its dimensional characteristics. These dimensional physical characteristics are regarded as some of the outputs which are observed in the cladding process. These outputs are being influenced by different variable input parameters associated with the laser cladding process.

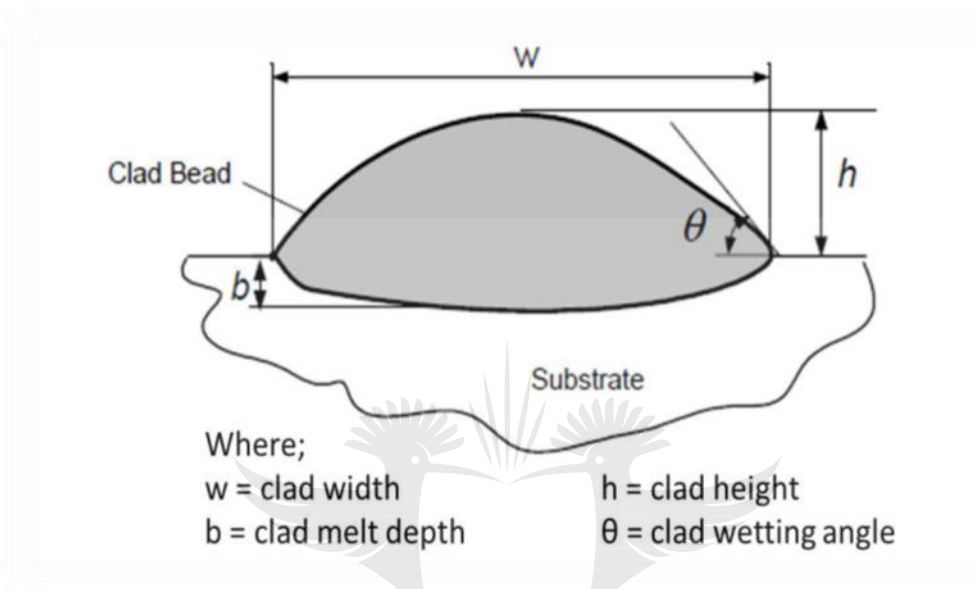


Figure 2. 5: A typical cross section of a single clad bead [22]

These input parameters include: laser power and its mode (continuous wave or pulsed), traverse speed, spot diameter, material properties, material feed rate, feeding direction, angle of feed, preheating and delivery gas flow rate [22]. The desired outputs which are commonly observed include: physical characteristics (clad width, height, and dilution or melt depth), microstructural characteristics and performance characteristics amongst others. In conclusion, Ochonogor et al. [53], however discussed different rapid solidification methods that have been put forward by some authors. The wear resistance of titanium alloys can be improved by applying special coatings to their surface using various methods. Laser surface alloying (LSA) has been reported to be a promising technique because of some advantages derived therewith. However, LSA often creates thermal distortions which result in severe residual stresses. But laser surface cladding (LSC) overcomes some of these obstacles since only a thin surface layer of the substrate melts during the process and combines with the additive materials to form the coatings. Laser cladding otherwise known as direct metal deposition

(DMD) which is an economical and highly flexible repair technique in the aero-engine, automobile, petroleum, and nuclear power station industries to mention just a few.

2.3.4 Reactive Hot Pressing (RHP)

Reactive hot pressing (RHP) refers to a process in which ceramic reinforcement is in situ formed through chemical reaction between elements and compound during hot pressing of mixture powders [1, 4]. Thus, the reactive hot pressing (RHP) process has been developed further by Tjong et al. [27] for fabricating the aluminium matrix composites reinforced with TiB_2 particulates on the basis of the exothermic dispersion (XD) technique [4]. Furthermore, researchers of recent successfully prepared in situ TiBw whisker reinforced Ti6Al4V composites by means of RHP. Powder mixtures containing Ti, Al-V master alloy, and TiB_2 were initially hot pressed at 1473 Kelvin (K) in a vacuum. Pressed billets were subjected to hot extrusion at 1323K. They reported that TiBw whiskers with a diameter of 0.1-3.5 μm and aspect ratio of 10-20 were in situ generated through the reaction between Ti and TiB_2 . They however used the RHP route to prepare TiB/Ti composites containing high volume content of TiBw whiskers (30-92%). In the case of TiB/Ti composites with TiB above 86 vol. %, a significant amount of TiB_2 phase remains. In another development [4] examined, the possibility of producing in situ TiB particle reinforced Ti composites by means of RHP route from four different mixtures of Ti-B, Ti- TiB_2 , Ti- B_4C and Ti-BN were observed. The powders from these mixtures were first blended thoroughly and then cold compacted. The green compacts were then degassed in a vacuum and hot pressed at 1523K for 1hour. X-ray diffraction (XRD) analysis confirmed the presence of TiB phase generated in the composites from four mixtures. Additional TiC phase was detected in the composite from Ti- B_4C mixture, while certain amount of TiB_2 remains in the Ti- TiB_2 mixture, indicating an incomplete conversion of TiB_2 to TiB. It was also reported that no titanium nitride were detected in the Ti-BN mixture [1, 4].

2.3.5 Rapid Solidification Processing (RSP)

Rapid solidification processing (RSP) route combines Ingot metallurgy (IM) and a rapid solidification technique to produce in situ MMCs. For instance, rapid solidification processing (RSP) of Ti-B or Ti-Si alloys accompanied by high cooling rates has been shown to be very effective in producing in situ Ti-based composites that contain large volume fractions of reinforcing particles. In the preparation of in situ Ti-based composites via the RSP route, rapidly solidified powders of Ti alloys containing boron (B) or silicon (Si) are initially produced by the plasma arc melting with centrifugal atomization (PAMCA) technique. Moreso, RSP route has been used to fabricate in situ TiC particulate reinforced Al-based composites [4, 27]. In situ formed TiC particles of 40-80 nm were reported to be distributed uniformly in the Al matrix with a grain size of 0.3-0.85 μm . The main advantage of RSP is its ability to produce alloy compositions not obtainable by conventional processing methods. Besides, RSP materials have excellent compositional homogeneity, small grain sizes, and homogeneously distributed fine precipitates or dispersoids [1, 4]. However, high power laser beam is an ideal source for surface modification of metals and alloys because very rapid heating and fast solidification can be achieved in metals during laser irradiation. This results in the formation of very fine microstructures in the laser modified surfaces [27]. Thus, these researchers studied the use of laser irradiation to deposit in situ TiB/Ti composites consisting of submicron and nanoscale TiB precipitates.

2.3.6 Self-Propagating High-temperature Synthesis (SHS)

Self-propagating high-temperature synthesis (SHS) or Combustion synthesis is a processing technique that involves using the energy released during exothermic reaction for the production of titanium matrix composites (TMCs). This process involves the exothermic chemical reactions and the heat liberated is sufficient to sustain the reaction through the rapid propagation of a combustion front without further addition of energy. High enthalpy of reaction is the major requirement for the propagation of a reaction in a self-sustaining mode. Abdulfatai [1] studied the combustion synthesis process involves mixing and compaction of powders of the constituent elements into a green compact, followed by igniting a portion of the green compact with a suitable heat source. SHS has been reported to be useful in the

production of near-net shape components and high purity products because of the possibility of all volatile impurities evaporating at very high temperatures. The researcher also reported that, with slight modification, combustion synthesis route can be used to produce titanium matrix composites. The main problem with this method is intrinsic porosity generation, where products formed expand due to the molar volume change from reactants to products, that resulting in the generation of intrinsic porosity. This researcher however found that such porosity can be reduced substantially by exothermic dispersion (XD) and combustion-assisted synthesis methods. A research study shows that, a self-propagating high-temperature synthesis (SHS) or combustion synthesis (CS) has been successfully used to produce TiC, TiB, TiC-TiB and Al-TiB₂ composites [1].

However, SHS is an attractive combustion synthesis method for a wide variety of advanced materials including ceramics, intermetallics, composites and functionally graded materials. This technique involves the conversion of chemical energy released by the exothermic reaction of raw powders to thermal energy once ignited by means of a heat source such as electrical spark, inductive wire, laser and furnace. The combustion wave is self-sustained and propagates across the specimen, converting the reactants into the final product. The combustion temperature can reach 5000 K and the wave propagation rate can be very fast. Volatile impurities are expelled as the wave propagates through the specimen due to the high temperature of the combustion wave. Thus, SHS is extremely attractive and its main advantages being the self-generation of energy required for the process, higher purity of the products due to volatilization of low boiling point impurity at elevated temperature, low energy inputs, very short processing times with high productivity due to very high reaction rates and relative simplicity of the process.

Therefore, the final products are very porous, typically 50% theoretical density. SHS plus mechanical pressing are commonly used to achieve fully dense TMCs [4, 27]. Tjong et al. [4], found that self-propagating high-temperature synthesis (SHS) was developed by Merzhanov and co-workers in the late 1960s, refers to as process in which materials with a sufficiently high heat of formation are synthesized in a combustion wave, which after ignition, spontaneously propagates throughout the reactants and converts them into the products. An important feature of SHS reactions is the self-sustaining reaction front in which

a heat of reaction of the order of -167 kJ/g mol is sufficient to maintain a propagating front. In conclusion, the SHS process has been extensively employed for the production of ceramic, intermetallic, and intermetallic matrix composites (IMCs) [4].

2.3.7 Exothermic Dispersion (XD) Process

Exothermic dispersion (XD) process, termed XDTM technology, was developed by Martin Marietta Laboratories, Baltimore, MD, USA in the 1980s [1, 4]. XD technology involves blending and compaction of elemental powders, followed by igniting the compact that initiated the exothermic reaction and generation of sustainable energy that produces the composites. XD technology was however used for the production of TiAl-TiB₂ composites, where elemental powders (boron, titanium and aluminium) were blended. It was reported that because of in situ development of reinforcements, the process eliminates oxide formation that could have weakened the interface between the reinforcement (TiB₂) and the matrix [1].

It was also reported that TiB₂ particles introduced via XD process offer substantial grain refinement and improved microstructural uniformity compared to un-reinforced TiAl. The XD process was reported to be very cheap with some limitations such as chemical and thermal stability of the dispersed phase. Another possible problem may arise when the reaction between composite forming elements are less exothermic. Exothermic dispersion (XD) process has been successfully used to produce variety of metal matrix composites (MMCs) with Ti, TiAl, and Ti₃Al as matrices and borides, nitrides and carbides as reinforcements but there is no mention of using the processing method to generate TMC composites from Ti and B₄C mixture [1]. Tjong et al. [4], reported the fabrication of the in situ TiB₂ reinforced with Al composite using XD process. Powder blends of Ti, Al and B were first cold-isostatically pressed at a pressure of 200 MPa and subsequently degassed in vacuum at 723 K for 1h. The Al-Ti-B compact is heated to 1073 K in an argon atmosphere and held at that temperature for 15 minutes. The resulting porous composite is canned and section-rolled into rods of 6 mm in diameter [4].

2.3.8 Chemical Vapour Deposition (CVD)

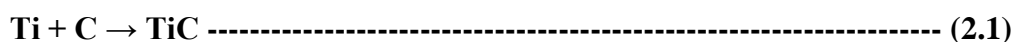
Deposition is a process of depositing a thin layer of film onto the surface of the wafer or an adhesive material. Vapour deposition processes usually take place within a vacuum chamber. There are two categories of vapour deposition processes: physical vapour deposition (PVD) and chemical vapour deposition (CVD). In PVD processes, the workpiece is subjected to plasma bombardment. In CVD processes, thermal energy heats the gases in the coating chamber and drives the deposition reaction. Therefore, chemical vapour deposition is done by putting the chemicals into a heated vacuum chamber containing a small thin disk of an adhesive material or a wafer. These chemical are fed into the chamber in a gas form [10]. Diefendorf et al. [28], studied that CVD process is an important method used for the fabrication of titanium diboride (TiB_2) fibres. Given the power and versatility of CVD, attempts to develop TiB_2 fibres were made only by using CVD. Experiments showed that in addition to process parameters such as temperature and reactant partial pressures, reactor geometry has a large influence on the deposit properties. A thorough understanding of what is occurring inside the reactor during the synthesis of TiB_2 is needed to guarantee better control of the CVD process and process optimization [28].

2.4 THERMODYNAMICS OF IN SITU REACTION SYSTEM

A great variety of processing techniques have been developed to fabricate in situ TMCs and numbers of reactive systems have been adopted by various researchers. However, the thermodynamic feasibility of these in situ reactions involved in fabricating in situ Ti based composites had been considered by many researchers. Therefore this section reviews the thermodynamics of in situ reactions for some typical and important reactive systems involved in the in situ formed reinforced TMCs such as Ti - C (graphite), Ti - B, Ti - TiB_2 , Ti - B_4C and Ti - $TiC/Ti - B_4C$ system.

2.4.1 Ti – C System

In situ TiC reinforced Ti matrix composites have been fabricated from Ti and C by means of combustion assisted casting (CAC) process. The thermodynamic feasibility of the reaction has been reported in terms of enthalpy, ΔH , and Gibbs free energy, ΔG reported by [1]. The equation of reaction of in situ TiC reinforcement is synthesized as:



The reaction enthalpy of formation, ΔH , and Gibbs free energy, ΔG , for the reaction between Ti and C was calculated using thermodynamic data studied by Abdulfatai and the variations of ΔH and ΔG with temperature for the reaction in equation 2.1 was also investigated [1]. ΔG is negative for the temperature ranges investigated, indicating that the reaction for the formation of TiC is feasible thermodynamically. However, the ΔH values are very large, indicating that a high quantity of heat will be released during the reaction [4].

2.4.2 Ti – B and Ti – TiB₂ System

Concerning the system involving titanium (Ti) and boron (B), the possible reactions that can occur were studied and reported as:

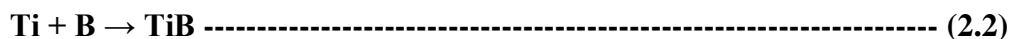


Figure 2.6 shows the generated Gibbs free energy (ΔG) against temperature (T) for reactions represented by equation 2.2 and 2.3 respectively. According to the figure, which shows that



ΔG for reaction in equation 2.3 is much less than that of reaction in equation 2.2. Although both TiB_2 and TiB are probable reinforcements, however, TiB_2 -reinforced TMCs cannot be synthesized by in situ reaction because TiB_2 is not stable when there is an excess of Ti [4]. Thus, TiB_2 is transformed to TiB as shown in the reaction represented by equation 2.4.

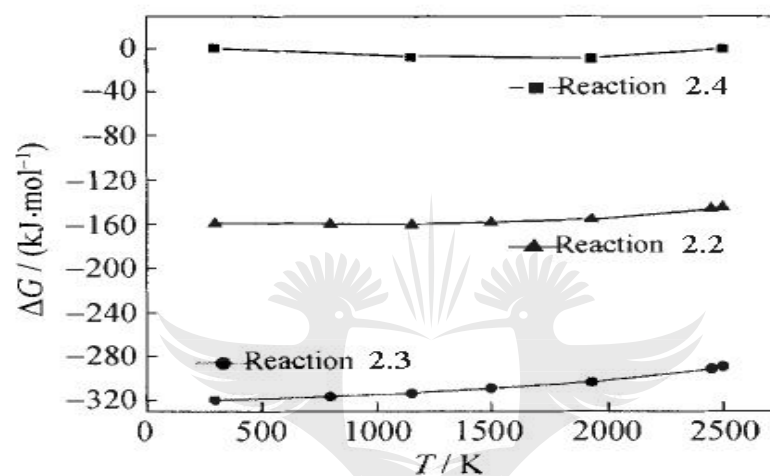


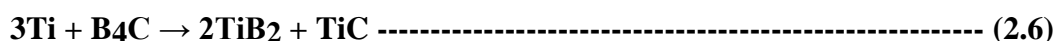
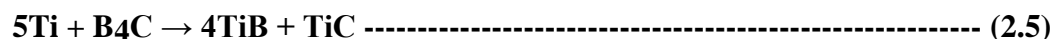
Figure 2. 6: The change of Gibbs free energy ΔG as a function of temperature for reaction equation 2.2, 2.3 and 2.4 [1]

However, Ti-TiB_2 system was used to fabricate in situ TiB whisker reinforced titanium matrix composites [1]. Equation 2.4 can apparently occur due to a negative free-energy change. Also, ΔH is negative, indicating that the reaction is exothermic [4].

2.4.3 Ti – B_4C System

TiB and TiC mixture-reinforced Ti matrix composites were reported to be fabricated by means of the combustion assisted cast (CAC) route [1]. Tjong et al. [4], also succeeded in fabricating a $(\text{TiB}+\text{TiC})/\text{Ti}$ composite from $\text{Ti-B}_4\text{C}$ mixture by means of the reactive hot pressing (RHP) route. These researchers however agreed that TiC , TiB and TiB_2 can be

synthesized by the chemical reaction between Ti and B₄C, and the chemical reactions that may take place are as follows:



Thus, the reaction formation enthalpy, ΔH , and Gibbs free energy, ΔG , for reactions in equation 2.5 and 2.6 were calculated using thermodynamic data. These results are shown in Figure 2.7 [1]. Figure 2.7 however shows that ΔG of the two reactions, equation 2.5 and equation 2.6 are all negative, which indicate that both reactions can take place. Moreover, the calculated reaction formation enthalpy, ΔH of each of the two reactions is very large, which indicates that quite a lot of heat is released during the reactions, i.e., exothermic.

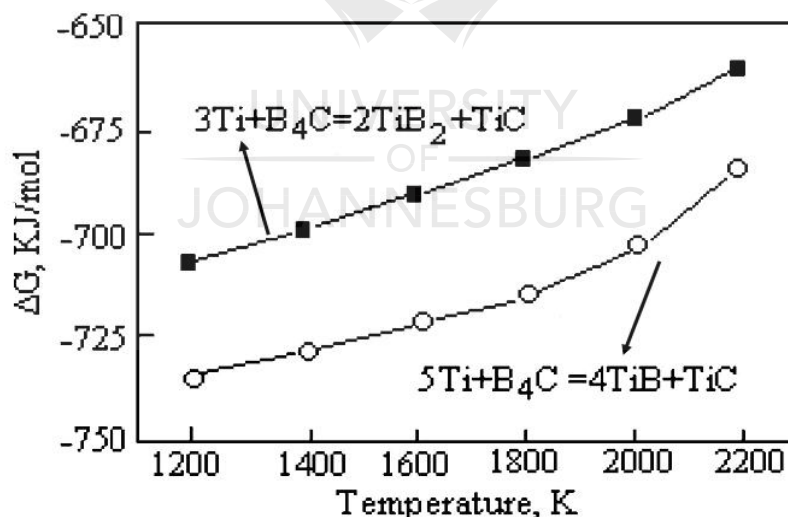


Figure 2. 7: Change of Gibbs free energy ΔG as a function of temperature for reactions of equation 2.5 and 2.6 [1]

Thus, subsequent fabrication of TiB and TiC reinforced Ti matrix composites from Ti-B₄C mixture using reactive hot pressing (RHP) reported by srivatsan et al. [25], explains and

proves that the thermodynamic calculations were correct and can be used to support further experiments.

2.4.4 Ti –TiC/Ti - B₄C system

During the processing of the titanium matrix composite by means of the combustion assisted cast (CAC) route, the temperature of the melt is so high that the TiC and TiB reinforcements synthesized by Self-propagating high-temperature synthesis (SHS) undergo disintegration and dissolution. When the melt is solidified, the TiC or TiB tends to precipitate from the Ti melt by means of nucleation and growth. Thus, the size and morphology of the in situ reinforcements are controlled by the solidification paths. Tjong et al., have investigated the effect of cooling rate and aluminium addition on the morphology and size of in situ formed TiC reinforcements in a Ti matrix. They show that both aluminium addition and an increase in the cooling rate of the melt can result in refinement of the reinforcements [4].

2.5 MECHANICAL PROPERTIES OF IN-SITU TMCs

The homogeneity of reinforcements and titanium matrix in a TMCs is of crucial important for high-performance engineering applications such as those in the automotive, chemical processing, nuclear power plant and aircraft industries. Uniform distribution of reinforcement in TMCs is very essential to achieve effective load-bearing capacity of the reinforcement while non-uniform distribution of reinforcement could bring about lower ductility, strength and toughness of the composites.

In situ method of fabricating TMCs generate fine ceramic particles that are uniformly distributed in the Ti matrix, leading to significant improvement in the yield strength, stiffness, creep and wear resistance of the materials. The explanation discussed by various researchers show the results of tensile properties of in situ titanium matrix composites (TMCs). The ductility of the TMCs is reduced significantly with increasing particle content and it is obvious that TiBw whisker exhibit a much larger reinforcing effect on the titanium matrix than the TiC particle. Many researchers have contributed to the study of tensile properties of in situ titanium matrix composites (TMCs) [4]. Considering the reinforcement materials used

in carrying out the tensile properties of in situ titanium matrix composites (TMCs). Tsang et al. (1996), used pure titanium as a reinforced material for the experimental analysis of in situ TMCs and the properties obtained are as follows: ultimate tensile strength (UTS) of 467 MPa, yield stress of 393 MPa, percentage elongation of 20.7% and elastic/young modulus is 109 GPa. Thus, various percentages of the reinforced materials were carried out for instance, Tsang et al. (1997), used 10 vol.% TiB/Ti reinforced. The results obtained are: UTS of 902 MPa, yield stress of 706 MPa, percentage elongation of 5.6% and elastic/young modulus of 131 GPa. Furthermore, Ranganath et al. (1996), used 15 vol.% (TiB + Ti₂C)/Ti as reinforced material and obtained the following values: UTS, yield stress and percentage elongation, i.e. 757 MPa, 690 MPa and 2.0% respectively. Similarly, Ni et al. (2006), performed an experiment with 10 vol.% (TiB + TiC)/Ti reinforced material and the following results were obtained: UTS of 817 MPa, percentage elongation of 0.55% and young modulus of 140 GPa but no value of yield stress was obtained. In conclusion, Ranganath et al. (1992), used 25 vol.% (TiB + TiC)/Ti as the reinforced material with the following results observed: UTS, yield stress and percentage elongation of 635 MPa, 471 MPa and 1.2% respectively. However, all these researchers' activities were reported by Tjong et al. (2000), [4].

These properties however generated a graph that shows the variation of compressive yield strength with temperature of the composites and unreinforced titanium at strain rates of $7 \times 10^{-4} \text{ s}^{-1}$ according to Figure 2.8. This figure shows that the strength of the composite is significantly higher than that of unreinforced titanium at temperatures ranging from 623 to 923 K. The researchers then suggested and concluded that the strength of (TiB + TiC)/Ti composite fabricated from the Ti-B₄C system is significantly higher than that of TiB/Ti composite produced from a Ti-TiB₂ system. They however suggested that the high strength of (TiB + TiC)/Ti composite could be produced from the presence of smaller reinforcements since the strength of the composites generally increases with decreasing size of the reinforcements.

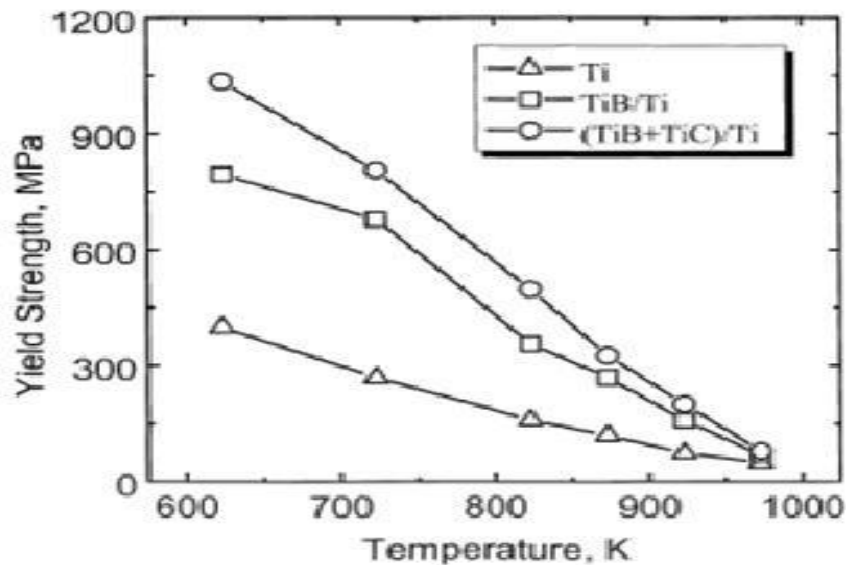


Figure 2. 8: Variation of compressive yield strength with temperature for 15 vol.% TiB/Ti and 15 vol.% (TiB+TiC)/Ti composites and unreinforced Ti [4]

Furthermore, creep properties of reinforced titanium matrix composites (TMCs) are very important especially for high temperature applications. However, couple of researchers also conducted a preliminary study on the tensile creep behaviour of TiB₂ and TiC-particulate reinforced Ti6Al4V composite at temperature from 500-650⁰C and stresses from 230-700 MPa. The obtained results show that, creep strain rates of TiB₂ and TiC reinforced composites were lower than those of the matrix alloy by two and one order of magnitude respectively. Further studied revealed that the creep fracture of composites in a high stress region was caused mainly by the debonding of the interface of TiB₂/ matrix and TiC/matrix and the cleavage of TiB₂ and TiC particles [1]. This researcher also carried out a report studied on the high temperature creep properties of in situ TiBw/TiAlV composite at 813 and 923K using rapid solidification processing (RSP) method. Results of their investigation show that TiB reinforcements decrease the creep rate by approximately two to three orders of magnitude when compared with the ingot metallurgy produced matrix alloy. However, the creep rates of the in situ composites are approximately one-order of magnitude lower than

those of monolithic powder metallurgy (PM) alloy. Another report carried out studied the steady-state compressive creep behaviour of $\text{Ti}_2\text{C}/\text{Ti}$ and $(\text{TiB} + \text{Ti}_2\text{C})/\text{Ti}$ composites at 823-923K and came up with results which show that steady-state creep rate of composites is two to three orders of magnitude lower than unreinforced Ti in the temperature range investigated. Figure 2.9 shows the variation of creep rate with stress for unreinforced Ti and 25 vol.% $\text{Ti}_2\text{C}/\text{Ti}$ composite.

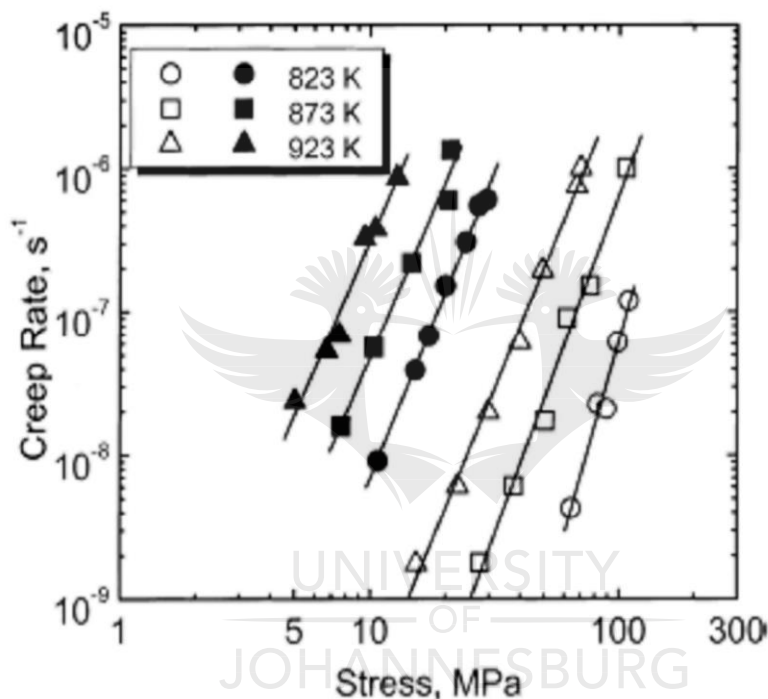


Figure 2. 9: Variation of steady-state creep rate with applied stress for unreinforced Ti (solid symbol) and 25 vol.% $\text{Ti}_2\text{C}/\text{Ti}$ composite (open symbol) [1]

Furthermore, Table 2.4 summarizes the apparent stress exponent and apparent activation energy for creep of the investigated materials. Thus, the value of apparent activation energies for creep is significantly higher than that for Ti, and increases with increasing volume fraction of reinforcements. The researcher however suggested that creep deformation of unreinforced Ti is governed by the climb-controlled creep mechanism.

Table 2.4: Apparent stress exponent and apparent activation energy for creep of composites titanium matrix composites (TMCs) and unreinforced titanium, Ti [1, 4]

Materials	Apparent stress exponent			Apparent activation energy (KJ/mol)
	823K	873K	923K	
Ti	4.3	4.1	4.1	236
10 vol.% (TiB+Ti ₂ C)/Ti	4.9	4.9	4.8	284
15 vol.% (TiB+Ti ₂ C)/Ti	7.2	4.7	4.1	336
25 vol.% Ti ₂ C/Ti	6.1	4.7	4.1	353

On the other hands, Tjong et al., [4] studied compressive creep behaviour of in situ 15 vol.% TiB/Ti and 15 vol.% (TiB + TiC)/Ti composites at 873-923 K. They reported that the creep rate of the composites is about one-order of magnitude lower than that of unreinforced Ti. They however, reported that the creep resistance of the (TiB + TiC)/Ti composite is higher than that of the TiB/Ti composite. The higher creep resistance of (TiB + TiC)/Ti composite were attributed to smaller size of reinforcements.

2.6 MICROSTRUCTURAL CHARACTERISTICS OF IN-SITU TMCs

Microstructural design has attracted increasing interest in modern development of hard coatings for wear-resistant applications [54]. It is however well known for instance that boride ceramics have high melting temperature, hardness, onset temperature of creep, and chemical stability at high temperatures [55]. Titanium diboride and boron carbide have both high melting points and high hardnesses. They also feature high Young's modulus and a good chemical stability most importantly B₄C for this report. However, TiB₂ and B₄C are difficult to sinter as pure materials due to a low self-diffusion coefficient and microstructural

coarsening. Thus, Composites based on the $\text{TiB}_2\text{-B}_4\text{C-WC}$ system are expected to retain a high level of hardness combined with a fine microstructure which would improve toughening mechanisms such as crack deflection [56]. Titanium diboride (TiB_2) and boron carbide (B_4C) are particularly useful for a variety of high-temperature applications due to their high hardness, high modulus, high electrical and thermal conductivities and as well as their exceptional corrosion and erosion resistance in many environments. But the difficulty in forming TiB_2 components is the major reason for its high cost and limited scope in engineering applications [57]. Studies have shown that small additions of Si_3N_4 or metallic elements such as Fe or Ni perform exceptionally well at reducing the temperatures and pressures required to sinter TiB_2 to near 100% density. TiC and TiN additions are common in the consolidation of TiB_2 , usually in high concentrations (>20%), because they facilitate sintering while inhibiting grain growth due to their immiscibility in TiB_2 [57].

Furthermore, ceramic materials such as borides, nitrides and carbides are a natural choice for several advanced structural applications due to their extraordinary hardness coupled with stability at high temperature. Continuous research on titanium-based ceramic materials have enabled them to emerge as one of the popular choices for temperature-critical applications because of their exceptional hardness coupled with an elastic modulus that exceeds the value of companion ceramics and is either comparable or better than that of metals. A titanium-based ceramic material of interest in the industrial sector is titanium diboride (TiB_2). It offers the potential for use in areas of cutting tools, wear resistant parts, as armour material, and even as cathode material for the Hall–Heroult cells. This is essentially attributed to its high hardness, elastic modulus, electric conductivity coupled with an intrinsic resistance to corrosion in molten metal environments [58].

2.6.1 Morphology, size and distribution of in-situ reinforcements in Ti – based Composites

In situ TiC reinforced TMCs have been fabricated through combustion assisted cast (CAC) routes by several researchers and TiC particles generated in TMCs are generally three-dimensional (3-D) dendrites [4]. On the other hand, some researchers also reported that the formation of this dendritic TiC reinforcements in the cast structure of combustion assisted cast (CAC) processed TMCs is mainly attributed to over-cooling of the composition during solidification. Tjong et al. [27], also studied that TiC has a cubic structure. Thus, when TiC nucleates, the growth rate in symmetric crystal planes is similar, therefore leading to the formation of equiaxed spherical particles. This claim has been proven to be correct by the in situ formation of equiaxed spherical TiC particles in the aluminium (Al) matrix composites developed by several other researchers [4]. Furthermore, others reported that TiB whiskers developed in the reactive hot pressing (RHP), processed TiB/Ti composite were in the form of elongated needles with a roughly hexagonal cross-section. In another development, a studied showed the formation of rod-like TiB in the CAC-processed (TiB+Ti₂C)/Ti composites.

In recent review developed, in-situ TMCs through reactive hot pressing (RHP) route from Ti-B, Ti-TiB₂, Ti-BN, and Ti-B₄C mixture with rod-like TiB reinforcements in situ formed in all the composites [4]. The microstructure of TiB/Ti and (TiB +TiC)/Ti formed was characterized by numerous rod-like reinforcements. The TiB whiskers in the TiB/Ti composite have a diameter of ~10 µm and a length of 40-400 µm, while those in the (TiB +TiC)/Ti composite have a diameter ~6 µm and a length of 25-250 µm. However, TiB exhibits a rod like shape, while TiC has spherical shape. All these researchers however pointed out that the spherical TiC particulates using reactive hot pressing (RHP) to process TMCs are quite different from dendritic reinforcements formed in combustion assisted cast (CAC) processed composites.

2.6.2 Factor affecting particle size and morphology

Consider the following factors that can significantly affect the particle size and morphology of the final TMCs include: cooling rate of the melt, synthesis temperature and holding time, as well as chemistry of matrix and reactants [1].

2.6.2.1 Cooling rate of the melt

Tjong et al. [4] studied the effect of cooling rate of melt on the reinforcement and final TMCs. They however fabricated the in situ TMCs using combustion assisted cast (CAC) route and were able to reveal that faster cooling yields smaller dendrites of TiC, encourages the formation of TiC dendrite arrays, and decreases the 'stoichiometry' of the TiC materials. Thus, effect of cooling rate of melt could be further investigated with regards to other processing methods with different starting materials for TMCs fabrication.

2.6.2.2 Synthesis temperature and holding time

Abdulfatai [1] studied and report the relationship between holding time and TiC particle radius at various temperatures. The researcher however reported that the size of the TiC particles tends to increase with increasing synthesis temperature and holding time. The researcher also reported that there is a significance difference in the size of the TiC particles generated in the samples that reacted with carbon-bearing gas for 5 minutes and the samples that reacted with carbon-bearing gas for 30 minutes at the same temperature of 1533 K. The TiC particles in the former sample are as small as 2 μm , while the TiC particles in the latter samples are as large as 10 μm . This indicates that there is coarsening of the in situ particles with increasing holding time.

2.6.2.3 Chemistry of matrix and reactants

Combustion assisted cast (CAC) process was used to fabricate (TiB +TiC)/Ti composites from Ti-B₄C [1]. The researcher however revealed that addition of aluminium (Al) exerts a

significant effect on primary TiC structure. This researcher also reported that there is a trend for the primary TiC to grow into an equiaxed grains and generate a fine structure after the addition of aluminium (Al). In another development Tjong et al. [4], fabricated TiB/Ti and (TiB +TiC)/Ti composites from Ti-TiB₂ and Ti-B₄C mixtures, respectively, under identical processing conditions. The reactants in both cases, TiB₂ and B₄C, have the same particle size of 3µm but the in situ formed TiB whiskers in the Ti-B₄C mixture are much smaller than those in Ti-TiB₂ mixture.

2.7 MICROHARDNESS CHARACTERIZATION OF CLADDED TMCs

Titanium alloy (Ti6Al4V) substrate has an average microhardness value of approximately 360 HV. One of the reasons for higher hardness in laser cladding process is that, volume fractions of unmelted carbide particles in the solidified deposits are significantly increased. Although, during re-solidification, some carbon came from the melted vanadium carbide (VC) particles can be pushed by the solidification front, due to it has low solubility in titanium, Ti [13], this eventually increases the percentage of carbon in this region. According to Ochonogor [74], which studied the uses of mixture of titanium and B₄C precursor powders to form a mixture of carbide and boride precipitates which however improved the hardness of the Ti6Al4V substrate from 350 HV to 600 HV. The precursor powders were placed in grooves machined to depths of 0.2 to 1.0 mm. New phases were formed typically TiC, TiB and TiB₂. The phases formed are characterized by high hardness which enhanced wear resistance.

Furthermore, this researcher however studied the surface modification of Ti6Al4V alloy to improve erosion wear resistance using a high power diode laser (HPDL) with a rectangular laser beam spot of multimode and uniform intensity laser. The process was carried out in a combined argon and nitrogen atmospheres. Result showed that the surface layers attained high hardness and significantly higher wear resistant, compared with the base material of

titanium alloy Ti6Al4V. The highest microhardness was displayed by the nitrogen surface layer on titanium alloy went up to 1300 HV_{0.2}. The surface layers formed are composites of titanium nitrides precipitations on the titanium alloy matrix. The result however was strongly attributed to the laser processing parameters adopted and also due to the partial pressure of nitrogen in the gas mixture of nitrogen-argon atmosphere. Based on the previous study, this researcher further investigated a developed modified Ti6Al4V alloy by laser surface alloying. Experiment were carried out at 1 kW CO₂ laser, 10.63 μm wavelength with focused beam of 65 mm. Laser treatment was performed on the samples coated by graphite and boron nitride powders in stream of nitrogen. The hardness value was determined under load of 1.96 N. Experimental results showed that laser treatment produced a surface layer which consists of hard ceramic TiC, TiN and TiB particles spaced in ductile martensitic matrix. The hardness obtained on cross-sectioned layer revealed a clear increase compared to the base material. The high hardness level (920 – 570 HV) was attributed to the formation of TiN, TiC and TiB hard phases. The thermoelectric power decreases noticeably with hardness increase.

On the other hand, similar investigation was conducted on Laser surface alloying of pure titanium with TiNBSiNi mixed powders. This experiment was carried out at 1.5 kW continuous wave CO₂ laser, with a beam diameter of 4 mm, at 25 % overlap. An alloyed layer consisting of Ti₆Ni₆Si₇, TiB₂ and TiN hard intermetallic compounds were formed. The alloyed layer showed a higher microhardness and a lower friction coefficient (COF) compared to that of the substrate. This researcher however concluded that, alloyed layer with such high hardness level and low friction coefficient can considerably improve the resistance to abrasion of the substrate. The treated sample showed a better oxidation resistance than the untreated substrate, which contributed to the high temperature and chemical stabilities of TiB₂, TiNi, TiN compounds formed in the alloyed layer [74].

In conclusion, the researcher carried out an investigation on friction and wear behaviour of Ti using laser surface alloying technique with Si, Al and Si + Al. Laser surface alloying (LSA) was carried out at 6 kW continuous wave CO₂ laser with a rectangular beam of 2.4 mm² area. The analysis conducted revealed that LSA with Si effectively improved the wear resistance of Ti than that by Si + Al or Al alone. The improved wear resistance in Si surface

alloyed samples was recognized to be due to presence of homogeneously distributed Ti_5Si_3 in the alloyed zone (AZ). Other results showed that LSA of pure Ti with Si, Al and Si + Al increases the microhardness of the AZ by two to four times. The increase in the microhardness was however attributed to the two-phase hyper-eutectic microstructure formed (Ti (Si) and Ti (Si + Al)). A similar improvement was also noticed in Ti (Al) which was due to the formation of solid solution hardening in a single-phase microstructure. The wear result showed that LSA significantly improved the wear resistance of laser surface-alloyed Ti that was subjected to wear testing with a hardened steel ball. The Ti (Si) system showed a better wear resistance followed by that of Ti (Si + Al) system and Ti (Al) system in decreasing order. LSA significantly reduced the coefficient of friction measured by quantitative wear testing.

2.8 WEAR CHARACTERISTICS OF CLADDED TMCs

Titanium and its alloys have been regarded as one of the productive and mostly used metal for industrial applications such as aerospace, marine, automobile, biomedical and food processing industries are strongly in demand of titanium due to their excellent properties. However, these alloys have found limited use in the mechanical engineering applications due to their poor tribological properties which includes poor abrasive wear resistance, poor fretting behaviour and high friction coefficient (COF). Moreover, these tribological properties could be improved and enhanced through the application of different surface treatments and coatings. As studied by Erinoshio et al. [75], the perfection in the mechanical properties of titanium and its alloys such as strength have greatly been accomplished through the addition of alloying metal composites. This researcher however stated that there are four main mechanisms that could be used to improve the tribological behaviour of titanium and its alloys and these are: increase the surface roughness, decrease the friction coefficient, increase the hardness and lastly the induction of a compressive residual stress. Shebani et al. [76], stated that wear can be defined as the removal of material from solid surfaces by mechanical action. Wear of materials is an everyday experience and has been observed and studied for a very long time. Hence, several factors are effects on the wear mechanisms such as normal load, hardness of material, sliding distance, sliding velocity and coefficient of sliding friction.

On the other hand, Fabio et al. [77], studied and discussed that the most used model for predicting wear is the linear wear law proposed by Archard. A common generalization of Archard's wear law is based on the assumption that the wear rate at any point on the contact surface is proportional to the local contact pressure and the relative sliding velocity. Wear can appear in many ways, depending on the material of the interacting contact surfaces, the operating environment, and the running conditions. In engineering terms, wear is often classified as either mild or severe. Mild wear results in smooth surfaces. Severe wear may occur sometimes, producing rough or scored surfaces which often will generate a rougher surface than the original surface. Severe wear can either be acceptable although rather extensive, but it can also be catastrophic which always is unacceptable. Mild and severe wear are distinguished in terms of the operating conditions, but different types of wear can be distinguished in terms of the fundamental wear mechanisms involved, such as: adhesive wear, abrasive wear, corrosive wear, and surface fatigue wear [78].

Adhesive wear occurs due to adhesive interactions between rubbing surfaces. It can also be referred to as scuffing, scoring, seizure, and galling, due to the appearance of the worn surfaces. Adhesive wear is often associated with severe wear, but is probably also involved in mild wear. As the name implies, adhesive wear involves strong adhesive forces between contacting surfaces.

Abrasive wear occurs when a hard surface or hard particles plough a series of grooves in a softer surface. The wear particles generated by adhesive or corrosive mechanisms are often hard and will act as abrasive particles, wearing the contact surfaces as they move through the contact.

Corrosive wear occurs when the contact surfaces chemically react with the environment and form reaction layers on their surfaces, layers that will be worn off by the mechanical action of the interacting contact surfaces. The mild wear of metals is often thought to be of the corrosive type. Another corrosive type of wear is fretting, which is due to small oscillating motions in contacts. Corrosive wear generates small sometimes flake-like wear particles, which may be hard and abrasive.

Surface fatigue wear, which can be found in rolling contacts, appears as pits or flakes on the contact surfaces; in such wear, the surfaces become fatigued due to repeated high contact

stresses. However, fretting (variously called fretting-corrosion or friction-oxidation) is a special combination of adhesive, corrosive, and abrasive wear [78-79]. Adhesive wear is one of the most prevalent types of wear.

Nevertheless, titanium is well known as a metal subject to severe welding or galling and otherwise having very poor friction properties. The preceding study on crystal structure effects suggested that improved friction properties could be obtained if titanium were alloyed in such a way as to (i) stabilize the hexagonal structure over a greater range of temperature and (ii) increase the c/a lattice ratio [80]. Additional studies showed that the shear force in hexagonal crystals varies with the relative spacing of the atoms within the crystals. In particular, the shear force is controlled by the ratio of the distance c (the spacing between hexagonal planes) to the distance a (the spacing between adjacent atoms in the hexagon). Various metals with hexagonal crystal structures have different values of c/a . Generally, friction declines with increasing c/a , and those metals that showed low friction give no evidence of gross surface welding.

As studied by Williams [81], stated that the common starting point in the analysis of wear is often the Archard wear equation which asserts that the wear volume, w is directly proportional to the product of the load, P on the contact and the sliding distance, s but inversely proportional to the surface hardness, H of the wearing material. The expression is given as: $w = K \times Ps/H$. The dimensionless constant K is the non-dimensional wear coefficient. On the other hand, Syafa'at et al. [82], also presented that Archard was the pioneer in developing the sliding wear model. Archard's wear equation postulates that the wear rate is defined by the volume worn away per unit sliding distance and the load. The wear depth can be computed related to the wear rate, sliding distance and contact pressure. The wear system considered is a pin-on-disc contact configuration in which the general Archard's wear equation is combined with finite element analysis (FEA) for predicting the wear.

Furthermore, Tian et al. [83], studied the wear properties of deposited composites coating of titanium borides and carbides reinforced composite coating which however exhibits excellent abrasive and adhesive wear resistance under sliding wear test conditions, because the strength and hardness of the surface of samples are significantly enhanced by the in situ formed

compounds. Alloyed layers are fabricated by laser surface alloying of pure titanium with B₄C and Ti mixed powders.

2.9 SUMMARY

Nevertheless, the investigations of laser metal deposition of titanium alloys with boron carbide reinforcement have been infrequently reported. As known to researchers and metallurgists, titanium alloys with boron carbide metal matrix composites (MMCs) have very high hardness, excellent wear and corrosion resistance, and high stability at elevated temperature. However, the aim of the present work is to produce composite coatings containing boron carbide, B₄C on the surface of titanium alloy, Ti6Al4V substrate by employing laser alloying technique and to investigate the evolving microstructure, microhardness and wear properties.



CHAPTER THREE

EXPERIMENTAL PROCEDURE

3.1 INTRODUCTION

This chapter provides detailed description of the starting materials, chemicals, equipment, methodology (procedures used in the experimental part of this research work), as well as characterization of the starting materials. The experimental arrangement used for the laser metal deposition and the characterization techniques used for the feedstock materials and deposits obtained from deposition process are also presented. The standard specification for titanium and titanium alloy bars and billets for the hot rolled substrate of Ti6Al4V was observed according to ASTM B348-13 [59]. The experimental set-up will however contain particle size analysis of the feedstock powders used and their microstructural characterization, laser deposition set-up, sample preparation for microstructural examination and description of the Scanning Electron Microscopy (SEM) equipped with Oxford Energy Dispersion Spectroscopy (EDS), Optical Microscopy (OM) and X-Ray Diffraction (XRD) techniques used for both powder and deposit characterization. Procedures for the microhardness test, wear test, corrosion test, erosion test, fracture toughness test and tensile test are also presented and discussed.

3.2 PARENT MATERIALS

The materials involved in this study are Ti6Al4V powder produced by Alfa Aesar Company and B₄C powder also supplied by the same company in Germany. The rectangular Ti6Al4V substrate with dimensions 102 mm x 102 mm x 7 mm is prepared for the laser metal deposition of the mixture powders. Ti6Al4V alloy samples were sandblasted and cleaned under tap water prior to the coating operation. Boron carbide powder, B₄C with particle size of about 22-59 µm, and titanium alloy powder with particle size of 45-90 µm, were deposited in the ratio of 1:4 in weight percent. The laser power used were varied between 800 W to 2400 W with 200 W interval. The beam diameter or spot size of 4mm was employed to melt the surface of the samples and the tracks were 50% overlapped for the multiple tracks

depositions in which 12mm focal distance was maintained from the nozzle to the surface of the substrate. During the laser surface melting process, the powders were dissolved into the melted pool, leading to alloying the surface of the samples with boron carbide. To protect the melt pool from oxidation during laser deposition process, argon gas was initiated at a pressure of 2 MPa to provide shielding. The powders were fed through a nozzle which was coaxial with the laser beam. The properties of Titanium alloy, Ti6Al4V used as substrate and as well as powder are described as follows: The substrate contains titanium alloy of Ti6Al4V with dimensions as 102 mm x 102 mm x 7 mm while the powder is 99.6 % pure and contains spherical particles in the 45 and 90 μm size range. The mechanical properties of Ti6Al4V obtained through forging followed by annealing is as follows: yield tensile strength ($\sigma_{0.2}$) 880 MPa, ultimate tensile strength 950 MPa, hardness (Hv) 349, young's modulus 113.8 GPa, Poisson's ratio 0.342, fracture toughness $75 \text{ MPa}\cdot\text{m}^{0.5}$ [60].

3.3 PROPERTIES OF B₄C METAL MATRIX COMPOSITES

Properties of boron carbide powder obtained from Alfa Aesar Company is described as: density of $> 2.48 \text{ g/cm}^3$, porosity of $< 0.5 \%$, average particle size of $< 15 \mu\text{m}$, Vickers hardness of 31 GPa, knoop hardness of 29 GPa, elasticity of 420 GPa, Weibull modulus of 15m, flexural strength of 450 MPa, compression strength of $> 2800 \text{ MPa}$, poisson number of 0.15, fracture toughness of $5 \text{ MPa}\cdot\text{m}^{0.5}$, coefficient of thermal expansion at $20 \text{ }^\circ\text{C}$ is $4.5 \times 10^{-6}/\text{K}$, specific heat at $20 \text{ }^\circ\text{C}$ is 1 J/gK , thermal conductivity at $20 \text{ }^\circ\text{C}$ is 40 W/mK , specific electrical resistance at $20 \text{ }^\circ\text{C}$ is $1 \Omega\text{cm}$ and purity of $> 99\%$.

3.4 EQUIPMENT

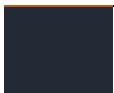
The equipment used for the experimental analysis of the laser metal deposition are as follows: Laser machine connected with kuka robot, coaxial nozzle, powder mixer machine together with hoppers connected to pipes and to the coaxial nozzle, wear test machine, hardness test machine for microhardness test, scanning electron microscopy for microstructure test, optical microscopy test and x- ray diffraction test machine. The equipment are described as follows:





Figure 3. 1: Laser metal deposition machine connected to kuka robot with coaxial nozzle

The laser equipment shown above is highly sophisticated and it was designed to operate at maximum power of 3 KW. Thus, its sensitivity can easily be noticed when the powder is contaminated due to improper cleaning of the hopper and other accessories connected to the laser machine. Also for two powders to be mixed to allow deposition to take place, there is need for powder mixer which contain hoppers of different powder. Figure 3.2 illustrates the powder mixing analyzer connected with two hoppers.



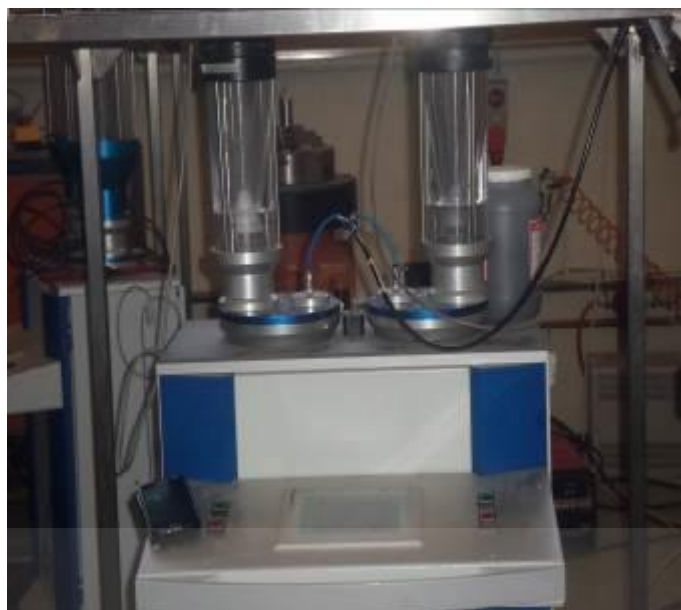


Figure 3. 2: Powder mixer analyser connected with hoppers

3.5 SPECIMEN PREPARATION

Proper specimen preparation is essential if the true microstructure is to be observed, identified, documented and measured. When a specimen is prepared properly, and the structure is revealed properly, or a phase or constituent of interest is revealed selectively and with adequate contrast, then the actual tasks of examination, interpretation, documentation and measurement are generally quite simple [61]. Before deposition process take place on the titanium block, the substrate should be clean and free of surface defects such as scratches or grinding marks. All scratches deeper than the finish produced should be removed by sanding through sandblasting process. Plate products should be free of gross stress raisers, very rough, irregular surface finishes, visible oxide scale and brittle alpha case (diffused-in oxygen layers) to achieve reasonable cold or warm formability. The titanium alloy block or the substrate has to be sandblasted and then cleaned with acetone and dry to roughen the surface and to facilitate laser energy absorption before taking for laser metal deposition process. Sandblasting machine is shown in the Figure 3.3:



Figure 3. 3: Sandblasting machine

3.5.1 Cutting

Bulk samples for subsequent laboratory cutting may be removed from larger pieces using methods such as core drilling, band or hack-sawing, flame cutting, or similar methods. However, when these techniques are used, precautions must be taken to avoid alteration of the microstructure in the area of interest. Laboratory abrasive-wheel cutting is recommended to establish the desired plane of polish. In the case of relatively brittle materials, cutting may be accomplished by fracturing the specimen at the desired location. The most commonly used cutting device in the metallographic laboratory is the abrasive cut-off machine. All abrasive-wheel cutting should be performed wet. An ample flow of coolant, with an additive for corrosion protection and lubrication should be directed into the cut. Wet cutting will produce a smooth surface finish and most importantly will guard against excessive surface damage caused by overheating. Thus, abrasive wheels should be selected according to the manufacturer's recommendations. Specimens must be fixed securely during cutting and however, cutting pressure should be applied carefully to prevent wheel breakage. Some materials such as commercially pure (CP) titanium are quite prone to cutting damage. Figure 3.4 shows the cutting machine used in this research:



Figure 3. 4: Cutting machine

These wheels consist of abrasive particles, mainly alumina or silicon carbide and filler in a binder material that may be a resin, rubber, or a mixture of both resin and rubber. Alumina (aluminium oxide) is the preferred abrasive for ferrous alloys while silicon carbide is the preferred abrasive for nonferrous metals and minerals. Furthermore, wheels (or cutting discs) have different bond strengths and are recommended based on the suitability of their bond strength and abrasive type for the material to be cut. Consequently, as the hardness of a material increases, abrasives become dull more quickly in which the binder must break-down and thereby release the abrasives when they become dull so that fresh abrasive particles are available to maintain the cutting speed and efficiency. Therefore, these wheels are simply known as the consumable wheels because they tend to wear away with usage. In conclusion, optimal cutting with the least damage to the specimen is obtained by keeping the pressure on each abrasive particle in the wheel constant and as low as possible by keeping the contact area between the wheel and the specimen constant and low. This idea is however called the minimum area of contact cutting (MACC) method [61].

3.5.2 Mounting

The primary purpose of mounting the samples is for metallographic preparation such as the grinding and polishing operations, etching and microscopy observation. While a secondary purpose is to protect and preserve extreme edges or surface defects during metallographic preparation. Hence, the method of mounting should in no way be injurious to the microstructure of the specimen in which pressure and heat are the most likely sources of injurious effects. The most common mounting method uses both pressure and heat to encapsulate the specimen with a thermosetting or thermoplastic mounting material. Common thermosetting resins include phenolic (PhenoCure resin), diallyl phthalate and epoxy (EpoMet resin) while methyl methacrylate (TransOptic resin) is the most commonly used thermoplastic mounting resin. Figure 3.5 shows a hot mounting machine used in the metallurgy laboratory:



Figure 3. 5: Hot mounting press

Both thermosetting and thermoplastic materials require heat and pressure during the moulding cycle, but after curing, mounts made of thermoplastic resins must be cooled under pressure to at least 70 °C while mount made of thermosetting materials may be ejected from the mould at the maximum moulding temperature.



Figure 3. 6: Mounted samples

However, cooling thermosetting resins under pressure to near ambient temperature before ejection will significantly reduce shrinkage gap formation. Thermosetting resin mount must never be rapidly cooled with water after hot ejection from the moulding temperature. This idea causes the metal to pull away from the resin producing shrinkage gaps which may promote poor edge retention simply because of the different rates of thermal contraction. Most importantly, mounted specimens are easier on the grinding/polishing surfaces than unmounted specimens [61].

UNIVERSITY
OF
JOHANNESBURG

3.5.3 Grinding and Polishing

Grinding should commence with a rough or plain grit size that establish an initial flat surface and remove the effects of cutting within a few minutes. An abrasive grit size of 180 to 240 (P180 to P280) is coarse enough to be used on rough surface. Hack-sawed, bandsawed, or other rough surfaces usually require abrasive grit sizes in the range of 120- to 180-grit. However, a satisfactory fine grinding sequence might involve SiC papers with grit sizes of 220- or 240-, 320-, 400-, and 600-grit. Thus, all grinding steps should be performed wet provided that water has no adverse effects on any constituents of the microstructure. Wet grinding minimizes specimen heating, and prevents the abrasive from becoming loaded with metal removed from the specimen being prepared. The depth of damage decreases with the

abrasive size but so does the metal removal rate. For a given abrasive size, the depth of damage introduced is greater for soft materials than for hard materials. Hence, for every hard material such as ceramics and sintered carbides, one or more metal-bonded or resin-bonded diamond disks with grit sizes from about 240- to 9- μm can be used. The grinding abrasives commonly used in the specimens' preparation are silicon carbide (SiC), aluminium oxide (Al_2O_3), emery ($\text{Al}_2\text{O}_3 - \text{Fe}_3\text{O}_4$), composite ceramics and diamond. Emery paper is rarely used due to its low cutting efficiency. SiC is more readily available as waterproof paper than aluminium oxide. Furthermore, alumina papers such as PlanarMet Al 120-grit paper, do have a better cutting rate than SiC for some metals. These abrasives are bonded to paper, polymeric or cloth backing materials of various weights in the form of sheets, discs and belts of various sizes. Limited use is made of standard grinding wheels with abrasives embedded in a bonding material. The abrasives may also be used in powder form by charging the grinding surfaces with the abrasive in a premixed slurry or suspension [61]. Figure 3.7 shows an automatic polishing machine with two rotating discs:



Figure 3. 7: Automatic polishing machine with two rotating discs

Polishing is a step in producing a deformation-free surface that is flat, scratch-free, and mirror-like in appearance whereby such a surface is necessary to observe the true microstructure. The polishing technique used should not introduce extraneous structures such as disturbed metal, pitting, dragging out of inclusions or staining. A compatible lubricant should be used sparingly to prevent overheating or deformation of the surface. Intermediate polishing should be performed thoroughly so that final polishing may be of minimal duration.

However, manual or hand polishing is usually conducted using a rotating wheel in which the specimen is being rotated in a circular path counter to the wheel rotation direction [61]. Hence hand-polishing techniques follow the following basic practices:

- **Specimen Movement:** The specimen may be held with one or both hands and it is rotated in a direction counter to the rotation of the polishing wheel. In addition, the specimen is continually moved back and forth between the centre and the edge of the wheel, thereby ensuring even distribution of the abrasive and uniform wear of the polishing cloth.
- **Polishing Pressure:** The correct amount of applied pressure must be determined by the experience. In general, a firm hand pressure is applied to the specimen.
- **Washing and Drying:** The specimen is washed by swabbing with a liquid detergent solution, rinsed in warm running water, then with ethanol, and dried in a stream of warm air. Alcohol can usually be used for washing when the abrasive carrier is not soluble in water or if the specimen cannot tolerate water. However, ultrasonic cleaning may be needed if the specimens are porous or cracked.
- **Cleanness:** The cleanness must be strictly observed to avoid contamination problems. This involves the specimen, the operator's hands, and the equipment.

Furthermore, polishing of specimens usually involves the use of one or more of the following abrasives: diamond, aluminium oxide (Al_2O_3), and amorphous silicon dioxide (SiO_2) in colloidal suspension. With the exception of diamond, these abrasives are normally suspended in distilled-water, but if the metal to be polished is not compatible with water, other suspensions such as ethylene glycol, alcohol, kerosene or glycerol, may be required [61]. In conclusion, pure titanium is soft and ductile, but is very easily damaged when cutting and grinding. Preparation of commercially pure titanium is very difficult, while preparation of the alloys is somewhat easier. Titanium is very difficult to cut and has low grinding and polishing rates.

3.5.4 Etching

Metallographic etching comprises of all the processes used to reveal particular structural characteristics of a metal that are not evident in the as-polished condition. Examination of a



properly polished specimen before etching may reveal structural aspects such as porosity, cracks, and non-metallic inclusions. Thus, microscopic examination of a properly prepared specimen will clearly reveal structural characteristics such as grain size, segregation, shape and size, and distribution of the phases and inclusions that are present. Etching is done by immersion or swabbing a sample in a suitable chemical solution that essentially produces selective corrosion. Swabbing is however preferred for the metals and alloys that form a tenacious oxide surface layer with atmospheric exposure such as stainless steels, aluminium, nickel, niobium, and titanium and their alloys. It is best to use surgical grade cotton that will not scratch the polished surface [61]. Etchants that reveal grain boundaries are very important for successful determination of the grain size. Therefore, Table 3.1 shows the summary of commonly used etchants for both metals and alloys:

Table 3. 1: commonly used etchants for metals and alloys [61]

Composition	Comments
100 ml water 1-3 ml HF 2-6 ml HNO ₃	Kroll's reagent for Ti alloys. Swab specimen 3-10 seconds or immerse specimen 10-30 seconds.
200 ml water 1 ml HF	For Ti, Zr and alloys. Swab or immerse specimen. Higher concentrations can be used but are prone to staining problems.
30 ml lactic acid 15 ml HNO ₃ 30 ml HF	For Ti alloys. Swab specimen up to 30 seconds. Decomposes, do not store. Good for alpha-beta alloys.
10-20 ml glycerol 10 ml HNO ₃ 10 ml HF	For Mo and Mo-Ti alloys. Immerse specimen for up to 5minutes.

Considering the fact that, distilled water was specified and used for laboratory purposes. It is however best to use reagent grade chemicals. Etchants can be quite dangerous and it is advisable to consult with a laboratory technician when dealing with etchants that may be potentially dangerous. For most metals and alloys, etching must be used to fully reveal the microstructure.

3.6 MIXING OF Ti6Al4V-B₄C POWDER

The mixing of titanium alloy, Ti6Al4V and the boron carbide, B₄C powders took place in the mixer connected with hoppers containing each powder. Both powders were mixed at different percentage as prescribed for laser deposition process in which the titanium alloy contains a portion of 80wt % while boron carbide contains a portion of 20wt % to complete the percentage at a powder flow rate of 4rpm for both powders. Furthermore, this mixing took place at constants scanning speed, gas flow rate but at ranges of power according to the processing parameters for the laser deposition process. Processing parameters is given in Table 3.2 shown:

Table 3. 2: Experimental matrix for the laser metal deposition

Sample	Laser Power (W)	Scanning Speed (m/min)	Powder Flow Rate (rpm)	Gas Flow Rate (L/min)
S1	800	1	4	2
S2	1000	1	4	2
S3	1200	1	4	2
S4	1400	1	4	2
S5	1600	1	4	2
S6	1800	1	4	2
S7	2000	1	4	2

S8	2200	1	4	2
S9	2400	1	4	2

Considering the processing parameters to carry out the experimental analysis, only laser power was varied between 800 W to 2400 W with an interval of 200 W for nine samples. Other parameters such as the scanning speed, powder flow rate and gas flow rate were kept at constant value. Thus, Figure 3.3 illustrates how the powders mixture were carried out at different proportion making a total of hundred percent in which 80wt % was allocated to the titanium alloy, Ti6Al4V powder and the remaining 20wt % allocated to boron carbide, B₄C powder to carry out the laser deposition process. Table 3.3 illustrates the powder system with the corresponding mixing proportion.

Table 3. 3: Powders with respective mixing proportion

Powders	Weight Percentage (wt.%)
Ti6Al4V	80
B ₄ C	20

However, deposition process using the laser machine is illustrated in the Figure 3.8 shown. The melt pool was deposited on the titanium alloy substrate at varied power with constants scanning speed, powder flow rate and gas flow rate. Therefore, this surface deposition will then be used for various characterizations such as microstructure, microhardness and wear tests in order to be able to investigate the resistance of the material in a highly stressed condition and exposure to unfavourable chemical and environmental conditions.

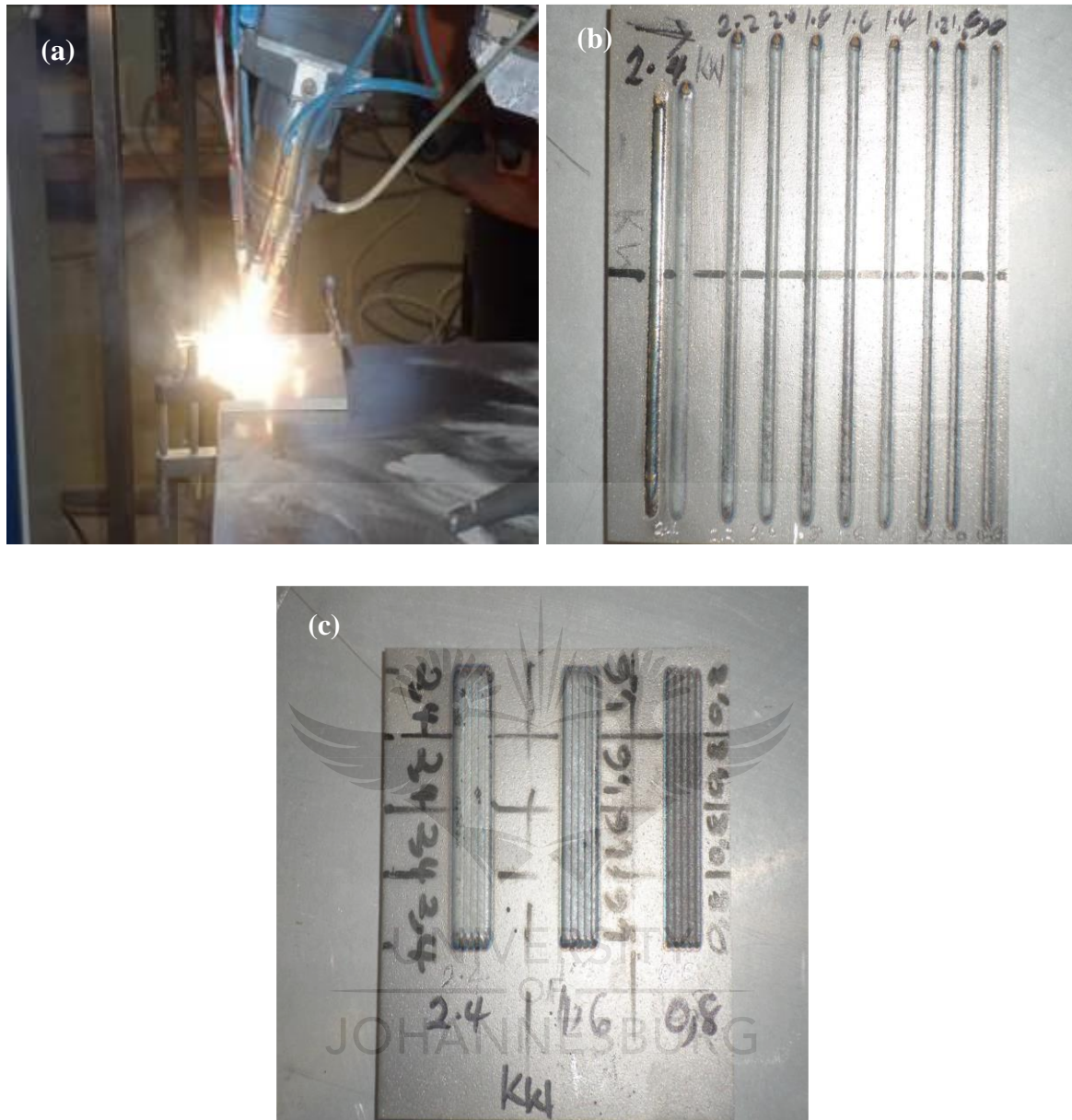


Figure 3. 8: (a) laser deposition process, (b) single track deposition of Ti6Al4V-B₄C composites and (c) multiple track deposition of Ti6Al4V-B₄C composites.

3.7 CHARACTERIZATION OF LASER PREPARED SAMPLES

Laser metal deposited samples or specimens prepared were characterized to determine the microstructure, microhardness, wear, and corrosion behaviours. In addition, various microscopic tests such as scanning electron microscopy (SEM) were carried out with energy dispersion spectroscopy (EDS), optical microscopy (OM), and x-ray diffraction (XRD). The samples for metallurgical examination and microhardness profiling were cut across the

deposition direction. The cut samples were mounted, ground and polished according to the standard metallurgical preparation of titanium and its alloys – ASTM E3-11 [62]. Thus, the polished samples were etched for microstructural examinations using Kroll's reagent according to Taylor and Weidmann, 2008 [63]. The etched samples were studied under the Olympus BX51M Optical Microscope which however revealed the various grain structures.

3.7.1 Scanning Electron Microscopy (SEM)

Scanning electron microscopy (SEM) represents a high performance method used to investigate the structure of a material. It is defined by: easiness to prepare samples to be tested, large diversity of information reached, good resolution associated with high field depth, large and continuous range of magnifying, etc. The examination of microstructures with SEM offers two benefits as compared to optical microscopy (OM): much more resolution and magnification, as well as very large field depth giving the impression that images obtained are outstanding. Thus, the field depth in OM when magnified 1200 times is 0.08 μm , while in SEM at 10000 times magnifying, the field depth is 10 μm . However, SEM is used for observation of specimen surfaces. The topography of the surface can be observed by two-dimensional scanning of the electron probe over the surface. The Figure 3.9 illustrates the capturing microstructural images of a specimen using scanning electron microscopy techniques.



Figure 3. 9: Scanning electron microscope

3.7.2 X-Ray Diffraction (XRD)

X-ray diffraction is one of the most important characterization tools used in solid state chemistry and materials science. X-ray diffraction has been in use for the characterization of crystalline materials and as well as the determination of their structure. Once the material has been identified, x-ray crystallography may be used to determine its structure, i.e. how the atoms pack together in the crystalline state and what the interatomic distance and angle are etc. However, diffraction is a physical phenomenon that consists in electromagnetic waves avoiding obstacles if the size of the obstacles compares to the wavelength. This phenomenon can be applied to the analysis of materials as the atom plans are placed at comparable distances to x-ray lengths. X-rays are electromagnetic waves similar to light, but whose wavelength is much shorter ($\lambda = 0.2 - 200 \text{ \AA}$). XRD is produced as a reflexion at well-defined angles. Every crystalline phase has its own diffraction image in which the diffraction image depends upon the material structure. The diffraction methods allow for the performance of the following studies: the determination of the crystalline structures, the phase quantitative and qualitative analysis, the study of phase transformations, the study of the crystallographic

texture, the size of the crystallites, and the internal stresses in the sample [64]. The Figure 3.10 illustrates the x-ray diffraction equipment:



Figure 3. 10: X-ray diffraction machine

3.7.3 Optical Microscopy

In principle, optical microscopes may be used to look through specimens ('in transmission') as well as at them ('in reflection'). Many materials, however, do not transmit light and so we are restricted to looking at the surface of the specimens with an optical microscope. The most commonly used microscope is the conventional light microscope. Microscopes are required for the examination of the microstructure of the metals and alloys. Optical microscopes are used for resolutions down to roughly the wavelength of light (about half a micron). With optical microscopy, the light microscope is used to study the microstructure in which optical illumination systems are its basic elements. For materials that are opaque to visible light (all metals, many ceramics and polymers), only the surface is subject to observation, and the light microscope must be used in a reflective mode. Contrasts in the image produced result from differences in reflectivity of the various regions of the microstructure. Thus, Figure 3.11 shows the physical arrangement of the optical microscopy:



Figure 3. 11: Optical Microscope

A careful and meticulous surface preparations are necessary to reveal the important details of the microstructure. The specimen surface must first be ground and polished to a smooth and mirror-like finish which is accomplished by using successively finer abrasive papers and powders. The microstructure is revealed by a surface treatment using an appropriate chemical reagent in a procedure termed etching. The etching reagents depend on the material used and after etching the specimen must be washed with alcohol and ether to remove the grease [65]. In a situation whereby the microstructure of a two phase alloy is to be examined, an etchant is chosen that produces a different texture for each phase so that the different phases may be distinguished from each other. In conclusion, optical microscopy can give information concerning a material's composition, previous treatment and properties. For instance, microstructural features commonly observed are:

- Grain size,
- Phases present,
- Distribution of phases,
- Chemical homogeneity, and
- Elongated structures formed by plastic deformation.

However, the examination of materials by optical microscopy is essential in order to understand the relationship between properties and microstructure. Useful information can be gained by examination with the naked eye of the surface of metal objects or of polished and etched sections. Structures which are coarse enough to be discernible by the naked eyes are termed macrostructures and for those which require magnification to be visible are termed microstructures.

3.8 MICROHARDNESS PROFILING

The microhardness characterization was performed on a digital microhardness tester of Vickers hardness machine. The hardness testers cover a unique test load range, suitable for many applications. The main purpose of the hardness test is to determine the ‘suitability’ of a material, or the particular treatment to which the material has been subjected. However, the hardness test is typically performed by measuring the ‘depth of indenter penetration’ or by measuring the ‘size’ of an impression left by an indenter, i.e. Vickers, Knoop and Brinell. Thus, the polished samples were indented using the digital microhardness Vickers hardness indenter. The indentation was carried out at a load setting of 500g and a dwell time of 15 seconds. However, the space between indentations was maintained at a distance of 10 μ m between each indentation throughout the hardness tests and at each interval ten indentations were taken and the average values were also recorded on each samples according to ASTM E384-11e1, 2011 [66]. Figure 3.12 illustrates the microhardness indenter used in this research:



Figure 3. 12: Digital Microhardness Indenter

3.9 WEAR ANALYSIS

The dry sliding wear tests were carried out using ball-on-disc tribometer equipment called CETRUMT-2 which operates with linear reciprocating motion drive. Measuring and evaluating the wear volumes and wear rates of respective samples, ball-on-disc tests were performed on the UNIVERSAL MICRO MATERIALS TESTER (UMT-2), produced by Centre for Tribology, Inc. (CETR), USA. However, the wear tests were performed using a tungsten carbide ball of about 10mm diameter with a constant stroke length of 2mm together with application normal load of 25N. Thus, the frequency for the reciprocating spindle was maintained at 5Hz together with speed of 5mm/s which was also maintained throughout the tests. Therefore, the dry sliding wear tests were carried out on the single track deposited samples of B₄C-Ti6Al4V composites according to the ASTM G133-05 [67]. Figure 3.13 shows the tribometer equipment used in carrying out dry sliding wear tests:



Figure 3. 13: CETRUMT-2 Tribometer

The coefficient of friction (COF) was observed during sliding process at a total time of 1000 seconds which was approximately 17 minutes allocated period per sample. For coefficient of friction, the average value from the plot was observed. Also, wear behaviour was however increased with time. The samples for the wear test were prepared according to the ASTM G133-05 specifications.

3.10 SUMMARY

In conclusion, the aim of this research was to carry out laser metal deposition (i.e. laser-cladding) on titanium alloy substrate, Ti6Al4V with boron carbide, B₄C metal matrix composites using hardness, wear and corrosion as criteria. Thus, B₄C metal matrix composite was developed on titanium alloy, Ti6Al4V as substrate with the aim of improving the hardness and wear properties by laser-cladding technique using a Rofin Sinar, Kuka Robot 3.0 KW maximum power output Ytterbium fibre laser system.

CHAPTER FOUR

RESULTS AND DISCUSSION

4.1 INTRODUCTION

The results obtained from this present study are presented and discussed in this section. The material characterizations include microstructure, microhardness, wear and corrosion of the composites deposited. However, the results obtained from optical microscopy (OM), scanning electron microscopy (SEM) with energy dispersion spectroscopy (EDS) as well as x-ray diffraction (XRD) were therefore analysed and reported accordingly.

4.2 PHYSICAL APPEARANCES OF DEPOSITIONS

The physical appearance of the laser deposited composites ($B_4C-Ti6Al4V$) is illustrated in Figure 4.1. From the single track deposition as shown, it was observed that the width of deposit increased as the laser power increases. The length of 90mm was observed for the samples from S1 to S8 while the length of 80mm was also observed for sample S9 in which the width for deposited coatings were increased between 2mm and 3mm. On the other hand, the multiple track depositions shown in Figure 4.2 were characterized with 60mm length and 10mm width with 50% overlapped.

The microstructure of the surface was observed to have coarse structure and gradually changes to fine and smooth surface structures as the laser power increases, the powders also characterized with a good deposit and a desirable melt pool during the deposition process as the laser power constantly increases.



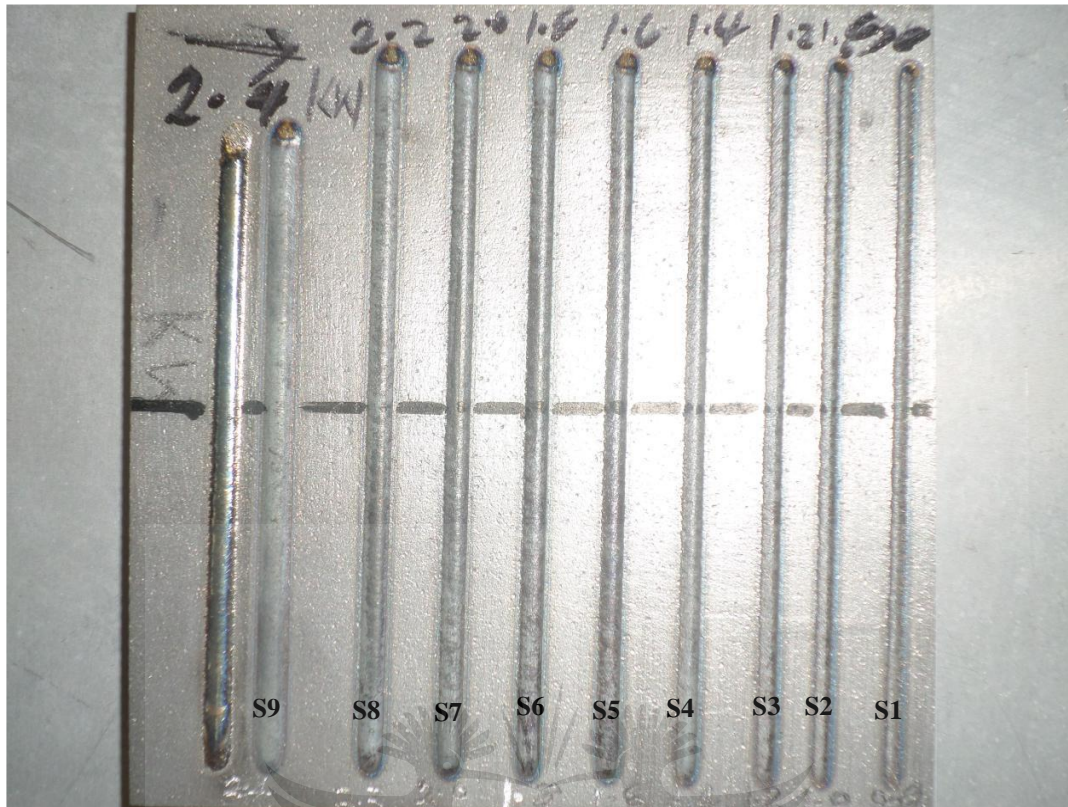


Figure 4. 1: The photograph of single track laser metal deposited samples S1-S9 on the substrate

The single track deposition of Figure 4.1 shows sample S1 to S9 with different parameter for each deposition in terms of laser power increasing from S1 to S9 in which other parameters such as scanning speed, powder flow rate and gas flow rate were kept constant throughout the deposition. Sample S1 and Sample S2 deposited with 800 W and 1000 W were observed to have pores which may be due to the laser power not enough to melt the powders in the melt pool during the deposition process. However, the bonding between the coating and the substrate appears physically good and their thickness also observed to be different as the laser power increases from samples S1 to S9 respectively. On the other hand, when considering the multiple track deposited on the substrate as shown in Figure 4.2:

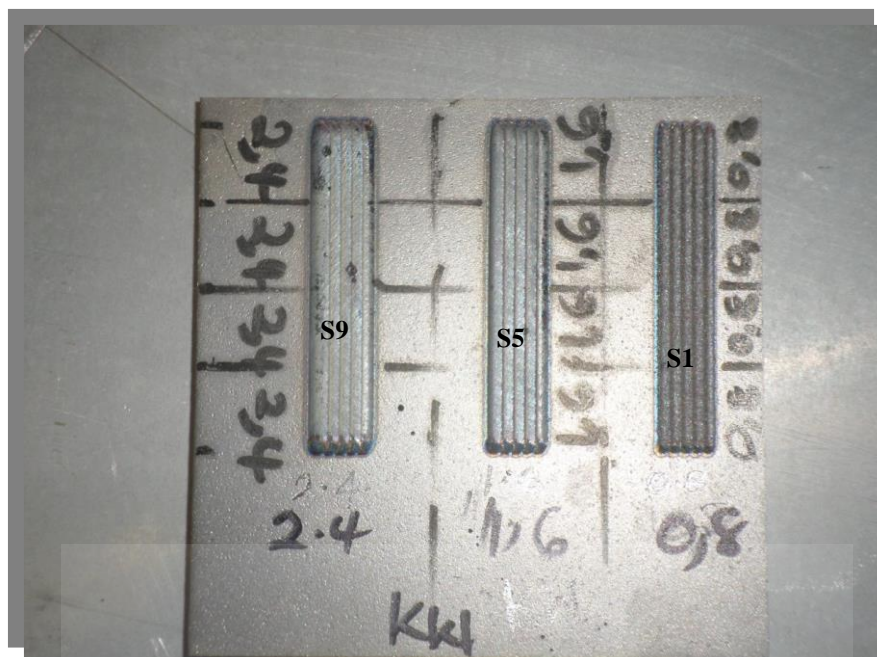


Figure 4. 2: The photograph of multiple track laser metal deposition of samples S1, S5 and S9

4.3 GEOMETRICAL ANALYSIS AND CHARACTERIZATION

The dilution analysis of the deposits were observed with the help of optical microscope by measuring the height, width and area of the clad as well as the heat affected zones for each deposition in order to determine the dilution rate. In order to study the effect of the laser power on the dilution rate, the thickness of the composite layers and the dilution layer were measured from the samples at low magnification using optical microscope. Dilution simply means the mixing of the deposit and the substrate material. Thus, the dilution thickness was obtained by subtracting the composite layer thickness from the total deposition length i.e., dilution thickness equals (total deposition length) minus (composite layer thickness) measured under the optical microscope. For the microstructure and geometrical quantities of the coatings to be analysed, metallographic samples were prepared and sectioned. These samples were prepared according to standard mechanical polishing procedures and then etched using Kroll's solution of 100 ml i.e. 92% distilled water (H₂O), 3 ml i.e. 2.75% hydrofluoric acid (HF) and 6 ml i.e. 5.5% nitric acid (HNO₃). However, for single laser track geometrical characterization in which the main variables of the cross section of laser track were measured according to Figure 4.3 shown.

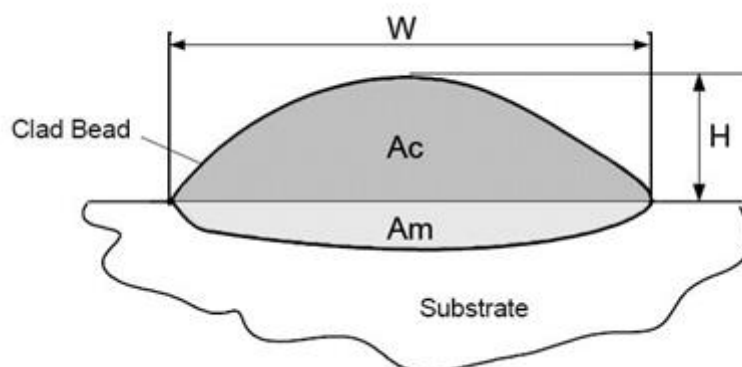


Figure 4. 3: Schematic view of cross section morphology of a single laser clad track showing main geometrical quantities [73]

These variables are given as follow: clad height H (μm), clad width W (μm), clad area A_c (μm^2) and molten area A_m (μm^2). Similarly, heat affected zone height and width were also measured. Thus, the dilution as well as aspect ratio were calculated whereby dilution, $D = A_m / (A_c + A_m)$ and aspect ratio, $AR = W/H$. Carcel et al. [73], observed that the most important geometric characteristics of a laser track are dilution and aspect ratios. The aspect ratio is described as the quantity which is related with the appearance of porosity and crack in the overlapping tracks. Therefore, in order to ensure a good overlapping, aspect ratio between 3 and 5 is recommended [73]. On the other hand, dilution quantifies the relative amount the substrate material that has been molten during the cladding process and mixed with the clad material. However, the aim of laser cladding is to cover one metal with another whereby reinforcing properties such as hardness or wear of the composite which form an interfacial bond without diluting the cladding metal with substrate material giving that dilution may degrade coating properties. Beneficially, some dilution may be required to guarantee a good metallurgical bond [73]. As shown in Figure 4.4 which illustrates the measurement of different samples at low magnification of 5x using optical microscope. On the other hand, Table 4.1 shows the processing parameters and geometrical quantities of single laser tracks for different samples carried out under the deposition process and dilution analysis.

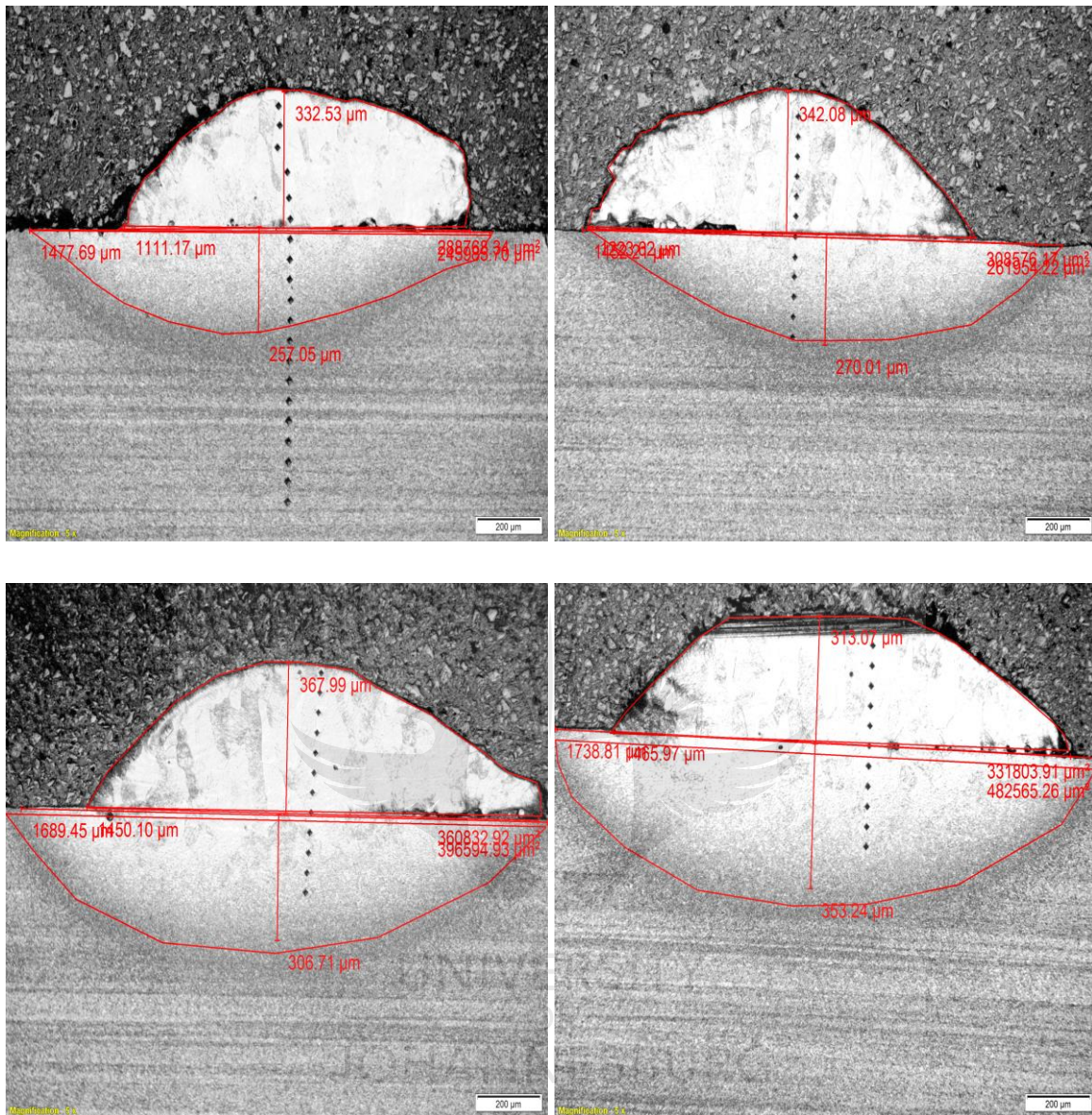


Figure 4. 4: Optical micrographs showed geometrical measurement for different composites

The dilution ratio evaluation to determine the rate of dilution as well as the various aspect ratios after deposition were carried out using the following equations expressed as:

$$D = \left(\frac{A_m}{A_m + A_c} \right) \times 100 \quad (4.1)$$

$$AR = \frac{W}{H} \quad (4.2)$$

Where, D = dilution ratio

Ac = clad area

W = clad width

Am = molten area

AR = aspect ratio

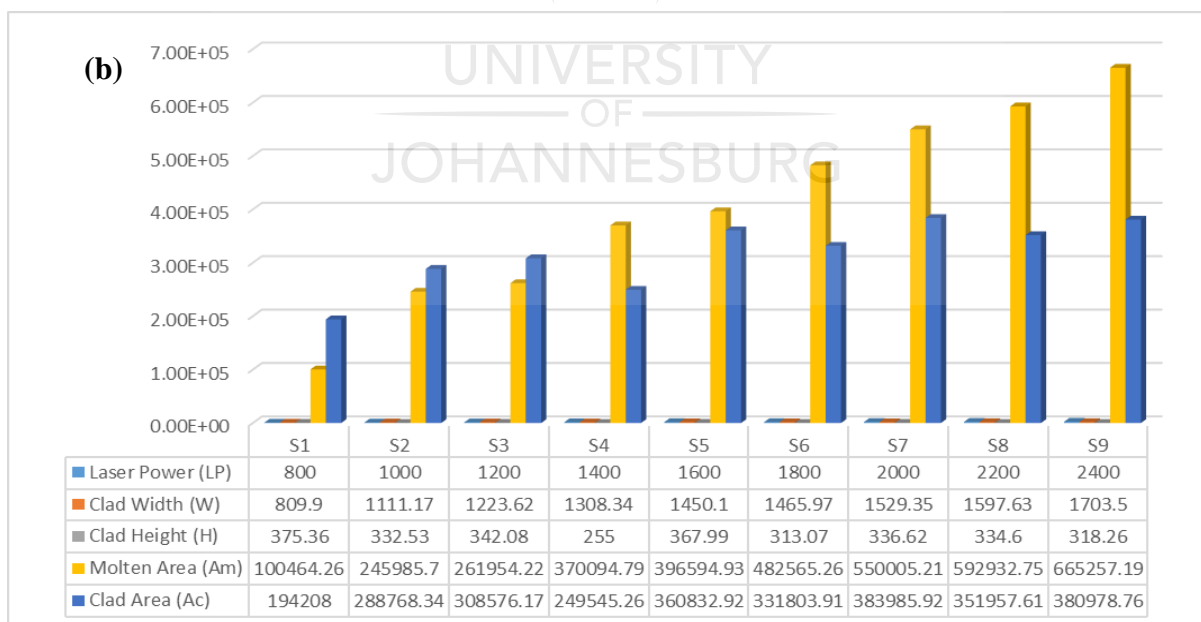
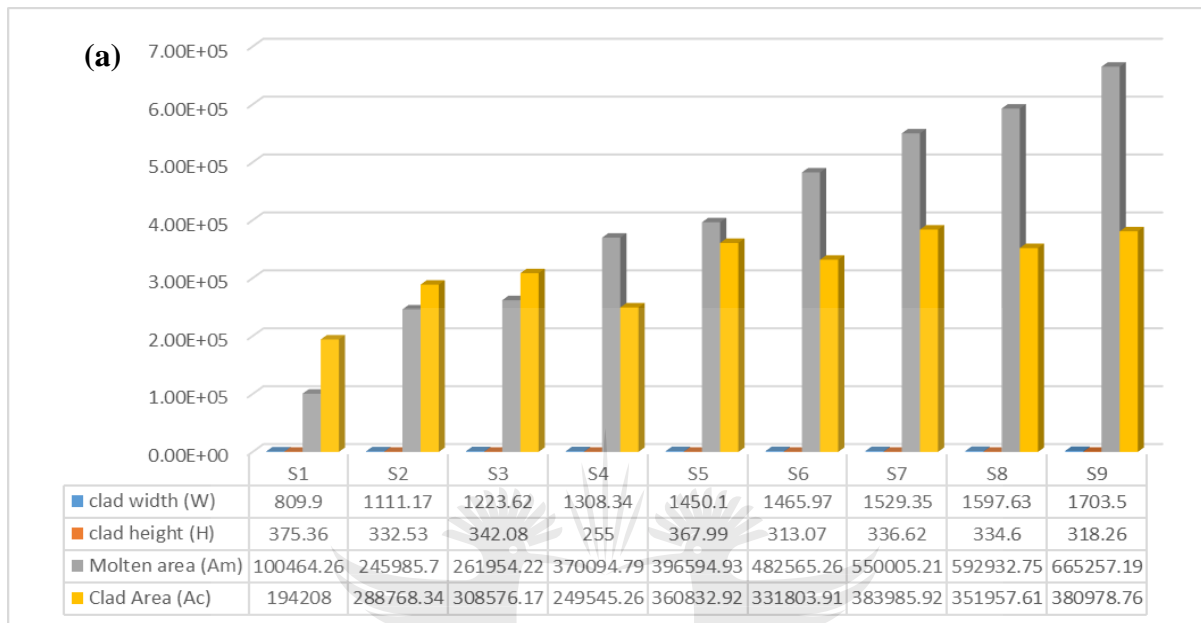
H = clad height

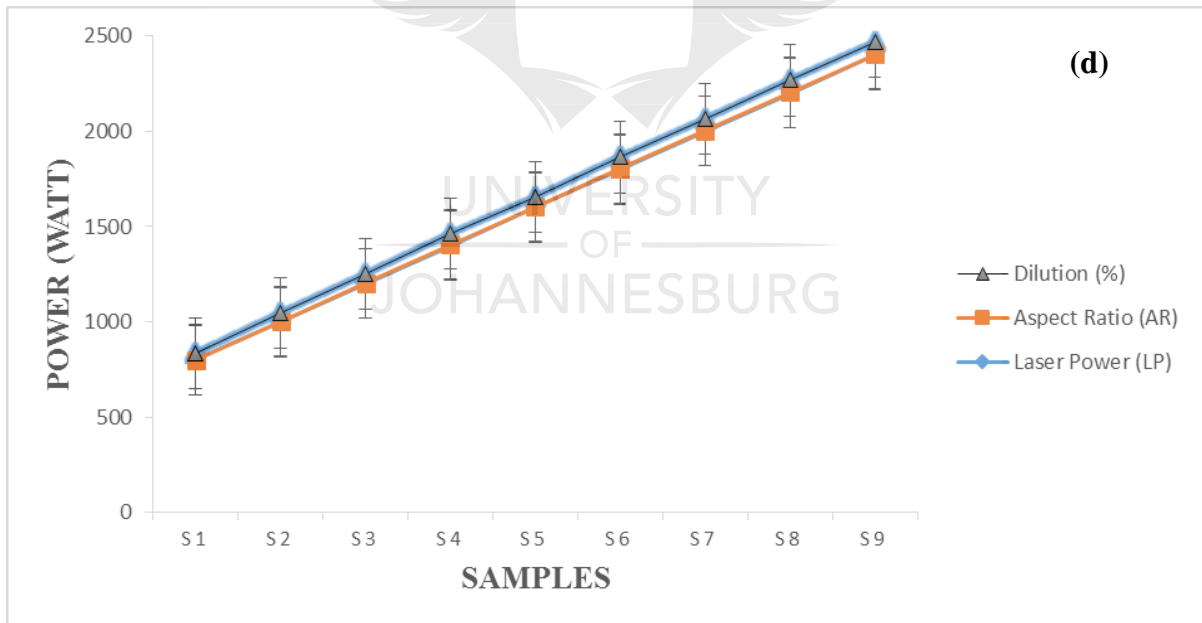
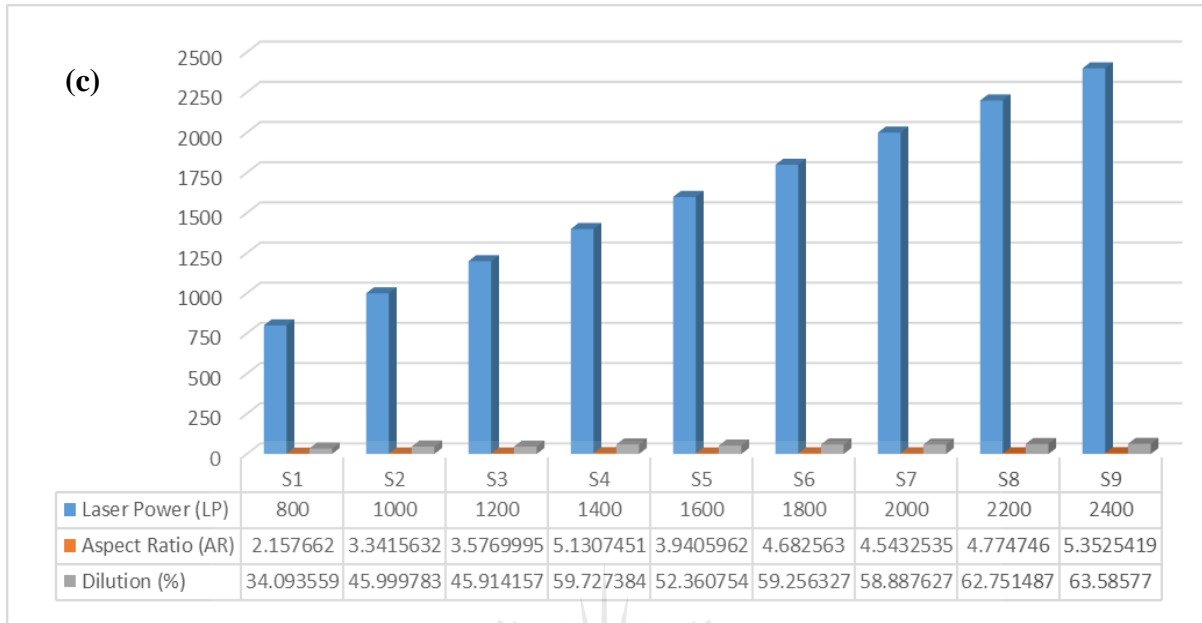
Furthermore, Table 4.1 shown however illustrates the variations in both dilution and the aspect ratios of the clad bead deposition.

Table 4. 1: Processing parameters and geometrical quantities of single laser tracks

Samples	Laser Power (W)	Scanning Speed (m/min)	Powder Flow Rate (g/min)	Gas Flow Rate (l/min)	Clad width, W (μm)	Clad height, H (μm)	Molten area, Am (μm^2)	Clad area, Ac (μm^2)	Aspect Ratio, AR	Dilution, D (%)
S1	800	1	6.68	2	809.90	375.36	100464.26	194208.00	2.16	34.09
S2	1000	1	6.68	2	1111.17	332.53	245985.70	288768.34	3.34	46.00
S3	1200	1	6.68	2	1223.62	342.08	261954.22	308576.17	3.58	45.91
S4	1400	1	6.68	2	1308.34	255.00	370094.79	249545.26	5.13	59.73
S5	1600	1	6.68	2	1450.10	367.99	396594.93	360832.92	3.94	52.36
S6	1800	1	6.68	2	1465.97	313.07	482565.26	331803.91	4.68	59.26
S7	2000	1	6.68	2	1529.35	336.62	550005.21	383985.92	4.54	58.89
S8	2200	1	6.68	2	1597.63	334.60	592932.75	351957.61	4.77	62.75
S9	2400	1	6.68	2	1703.50	318.26	665257.19	380978.76	5.35	63.59

Thus, the following Figures shown illustrate the behaviour of both aspect ratio and dilution as the laser power of the coatings increases.





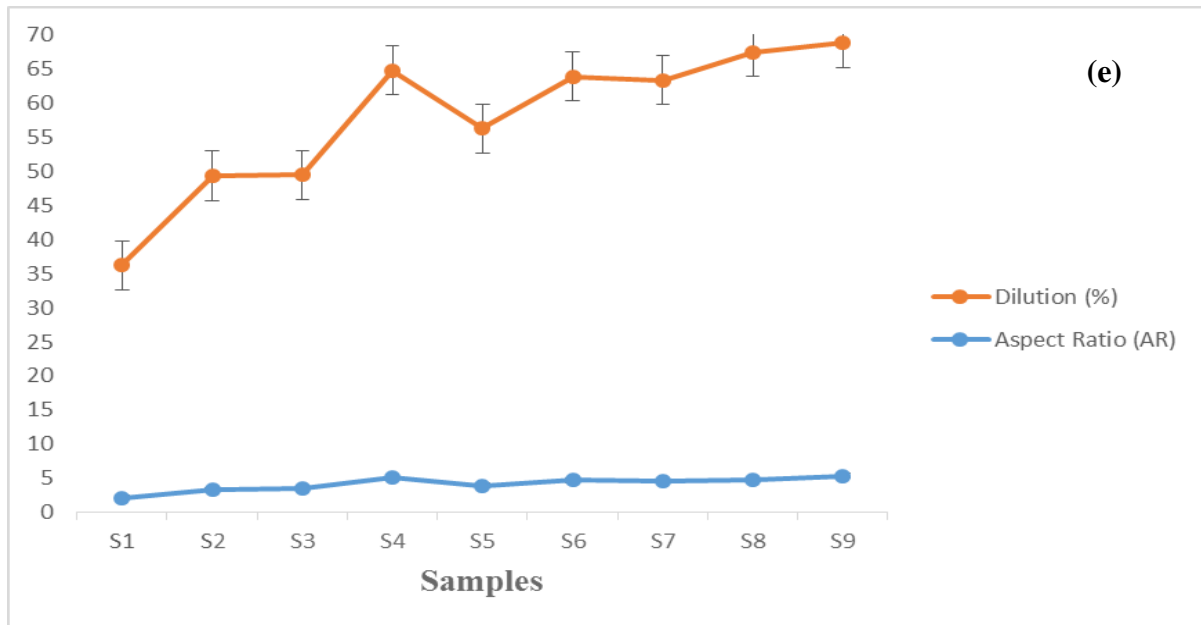


Figure 4. 5: Dilution ratio of B₄C-Ti6Al4V single clad track composite coatings

From this preliminary optimization tests, samples 1, 2 and 3 corresponding to samples S1, S2 and S3 which however correspond to the laser power of 800 W, 1000 W and 1200 W respectively and to a scanning speed of 1 m/min with powder flow rate of 6.68 g/min and gas flow rate of 2 l/min, dilution of approximately 34% and 46% with aspect ratio of 2.16 as well as between 3.34 and 3.58 were the best in terms of defectology for the combined with acceptable geometrical characteristics. These results are similar to what was obtained by Carcel et al. [73]. In conclusion, as the laser power of the coatings increases, dilution also increases which obviously characterized by the higher proportion of titanium alloy as a result of the heat input from the laser machine that corresponds to the power output of the molten pool which consequently caused increase in the dilution ratio.

4.4 MICROSTRUCTURAL EVALUATION

The microstructure of the substrate is characterized by the alpha and the beta phases as shown in Figure 4.6(a). The alpha phases are the light snow-flakes grain structures while the beta phases are the dark snow-flakes grain structures. However, alpha phase dominates more grain structures than the beta phase and alpha phase was characterized by hard particles while the

beta phase on the other hand was characterized by the soft particles. This is due to the fact that the laser power of 800 W and 1000 W respectively for the deposited composites shown in Figures 4.6 (b) and (c) were not enough to provide adequate heat input to fuse the deposit to the surface of the substrate. Defects were also observed such as porosity in the clad, and it was observed as a result of the low laser power used to create the melt pool on the substrate. However, observation of the coating surface microstructure indicated the lamellar packing, which was associated with deposition process. Oxidation was noted to occur at the surface of the deposition. Therefore, there were two kinds of pores observed after the deposition process, one was open pores that existed in the contact area between layer and layer, and the other was the closed pores that existed inside the melted particles. Thus, these pores were associated with decrease in laser power during deposition process. Also, these pores could have experienced entrapment of gas such as oxygen which may have been reacted with carbon to form carbon-oxide gas during the laser metal deposition (LMD) process.

However, merely looking at the Figure 4.6 (b), (c) and (d), it shows that there is a poor bonding between the deposited clad bead and substrate which may be characterized by some boron carbide particles could have hindered the free flow of titanium alloy during deposition process. On the other hand, poor bonding may be due to certain larger size of boron carbide particles in the melt pool hindering the movement of titanium alloy and creating void at the interface at some certain positions. It was noted that within the deposition interface, there were many unmelted entrapped particles in which these were however observed to be solid boron carbide particles that did not melt together with the deposited material during the LMD process. Thus, this can be correlated with the high melting temperature of boron carbide which is between 2500 °C and 2700 °C. Hence the heat output or laser power was not sufficient enough to melt the boron carbide particles completely before solidification of deposited clad bead.

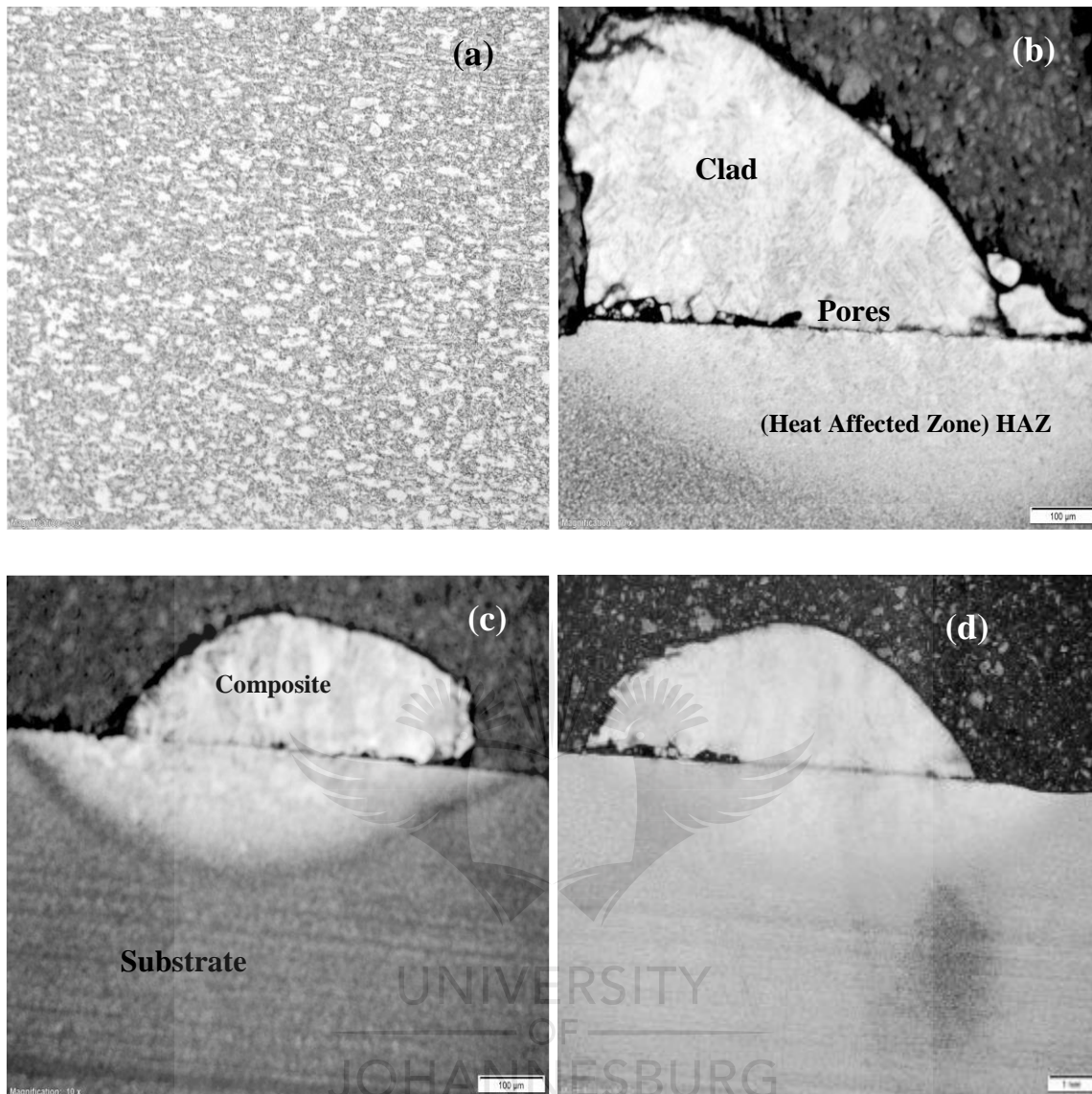


Figure 4. 6 : (a) Optical microstructure of the substrate, (b), (c) and (d) Macrographs of B₄C-Ti₆Al₄V composites deposited with laser power of 800 W, 1000 W and 1200 W

4.4.1 Microstructural Characterization

The microstructures of samples S1 to S9 were observed at low and high magnifications under the optical microscope in the metallurgy laboratory. The following micrographs show various images at different magnifications.

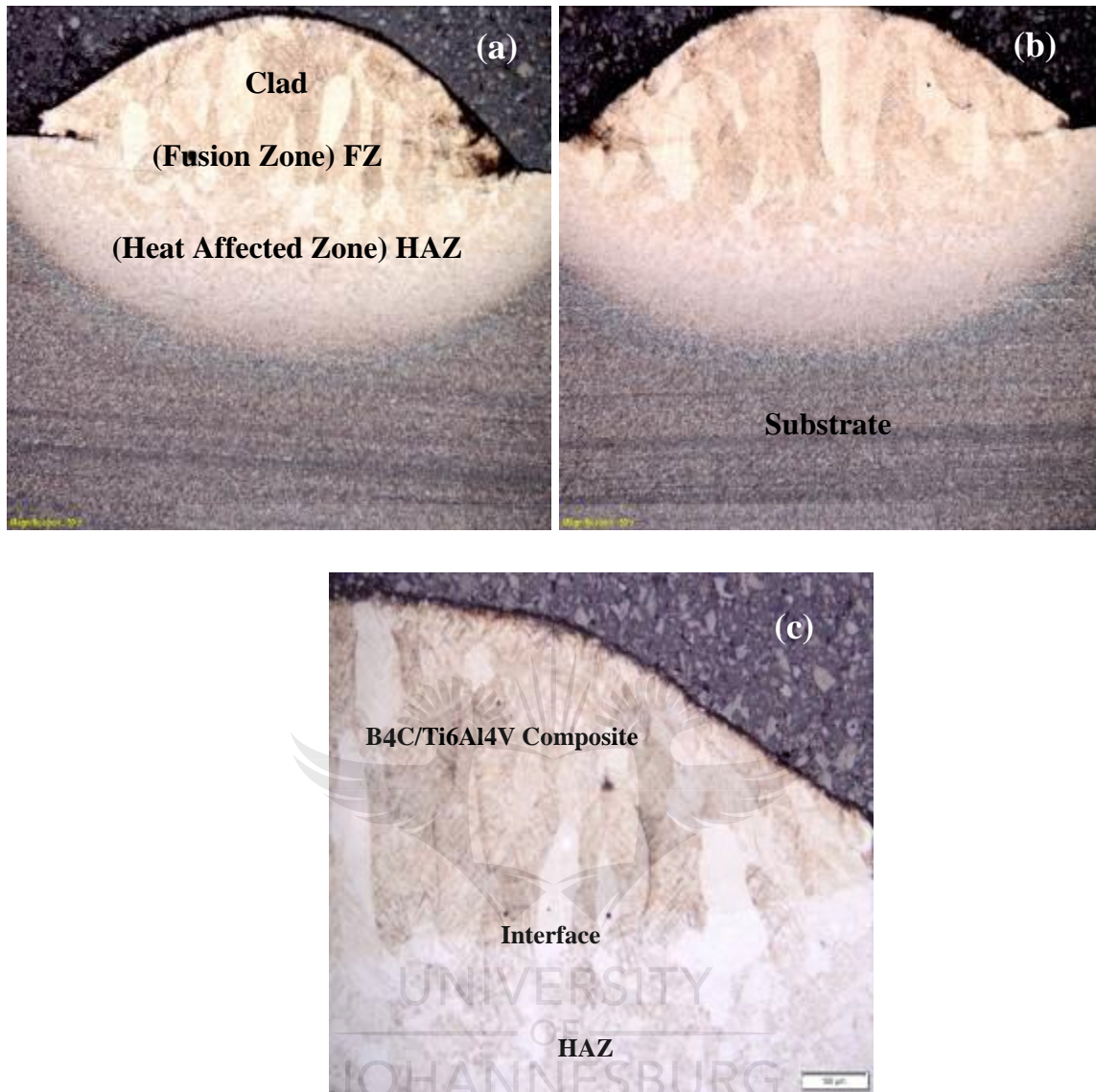


Figure 4. 7: Optical micrographs of laser deposited Ti6Al4V-B4C composites deposited at varying laser powers, (a) 2000 W; (b) 2200 W; (c) 2400 W

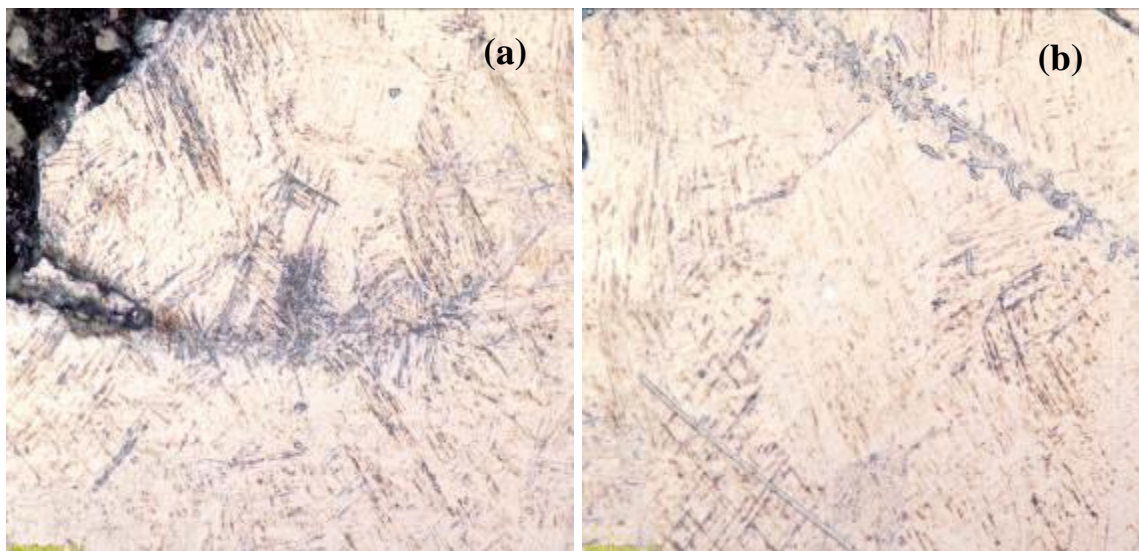
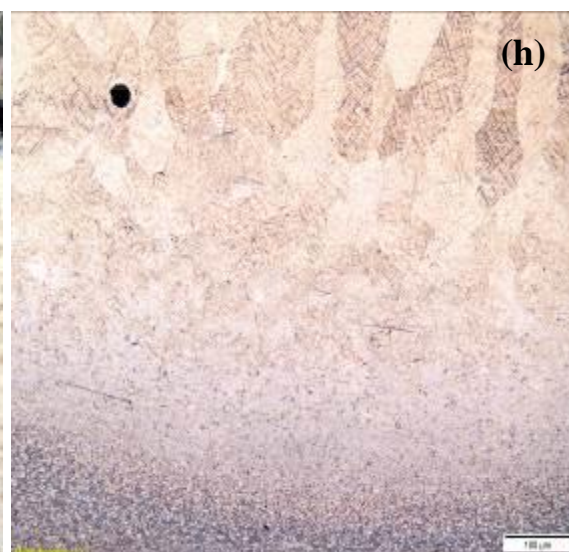
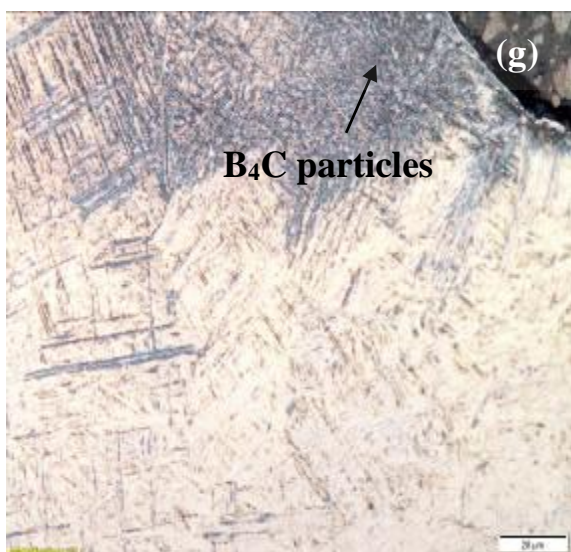
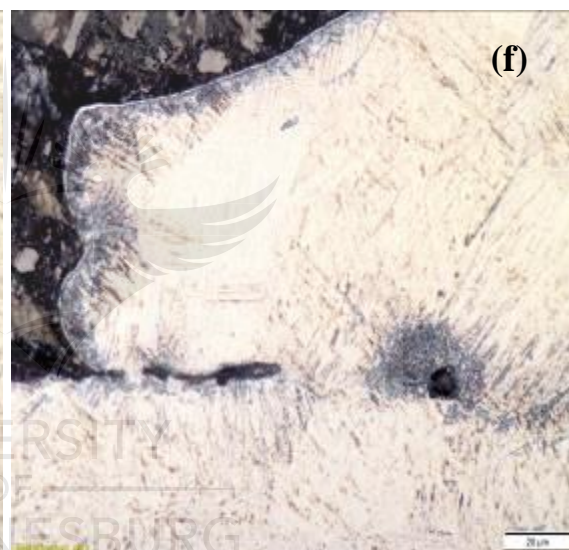
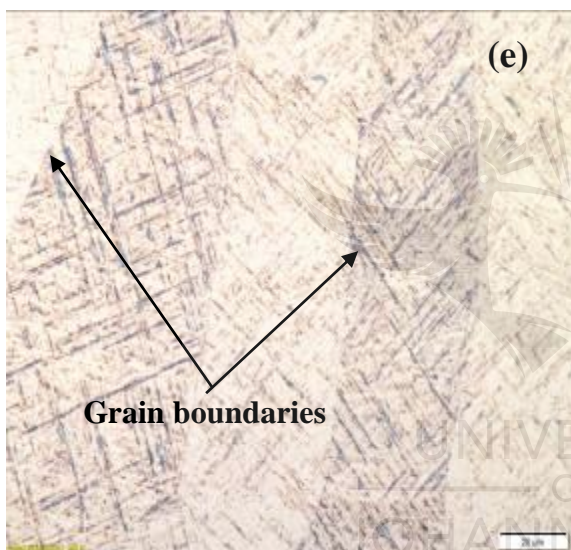
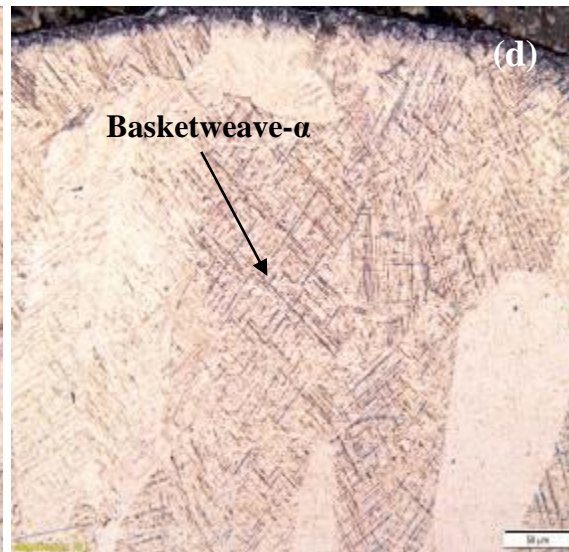
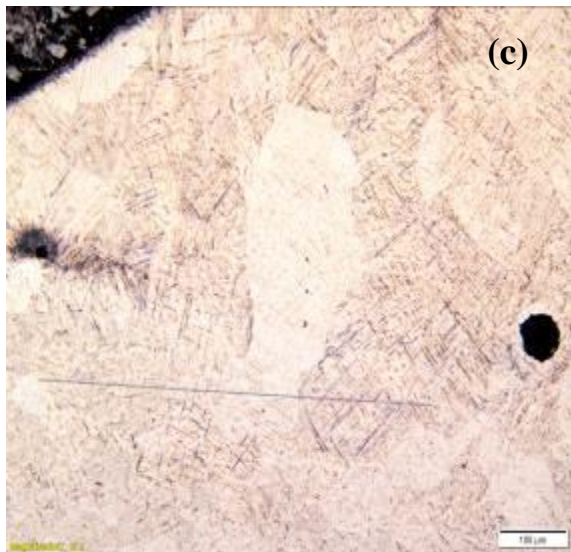


Figure 4. 8: Optical micrographs of B₄C-Ti6Al4V composite deposited at 1800 W laser power





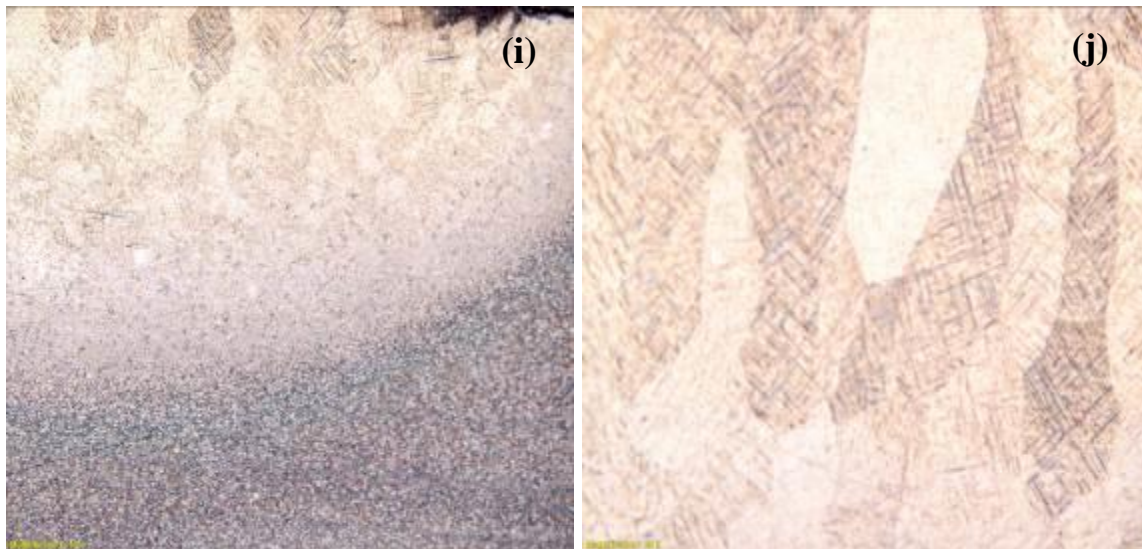
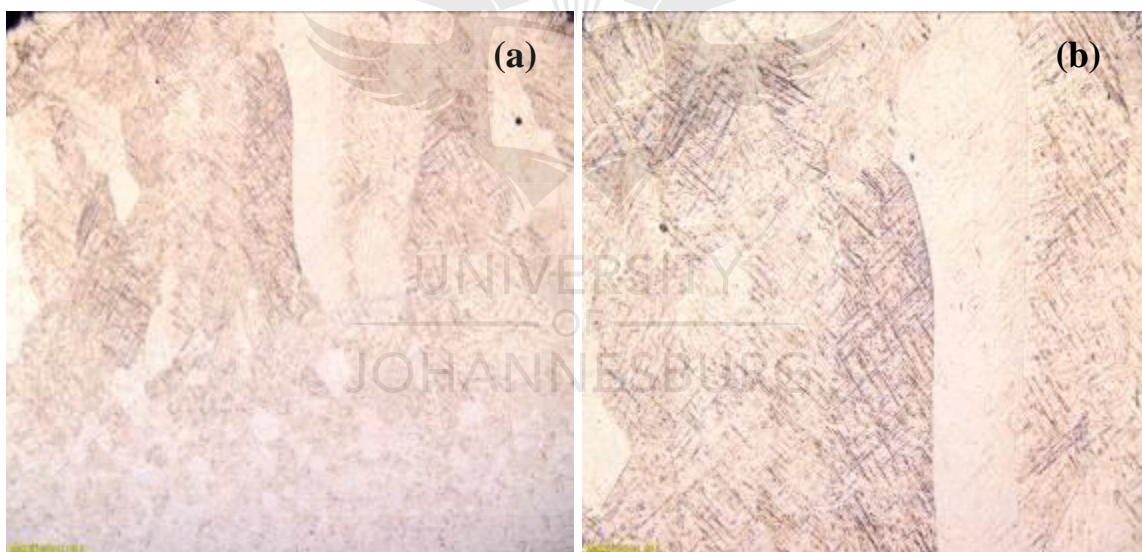
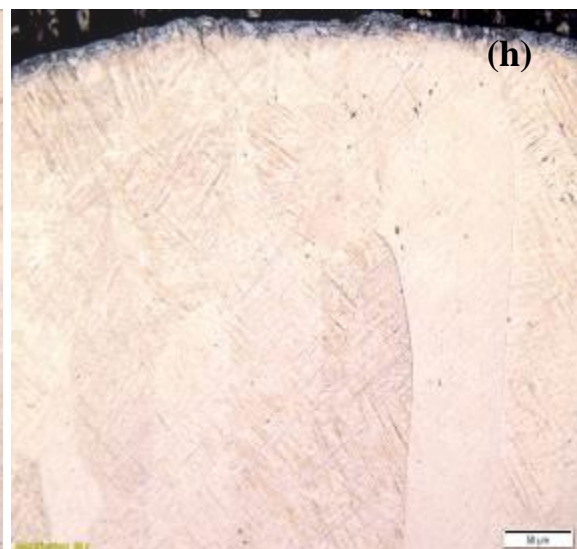
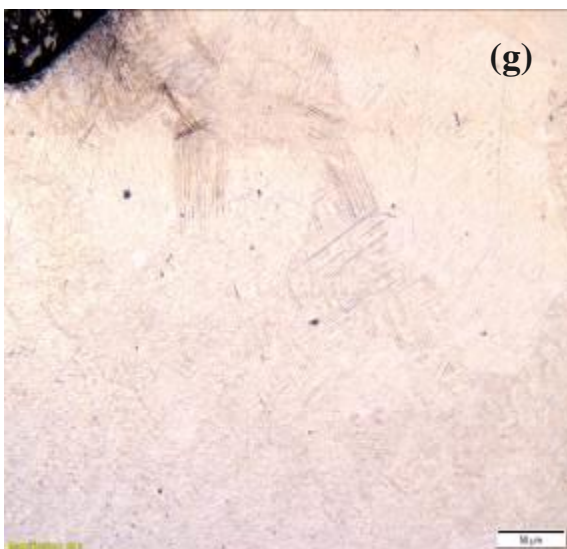
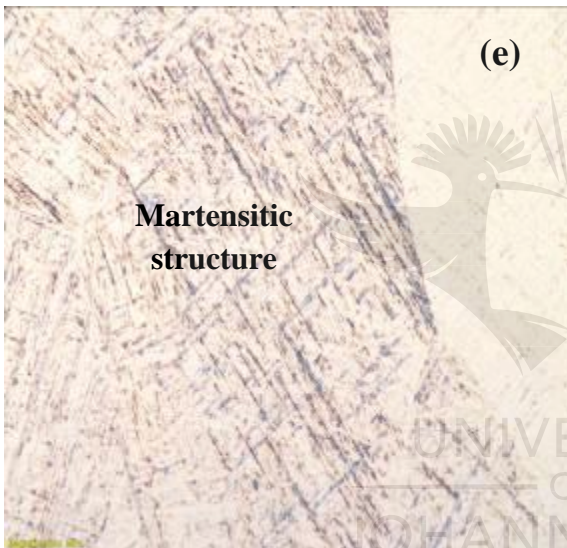
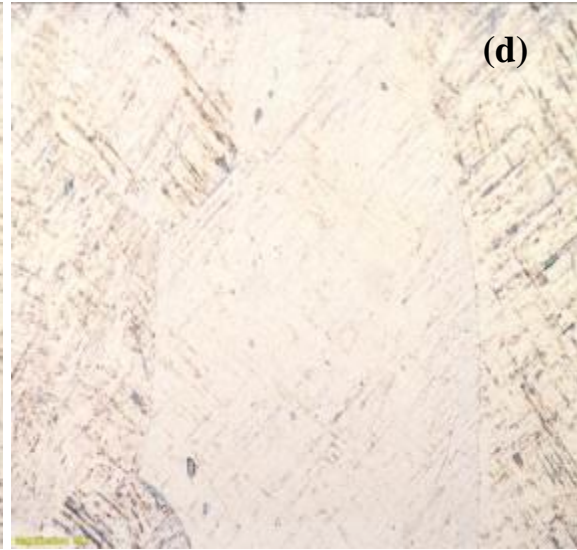
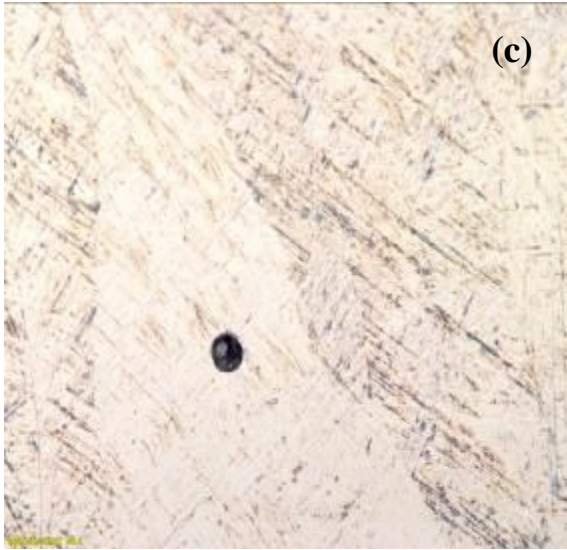


Figure 4. 9: Optical micrographs of B₄C-Ti6Al4V composite deposited at 2000 W laser power





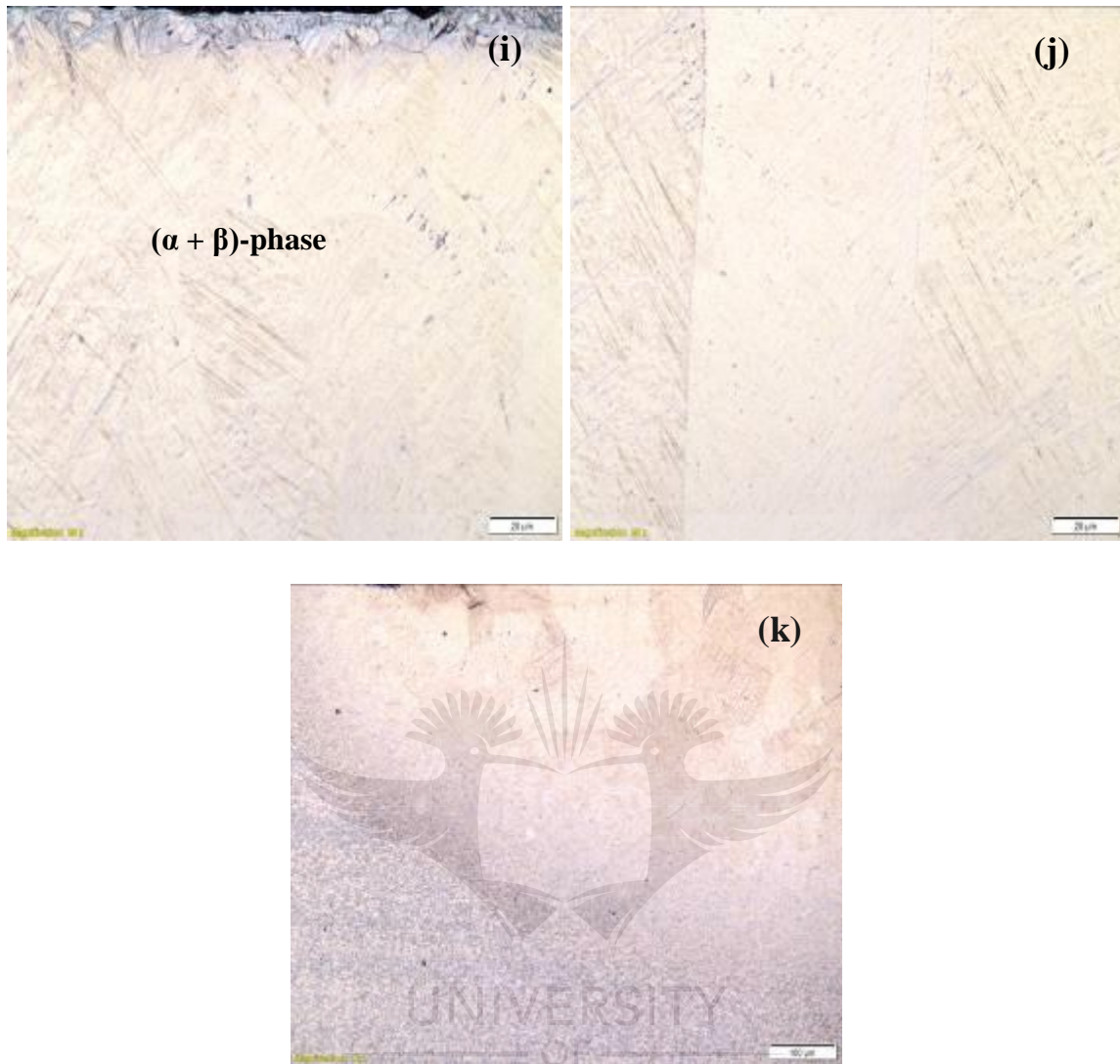
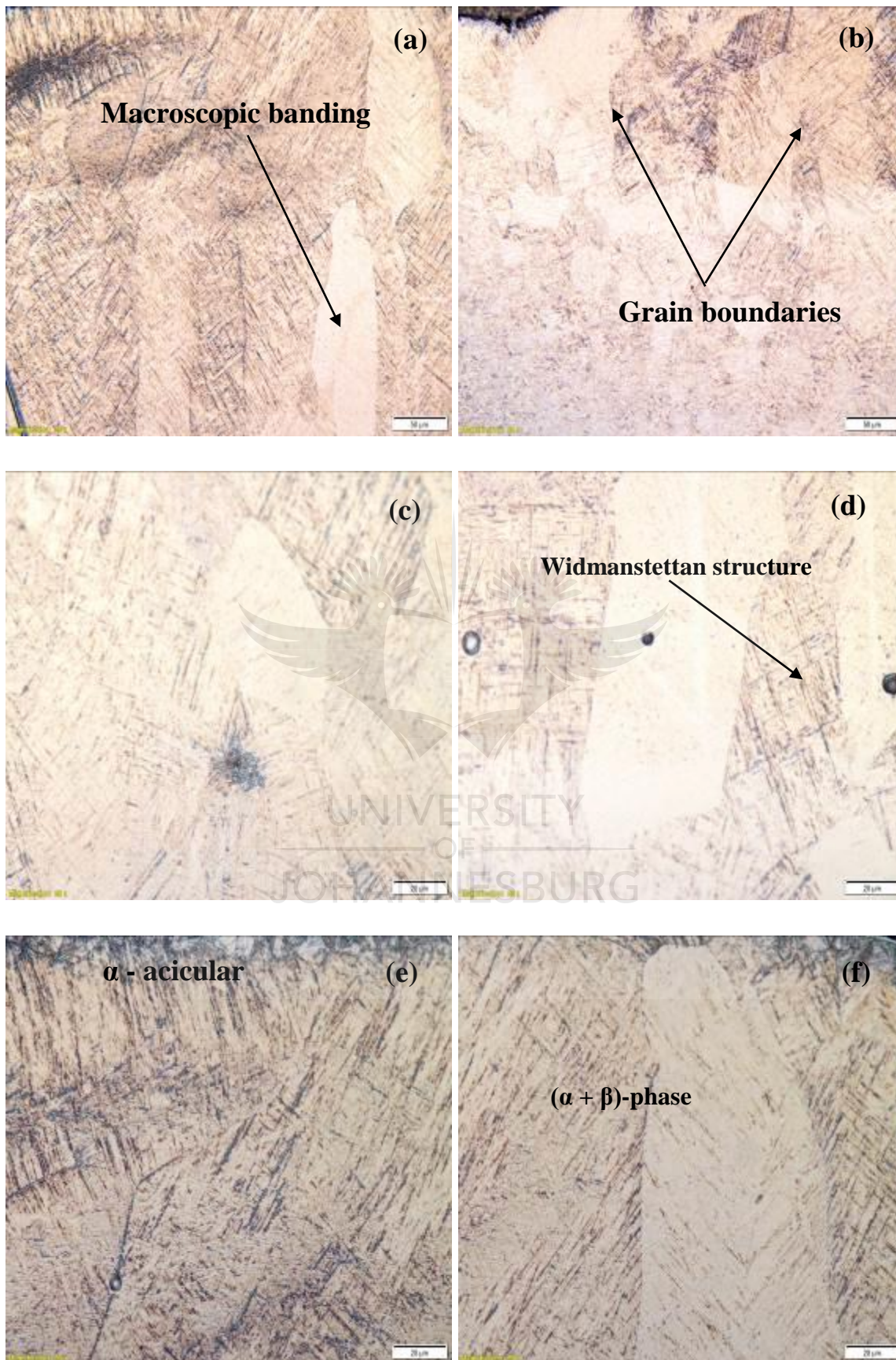
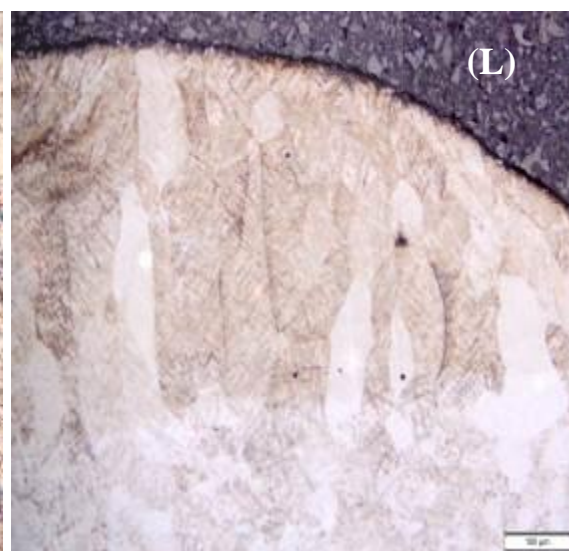
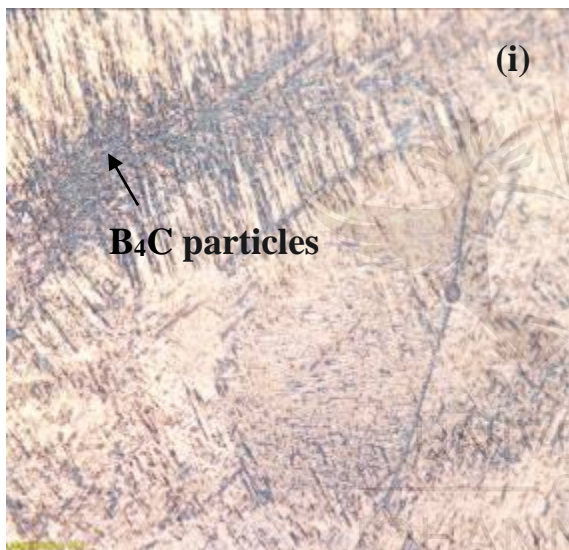
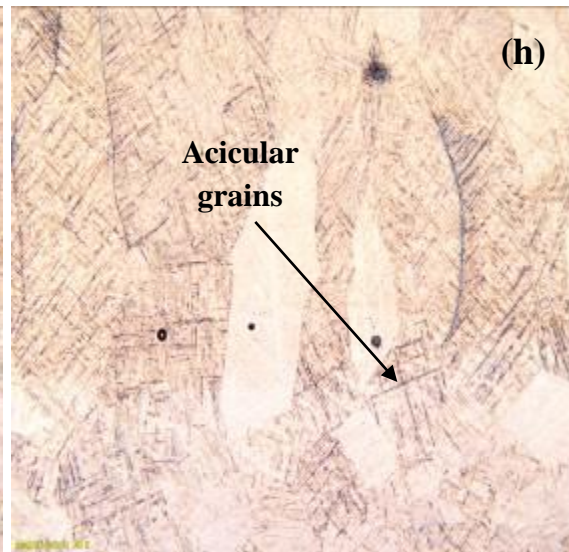
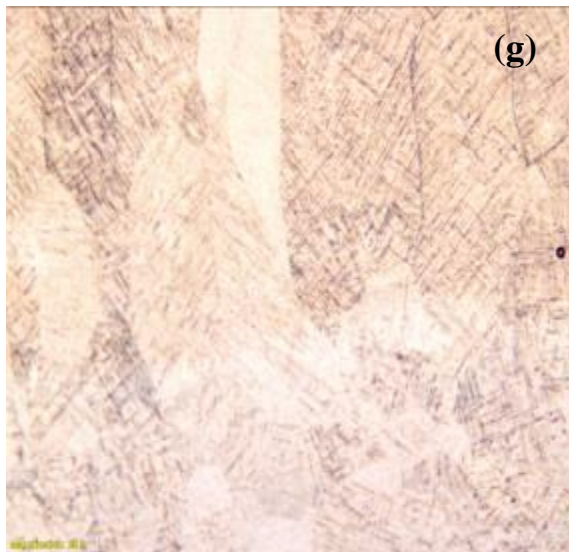
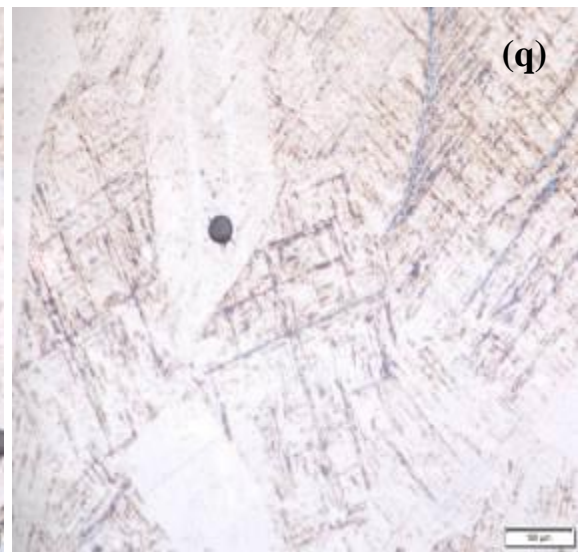
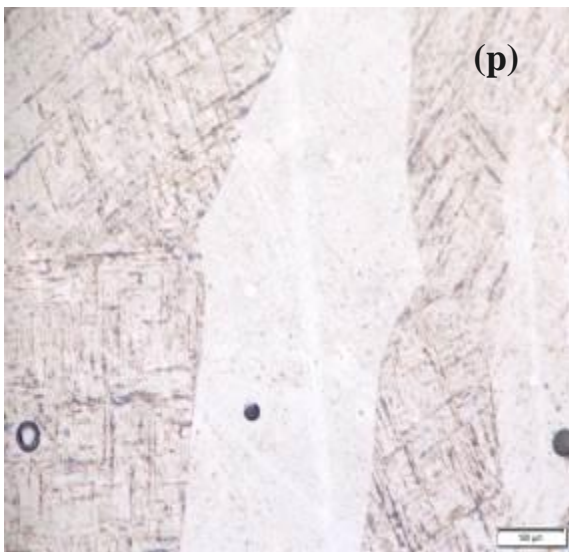
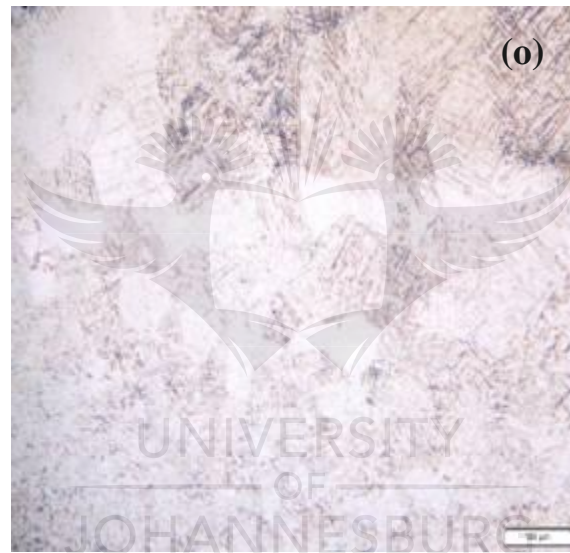
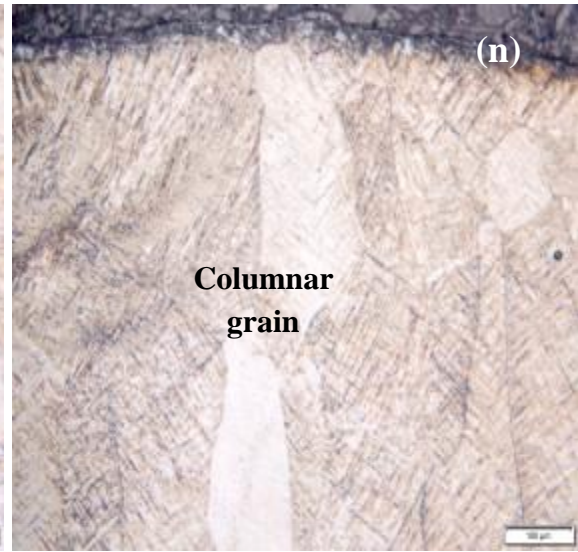
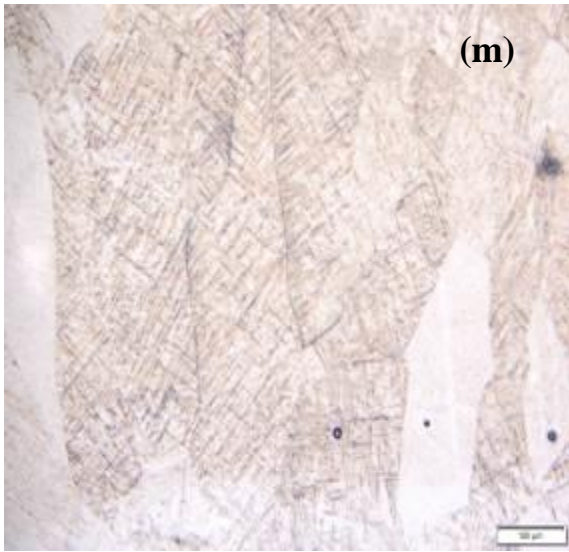


Figure 4. 10: Optical micrographs of B₄C-Ti6Al4V composite deposited at 2200 W laser power







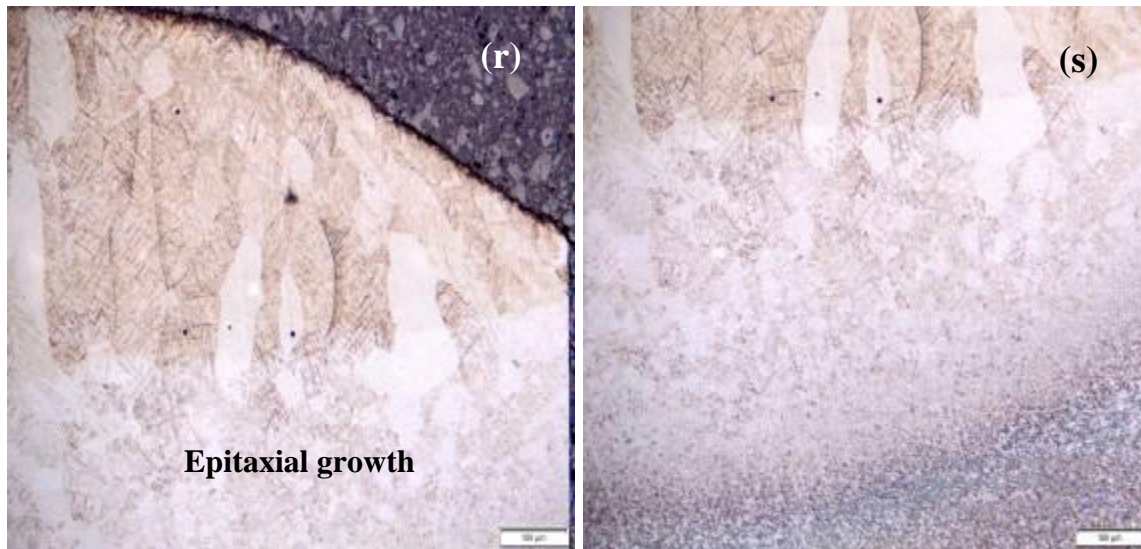


Figure 4. 11: Optical micrographs of B₄C-Ti6Al4V composite deposited at 2400 W laser power

A careful and critical observation was put in place when studying the microstructures of the composites. It was however found out that the level of porosities observed decreases as the laser power increases. The level of homogeneity was observed as the laser power also increases and in actual sense, the content of boron carbide particles in the composites were formed on the top layer of the deposit which actually behaves like a shielding structure or coated film-like structure on the deposition's surface. This property however serves as the properties that is responsible for the resistance to wear as well as the corrosion due to the higher concentration of boron carbide particles deposited at the utmost surface of the deposit. Thus, Fei et al. [72], observed that, this property is characterized with the martensitic microstructure which shows a significant microhardness increase and corrosion resistance improvement.

On the other hand, as the laser power increases, the pores in the composites dissolve in the melt pool prior to solidification. For other clarification, the micrographs revealed that, grain growths were observed on the heat affected zone and these were however attributed to the increase in the laser power. Furthermore, the basket weave martensitic structure which was presented in Figure 4.11 (a) and (d) resulting from heat input through laser metal deposition (LMD) process. Basketweave- α has however been known to benefit the mechanical properties of titanium alloy (Ti6Al4V). Therefore, using laser LMD process, parts produced

are prone to porosity from lack-of-fusion and gas entrapment which can simply have a detriment effect on the mechanical properties. However, the microscopic banding was observed to have an epitaxial growth on the globular microstructure which was shown in Figure 4.11(r) between the fusion zones (FZ) or at the interface and the heat affected zone (HAZ) of the deposited composites. Thus, the formation of protective oxide layer on the surface of the deposits permits part of the wear and corrosive resistance.

4.4.2 Porosity Analysis and Characterization

To perform porosity analysis on the deposited composites, after the deposition process, the samples were sectioned for porosity analysis and microstructure studies. The sectioned samples were however mounted, ground and polished according to standard metallurgical preparation of titanium alloys. The polished samples were then etched using Kroll's reagent. Porosity analysis was observed using the optical microscope equipped with ANALYSIS Docu image processing software to establish the percentage porosity, pore count and the maximum pore size of the composites. The maximum size of the pores were also observed by measuring the pores sizes at different areas and then take the maximum value for each sample. However, the processing parameters observed during the laser metal deposition (LMD) process are of utmost important as they may facilitate properties such as porosity defect. On the other hand, Mahamood et al. [71], described that porosity in the laser metal deposited samples or parts was being seen as a defect in most manufacturing and medical implant applications. These researchers however reported that, porosity defect provide a great important factor in the healing process and proper integration of medical implants and body tissues for required implants.

Furthermore, titanium alloy such as Ti6Al4V has proven itself beyond reasonable doubt and thereby used as medical implants due to its outstanding hardness, wear and corrosion resistance properties and superior biocompatibility. Figures 4.12 shows the porosity behaviours of the samples at different laser powers in which the degree of their porosities varies as the laser power increases and thereby arrived at a laser power in which no porosity was observed and then further experience significant amount of porosity as the laser power further increases.



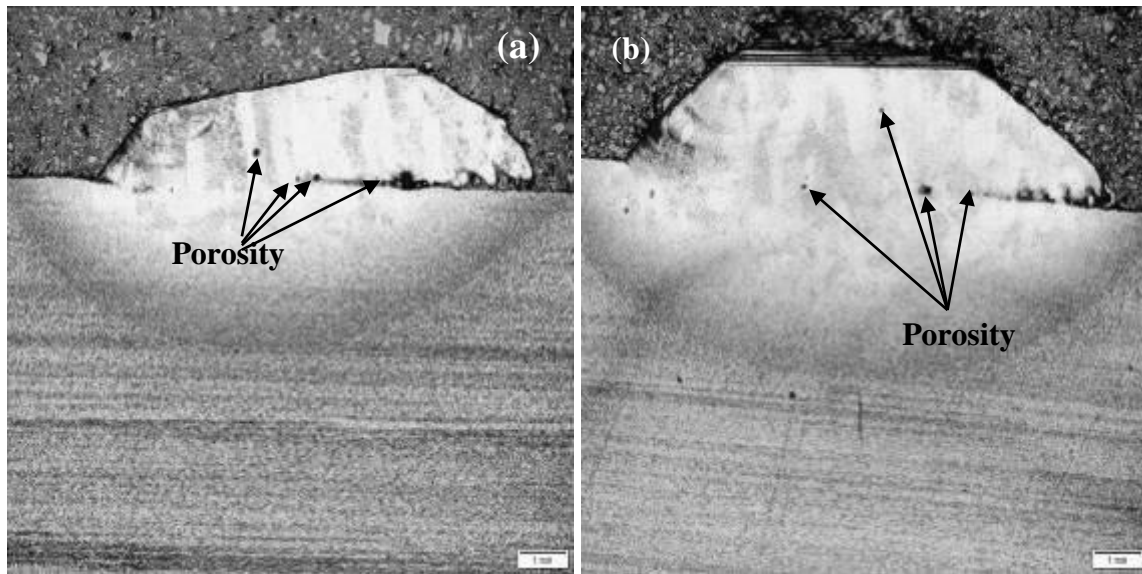


Figure 4. 12: Micrographs of samples (S4 and S6) at (a) 1400 W laser power, (b) 1800 W laser power

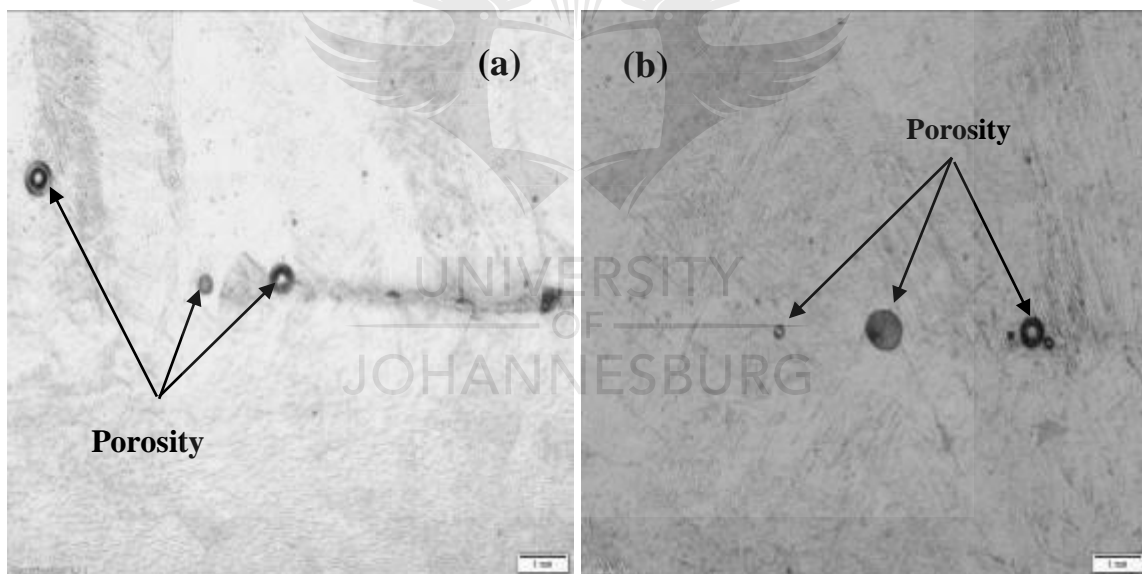


Figure 4. 13: Micrographs of sample 4 and 6 (S4 and S6) at high magnification with laser power of (a) 1400 W and (b) 1800 W

Interestingly, at a certain laser power of 2200 W, there was no porosity observed in the characterized sample. No unmelted powders were observed in the clad after solidification. Figure 4.14 depicts that the sample deposited with a laser power of 2200 W was characterized with no porosity.

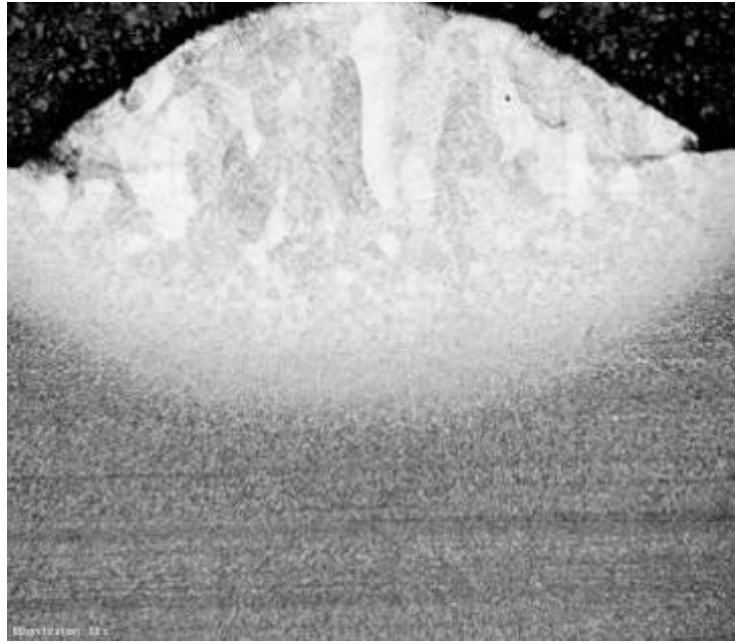


Figure 4. 14: Micrograph of Ti6Al4V-B₄C composite of sample S8 at laser power of 2200 W

This composite was observed and characterized to be porous-free deposit and thereby resulted in a fully densified deposit. Perhaps, there was a sufficient heat input generated by the laser system which however, provides adequate laser power to the melt pool whereby no unmelted powder remains in the molten pool after solidification. Considering Table 4.2 which presents the average percentage porosity and the maximum pore sizes of the samples. Thus, the bar chart of the percentage porosity is shown in Figure 4.15.

Table 4. 2: Average percentage porosity and maximum pore size of various samples

Samples	Average porosity (%)	Maximum pore size (μm)
S1	0.45	158.01
S2	0.16	66.63
S3	0.12	33.96
S4	0.44	132.79
S5	0.31	153.47

S6	0.30	143.79
S7	0.09	64.45
S8	No porosity	Nil
S9	0.03	27.50

However, Figure 4.15 illustrates the variation of average porosity as well as the maximum pore size of the composite for various samples which was presented in a bar chart.

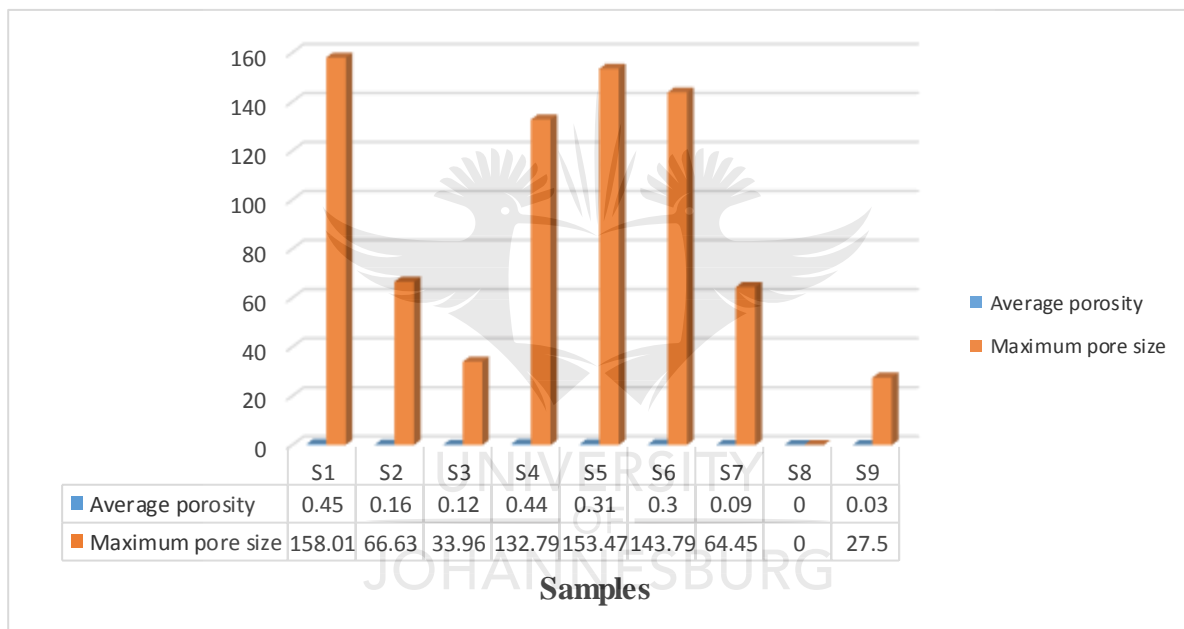


Figure 4. 15: The variation of average porosity and maximum pore size of composites for different samples

4.4.3 Scanning Electron Microscopy (SEM) Analysis

The scanning electron microscopy (SEM) images of the composites at various laser powers and their corresponding energy dispersion spectroscopy (EDS) analysis are presented in Figures shown as follow:

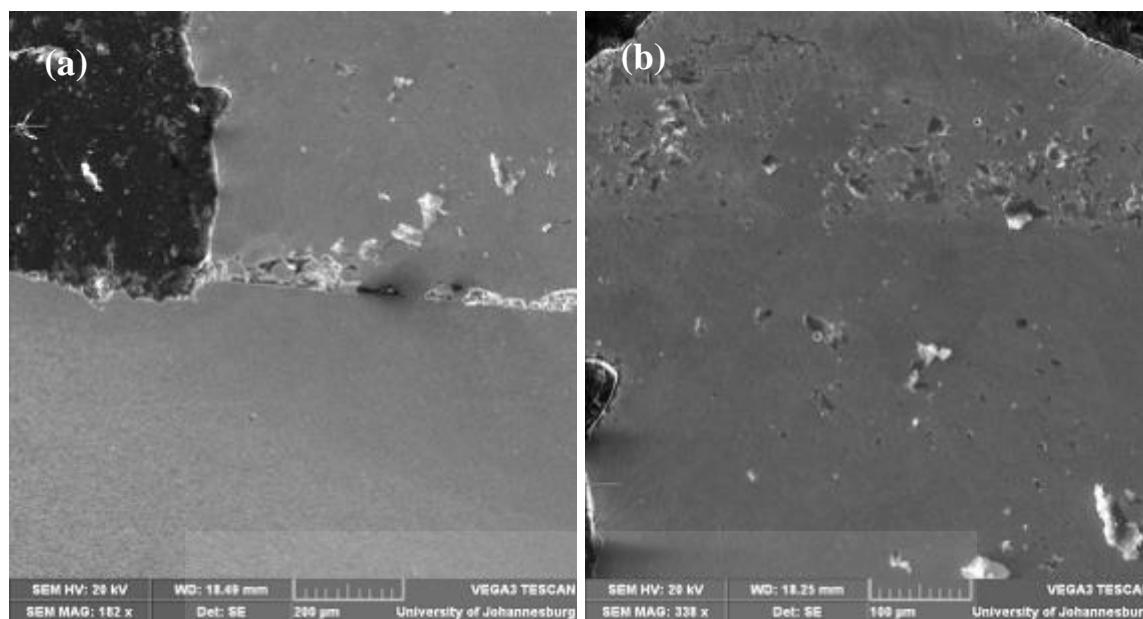


Figure 4. 16: SEM micrographs of B₄C-Ti6Al4V composite at laser power of 800 W at low and high magnification

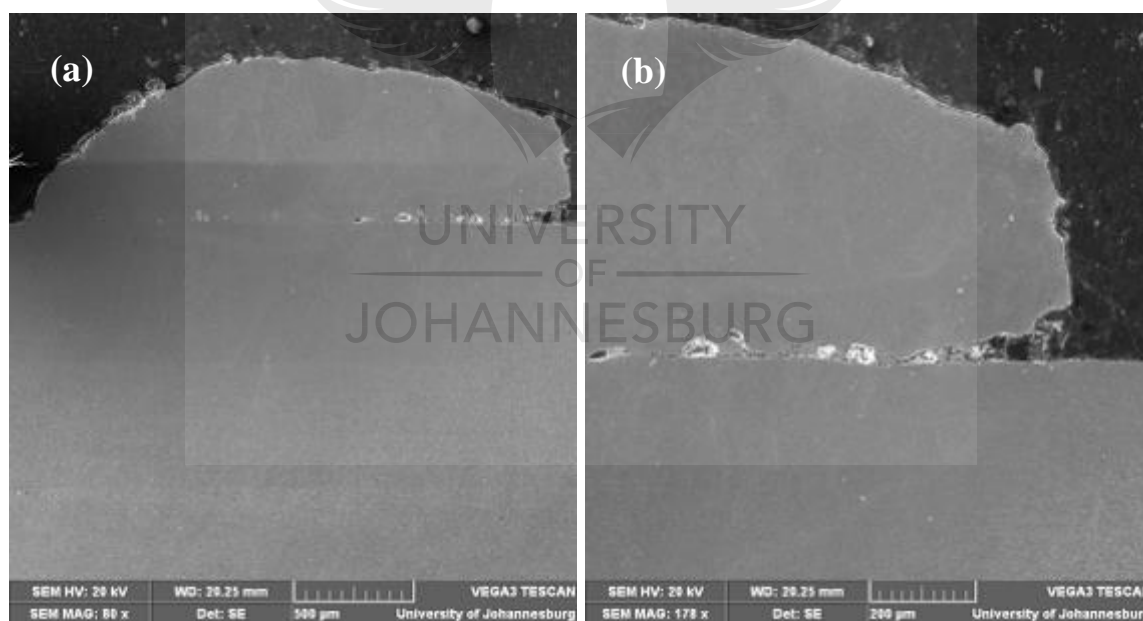


Figure 4.17: SEM micrographs of B₄C-Ti6Al4V composite at laser power of 1000 W at low and high magnification

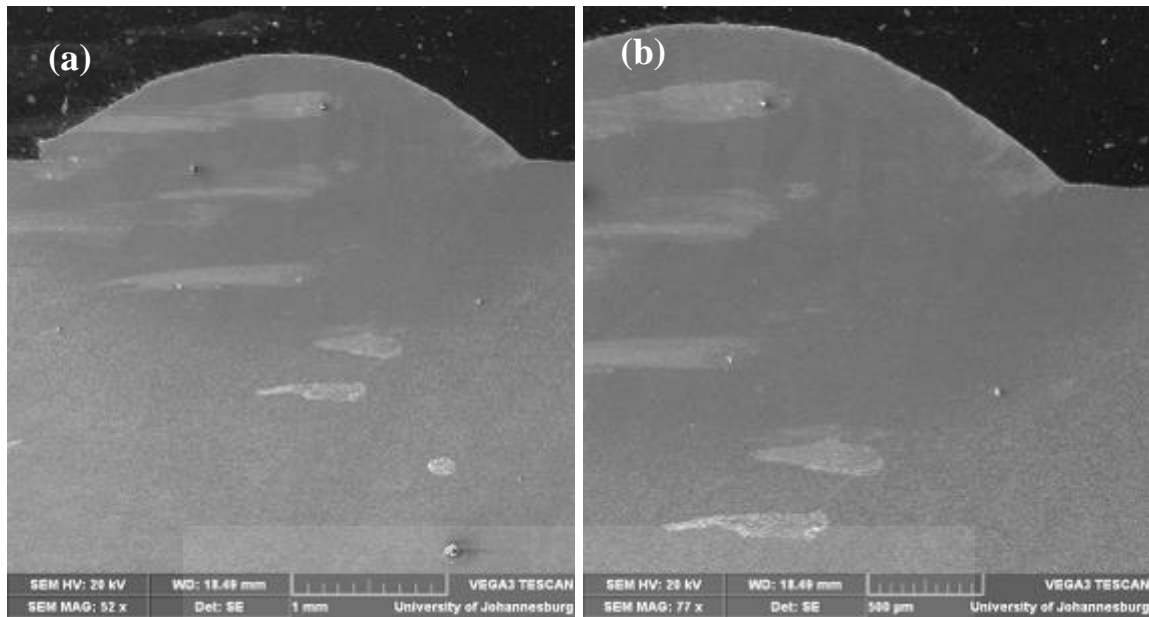


Figure 4.18: SEM micrographs of B₄C-Ti6Al4V composite at laser power of 2000 W at low and high magnification

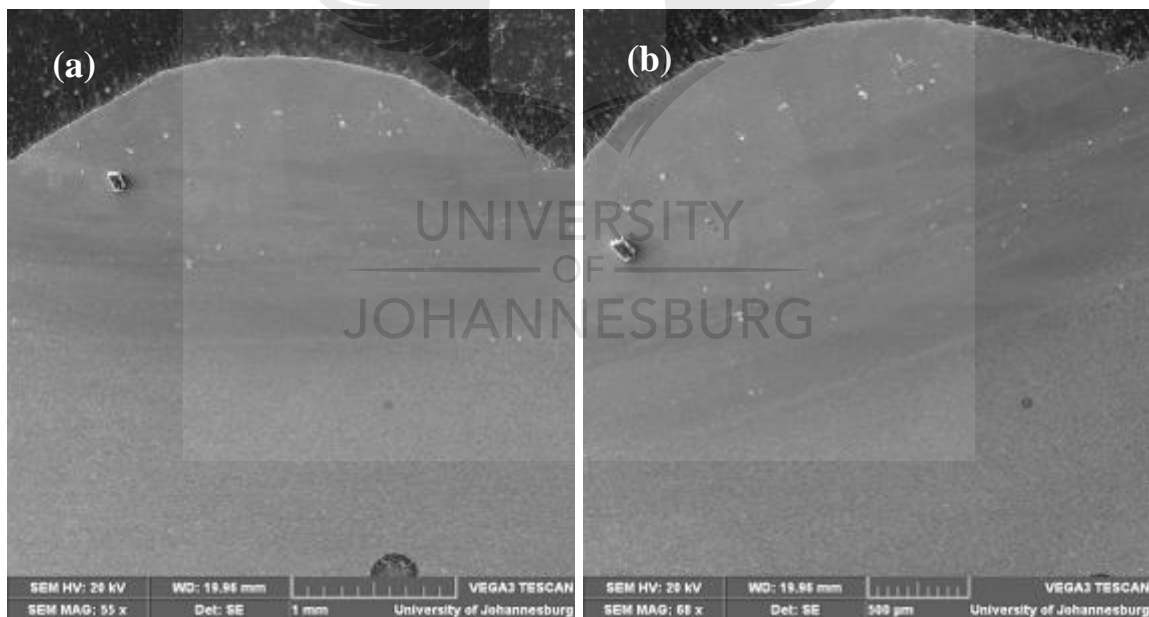


Figure 4.19: SEM micrographs of B₄C-Ti6Al4V composite at laser power of 2200 W at low and high magnification

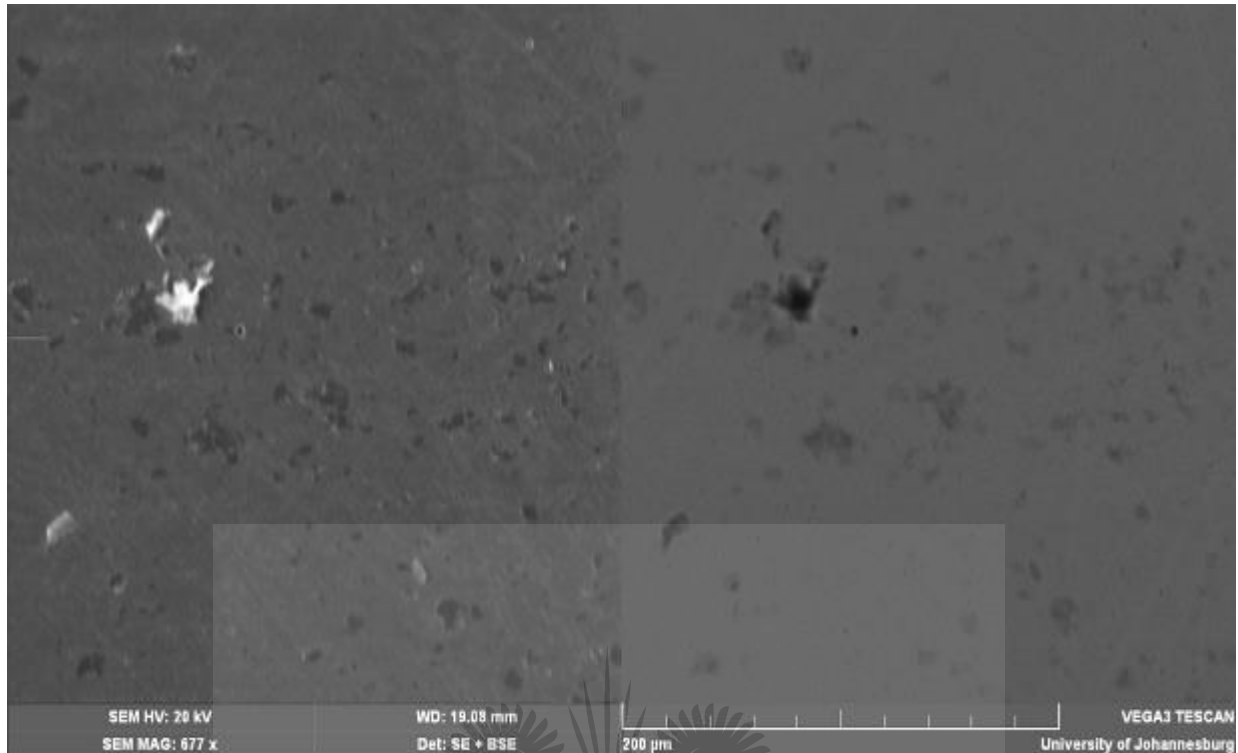


Figure 4.20: SEM micrograph showing backscattered morphology of B₄C-Ti6Al4V composite at laser power of 2200 W at magnification of 677 x

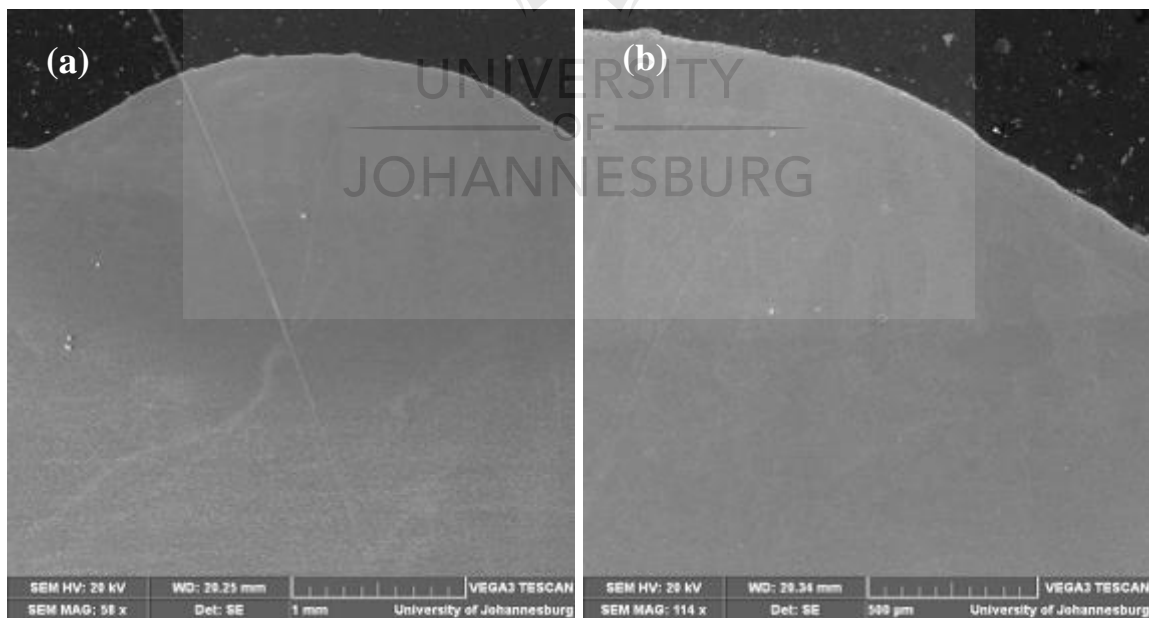


Figure 4.21: SEM micrographs of B₄C-Ti6Al4V composite at laser power of 2400 W at low and high magnification

The Figures from 4.22 to 4.27 show the SEM micrographs with EDS spectra for B₄C-Ti6Al4V composites at various laser power.

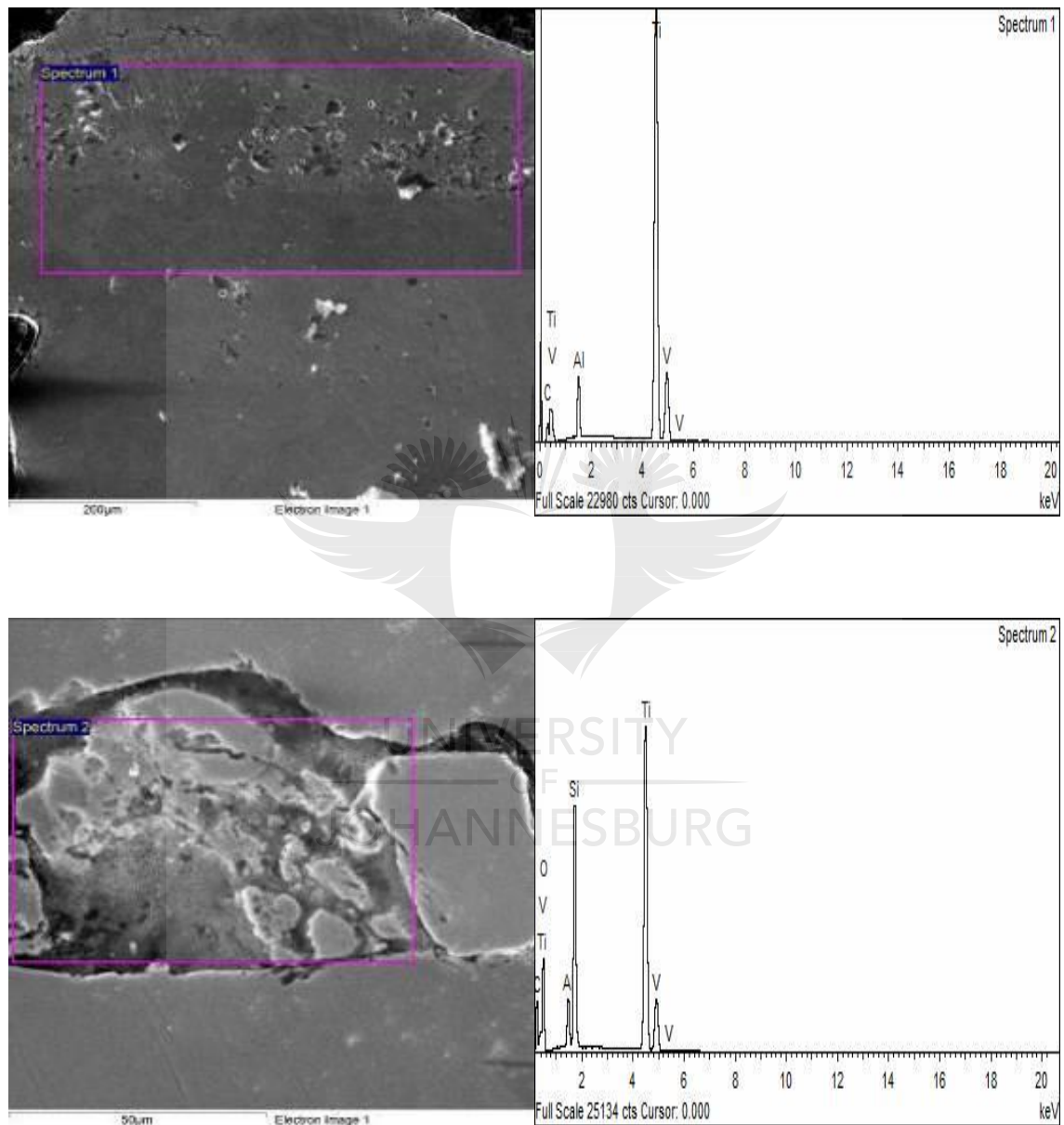


Figure 4.22: The SEM images and EDS spectrum of B₄C-Ti6Al4V composite at 800 W laser power

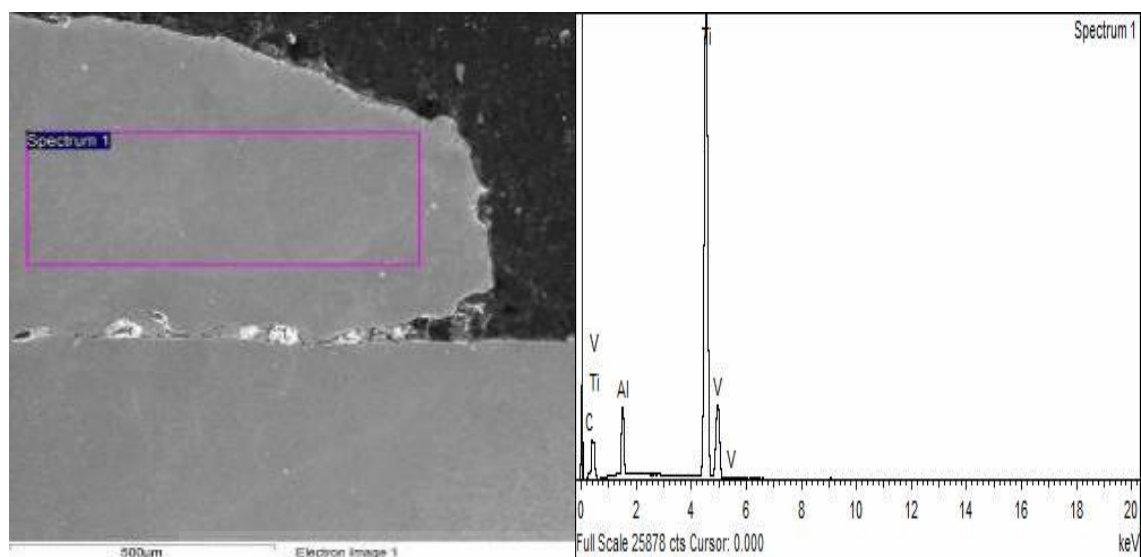


Figure 4.23: The SEM image and EDS spectrum of B₄C-Ti6Al4V composite at 1000 W laser power

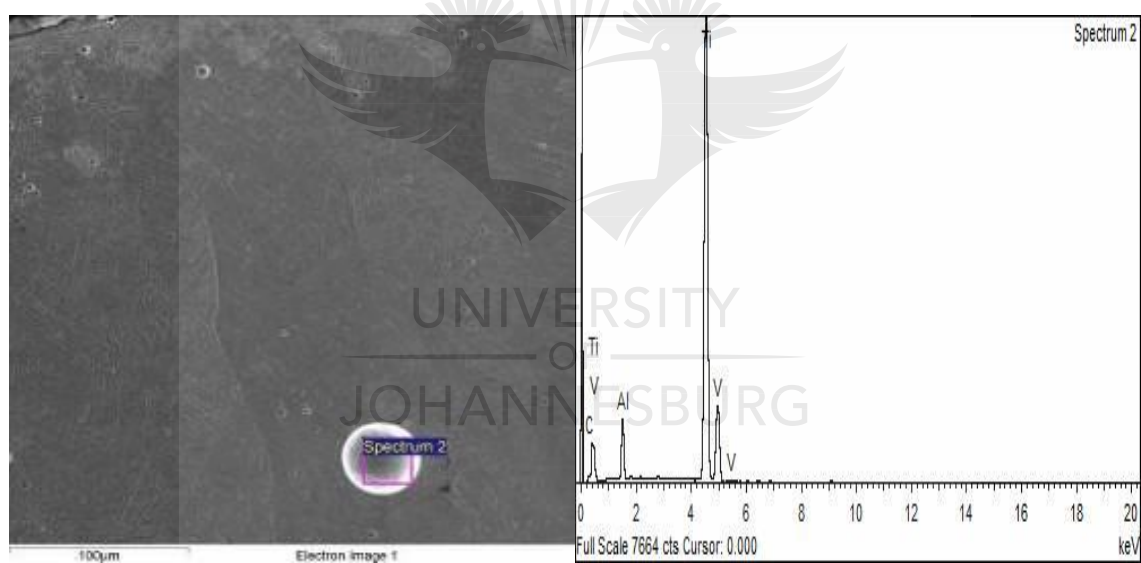


Figure 4.24: The SEM image and EDS spectrum of B₄C-Ti6Al4V composite at 1400 W laser power

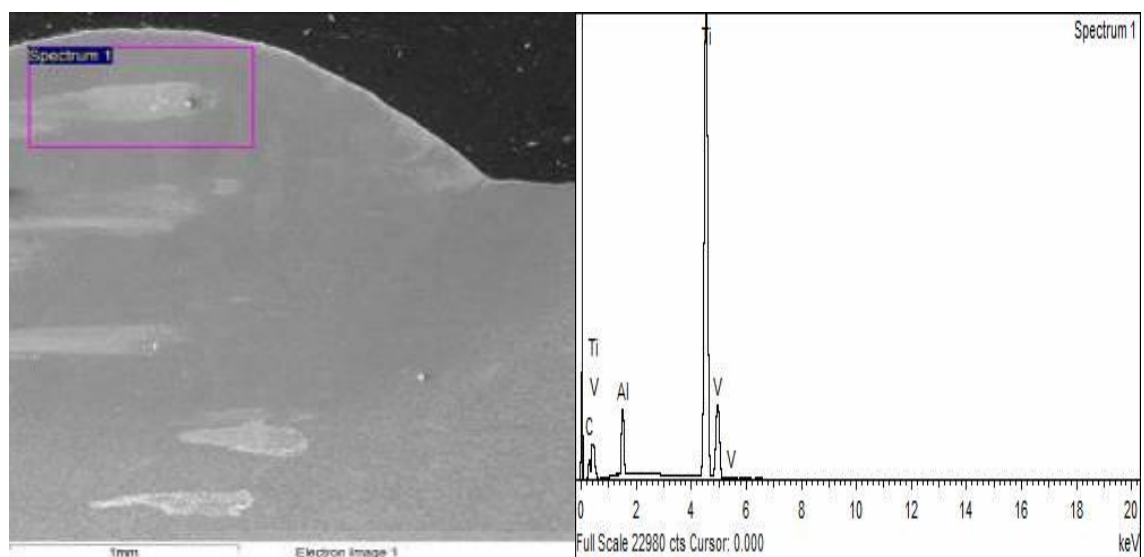
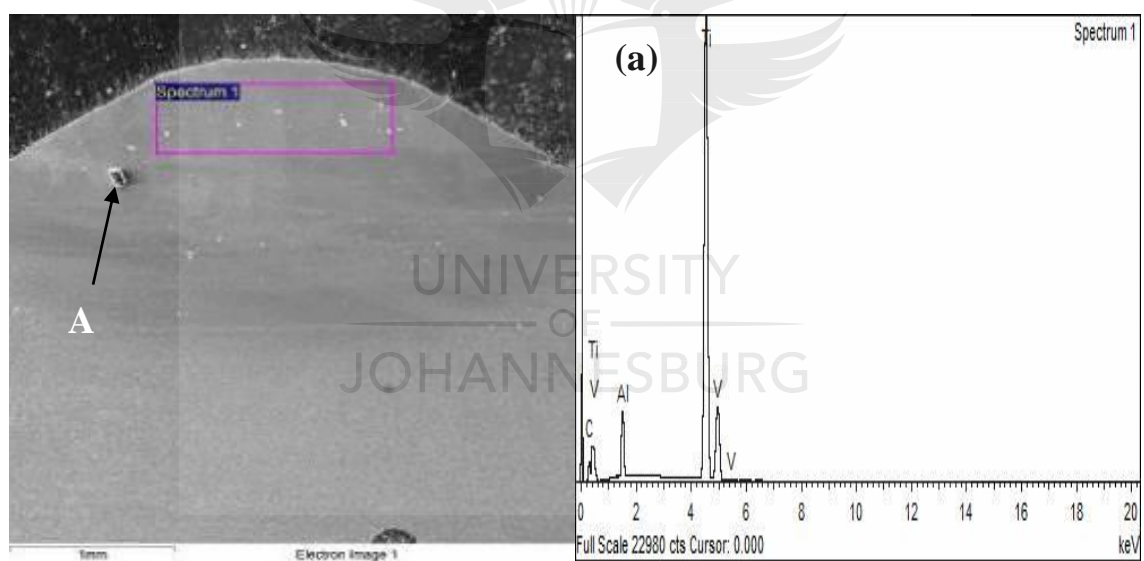


Figure 4.25: The SEM image and EDS spectrum of B₄C-Ti6Al4V composite at 2000 W laser power



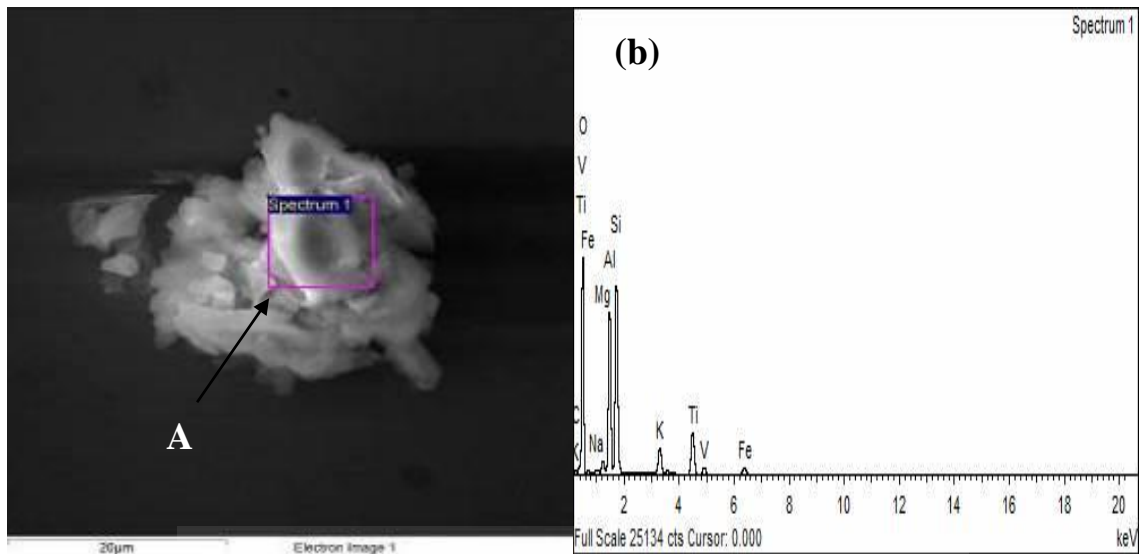


Figure 4.26: The SEM images and EDS spectrum of B₄C-Ti₆Al₄V composite at 2200 W laser power

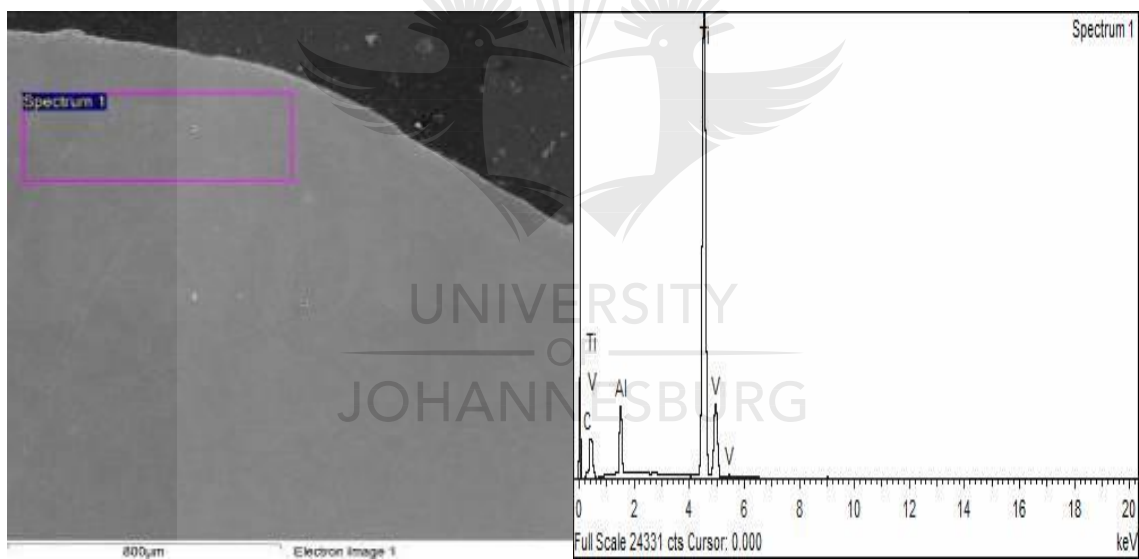


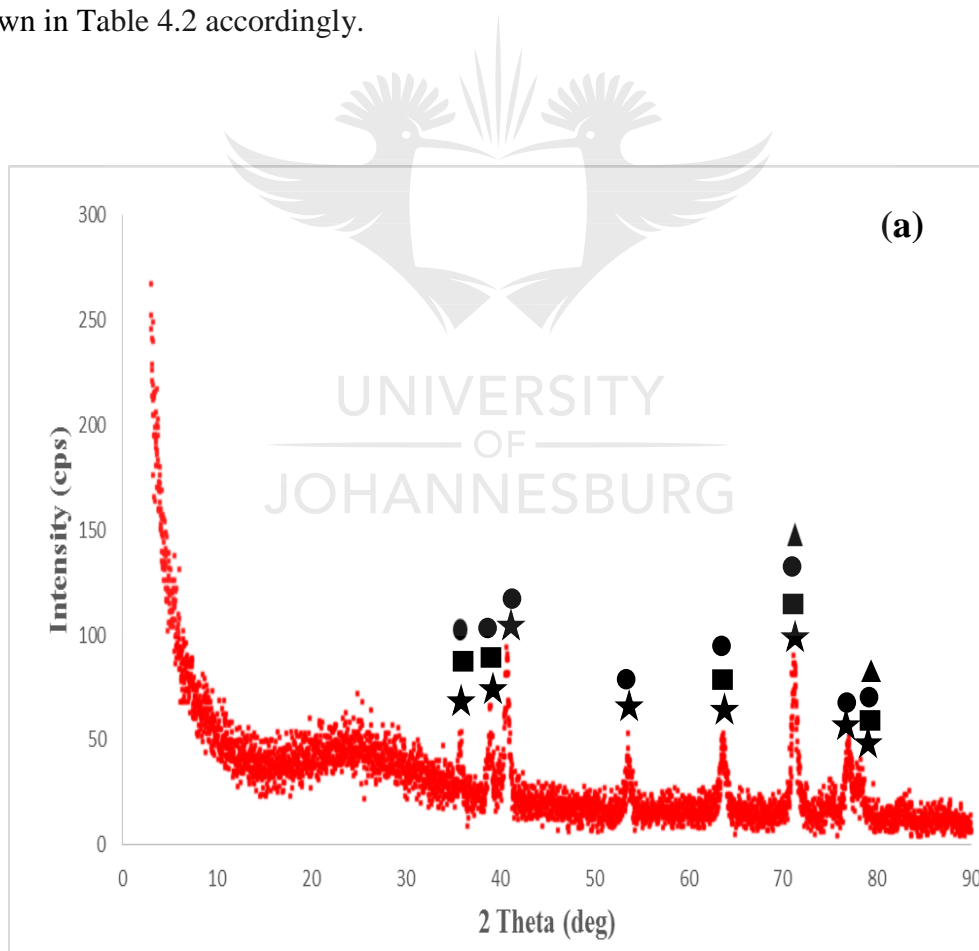
Figure 4.27: The SEM image and EDS spectrum of B₄C-Ti₆Al₄V composite at 2400 W laser power

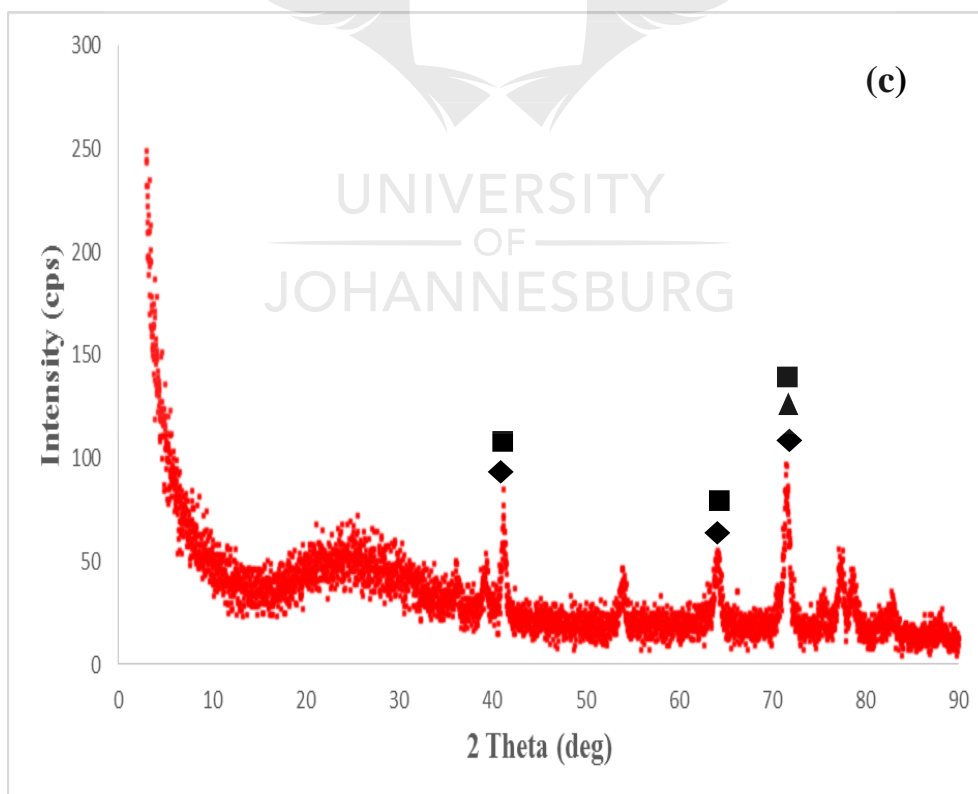
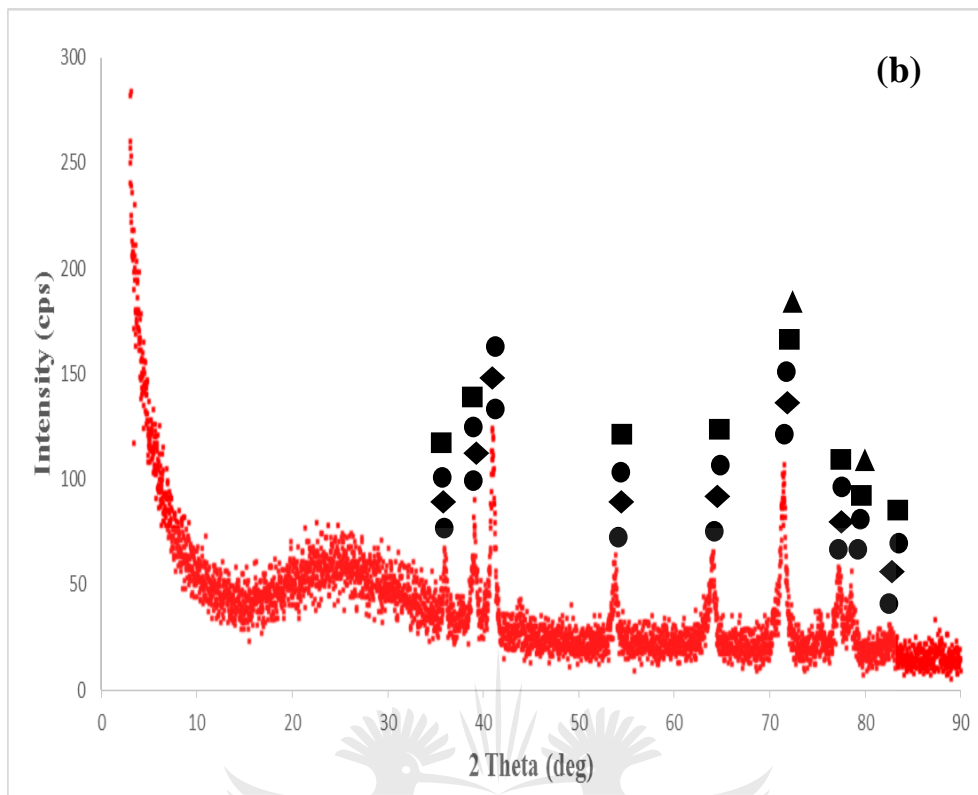
From the results of the EDS spectra showed, it was observed that titanium was the most prominent element in the composites with minor carbon element. The results obtained displayed no traces of boron element which could be as a result of completely dispersed of the boron element in the composites. On the other hand, the EDS spectra from Figure 4.22 showed that there were poor bonding between the deposited layer and the substrate layer in

which oxygen element was observed in the composites as a result of entrapment of gas before solidification during the deposition process. Furthermore, the EDS spectrum from Figure 4.26 (b) report showed that there were certain number of impurities observed in the deposit at a spot in which the elemental impurities include oxygen, iron, silicon, sodium, magnesium and potassium.

4.4.4 X-Ray Diffraction (XRD) Analysis

The phase purity of different samples was investigated by x-ray diffraction (XRD) analysis. XRD patterns of selected samples are shown in Figure 4.28 (a) to (d) which exhibited by various crystalline phases. The results obtained from the XRD analysis data are summarized and shown in Table 4.2 accordingly.





UNIVERSITY
OF
JOHANNESBURG

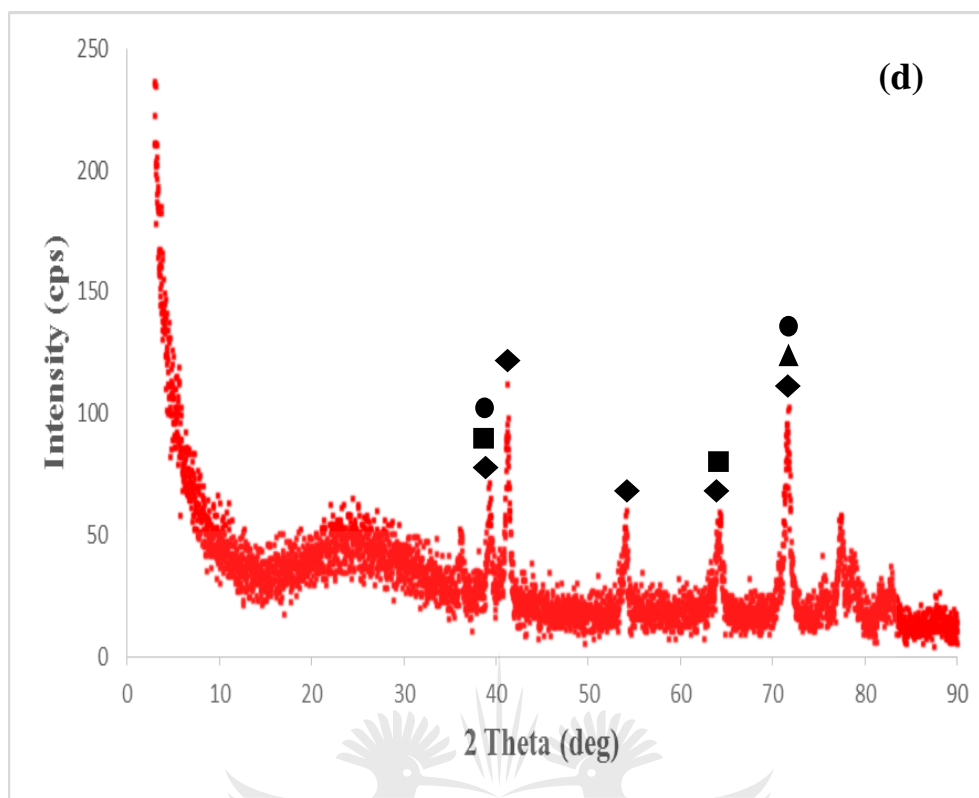


Figure 4.28: x-ray diffraction (XRD) patterns of sample S1, S6, S8 and S9 at laser power 800 W, 1800 W, 2200 W and 2400 W respectively

The Figures 4.28 (a) to (d) showed present various crystalline phases for different selected coatings. In Figure 4.28 (a), XRD patterns characterized strong diffraction peaks at 40.69° and 71.15° and indicating the dominance of titanium vanadium carbide and titanium phases. On the other hand, in Figure 4.28 (b), XRD patterns characterized strong diffraction peaks at 38.92° , 40.93° and 71.35° and indicating the dominance of titanium, vanadium carbide and titanium boride phases. Furthermore, in Figure 4.28 (c), XRD patterns exhibited strong diffraction peaks at 41.23° and 71.48° which however indicating the dominance of vanadium carbide and titanium boride phases. Finally in the Figure 4.28 (d), XRD patterns exhibited strong diffraction peaks at 41.18° and 71.57° in which the phases were characterized by vanadium carbide. Therefore from Figure 4.28 (a) to (d), they were shown that the diffraction patterns peak intensity of the coatings slightly increases with increasing laser power. These

results however suggested that the coatings were composed of slightly low traces of impurities or no irregular impurity of crystalline was observed.

Table 4.3(a) and 4.3(b) illustrates the various phases observed during the x-ray diffraction (XRD) for different sample coatings.

Table 4. 3(a): Phase analysis

Samples	Phases obtained from XRD analysis	Chemical formula	Comments
S1	Titanium vanadium carbide, titanium boride, titanium diboride, titanium	(Ti _{0.33} V _{1.67} C),	Main
		TiB, TiB ₂ , Ti	Secondary
S2	Titanium vanadium carbide, titanium, titanium boride	(Ti _{0.33} V _{1.67} C), Ti, TiB	Main Secondary
S3	Titanium vanadium carbide, titanium, titanium boride, titanium diboride	(Ti _{0.33} V _{1.67} C), Ti, TiB, TiB ₂	Main Secondary
S4	Titanium vanadium carbide, titanium, titanium boride, titanium diboride	(Ti _{0.33} V _{1.67} C), Ti, TiB, TiB ₂	Main Secondary
S5	Titanium vanadium carbide, titanium boride, titanium	(Ti _{0.33} V _{1.67} C), TiB, Ti	Main Secondary

Table 4. 3(b): Phase analysis

Samples	Phases obtained from XRD analysis	Chemical formula	Comments
S6	Titanium, vanadium carbide, titanium boride, titanium diboride	Ti, V ₂ C, TiB, TiB ₂	Main Secondary
	S7	Titanium vanadium carbide, aluminium titanium vanadium, titanium boride, titanium diboride	(Ti _{0.33} V _{1.67} C), Al _{0.5} Ti _{0.5} V, TiB, TiB ₂
S8	Vanadium carbide, titanium boride, titanium diboride	V ₂ C, TiB, TiB ₂	Main Secondary
		S9	Vanadium carbide, titanium boride, titanium, titanium diboride

In conclusion to the x-ray diffraction (XRD) patterns, the crystalline phases are marked as follow: titanium vanadium carbide, Ti_{0.33} V_{1.67} C (★); titanium boride, TiB (■); titanium, Ti (●); titanium diboride, TiB₂ (▲); vanadium carbide, V₂C (◆); aluminium titanium vanadium, Al_{0.5} Ti_{0.5} V (▼).

4.5 MICROHARDNESS PROFILING

The microhardness profiles of the composites were carried out on all the deposited samples from S1 to S9. Figure 4.29 shown illustrates the average Vickers Hardness values together with their corresponding standard deviations. The Vickers microhardness values of the composites were however measured under a load of 500 g at dwell time of 15 seconds on a digital microhardness tester. Prior to hardness measurements, the composites were sectioned, ground and polished by fine MD chem grinding disc with oxide polishing (OP-S) suspension to obtain a mirror-like finish on the surface in order to allow accurately measured indentations.

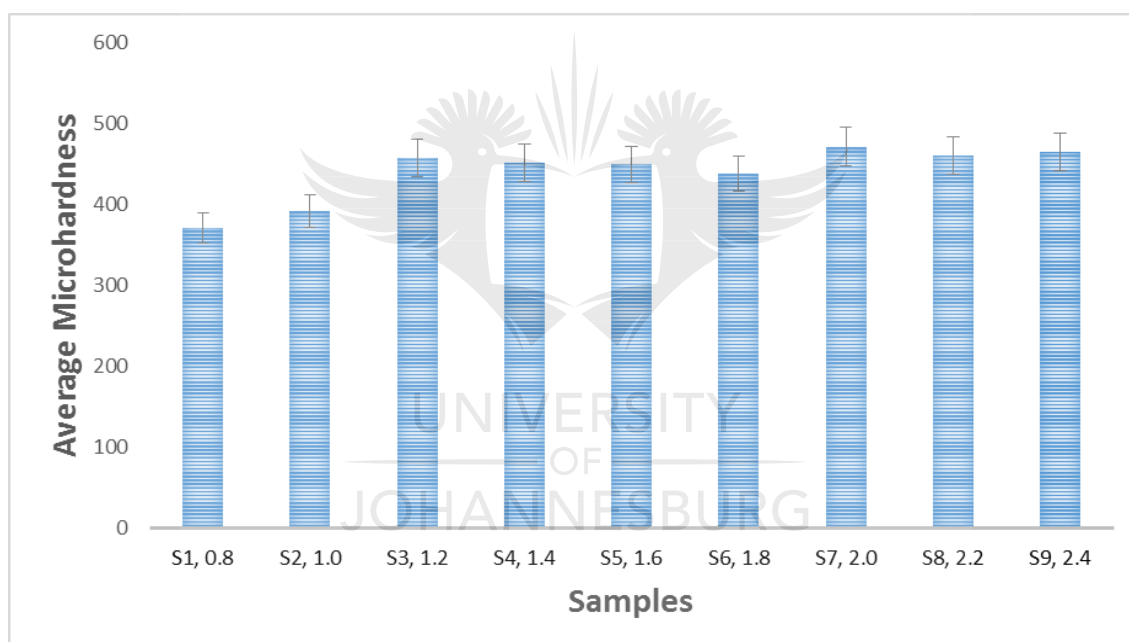


Figure 4.29: Average Vickers microhardness profiles of the deposited composites

According to Figure 4.29 which illustrates that the hardness value increases as the laser power increases. However, at a certain instance, the hardness values decrease as the laser power increase and then the hardness value got to the peak and later decreases almost at constant hardness value as the laser power continue to increase. Therefore, sample S7 at a laser power of 2000 W was observed to have the highest hardness value. Thus, the variation in hardness values set as criteria to improve the ductility property of the composites. It is

however observed that, increase in laser power influences the microstructure of the deposit which changes it from rough and coarse surfaces to less coarse and fine surfaces which eventually tends to increase the hardness of the deposits. Nevertheless, it can be seen from the graph that the optimum laser power for the deposited composites were observed between 2000 W and 2400 W.

4.6 WEAR CHARACTERIZATION

The materials of the contact pair were titanium alloy substrate (Ti6Al4V) embedded with deposited titanium alloy and boron carbide (Ti6Al4V-B₄C) composites adhered to the sliding plate at the lower cylinder part of the test ball. Furthermore, geometrical measurement after the test was observed on the samples with which normal load of 25 N was applied during process and at 5 Hz oscillatory frequency with 2 mm stroke for approximately 17 minutes (i.e., 1000 seconds) for each sample at speed of 5 mm/s. The tests were conducted in ambient air environment without any lubrication applied.

4.6.1 SEM characterization of wear track

The SEM images of worn scar for respective coatings were shown in Figure 4.30 (a) to (f) at constant applied load of 25 N. Worn surfaces were characterized by wear debris and severe wear were observed apparently in all the wear samples. However, the worn surfaces were pronounced by spherical shape in all the samples. Samples S1 and S2 from the Figure 4.30 (a) and (b) shown were pronounced by mild wear when compared to other samples which could be due to loss of ductility properties within the deposited composite.

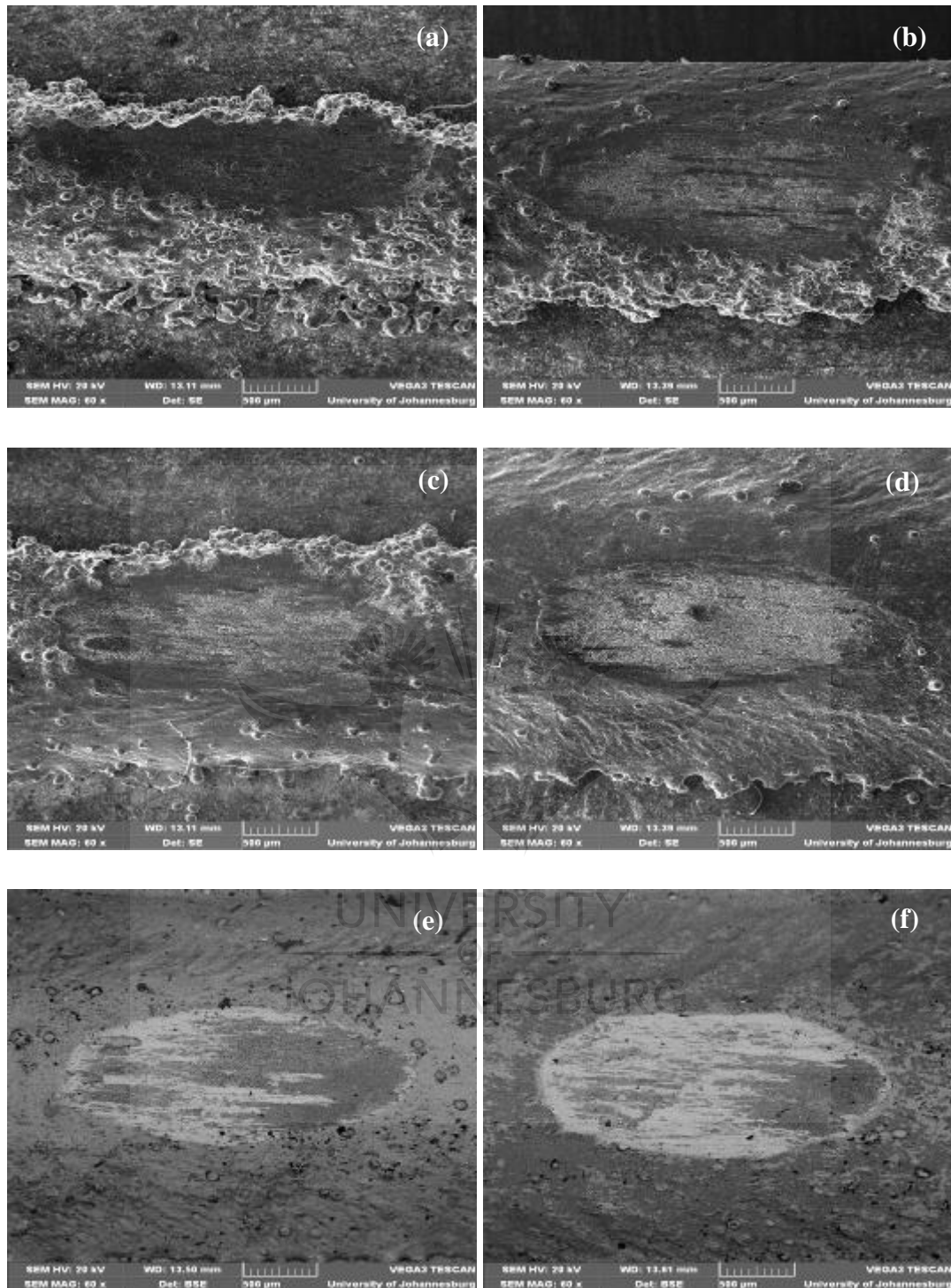


Figure 4.30: The SEM images of wear scar on the deposited B_4C -Ti6Al4V composite flat that was worn against a tungsten carbide, WC ball; (a) sample S1 at laser power of 800W, (b) sample S2 at laser power of 1000 W, (c) sample S3 at laser power of 1200 W, (d) sample S7 at laser power of 2000 W, (e) sample S8 at laser power of 2200 W and (f) sample S9 at laser power of 2400 W

However, wear of the tungsten carbide ball was deliberately ignored when wear volume of the linear deposited composite samples were calculated. Therefore, wear volumes as well as the wear rates of the linearly operated deposited composite under the normal load application and constantly controlled speed were calculated according to Archard's wear model equations [68]. Thus, Archard's wear law equations for sliding wear are normally expressed as follows:

$$\frac{V}{s} = k \cdot \frac{F_N}{H} \quad (4.3)$$

$$K_D = \frac{V}{F_N \cdot s} \quad (4.4)$$

Where V = wear volume, s = sliding distance, F_N = normal load, H = hardness of the worn surface and K = dimensionless wear rate. Considering the equation to calculate the wear volume on a flat sample of the linearly sliding wear composites given as follows:

$$V_f = L_s \left[R_f^2 \arcsin\left(\frac{W}{2R_f}\right) - \frac{W}{2} (R_f - h_f) \right] + \frac{\pi}{3} h_f^2 (3R_f - h_f) \quad (4.5)$$

Where V_f = wear volume or material loss, h_f = wear depth, W = width, L_s = stroke length and R_f = radius of the two spherical ends, h_f is however given as:

$$h_f = R_f - \sqrt{R_f^2 - \frac{W^2}{4}} \quad (4.6)$$

But equation 4.6 can also be written as follows:

$$R_f = \frac{4h_f^2 + W^2}{8h_f} \quad (4.7)$$

On the other hand, [69-70] however developed analytical method for wear of the flat specimen generated by reciprocating sliders with compound tip curvature in which the equation given in 4.5 was used to evaluate its wear volume.

$$V_f = L_s \left[R_f^2 \arcsin \left(\frac{W}{2R_f} \right) - \frac{W}{2} (R_f - h_f) \right] + \pi \frac{(L - L_s)}{3W} [h_f^2 (3R_f - h_f)] \quad (4.8)$$

Where, L and W are the length and width of the wear scar respectively.

The analysis of the wear scar geometry was done with optical microscopy (OM) and then using scanning electron microscopy (SEM) to further measured the various parameters involved in the evaluation of wear volume as well as the wear rates and depth of the wear scar for different samples undergone wear test. The relative wear of the ball and the flat specimen yields different geometric variations according to ASTM G133-05 [67]. However, the actual shape of the worn out groove was well understood from the OM and SEM analysis in which the depths and other dimensions measured by scanning electron microscopy (SEM) methods were however used to evaluate the wear volume together with wear rate of deposited composites. Table 4.5 presented in appendix G shows the wear measured variables on deposited coatings for every sample. The wear scar variables for the deposited composites measured by scanning electron microscope (SEM) and evaluated were also presented in Table 4.5 shown in appendix G and however used to analyse the characteristics of individual samples. Figure 4.31 illustrates the behaviour of wear depth, width, stroke length, wear volume and wear rate of respective samples.

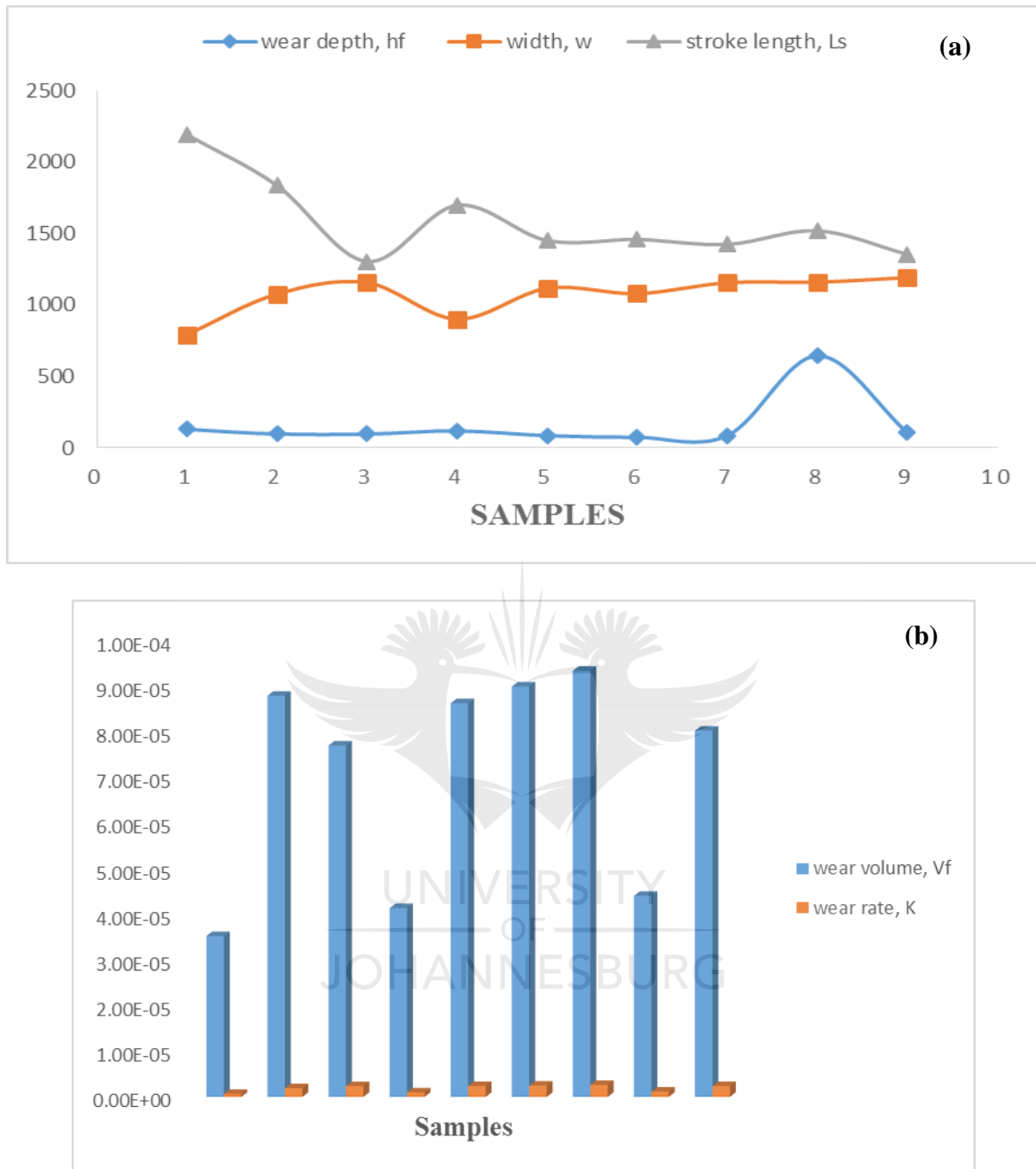


Figure 4.31: Multiple bar charts of the wear depth, width, stroke length, wear volume and wear rate for the deposited composites samples

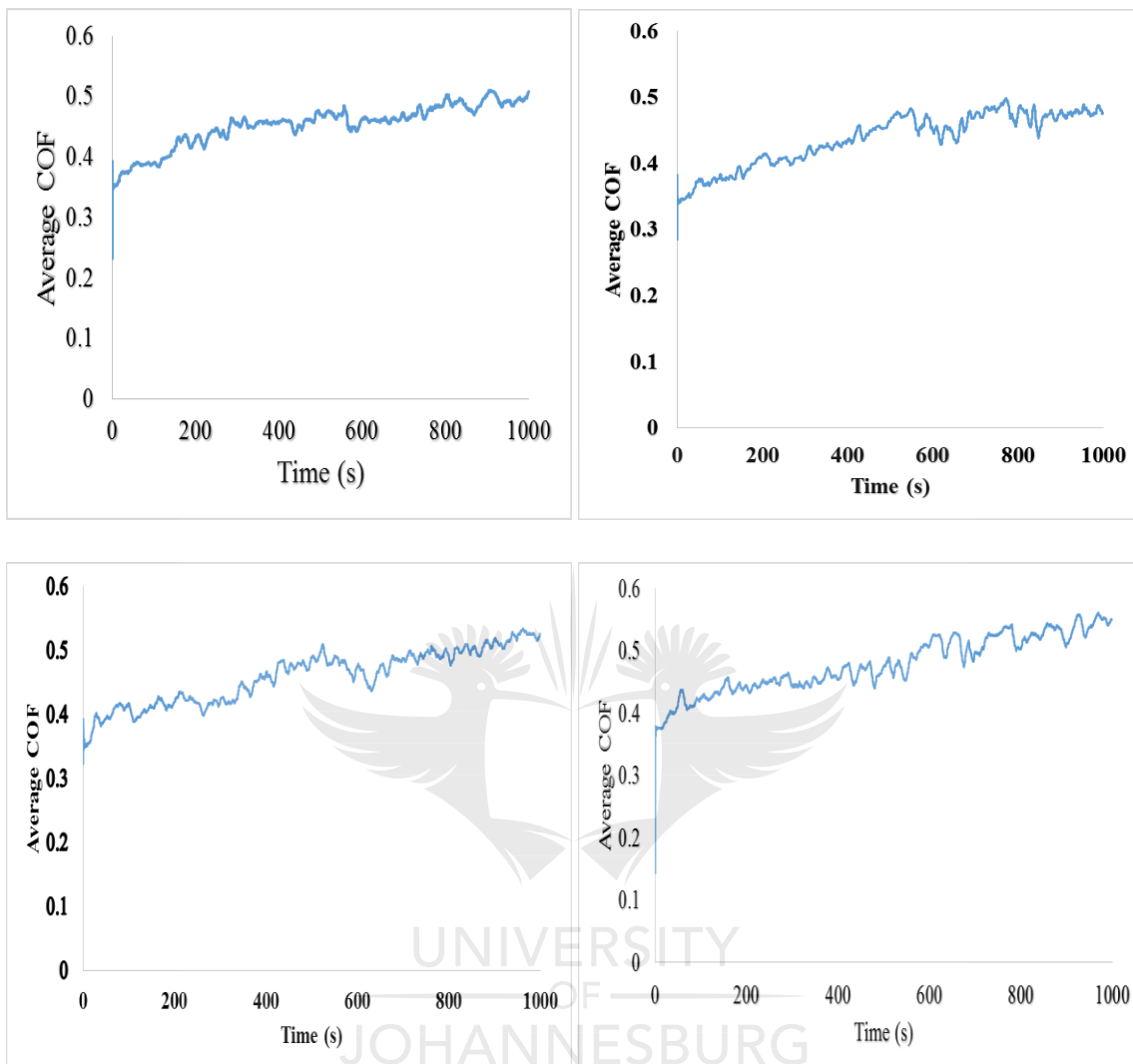
Figures 4.31 (a) and (b) clearly represent the wear depth, width, stroke length, wear volume and wear rate information of all deposited samples. Of all the deposited composites, sample S6 at laser power of 1800 W was identified to have the lowest wear depth of 74.6 μm while S8 at laser power of 2200 W was however observed to have the highest wear depth with

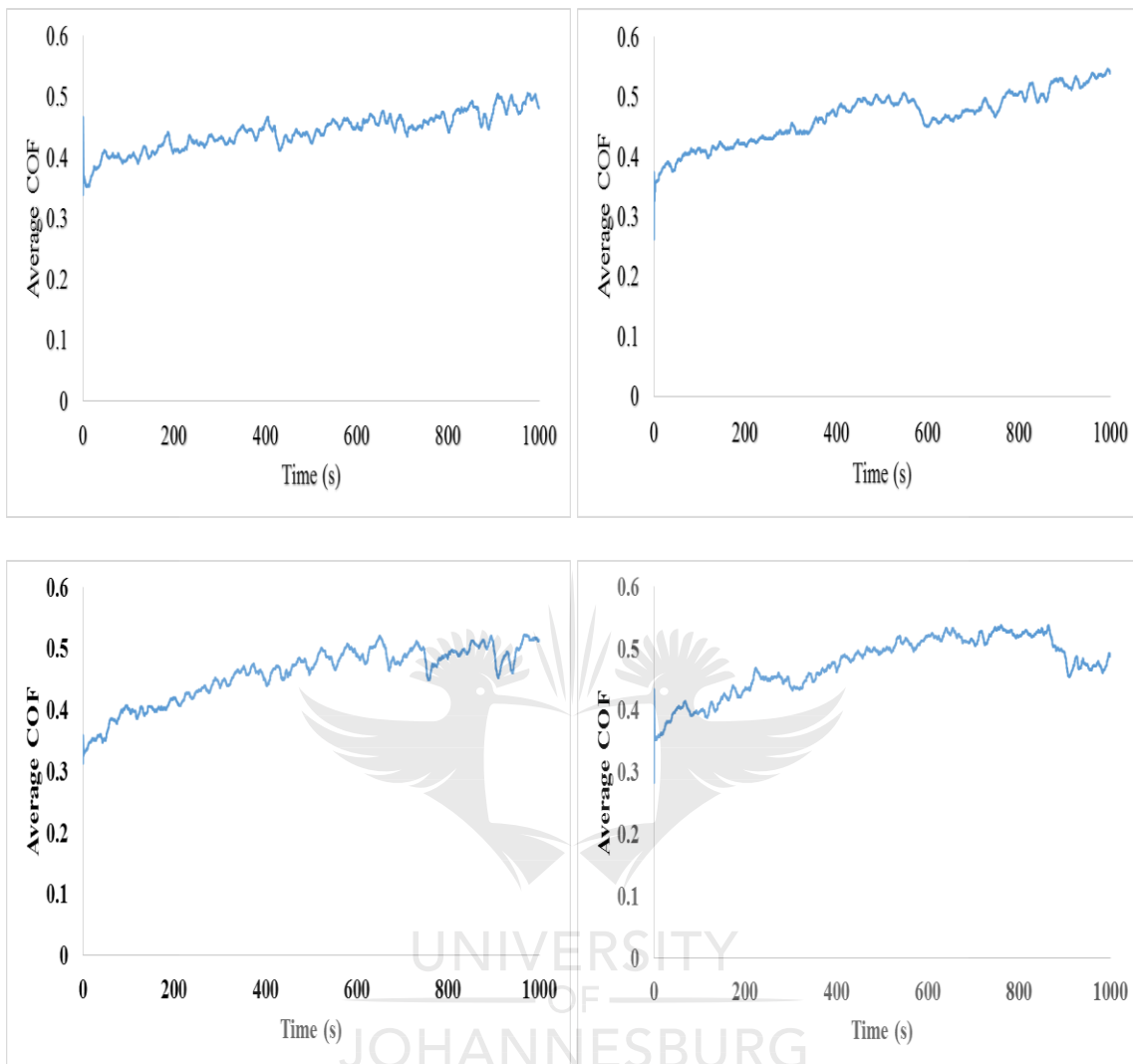
646.3 μm . Thus, sample S6 showed profound ductile property than sample S8 which could be due to more heat input that was applied to sample S8 when compared to sample S6. On the other hand, some particles of B₄C that might have formed unmelted powder in the melt pool after solidification of the composites may also be the reason for sample S6 having the lowest wear depth among the rest of the samples.

Furthermore, both wear volume and wear rate were characterized by irregular behaviour whereby the samples were observed to experience both increase and decrease as the laser power increases across the deposited composites. From all the deposited composites observed, sample S1 deposited at laser power of 800 W has the lowest wear volume of $35.2 \times 10^{-3} \text{ mm}^3$ while sample S7 deposited at laser power of 2000 W possesses the highest wear volume of $93.3 \times 10^{-3} \text{ mm}^3$. Similar to wear volume characteristics, sample S1 was also observed to have the lowest wear rate of $6.42 \times 10^{-4} \text{ mm}^3/\text{Nm}$ while sample S7 was however observed to experience the highest wear rate of $2.62 \times 10^{-3} \text{ mm}^3/\text{Nm}$. In addition to these results, it was observed that both wear volume and wear rate were proportional to laser power whereby increase in laser power for respective samples influences both the wear volume and wear rate of the deposited composites.

4.6.2 Dry Wear Characteristics of the Deposited Coatings

Considering the variations of friction coefficient (COF) versus time taken curves for Ti6Al4V-B₄C composites are illustrated in Figure 4.24 shown. Various COF curves were obtained under applied load of 25 N, frequency of 5 Hz, 2 mm stroke and at a speed of 5 mm/s against a tungsten carbide ball with the experimental process of ball-on-disk tests. The test was however conducted in ambient air environment without any application of lubricant. Figure 4.32 presented showed various changes in friction coefficient of deposited coating samples with respect to time change.





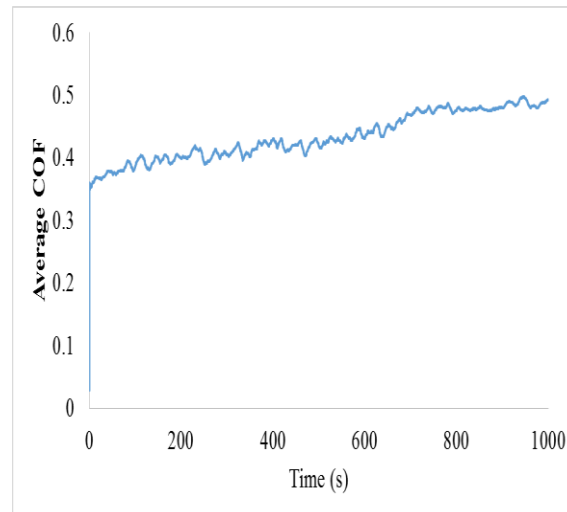


Figure 4.32: Friction coefficients (COF) of deposited composite coatings versus time taken at constant normal load of 25 N and 5 mm/s speed under varying laser power of samples in a dry condition

The Figure 4.32 presented the various behaviours of coefficient of friction against time taken for the deposited composites. Under constant parameters which include the applied load of 25 N, speed of 5 mm/s, stroke of 2 mm and reciprocating frequency of 5 Hz. The coefficient of friction for respective samples was measured in which sample S1 was observed to experience a slight increase from 0.354 to 0.434 of COF at time of 200 seconds. However, there is a sharp increase in COF and attain a maximum value of 0.509 at above 900 seconds. On the other hand, sample S2 showed a significant increase of COF at a range between the values of 0.375 and 0.481. This result was observed at the time of approximately 550 seconds. Furthermore, this sample however experienced irregular decrease and increase between 600 and 800 seconds at COF values between 0.444 and 0.484 respectively. Sample S3 was observed to be profound by successive increment in COF between 0.414 and 0.505 corresponding to time between 100 and 525 seconds. The coating drops in COF value of 0.436 at about 630 seconds and eventually rise continuously at COF of 0.532 corresponding to 960 seconds. This sample showed progressive increment in COF with the lowest value of 0.432 and highest value of 0.557 corresponding to 900 seconds. Therefore, the results observed showed significant characteristics that wear actually increases with time as the laser power for deposited composites also increases.

In conclusion to the COF behaviour with time, sample S5 was observed to be profound with almost the same characteristics as sample S6 while sample S6 was observed to show constant

increase in COF from 0.41 to 0.50 which corresponds to 100 and 550 seconds respectively. Both sample S7 and S8 were significantly characterized with successive change in COF against time. These composites were observed to have their highest COF values of 0.52 and 0.54 respectively. In addition to these behaviours, the deposited composites experienced the COF values at different time whereby sample S7 was observed between 100 and 900 seconds while sample S8 observed between 200 and 800 seconds respectively. Deposited composites of sample S9 was profound with almost linear curve and possesses highest COF value of 0.5 corresponding to time of 950 seconds. Lastly, the COF values for the test were observed to be between 0.50 and 0.56 in which samples S2, S5 and S9 have lowest value of COF corresponding to 0.50. On the other hand, sample S4 has the highest COF value of 0.56. However, the COF value remained between the range of 0 and 0.56 throughout the test. Also, deposited composites coating otherwise represented as samples whose possessed by lowest COF thus being fairly resistant to wear damage.

4.7 SUMMARY

There is no doubt that laser metal deposition (LMD) parameters play an important role in fabricating coatings with superior properties. The parameters mainly include laser power, laser scanning speed, laser beam diameter, powder flow rate and as well as gas flow rate, whereby these parameters may be regarded as the optimization process parameters. However, optimization simply means the selection of the best combination of different fabricating parameters. On the other hand, this study has varied numerous amounts of quantitative and qualitative properties and which has helped in the characterization of the titanium alloy (Ti6Al4V) with the addition of boron carbide (B₄C). Furthermore, different tests were carried out after the deposition process of the coatings; which include the microstructural evaluation, microhardness profiling, geometrical analysis, porosity analysis and wear test. Thus, the main aim of this study was to use hardness and wear as criteria for titanium alloys beneficiation reinforced with boron carbide in the industries as well as the biomedical implants.

CHAPTER FIVE

CONCLUSIONS AND FUTURE WORK

5.1 INTRODUCTION

The aim of this research work is to study the laser metal deposition process of Ti6Al4V reinforced with B₄C particulate to improve the material properties and then find the best combination of process parameters for the metal matrix composites (MMCs). The optimization of process parameters for the LMD process was achieved by characterizing as well as quantifying the deposition produced through metallurgical evaluation, mechanical testing, scanning electron microscope (SEM) with energy dispersive spectroscope (EDS), x-ray diffraction (XRD) analysis, geometrical measurements, porosity analysis and wear test in order to achieve superior coatings with limited or no impurities after solidification of the deposits. A comprehensive literature review presented in chapter 2, has however discussed in detail the LMD process with the significance of its essential process parameters. Conventional fabrication processes such as powder metallurgy (PM), reactive hot pressing (RHP) amongst other have been reported and discussed through LMD process for the metal matrix composites (MMCs) coatings.

Thus, the knowledge gaps identified in the literature is that there was no detailed characterization in terms of microstructure, mechanical and wear for the LMD process between Ti6Al4V and B₄C composite as however dealt with in this study. The detailed experimental procedures employed in this research work were presented in chapter 3. These include the various methods of analysis conducted on the deposited composites coating samples mentioned as follow: microstructural characterization (through optical micrograph; scanning electron spectroscope with energy dispersive and x-ray diffraction), microhardness testing, geometrical measurements for dilution as well as aspect ratios and wear. Furthermore, the decisions on the final experimental matrix for the laser metal deposition employed in this research work were based on the analysis of the deposition of outstanding quality depositions produced during the preliminary investigation phase.

On the other hand, range of process parameters were employed in which laser power was varied while other parameters such as scanning speed, powder flow rate and gas flow rate were kept constant throughout the experiment in order to achieve deposited coatings with limited or no defects such as pores, cracks and forms of impurities (e.g. slag inclusions) after solidification of deposited composites coating. Other conclusion based on the preliminary investigation was to finalize the laser beam spot size by changing the spot size from 2 mm to 4 mm throughout the experiment to achieve the best results. Moreover, recommendations are highlighted for the future work that may be conducted based on this research work to further the state of this study.

5.2 CONCLUSIONS

The results and discussions of the laser metal depositions produced with the final experimental matrix comprising 9 deposited samples were presented in chapter 4. This section reports the overview and summary of the analyses conducted on the deposited composites coating together with the observed trends for each and every samples. The common trend observed after solidification of the deposits according to the process parameters, was that the intermetallic bonding increases as laser power increases but the porosity decreases accordingly across the entire samples. The deposits produced at the lowest laser power of 800 W was observed to have the poorest intermetallic bonding while those with laser power between 2000 W and 2400 W were observed to have intermetallic bonding which was attributed to the higher heat input introduced and whereby most unmelted powder particles were dispersed in the melt pool and any traces of entrapment gas must have escaped before solidification. The interrelationships observed between the experimental matrix and the deposited composites properties are discussed later.

The macrographs of the deposited composites revealed that the samples with laser powers between 800 W and 1800 W were characterized with pores and poor intermetallic bonding at the interface or fusion zone which is however observed that there was no sufficient heat to dissolve the unmelted powder particles in the melt pool before solidification. On the other hand, samples deposited with laser powers between 2000 W and 2400 W were however profound with good intermetallic bonding and very less porosity in which the one with laser

power of 2200 W was observed to be the best of them all in terms of intermetallic bonding and susceptibility to porosity. Optical micrographs of all the deposited samples were noted with microstructural zones such as fusion zone (FZ) and heat affected zone (HAZ) and observed in the cross-sections which was a typical LMD of titanium matrix composites (TMCs).

The microhardness profiles of the deposited samples were correlated with the microstructures of the fusion interfaces, it was found that higher Vickers microhardness values measured corresponded with the intermetallic compounds in those regions. Furthermore, scanning electron microscope (SEM) with energy dispersive spectroscopy (EDS) analyses showed that the hardness value (between the deposits and substrates) at the interfacial regions varies due to the distribution pattern of the intermetallic phases involved, as well as the variation in the amount of deformation the material had eventually experienced. Therefore, deposited samples with laser power between 2000 W and 2400 W were observed to have the highest range of hardness values whereby sample with laser power of 800 W has the lowest hardness value of 371 HV while sample with laser power of 2000 W has the highest hardness value of 471 HV.

The x-ray diffraction (XRD) analysis patterns of the deposited composites coating revealed that there were intermetallic compounds formed at the deposited interfaces through the LMD process produced in this research work, in which the most common intermetallics mainly being $\text{Ti}_{0.33}\text{V}_{1.67}\text{C}$ and V_2C whereas the secondary were TiB and TiB_2 ceramics due to the presence of higher titanium alloy proportion. However, the TiB and TiB_2 intermetallic compounds were expected and therefore observed throughout the test at different heat input which is corresponding to laser power.

The wear tests for the deposited composites coating on every samples were conducted using dry sliding wear process on ball-on-disc tribometer equipment. Both wear volume and wear rate for each and every deposited composites coating samples were calculated using the proposed Archard's wear equation. For obvious reason, deposited composites sample with laser power of 800 W has the lowest in both wear volume and wear rate while sample with laser power of 2000 W was exhibited the highest in both wear volume and wear rate in which the result was attributed to amount of heat input to the deposition, that is, as the laser power

increases the wear volume together with wear rate experience increase to some extent before decreases to certain level and then rise again. These results were however observed with irregular increase-decrease characteristics in both cases. On the other hand, coefficient of friction (COF) also has an influence on deposited composites coating in which samples with laser power of 1000 W, 1600 W and 2400 W respectively were observed to have the lowest COF while sample with laser power of 1400 W has the highest COF. Thus, the properties of high microhardness, low friction coefficient (COF) and excellent wear resistance of the alloyed layer (i.e. substrate) were attributed to the formation of hard ceramics compounds.

Nevertheless, the proposed aims and objectives of this research work were successfully accomplished. Depositions of titanium alloys and boron carbide metal matrix composites on titanium alloy substrates using laser metal deposition process were produced, and detailed characterizations were conducted. Based on the range of experimental matrix process parameters adopted, the research work has been able to establish an optimized process parameters between laser power of 2000 W and 2400 W whereby other parameters such as scanning speed, powder flow rate and gas flow rate corresponding to 1 m/min, 4 rpm or 6.68 g/min and 2 l/min respectively were kept constant throughout the deposition process. Therefore, successful LMD process between titanium alloys and boron carbide metal matrix composites for surface engineering applications with limited or defects free and without identified impurities were produced. Finally, these results showed that the optimized process parameters evaluated in this research can be recommended for industrial purposes.

5.3 FUTURE WORK

Despite the fact that significant work has already been achieved in this research work, there are still some aspects of the research that require further investigations and these include:

- Percentage composition of 80 wt.% to 20 wt.% powder mixtures between Ti alloy and B₄C metal matrix composites using laser metal deposition process were successfully deposited on Ti alloy substrate. The observed XRD analysis confirmed that Ti_{0.33}V_{1.67}C and V₂C were the main phases present with small amount of TiB and TiB₂ in which there was a shift noticed in the major Ti peak. This was suspected to be as a

result of small amount of C and B were actually dissolved in the Ti6Al4V-B₄C matrix during the deposition process. This however require review of the percentage composition between Ti6A4V and B₄C to be in proportion such as 75/25, 60/40 and 50/50 by percentage weight (wt.%) in order to have an excellent Vickers hardness and wear quality.

- Scanning speed of the deposited composites coatings should be varied as to figure out the cooling rate of the deposits at various scan speed before solidification.
- Corrosion test is required to be carried out on the deposited composites coating in varying environments to be able to figure out the compatibility of the material properties for biomedical implants.
- Fracture toughness test of the deposited coating should be investigated in conformity when compared to human tissues for biocompatibility applications.
- The erosive and corrosive wear performance of this coating with higher reinforcement fractions could be compared to check whether there is any significant improvement in its performance when compared to the results presented in this research work.
- The inclusion of particulates or whisker reinforcement in Ti6Al4V may reduce its corrosion performance, thus a study of the corrosion performance of the Ti6Al4V-B₄C composites coating and untreated Ti6Al4V could be investigated.
- The validity of the modification process employed by attaching fine B₄C on Ti6Al4V can be verified by using other deposition process. Hence, this process can be used to develop new materials with better properties for specific applications.
- Post deposition processing or treatment can be studied with their effect on the properties of composites parts fabricated. This will however allow composites with excellent properties to be developed with little or no defects such that they can be integrated into a range of materials to be heavily used in the manufacturing industries.

- In the future, functionally graded MMCs will be more used in ground transport and aerospace applications, however, the challenges of incomplete homogenisation of microstructure and anisotropy of their mechanical properties must be overcome.

The tests listed above together with the completed work in this research study would provide a comprehensive study on the LMD (cladding) process of titanium alloys and boron carbide metal matrix composites for surface engineering applications.



REFERENCES

- [1] Abdulfatai Jimoh, PhD Thesis: 2010. The Particulate-Reinforcement of Titanium Matrix Composites with Borides. The Faculty of Engineering and the Built Environment, University of the Witwatersrand, South Africa.
- [2] Francois Thevenot, 1990. Boron Carbide – A comprehensive report; Journal of the European Ceramic Society 6 pp. 205-225.
- [3] Tian, Zhang and Wang, 2008. Study on the microstructures and properties of the boride layers laser fabricated on Ti–6Al–4V alloy. Elsevier journal of materials processing technology 209, pp. 2887–2891.
- [4] Tjong and Ma, 2000. Microstructural and mechanical characteristics of in situ metal matrix composites. A review journal, materials science and engineering, 29 pp. 49-113.
- [5] Kim, Chung and Kang, 2001. In situ formation of titanium carbide in titanium powder compacts by gas-solid reaction, Elsevier journal of composites, part A 32, pp. 731-738.
- [6] Yang, Lu, Xu, Qin and Zhang, 2006. In situ synthesis of hybrid and multiple-dimensioned titanium matrix composites, Elsevier journal of alloys and compounds 419, pp. 76-80.
- [7] Levin, Frage and Dariel, 2000. A novel approach for the preparation of boron carbide-based cermets, Elsevier international journal of refractory metals and hard materials 18, pp. 131-135.
- [8] Hamdi Sencer Yilmaz, Master Dissertation: 2004. Characterization of Silicon Carbide Particulate Reinforced Squeeze Cast Aluminium 7075 Matrix Composite. The

department of metallurgical and materials engineering, graduate school of natural and applied sciences of Middle East technical university.

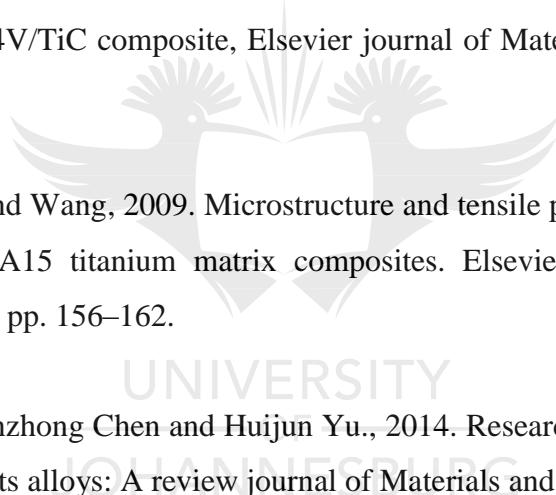
- [9] Naresh Prasad, PhD Thesis: 2006. Development and characterization of metal matrix composite using red mud an industrial waste for wear resistant applications. The department of mechanical engineering, national institute of technology Rourkela -769 008, India.
- [10] Dag Lukkassen and Annette Meidell, 2007. Advanced Materials and Structures and their Fabrication Processes. Book manuscript, Narvik University College, HiN.
- [11] Janne Nurminen, Jonne Nakki and Petri Vuoristo, 2009. Microstructure and properties of hard and wear resistant MMC coatings deposited by laser cladding, Elsevier Int. Journal of Refractory Metals & Hard Materials 27, pp. 472–478.
- [12] Ashby, Material Selection in Mechanical Design; Types of Materials, IE 351, Lecture 3, Slide 1-55, PowerPoint lecture presentation, page 26, Accessed August 2014.
- [13] El-Labban, Mahmoud and Al-wadai, 2014. Laser cladding of Ti-6Al-4V alloy with vanadium carbide particles, Apem journal of Advances in Production Engineering & Management, Vol. 9, No 4, pp. 159-167.
- [14] Sudipt Kumar “10404002” and Ananda, J., Theerthan “10304037”, 2008. Bachelor of Technology thesis on metal matrix composites (MMCs), Production and characterisation of aluminium fly-ash composite using stir casting method; Department of Metallurgical & Materials Engineering National Institute of Technology Rourkela.
- [15] Dinesh Kumar and Jasmeet Singh, 2014. Comparative Investigation of Mechanical Properties of Aluminium Based Hybrid Metal Matrix Composites. International Journal of Engineering Research and Applications (IJERA) ISSN: 2248-9622.

- National Conference on Advances in Engineering and Technology (AET- 29th March 2014).
- [16] General Introduction Module-1; General Introduction M1.1 Introduction of Composites; Historical Development / Historical overview; Page 1-35.
- [17] William Johnson and Alan Nagelberg, 1995. Application of Phase Diagrams to the Production of Advanced Composites. Lanxide Corporation Newark, Delaware 19714.
- [18] Ramesh and Ravichandran, 1990. Dynamic behaviour of a boron carbide-aluminium cermet: experiments and observations. Elsevier Journal of Mechanics of Materials 10, pp. 19-29.
- [19] James K. Wessel, 2004. Handbook of Advanced Materials, Enabling New Designs. A John Wiley & Sons, Inc., Publication, New Jersey, Published simultaneously in Canada. Wiley-Interscience publication, ISBN 0-471-45475-3.
- [20] Nicholas Clinning, Masters Dissertation, 2012. Thermomechanical processing of blended powder Ti-6Al-4V alloy, Centre for Materials Engineering, University of Cape Town, South Africa.
- [21] Titanium Alloy Guide, RMI Titanium Company, an RTI International Metals, Inc. Company. Website at: www.RMITitanium.com
- [22] Peter Kayode Farayibi, PhD Thesis, 2014. Laser Cladding of Ti-6Al-4V with Carbide and Boride Reinforcements using Wire and Powder Feedstock, Department of Mechanical, Materials and Manufacturing Engineering, University of Nottingham, United Kingdom.
- [23] Selva Kumara, Chandrasekar, Chandramohan and Mohanraj, 2012. Characterisation of titanium–titanium boride composites processed by powder metallurgy techniques. Elsevier journal of materials characterization 73, pp. 43-51.

- [24] Shahbahrami, Golestani Fard and Sedghi, 2011. The effect of processing parameters in the carbothermal synthesis of titanium diboride powder. Elsevier journal, *Advanced Powder Technology* 23, pp. 234–238.
- [25] Srivatsan, Guruprasad, Black, Radhakrishnan and Sudarshan, 2005. Influence of TiB₂ content on microstructure and hardness of TiB₂–B₄C composite. Elsevier journal, *Powder Technology* 159, pp. 161 – 167.
- [26] Bahman Nasiri-Tabrizi, Touraj Adhamin and Reza Ebrahimi-Kahrizsangi, 2013. Effect of processing parameters on the formation of TiB₂ nanopowder by mechanically induced self-sustaining reaction. Elsevier journal, *Ceramics International* 40, pp. 7345–7354.
- [27] Tjong and Yiu-Wing Mai, 2007. Processing-structure-property aspects of particulate- and whisker-reinforced titanium matrix composites. Elsevier *Journal of Composites Science and Technology* 68, pp. 583–601.
- [28] Diefendorf and Mazlout, 1994. Dynamic model for the chemical vapour deposition (CVD) processing of TiB₂ fibres. *Journal of Composites Science and Technology* 51, pp. 181-191.
- [29] Deyong Wang, Huihua Wang, Shuchen Sun, Xiaoping Zhu and Ganfeng Tu, 2014. Fabrication and characterization of TiB₂/TiC composites. Elsevier *Int. Journal of Refractory Metals and Hard Materials* 45, pp. 95–101.
- [30] Mary, Jamieson, Nick Serpone and Ezio Pelizzetti, 1987. *Titanium*: Elsevier Science Publishers B.V., Amsterdam – Printed in the Netherlands; *Coordination Chemistry Reviews* 78, pp. 147-251.

- [31] Wang, Ma, Li, Dong and Wang, 2011. Effect of boron addition on microstructure and mechanical properties of TiC/Ti6Al4V composites. ELSEVIER, Journal of Materials and Design 36, pp. 41–46.
- [32] Indrani Sen, Tamirisakandala, Miracle and Ramamurty, 2007. Microstructural effects on the mechanical behaviour of B-modified Ti–6Al–4V alloys. ELSEVIER, journal of Acta Materialia 55, pp. 4983–4993.
- [33] Shibayan Roy, Apu Sarkar and Satyam Suwas, 2010. Characterization of deformation microstructure in Boron modified Ti–6Al–4V alloy. ELSEVIER, Journal of Materials Science and Engineering A528, pp. 449–458.
- [34] Arrazola, Garay, Iriarte, Armendia, Marya and Le Maitre, 2008. Machinability of titanium alloys (Ti6Al4V and Ti555.3). ELSEVIER, a review journal of materials processing technology 209, pp. 2223–2230.
- [35] Bolzoni, Montealegre Meléndez, Ruiz-Navas and Gordo, 2012. Microstructural evolution and mechanical properties of the Ti–6Al–4V alloy produced by vacuum hot-pressing. ELSEVIER, journal of Materials Science and Engineering A546, pp. 189–197.
- [36] Shibayan R. and Satyam S., 2012. The influence of temperature and strain rate on the deformation response and microstructural evolution during hot compression of a titanium alloy Ti–6Al–4V–0.1B. ELSEVIER, Journal of Alloys and Compounds 548, pp. 110–125.
- [37] Murr, Quinones, Gaytan, Lopez, Rodela, Martinez, Hernandez, Martinez, Medina and Wicker, 2008. Microstructure and mechanical behaviour of Ti–6Al–4V produced by rapid-layer manufacturing, for biomedical applications – A review article, ELSEVIER, journal of mechanical behaviour of biomedical materials 2, pp. 20-32.

- [38] Mogilevsky, Gutmanas, Gotman and Telle, 1995. Reactive Formation of Coatings at Boron Carbide Interface with Ti and Cr Powders. *Journal of the European Ceramic Society* 15, pp. 527-535.
- [39] Srivatsan, Sudarshan and Laverniaj, 1995. Processing of Discontinuously-reinforced metal matrix composites by rapid solidification. *Elsevier journal, Progress in materials science* Vol. 39, pp. 317-409.
- [40] Meyers, Mishra and Benson, 2005. Mechanical properties of nanocrystalline materials. *Elsevier journal, Progress in materials science* 51, pp. 427–556.
- [41] Jianbo Jia, Kaifeng Zhang and Shaosong Jiang., 2014. Microstructure and mechanical properties of Ti-22Al-25Nb alloy fabricated by vacuum hot pressing sintering. *Journals of Materials Science and Engineering A*, www.elsevier.com/locate/msea
- [42] Ville Matilainen., 2012. Benchmarking of laser additive manufacturing process. An article of Lappeenranta University of Technology (LUT), Faculty of technology and metal technology BK10A0401 Bachelor's thesis and seminar.
- [43] Yongzhong Zhang, Zengmin Wei, Likai Shi and Mingzhe Xi., 2007. Characterization of laser powder deposited Ti–TiC composites and functional gradient materials. *Elsevier journal of materials processing technology* 206, pp. 438–444.
- [44] Akinlabi E. T. and Akinlabi S. A., 2015. Characterization of Functionally Graded Commercially Pure Titanium (CPTI) and Titanium Carbide (TiC) Powders, *Proceedings of the World Congress on Engineering, Vol. II, WCE 2015, July 1 – 3, 2015, London, U.K.*
- [45] Mahamood R. M., Akinlabi E. T., Shukla M. and Pityana S., 2014. Characterization of Laser Deposited Ti6Al4V/TiC Composite Powders on a Ti6Al4V Substrate, *Lasers in Eng. Vol. 29. Pp. 197-213.*

- [46] Mahamood R. M., Akinlabi E. T., Shukla M. and Pityana S., 2014. Effect of processing parameters on the properties of laser metal deposited Ti6Al4V using design of experiment, IAENG Transactions on Engineering Sciences, Taylor & Francis Group, London, ISBN 978-1-138-00136-7. Pp. 331-339.
- [47] Mahamood R. M., Akinlabi E. T., Shukla M. and Pityana S., 2013. Material Efficiency of Laser Metal Deposited Ti6Al4V: Effect of Laser Power, International Association of Engineers, Engineering Letters, 21:1, 2013, ISSN: 1816-093X (Print); 1816-0948 (Online).
- [48] Mahamood R. M., Akinlabi E. T., Shukla M. and Pityana S., 2013. Scanning velocity influence on microstructure, microhardness and wear resistance performance of laser deposited Ti6Al4V/TiC composite, Elsevier journal of Materials and Design vol. 50, pp. 656–666.
- [49] Liu, Zhang, Li and Wang, 2009. Microstructure and tensile properties of laser melting deposited TiC/TA15 titanium matrix composites. Elsevier Journal of Alloys and Compounds 485, pp. 156–162.
- [50] Fei Weng, Chuanzhong Chen and Huijun Yu., 2014. Research status of laser cladding on titanium and its alloys: A review journal of Materials and Design 58, pp. 412–425.
- [51] Anoop N. Samant and Narendra B. Dahotre, 2008. Laser machining of structural ceramics—A review Journal of the European Ceramic Society 29, pp. 969-993.
- [52] Yilbas and Karatas, 2014. Laser treatment of boron carbide surfaces: Metallurgical and morphological examinations. Elsevier Journal of Alloys and Compounds 603, pp. 125–131.
- [53] Ochonogor, Meacock, Abdulwahab, Pityana and Popoola, 2012. Effects of Ti and TiC ceramic powder on laser-cladded Ti–6Al–4V in situ intermetallic composite, Elsevier journal of Applied Surface Science vol. 263, pp. 591–596.
- 

- [54] Paul H. Mayrhofer, Christian Mitterer, Lars Hultman and Helmut Clemens, 2006. Microstructural design of hard coatings. Elsevier journal, Progress in Materials Science 51, pp. 1032–1114.
- [55] Bogomol, Nishimura, Vasylykiv, Sakka and Loboda, 2009. Microstructure and high-temperature strength of B₄C–TiB₂ composite prepared by a crucibleless zone melting method. Elsevier Journal of Alloys and Compounds 485, pp. 677–681.
- [56] Tuffe, Dubois, Fantozzi and Barbier, 1996. Densification, Microstructure and Mechanical Properties of TiB₂-B₄C Based Composites. Elsevier, Int. Journal of Refractory Metals and Hard Materials 14, pp. 305-310.
- [57] Peters, Cook, Haringa and Russell, 2009. Microstructure and wear resistance of low temperature hot pressed TiB₂. Elsevier, Wear 266, pp. 1171–1177.
- [58] Srivatsan, Guruprasad, Black, Petraroli, Radhakrishnan and Sudarshan, 2005. Microstructural development and hardness of TiB₂-B₄C composite samples: Influence of consolidation temperature. Elsevier Journal of Alloys and Compounds 413, pp. 63–72.
- [59] ASTM B348-13. Standard specification for titanium and titanium alloy bars and billets for the hot rolled substrate of Ti6Al4V.
- [60] Ming Yan and Peng Yu., 2015. An Overview of Densification, Microstructure and Mechanical Property of Additively Manufactured Ti-6Al-4V — Comparison among Selective Laser Melting, Electron Beam Melting, Laser Metal Deposition and Selective Laser Sintering, and with Conventional Powder Metallurgy, (<http://creativecommons.org/licenses/by/3.0>).
- [61] George F. Vander Voort; Buehler-summet, 2007. The science behind material preparation – A guide to material preparation and analysis: www.buehler.com

- [62] ASTM E3-11, 2011. Standard guide for preparation of metallurgical/metallographic specimens, ASTM international book of standards, volume 03.01.
- [63] Taylor B. and Weidmann E., 2008. Metallographic preparation of titanium, Struers Application Notes, Available online at http://www.struers.com/resources/elements/12/104827/Application_Note_Titanium_English.pdf, access August, 2014.
- [64] Jumate Elena and Manea Daniela Lucia, 2012. Application of x-ray diffraction (XRD) and scanning electron microscopy (SEM) methods to the Portland cement hydration processes. *Journal of Applied Engineering Sciences*, pp. 35-42.
- [65] Venkannah S., 2004. Materials Science-Mech 2121. Mechanical and production engineering department, faculty of engineering, university of Mauritius.
- [66] ASTM E384-11e1, 2011. Standard test method for Knoop and Vickers Hardness of materials, ASTM international book of standards, volume 03.01.
- [67] ASTM Standard G133-05, 2005. Standard Test Method for Linearly Reciprocating Ball-on-Flat Sliding Wear, Annual Book of ASTM Standards, volume 03.02.
- [68] Xuejin Shen, Lei Cao and Ruyan Li, 2010. Numerical Simulation of Sliding Wear based on Archard's Model. Supported paper by high and new engineering program of shanghai (No. D.51-0109-09-001) and the shanghai university innovation fund (No. A. 16-0109-09-724).
- [69] Jun Qu and John J. Truhan, 2006. An efficient method for accurately determining wear volumes of sliders with non-flat wear scars and compound curvatures. *Elsevier journal of wear* 261, pp. 848-855.

- [70] Sharma S., Sangal S. and Mondal K., 2013. On the optical microscopic method for the determination of ball-on-flat surface linearly reciprocating sliding wear volume. Elsevier journal of wear 300, pp. 82-89.
- [71] Rasheedat M. Mahamood, Esther T. Akinlabi, Mukul Shukla and Sisa Pityana, 2014. Characterizing the Effect of Processing Parameters on the Porosity of Deposited Titanium Alloy Powder. Proceeding of the International MultiConference of Engineers and Computer Scientists, Volume II, IMEC, March 12-14, Hong Kong.
- [72] Fei Weng, Chuanzhong Chen and Huijun Yu, 2014. Research status of laser cladding on titanium and its alloys: A review Journal by Elsevier, journal of materials and design 58, pp. 412-425.
- [73] Carcel B., Serrano A., Zambrano J., Amigo V. and Carcel A. C., 2014. Laser cladding of TiAl intermetallic alloy on Ti6Al4V. Process optimization and properties. 8th International Conference on Photonic Technologies LANE 2014. Elsevier journal of Physics Procedia 56, pp. 284-293.
- [74] Onyeka Franklin Ochonogor, M Tech Dissertation, 2013. Laser based in-situ Formation of Ceramic Coatings on Titanium. Department of Chemical and Metallurgical Engineering, Faculty of Engineering and the Built Environment, Tshwane University of Technology, South Africa.
- [75] Mutiu Erinosh, Esther Akinlabi and Sisa Pityana, 2015. Microstructure and dry sliding wear characteristics of the laser metal deposited Ti6Al4V/Cu composites. Proceeding of the 3rd international conference on laser and plasma application in material sciences.
- [76] Shebani A. and Pislaru C., 2015. Wear measuring and wear modelling based on Archard, ASTM and Neutral Network Models. International Science Index, Mechatronics Engineering Vol.9, No 1.

- [77] Fabio A. Dorinia and Rubens Sampaio, 2011. Some results on the random wear coefficient of Archard's model. Asociación Argentina de Mecánica Computacional, Mecánica Computacional Vol XXX, págs. 3297-3308 (artículo complete) Oscar Möller, Javier W. Signorelli, Mario A. Storti (Eds.) Rosario, Argentina, 1-4 Noviembre 2011.
- [78] Sören Andersson, 2010. Wear Simulation, Advanced Knowledge Application in Practice, Igor Fuerstner (Ed.), and ISBN: 978-953-307-141-1, InTech, Available from: <http://www.intechopen.com/books/advanced-knowledgeapplication-in-practice/wear-simulation>.
- [79] Masego Liberty Lepule, M Tech Dissertation: 2013. Tribo-corrosion Characteristics of Laser Deposited Titanium-Based Smart Coatings. Department of Chemical and Metallurgical Engineering, Faculty of Engineering and the Built Environment, Tshwane University of Technology, South Africa.
- [80] Edmond E. Bisson, 1968. Various modes of wear and their controlling factors. 71st Annual Meeting of the American Society for Testing and Materials San Francisco, California, June 23-28, 1968. Lewis Research Centre National Aeronautics and Space Administration Cleveland, Ohio.
- [81] Williams J. A., 1999. Wear modelling: analytical, computational and mapping: a continuum mechanics approach. Elsevier journal of wear vol. 225-229, pp. 1-17.
- [82] Syafa'at, Budi Setiyana, Muchammad and Jamari, 2013. Sliding Wear Modeling of Artificial Rough Surfaces. International Journal of Science and Engineering, Vol. 4(1)2013:21-23, January 2013, ISSN: 2086-5023.
- [83] Tian, Chen, Chen and Liu, 2005. Wear properties of alloyed layers produced by laser surface alloying of pure titanium with B4C and Ti mixed powders. Journal of materials science vol. 40 pp. 4387 – 4390.

APPENDIX A

PROPERTIES OF BORON CARBIDE (B₄C) POWDER AS-RECEIVED

Certificate of Analysis

Alfa Aesar®
A Johnson Matthey Company

Product Number: 10922
Product: Boron carbide 99+ %
Lot no: 61200108

Density	> 2.48 g/cm ³
Porosity	< 0.5 %
Average particle size	< 15 μm
Phase composition	B ₄ C, C
Vickers hardness	31 GPa
Knoop hardness	29 GPa
Elasticity (E)	420 GPa
Weibull modulus	15 m
Flexural strength, 4-point (σ _B)	450 MPa
Compression strength	> 2800 MPa
Poisson number (ν)	0.15
Fracture toughness	5 MPa·m ^{0.5}
Coefficient of thermal expansion	
(α) 20 °C - 500 °C	4.5 10 ⁻⁶ / K
(α) 500 °C - 1000 °C	7.2 10 ⁻⁶ / K
Specific heat at 20 °C	1 J/g K
Thermal conductivity at 20 °C (λ)	40 W/m K
Heat stress parameters (calculated)	
R ₁ = σ _B · (1 - ν) / (α · E)	202 K
R ₂ = R ₁ · λ	8 W/mm
Specific electrical resistance at 20 °C	1 Ωcm
Purity	> 99 %

Retest Date: February 2022

This document has been electronically generated and does not require a signature.

www.alfa.com

NORTH AMERICA
Tel: +1-800-343-0660 or
+1-978-521-6300
Fax: +1-800-322-4757
Email: info@alfa.com

GERMANY
Tel: 00800 4566 4566 or
+49 721 84007 280
Fax: 00800 4577 4577 or
+49 721 84007 300
Email: Eurosales@alfa.com

UNITED KINGDOM
Tel: 0800-801812 or
+44 (0)1524-850506
Fax: +44 (0)1524-850608
Email: UKsales@alfa.com

FRANCE
Tel: 0800 03 51 47 or
+33 (0)3 8862 2690
Fax: 0800 10 20 67 or
+33 (0)3 8862 6864
Email: frventes@alfa.com

INDIA
Tel: +91 8008 812424 or
+91 8008 812525 or
+91 8008 812626
Fax: +91 8418 260060
Email: india@alfa.com

CHINA
Tel: +86 (010) 8567-8600
Fax: +86 (010) 8567-8601
Email: saleschina@alfa-asia.com


KOREA
Tel: +82-2-3140-6000
Fax: +82-2-3140-6002
Email: saleskorea@alfa-asia.com

Safety data sheet
according to 1907/2006/EC, Article 31

Page 1/4

Printing date 01.07.2013

Revision: 31.08.2010

SECTION 1: Identification of the substance/mixture and of the company/undertaking	
1.1 Product identifier	Boron carbide
Trade name	10922
Stock number:	12069-32-8
CAS Number:	235-111-5
EC number:	
1.2 Relevant identified uses of the substance or mixture and uses advised against.	
Identified use:	SU24 Scientific research and development
1.3 Details of the supplier of the safety data sheet	
Manufacturer/Supplier:	Alfa Aesar GmbH & Co.KG A Johnson Matthey Company Zeppelinstr. 7b 76185 Karlsruhe / Germany Tel: +49 (0) 721 84007 280 Fax: +49 (0) 721 84007 300 Email: tech@alfa.com www.alfa.com
Informing department:	Product safety Tel + +049 (0) 7275 988687-0
1.4 Emergency telephone number:	Carechem 24: +44 (0) 1235 239 670 (Multi-language emergency number) Poison Information Center Mainz www.giftinfo.uni-mainz.de Telephone: +49(0)6131/19240
SECTION 2: Hazards identification	
2.1 Classification of the substance or mixture	Classification according to Regulation (EC) No 1272/2008
	GHS07
Acute Tox. 4	H332 Harmful if inhaled.
Skin Irrit. 2	H315 Causes skin irritation.
Eye Irrit. 2	H319 Causes serious eye irritation.
STOT SE 3	H335 May cause respiratory irritation.
Classification according to Directive 67/548/EEC or Directive 1999/45/EC	
<input checked="" type="checkbox"/> Xn; Harmful	
R20:	Harmful by inhalation.
<input checked="" type="checkbox"/> Xi; Irritant	
R36/37/38:	Irritating to eyes, respiratory system and skin.
Information concerning particular hazards for human and environment:	Not applicable
Other hazards that do not result in classification	No information known.
2.2 Label elements	
Labelling according to Regulation (EC) No 1272/2008	The substance is classified and labelled according to the CLP regulation.
Hazard pictograms	GHS07
Signal word	Warning
Hazard statements	H332 Harmful if inhaled. H315 Causes skin irritation. H319 Causes serious eye irritation. H335 May cause respiratory irritation.
Precautionary statements	P261 Avoid breathing dust/fume/gas/mist/vapours/spray. P305+P351+P338 IF IN EYES: Rinse cautiously with water for several minutes. Remove contact lenses, if present and easy to do. Continue rinsing. P302+P352 IF ON SKIN: Wash with plenty of soap and water. P321 Specific treatment (see on this label). P405 Store locked up. P501 Dispose of contents/container in accordance with local/regional/national/international regulations.
2.3 Other hazards	
Results of PBT and vPvB assessment	
PBT:	Not applicable.
vPvB:	Not applicable.
SECTION 3: Composition/information on ingredients	
3.1 Substances	
CAS# Designation:	12069-32-8 Boron carbide
Identification number(s):	
EC number:	235-111-5
SECTION 4: First aid measures	
4.1 Description of first aid measures	
After Inhalation	Supply fresh air. If required, provide artificial respiration. Keep patient warm. Consult doctor if symptoms persist.
After skin contact	Seek immediate medical advice. Instantly wash with water and soap and rinse thoroughly.
After eye contact	Seek immediate medical advice.
After swallowing	Rinse opened eye for several minutes under running water. Then consult doctor. Seek medical treatment.
4.2 Most important symptoms and effects, both acute and delayed	No further relevant information available.
4.3 Indication of any immediate medical attention and special treatment needed	No further relevant information available.
SECTION 5: Firefighting measures	
5.1 Extinguishing media	CO2, extinguishing powder or water jet. Fight larger fires with water jet or alcohol-resistant foam.
5.2 Special hazards arising from the substance or mixture	If this product is involved in a fire, the following can be released: Carbon monoxide and carbon dioxide Boron oxide
5.3 Advice for firefighters	Wear self-contained breathing apparatus. Wear full protective suit.

DE/E
(Contd. on page 2)

Safety data sheet
according to 1907/2006/EC, Article 31

Page 2/4

Printing date 01.07.2013

Revision: 31.08.2010

Trade name **Boron carbide**

(Contd. of page 1)

SECTION 6: Accidental release measures

6.1 Personal precautions, protective equipment and emergency procedures	Wear protective equipment. Keep unprotected persons away. Ensure adequate ventilation.
6.2 Environmental precautions:	Do not allow material to be released to the environment without proper governmental permits. Do not allow product to reach sewage system or water bodies. Do not allow to enter the ground/soil.
6.3 Methods and material for containment and cleaning up:	Dispose of contaminated material as waste according to item 13. Ensure adequate ventilation.
Prevention of secondary hazards:	No special measures required.
6.4 Reference to other sections	See Section 7 for information on safe handling See section 8 for information on personal protection equipment. See Section 13 for information on disposal.

SECTION 7: Handling and storage

7.1 Precautions for safe handling	Keep containers tightly sealed. Store in cool, dry place in tightly closed containers. Ensure good ventilation/exhaustion at the workplace.
Information about protection against explosions and fires:	No information known.
7.2 Conditions for safe storage, including any incompatibilities	
Storage Requirements to be met by storerooms and containers:	No special requirements.
Information about storage in one common storage facility:	Store away from oxidizing agents.
Further information about storage conditions:	Keep container tightly sealed. Store in cool, dry conditions in well sealed containers. No further relevant information available.
7.3 Specific end use(s)	

SECTION 8: Exposure controls/personal protection

Additional information about design of technical systems:	Properly operating chemical fume hood designed for hazardous chemicals and having an average face velocity of at least 100 feet per minute.
8.1 Control parameters	
Components with critical values that require monitoring at the workplace:	Not required.
Additional information:	No data
8.2 Exposure controls	
Personal protective equipment	
General protective and hygienic measures	The usual precautionary measures should be adhered to in handling the chemicals. Keep away from foodstuffs, beverages and food. Instantly remove any soiled and impregnated garments. Wash hands during breaks and at the end of the work. Avoid contact with the eyes and skin. Maintain an ergonomically appropriate working environment. Use breathing protection with high concentrations. Check protective gloves prior to each use for their proper condition. The selection of the suitable gloves does not only depend on the material, but also on further marks of quality and varies from manufacturer to manufacturer. Impervious gloves Not determined
Breathing equipment:	
Protection of hands:	Safety glasses Face protection Protective work clothing.
Material of gloves	
Penetration time of glove material	
Eye protection:	
Body protection:	

SECTION 9: Physical and chemical properties**9.1 Information on basic physical and chemical properties**

General Information	
Appearance:	
Form:	Powder
Colour:	Black
Smell:	Odourless
Odour threshold:	Not determined.
pH-value:	Not applicable.
Change in condition	
Melting point/Melting range:	2350 °C
Boiling point/Boiling range:	>2500 °C
Sublimation temperature / start:	Not determined
Inflammability (solid, gaseous)	Not determined.
Ignition temperature:	Not determined
Decomposition temperature:	Not determined
Self-inflammability:	Not determined.
Danger of explosion:	Product is not explosive.
Critical values for explosion:	
Lower:	Not determined
Upper:	Not determined
Steam pressure:	Not applicable.
Density at 20 °C	2.51 g/cm ³
Relative density	Not determined.
Vapour density	Not applicable.
Evaporation rate	Not applicable.
Solubility in / Miscibility with	
Water:	Insoluble
Partition coefficient (n-octanol/water):	Not determined.
Viscosity:	
dynamic:	Not applicable.
kinematic:	Not applicable.

(Contd. on page 3)
DE/E

Safety data sheet
according to 1907/2006/EC, Article 31

Page 3/4

Printing date 01.07.2013

Revision: 31.08.2010

Trade name Boron carbide	
(Contd. of page 2)	
9.2 Other information	No further relevant information available.
SECTION 10: Stability and reactivity	
10.1 Reactivity	No information known.
10.2 Chemical stability	Stable under recommended storage conditions.
Thermal decomposition / conditions to be avoided:	No decomposition if used and stored according to specifications.
10.3 Possibility of hazardous reactions	No dangerous reactions known
10.5 Incompatible materials:	Oxidizing agents
10.6 Hazardous decomposition products:	Carbon monoxide and carbon dioxide Boron oxide
SECTION 11: Toxicological information	
11.1 Information on toxicological effects	Harmful if inhaled.
Acute toxicity:	
LD/LC50 values that are relevant for classification:	No data
Skin irritation or corrosion:	Causes skin irritation.
Eye irritation or corrosion:	Causes serious eye irritation.
Sensitization:	No sensitizing effect known.
Germ cell mutagenicity:	No effects known.
Carcinogenicity:	EPA-I: Data are inadequate for an assessment of human carcinogenic potential.
Reproductive toxicity:	No effects known.
Specific target organ system toxicity - repeated exposure:	No effects known.
Specific target organ system toxicity - single exposure:	May cause respiratory irritation.
Aspiration hazard:	No effects known.
Additional toxicological information:	To the best of our knowledge the acute and chronic toxicity of this substance is not fully known.
SECTION 12: Ecological information	
12.1 Toxicity	
Aquatic toxicity:	No further relevant information available.
12.2 Persistence and degradability	No further relevant information available.
12.3 Bioaccumulative potential	No further relevant information available.
12.4 Mobility in soil	No further relevant information available.
Additional ecological information:	
General notes:	Do not allow material to be released to the environment without proper governmental permits. Generally not hazardous for water. Avoid transfer into the environment.
12.5 Results of PBT and vPvB assessment	Not applicable.
PBT:	Not applicable.
vPvB:	Not applicable.
12.6 Other adverse effects	No further relevant information available.
SECTION 13: Disposal considerations	
13.1 Waste treatment methods	Hand over to disposers of hazardous waste.
Recommendation:	Must be specially treated under adherence to official regulations. Consult state, local or national regulations for proper disposal.
Uncleaned packagings:	
Recommendation:	Disposal must be made according to official regulations.
SECTION 14: Transport information	
UN-Number	
ADR, IMDG, IATA	None
14.2 UN proper shipping name	
ADR, IMDG, IATA	None
14.3 Transport hazard class(es)	
ADR, IMDG, IATA	None
Class	
Packing group	
ADR, IMDG, IATA	None
14.5 Environmental hazards:	Not applicable.
14.6 Special precautions for user	Not applicable.
14.7 Transport in bulk according to Annex II of MARPOL73/78 and the IBC Code	Not applicable.
Transport/Additional information:	Not dangerous according to the above specifications.
SECTION 15: Regulatory information	
15.1 Safety, health and environmental regulations/legislation specific for the substance or mixture	
Australian Inventory of Chemical Substances	Substance is listed.
Standard for the Uniform Scheduling of Drugs and Poisons	Substance is not listed.
National regulations	
Information about limitation of use:	Employment restrictions concerning young persons must be observed. For use only by technically qualified individuals.
Water hazard class:	Generally not hazardous for water.
Other regulations, limitations and prohibitive regulations	
ELINCS (European List of Notified Chemical Substances)	Substance is not listed.
Substances of very high concern (SVHC) according to REACH, Article 57	Substance is not listed.
REACH - Pre-registered substances	Substance is listed.

(Contd. on page 4)
DE/E

Safety data sheet
according to 1907/2006/EC, Article 31

Printing date 01.07.2013

Revision: 31.08.2010

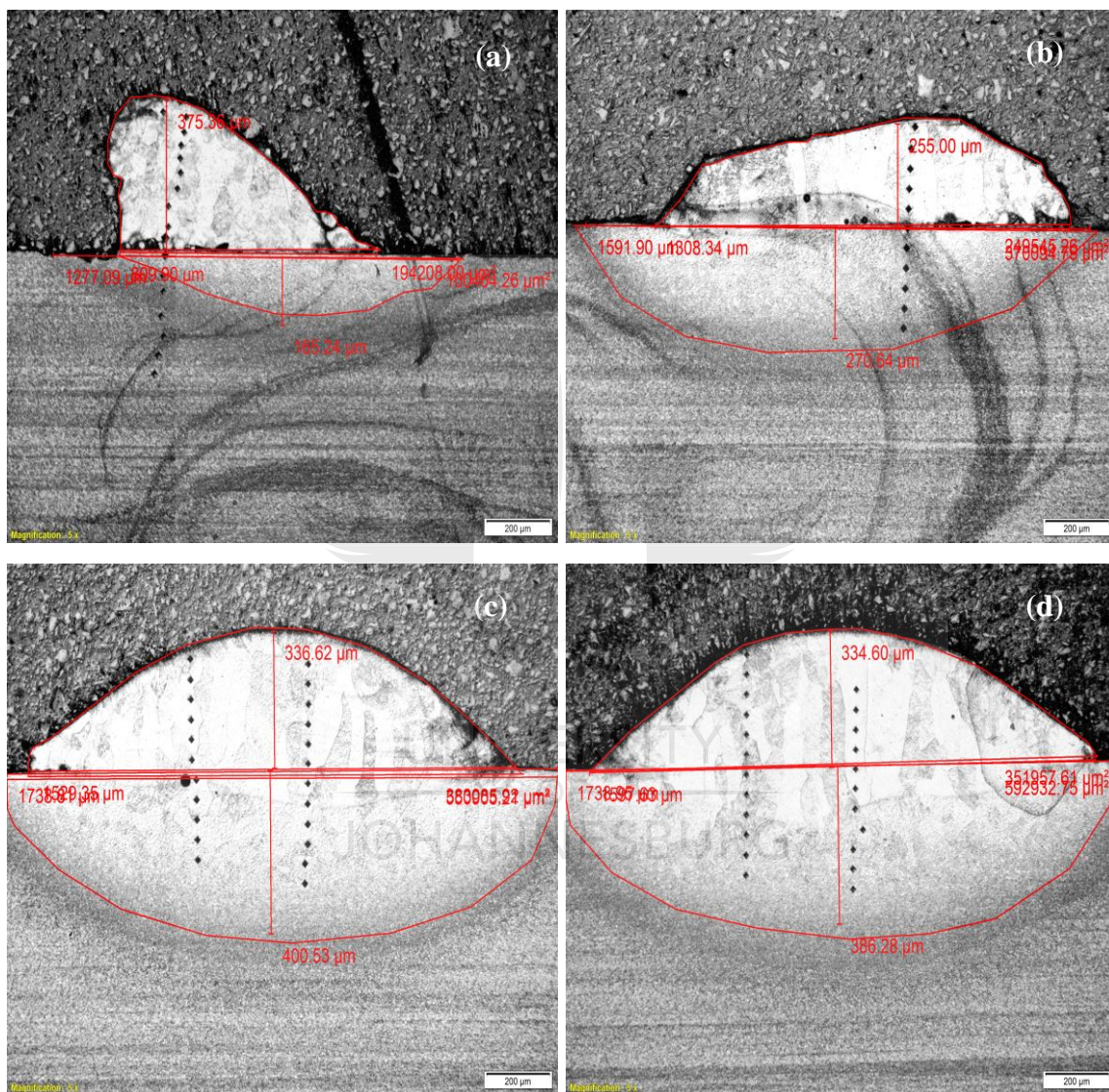
Trade name Boron carbide	
15.2 Chemical safety assessment:	A Chemical Safety Assessment has not been carried out. (Contd. of page 3)
<p>SECTION 16: Other information Employers should use this information only as a supplement to other information gathered by them, and should make independent judgement of suitability of this information to ensure proper use and protect the health and safety of employees. This information is furnished without warranty, and any use of the product not in conformance with this Material Safety Data Sheet, or in combination with any other product or process, is the responsibility of the user.</p> <p>Department issuing data specification sheet: Health, Safety and Environmental Department.</p> <p>Abbreviations and acronyms:</p> <p>RID: Règlement international concernant le transport des marchandises dangereuses par chemin de fer (Regulations Concerning the International Transport of Dangerous Goods by Rail) IATA-DGR: Dangerous Goods Regulations by the "International Air Transport Association" (IATA) ICAO: International Civil Aviation Organization ICAO-TI: Technical Instructions by the "International Civil Aviation Organization" (ICAO) ADR: Accord européen sur le transport des marchandises dangereuses par Route (European Agreement concerning the International Carriage of Dangerous Goods by Road) IMDG: International Maritime Code for Dangerous Goods IATA: International Air Transport Association GHS: Globally Harmonized System of Classification and Labelling of Chemicals EINECS: European Inventory of Existing Commercial Chemical Substances CAS: Chemical Abstracts Service (division of the American Chemical Society) LC50: Lethal concentration, 50 percent LD50: Lethal dose, 50 percent</p>	

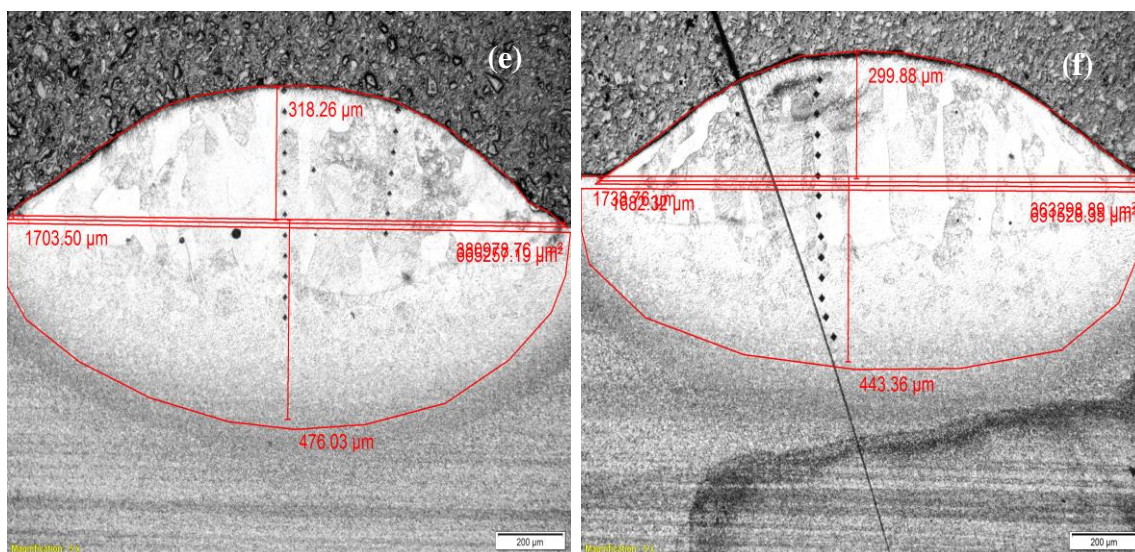


UNIVERSITY
OF
JOHANNESBURG

APPENDIX B

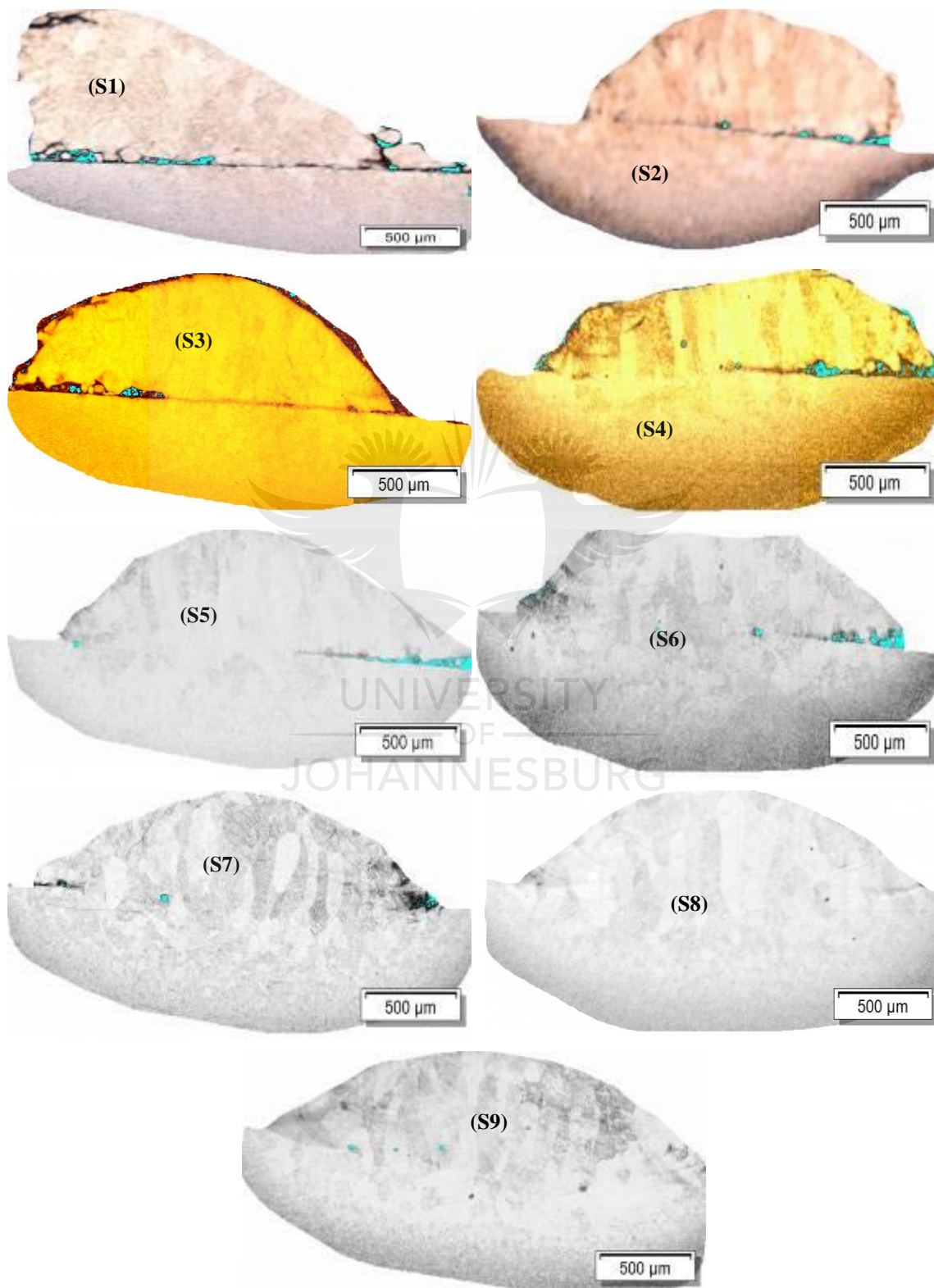
GEOMETRICAL MEASUREMENT OF LASER CLAD DEPOSITIONS





APPENDIX C

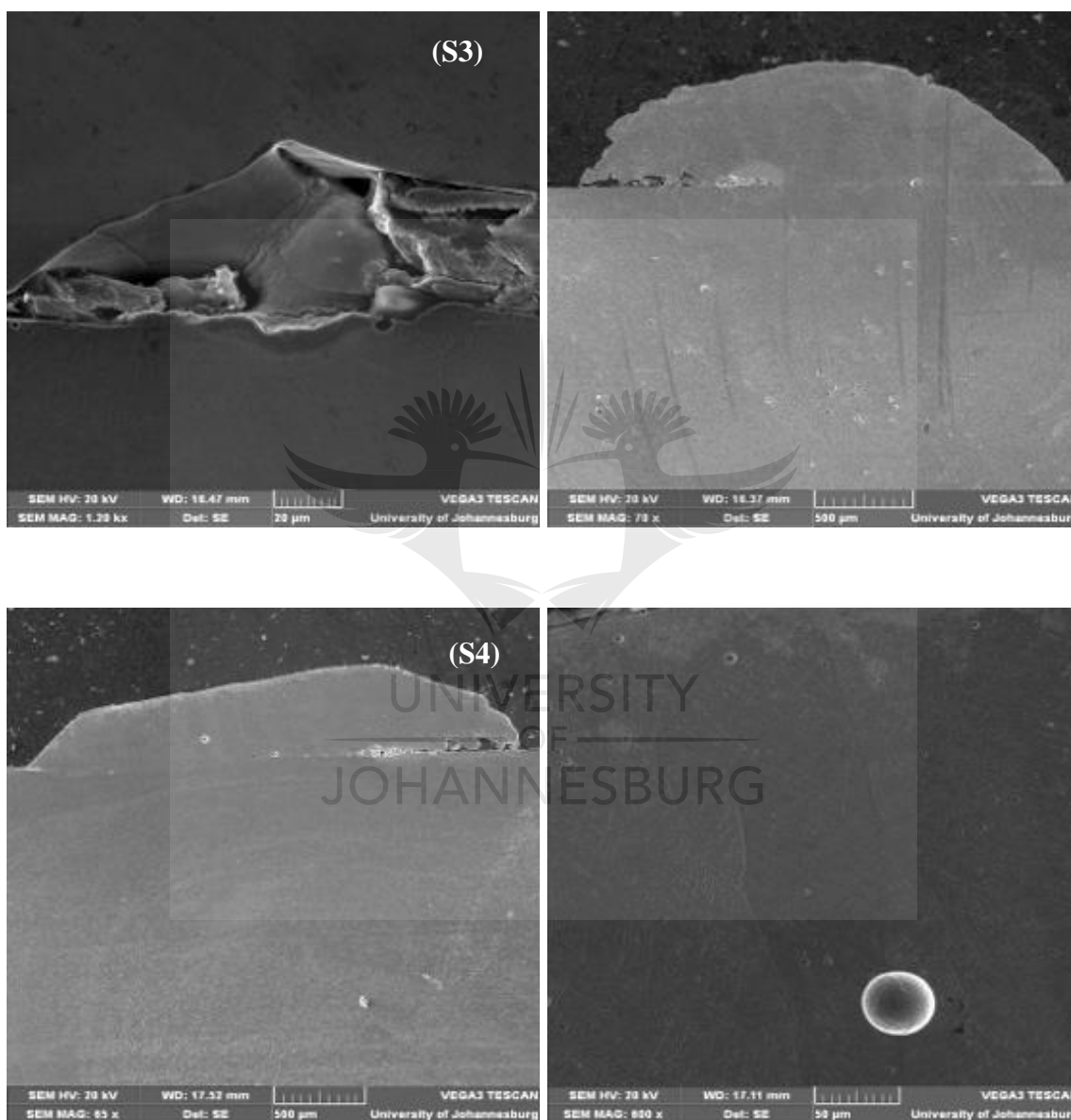
POROSITY ANALYSIS OF LASER CLAD DEPOSITIONS

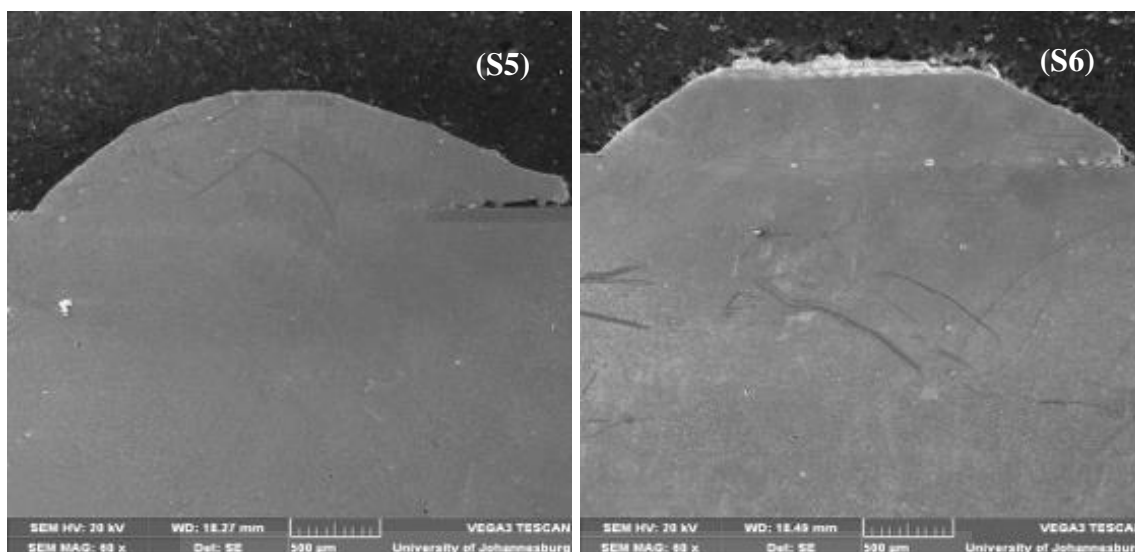


APPENDIX D

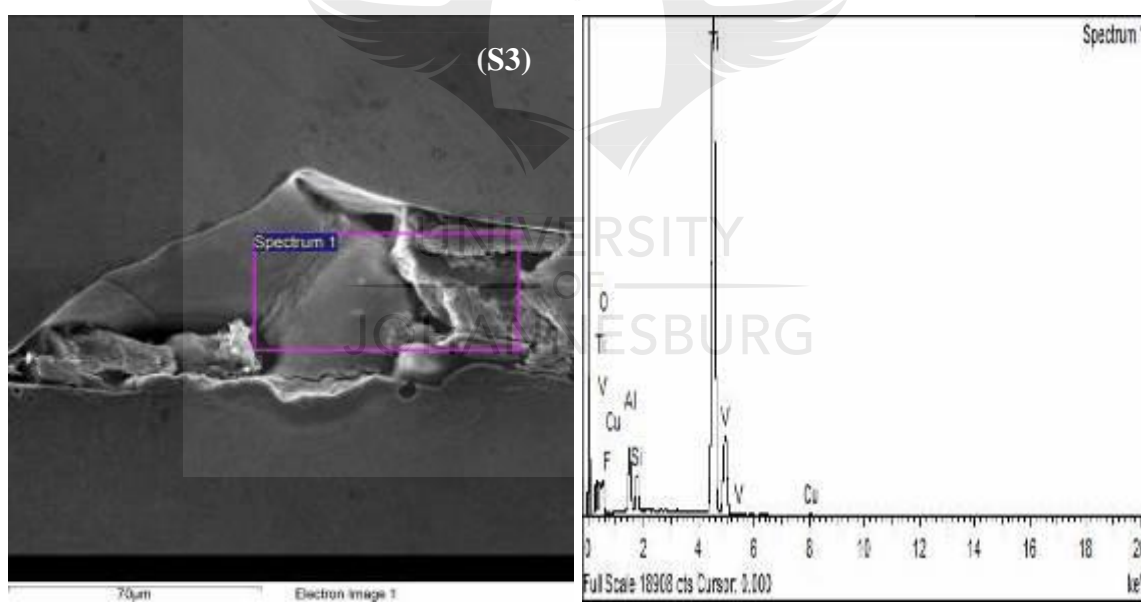
SEM AND EDS ANALYSIS OF LASER CLAD SAMPLES

D1. SEM of the deposited clad samples





D2. EDS of the deposited clad samples



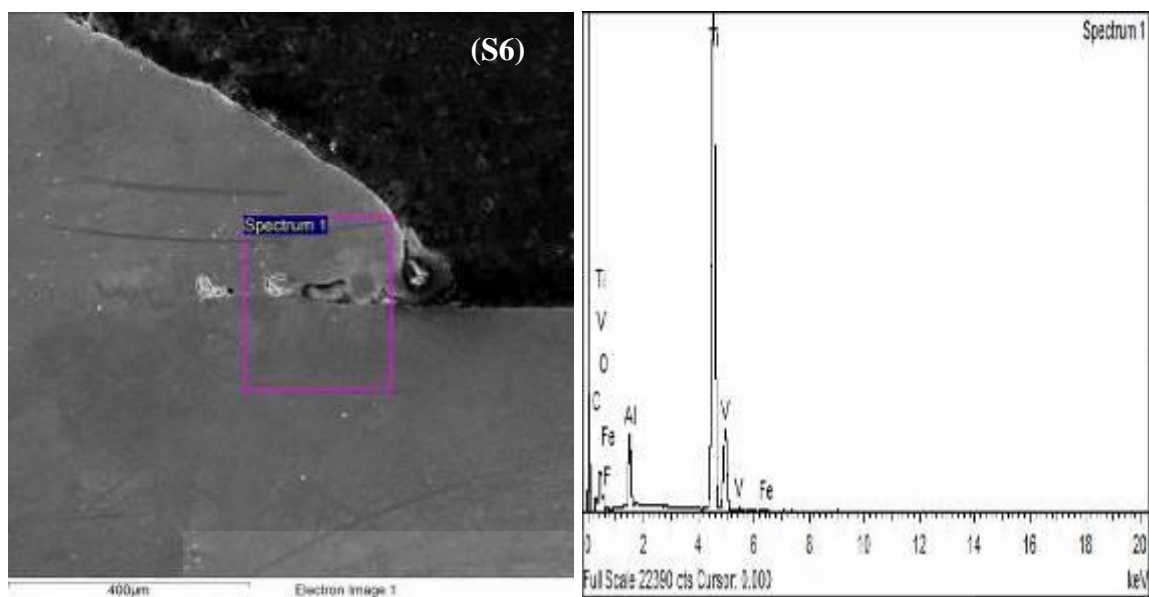
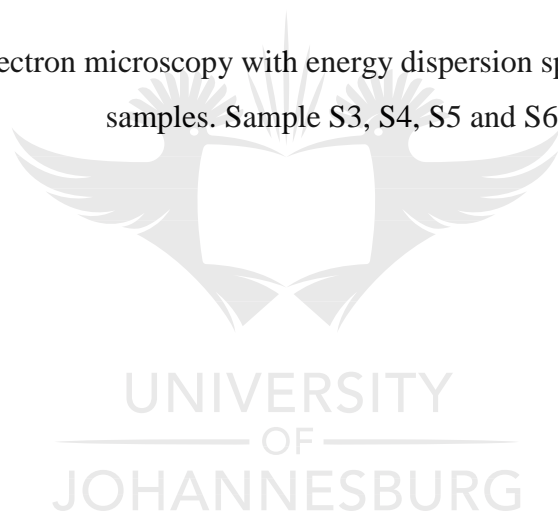
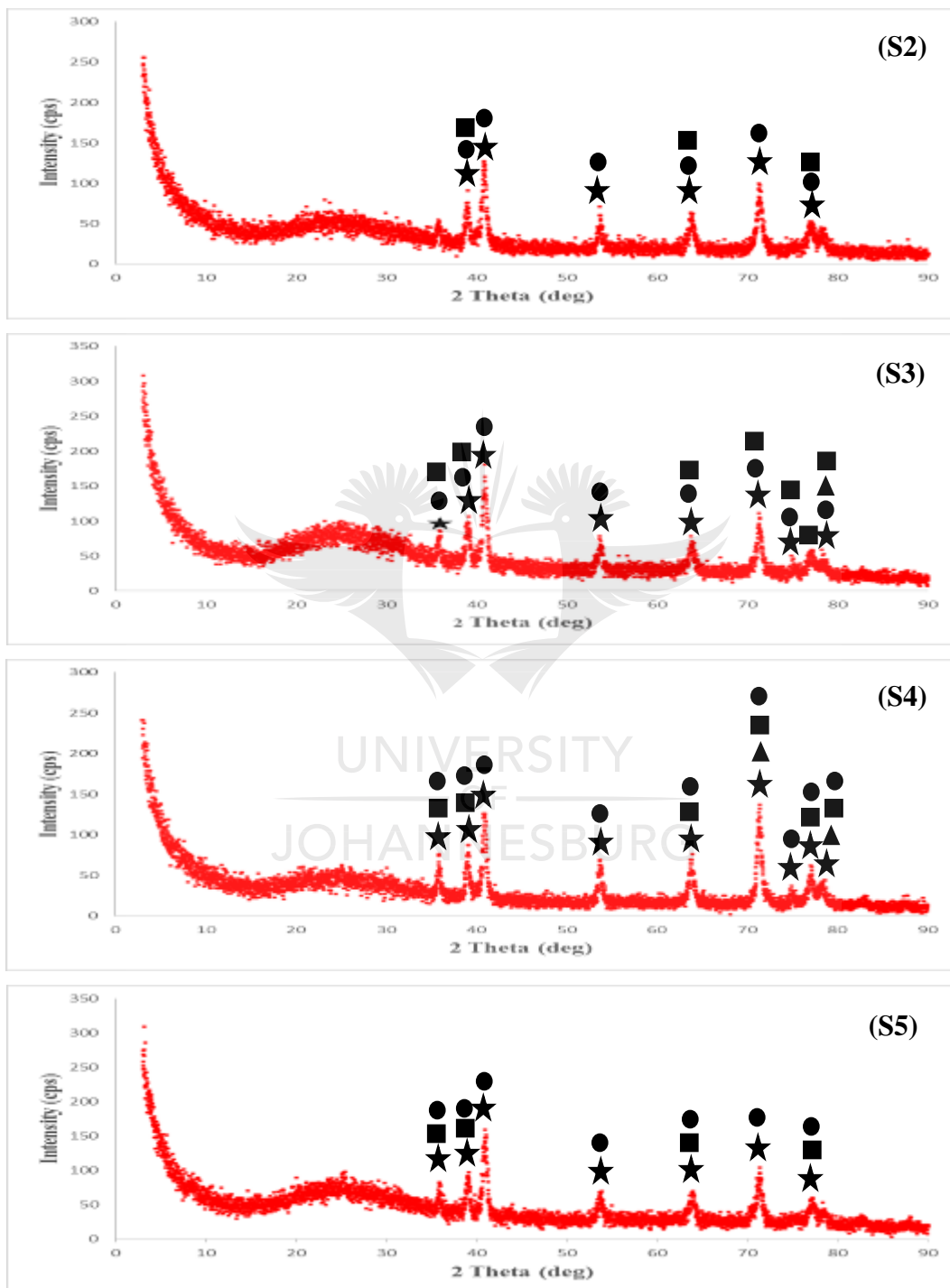


Figure D: Scanning electron microscopy with energy dispersion spectroscopy of different samples. Sample S3, S4, S5 and S6.



APPENDIX E

XRD ANALYSIS OF LASER CLAD SAMPLES



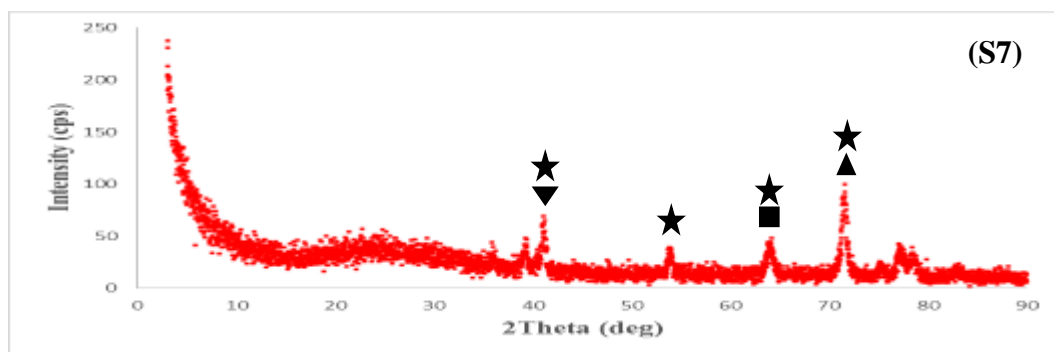


Figure E: x-ray diffraction (XRD) analysis of various samples: sample S2, S3, S4, S5 and S7.



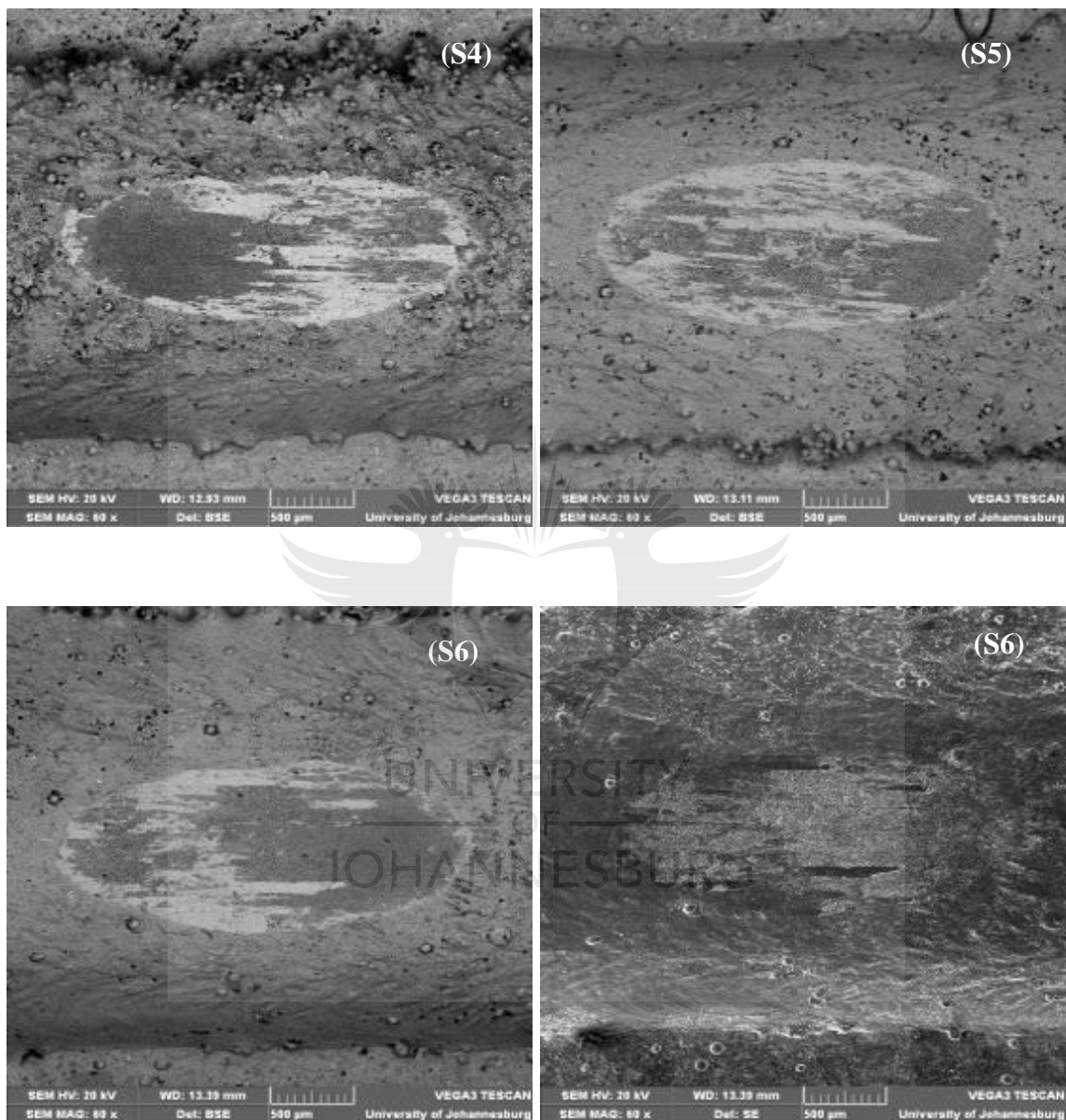
APPENDIX F**WEAR ANALYSIS OF LASER CLAD SAMPLES**

Figure F: wear scars photographs of different samples: sample S4, S5 and S6.

APPENDIX G

WEAR TRACK MEASUREMENT ANALYSIS AND VARIABLE EVALUATION

Samples	Wear depth, hf (μm)	Wear track radius, Rf (μm)	Width, w (μm)	Stroke length, Ls (μm)	Length, L (μm)	Wear volume, Vf (mm ³)	Wear rate, K (mm ³ /Nm)
S1	130.70	667.53	793.50	2193.17	2982.77	0.0352	0.0006421
S2	97.50	1538.13	1077.83	1837.82	2730.06	0.0878	0.0019109
S3	97.00	1773.24	1156.89	1305.03	2215.03	0.0769	0.0023574
S4	119.70	910.70	902.65	1699.80	2460.02	0.0413	0.0009722
S5	86.40	1852.32	1118.24	1452.57	2447.60	0.0862	0.0023729
S6	74.60	1994.51	1080.77	1459.70	2455.38	0.0898	0.0024609
S7	86.60	1976.43	1157.27	1425.22	2239.60	0.0933	0.0026175
S8	646.30	583.77	1160.83	1520.90	2321.77	0.0440	0.0011572
S9	106.70	1721.26	1193.20	1354.86	2325.65	0.0802	0.0023666



UNIVERSITY
OF
JOHANNESBURG





UNIVERSITY
OF
JOHANNESBURG

